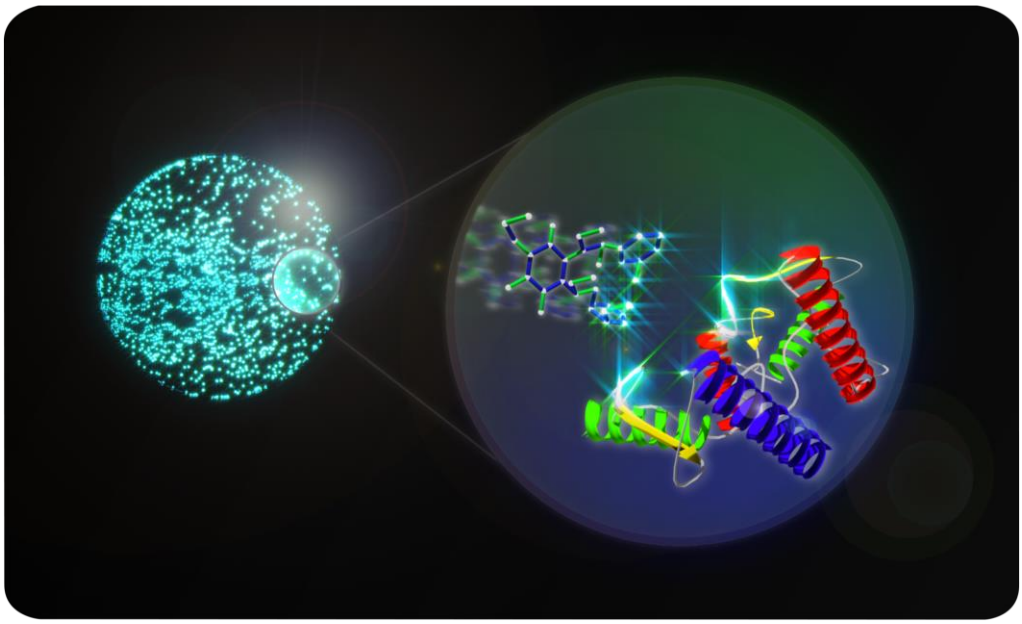
New approaches to detect and inhibit quorum sensing activity in *Pseudomonas aeruginosa*



Ivan H. G. Lafayette, BSc Hons Biotechnology, MRes in Toxicology

Thesis submitted to the University of Nottingham for the degree of Doctor of Philosophy in Molecular Microbiology

June 2016

“Everybody is a genius. But if you judge a fish by its ability to climb a tree, it will live its whole life believing that it is stupid.”

Unknown author

Unless otherwise acknowledged, the work presented in this thesis is my own. No part has been submitted for another degree at the University of Nottingham or any other institute of learning.

Ivan Lafayette

June 2016

Acknowledgments

A science PhD is before anything else a personal victory, a statement of commitment, of drive, passion and intellectual competences that go far beyond what seems to be humanly possible. It can only succeed when there is a visionary insight to what emergent challenges affect us all, embracing us in a common purpose as a team, unified, for the greater good. With this premise in mind I would like to recognise the incredible worth of a number of people and organisations that supported me throughout this research project. Firstly, I must thank the University of Nottingham and the Biotechnology and Biological Sciences Research Council (BBSRC) for continuously investing in pertinent research projects that allow students to be trained in world-class research laboratories. With all my heart I want to thank my supervisors, especially Prof Dr Miguel Cámara, Dr Stephan Heeb and Prof Dr David Barret, for giving me the opportunity of progressing as a scientist when they trusted me this PhD studentship. I recognise their remarkable guidance and effort when constantly going far above their professional obligations to help me reach the level of knowledge and insight I have gained. Likewise, I'd like to acknowledge the important contributions from our partner GreenPharma (in the person of Quoc-Tuan DO), and supervisors Paul Williams, Kim Hardie, Steve Atkinson, Ram Chaabra and Steve Diggle.

I'd also like to address my deepest gratitude to a team of Post-docs that collaborated with me throughout the many labs where I developed this research, especially Felix Dafhnis (a true brother) without whom this day would have been impossible. And the inestimable involvement of James Lazenby, Jean Dubern, Manuel Romero, Fadi Soukarieh, Sala Abdelrazig, Matt Fletcher, Anne Henstra and Katrin Schwarz, as well as all support from fellow PhD colleagues.

I address my enormous appreciation to a tireless team of specialised technical staff that thoroughly supported my research endeavours, especially Nigel Halliday, Catherine Orthori, Allex Truman and David Onion.

I would like to extend my thanks to true friends I made in the Centre for Biomolecular Sciences (CBS), and that I will always keep in my heart. From the pool of names allow me to elevate the likes of Anja Wiechmann, Hazel Silistre, Inma Madrigal, Andres Vallellano, Irene Escriba, Jorge Catala and Hamad Al-Harbi. They were indeed true valuable supporters through this process.

And because projects can never be successfully completed without a body of great supporting staff, I would like to address my sincerest friendship and appreciation to Tullia Randall and Shelley Alsop that always greated me with the most amazing kindness I could ask. And the support provided by Leanne Mitchell, Ian Hall, Louise Cupitt, Carole White, Jane Doughty, Slawomir Bianketti, Nicolla Smith, Evangelos Karwonis, Jacky Webb, Magda Lindstrom, Terri Mawson and Kate Beaumont.

These acknowledgements would never be completed without recognition of the immense support obtained from Felicity Baker which advice helped me be the best version of myself.

But above all I want to thank my family for their constant and positive presence, infinite love and unconditional support. My son Benjamin that was the true catalyst of my persistance, my wife Daniela that never stopped trusting my worth, my sister and my mother.

If at any point I forgot anyone, please accept my sincerest apoligies and rest assured that your names will always be written in my heart alongside all those hereby listed.

List of contents

Acknowledgments iii

List of Contents v

List of Figures xiii

List of Tables xvii

Abreviations xx

Abstract 1

Chapter 1. Introduction 5

1. Pseudomonas aeruginosa 5

1.1. *P. aeruginosa* as a nosocomial threat and a financial burden 6

1.2. *P. aeruginosa* virulence 6

1.2.1. Pyocyanin 9

1.2.2. Exoproteases 10

1.2.2.1. Elastases A and B 10

1.2.2.2. Protease IV 11

1.2.2.3. Alkaline protease (AprA) 11

1.2.3. Rhamnolipids 12

1.2.4. Type IV pili 13

1.2.5. Flagella 13

1.2.6. Lectins 13

1.2.7. Biofilm determinants 14

1.2.7.1. Pel 15

1.2.7.2. Psl 15

1.2.7.3. Extracellular DNA (eDNA) 16

1.3. Role of quorum sensing in the virulence of *P. aeruginosa* 16

1.3.1. *N*-acylhomoserine lactone quorum sensing signalling ... 16

1.3.2. Alkyl quinolone quorum sensing system 19

1.3.2.1. Biosynthesis of alkylquinolones 19

1.4. Role of AQs in the regulation of gene expression 21
1.4.1. Regulation of the pqs genes and relationships with the AHL-QS systems 23
1.5. Novel regulatory pathways influence PA virulence phenotypes 27
1.6. Impact of QS molecules in infection 29
1.6.1 Effect on interaction between polymicrobial communities 29
1.6.2 Effects on bacterial host-cell interactions 31
1.7. Approaches to treat PA infections 33
1.7.1. MDR PA and the need for alternative therapeutic approaches 33
1.7.2. Quorum sensing inhibition 40
1.7.2.1 Signal biosynthesis Inhibitors 38
1.7.2.1.1. Targeting AHLs 38
1.7.2.1.2. Targeting AQs 39
1.7.2.2. Signal molecule scavengers 40
1.7.2.2.1. Signal degrading enzymes 40
1.7.2.2.2. Degradation of AHLs 40
1.7.2.2.3 Degradation of AQs 42
1.7.2.2.4. Antibodies 43
1.7.2.2.5. Polymers 45
1.7.3. Receptor antagonists 45
1.7.3.1. PqsR inhibition 46
1.8. Objectives 53

Chapter 2. Material and Methods 55
2.1. Bacterial strains 55
2.2. Plasmids 56
2.3 Oligonucleotide primers 57
2.4. General Chemicals 60
2.4.1. Antibiotics and IPTG 60

2.4.2. Synthetic AHLs and AQs 61
2.5. General procedures 61
2.5.1. Growth media preparation 61
2.5.1.1. Luria Bertani (LB) medium 61
2.5.1.2. M9 minimal medium 62
2.5.1.3. RPMI-1640-based cell culture media (CCM..... 62
2.5.2. Growth and storage of bacterial strains 62
2.5.2.1. Small and large scale growth of bacterial strains 63
2.5.2.2. Long-term storage and revival of bacterial strains 63
2.5.3. DNA qualitation and quantification 63
2.5.4. DNA manipulation 64
2.5.4.1. Isolation of chromosomal DNA 64
2.5.4.2. Isolation of plasmid DNA 64
2.5.4.3. DNA ligation 65
2.5.4.3.1. DNA restriction enzymes 65
2.5.5. DNA agarose gel electrophoresis 66
2.5.5.1. DNA molecular weight markers 66
2.5.5.2. Extraction and purification of DNA from agarose gels 66
2.5.6. Polymerase Chain Reaction (PCR) amplification 70
2.5.7. Purification of PCR products 67
2.5.8. Cloning of PCR products 68
2.5.5.8.1. DNA sequencing 68
2.5.5.8.1.1. Obtaining DNA sequence data 68
2.5.5.8.1.2. DNA sequencing analysis 68
2.5.5.9. Transformation 69
2.5.5.9.1. Preparation of electrocompetent *E. coli* cells 69

2.5.5.9.2. Electroporation of *E. coli* cells ……. 69
2.5.5.9.3. Preparation of electrocompetent *Pseudomonas aeruginosa* cells …….. 70
2.5.5.9.4. Electroporation of electrocompetent PA cells …….. 70
2.6. Quorum sensing signaling molecules (QSSM) analysis … 70
2.6.1. QSSM extractions from bacterial supernatants …… 70
2.6.2. Liquid chromatography-mass spectrometry for detection of QSSM …….. 71
2.7. Virulence phenotype assays ……..…..… 73
2.7.1. Determination of bioluminescence and optical density of *lux* bioreporter strains using microtitre plate …….. 73
2.7.2. Quantification of Pyocyanin in overnight bacterial extracts …… 74
2.7.3. Biofilm assay using glass chamber slides …….. 74
2.8. Cytotoxicity assays ……. 76
2.8.1. Alamar Blue lymphocyte proliferation assay …… 76
2.8.2. Flow Cytometry cytotoxicity assay …… 76
2.9. Ligand-Receptor affinity prediction ……..…… 77
2.9.1. Protein preparation …….. 77
2.9.2. Ligand preparation …… 78
2.9.3. Molecular Docking …….. 78
2.9.4. Extraction solvents …….. 79
2.9.5. Preparation of standard mixtures …… 79
2.9.6. Preparation of growth media …….. 81
2.9.6.1. Luria BertaniMedia …….. 81
2.9.6.2. Long term storage of bacterial strains …….. 81
2.9.6.3. Bacterial growth conditions …….. 82
2.9.6.4. Preparation of bacterial extracts …….. 82
2.10. LESA-MS infusion optimisation methodology …… 83
2.10.1. LESA-MS optimisation methodology …… 84

2.10.2. Optimisation of surface for sample analysis …… 86

Chapter 3. Highthroughput screening for identifying novel potent PqsR inhibitors …… 88

3.1.1. Development of PqsR antagonists …… 88

3.1.1.1. Preliminary studies towards final pool of QS inhibiting candidates …… 105

3.2 Hit optimisation of PqsR inhibitors in *Pseudomonas aeruginosa* …… 106

3.2.1. Effect of the GP QS-inhibiting compounds on the activity of *pqsA* and P_{Km} …… 107

3.2.2. Synergistic effect of the PqsR inhibitors on CTX::P_{pqsA}-*luxCDABE* …… 111

3.3. Effect of PqsR inhibitors on AQ-dependent virulence factor production …… 116

3.3.1. QSIs effects on the production of lectins …… 116

3.3.1.1. Synergistic effects on *lecA/lecB* expression in PAO1-N after double exposure to PqsR inhibitors ….. 119

3.3.2. Effect of PqsR inhibitors on pyocyanin production ……. 124

3.3.3. Effect of PqsR on biofilm formation …… 127

3.3.3.1. Images of PAO1-L::mCherry biofilm formation after exposure to the top four GP QS-inhibiting compounds at their IC_{50}s …… 128

3.3.3.2. Analysis of a PAO1-L::mCherry putative dual behaviour response …… 130

3.4. Impact of PqsR inhibitors on AQs biosynthesis ……. 135

3.5. Cytotoxic effect of PqsR inhibitors on eukaryotic cells …… 138

3.5.1. Previous assays towards an optimised cytotoxicity protocol …… 138

3.5.2. Cytotoxic Effects of GP PqsR-inhibiting compounds on Eukaryotic cells (T Lymphocyte Jurkatt cells) 143
3.6. Summary of characterisation of PqsR-inhibitors 147
3.7. Discussion 152

Chapter 4. Engineering of a *pqsA-pqsR lux*-based biosensor in *E. coli* 175
4.1. Engineering of a *pqsA-pqsR* lux-based biosensor in *E. coli* 175
4.1.1. General schematic of the construct 175
4.1.2. Implementation of the bioengineering strategy 178
4.2. Bioluminescence assays 186
4.2.1. PAIL001 response to 50 µM C7-PQS and 1 mM IPTG ... 189
4.2.2. PAIL001 responsiveness after overnight exposure to 1 mM IPTG 191
4.2.3. PAIL003 [*lasR* mutant] 193
4.2.4. PAIL004 [*rhlR* mutant] 195
4.2.5. Effect of overnight IPTG exposure in the reporter activity of PAIL004 197
4.3. Corrective measures towards a functional system in *E. coli* 199
4.4. Discussion 204

Chapter 5. Optimisation of liquid extraction surface analysis (LESA) as a new methodology for rapid screening of quorum sensing moelecules in *ex vivo* PA bacterial extracts 214
5.1.1. Abstract 214
5.2. Introduction 215

5.2.1. Clinical and economic consequences of hospital-acquired PA infections 215
5.2.2. Traditional PA qualitative and quantitative detection methods 217
5.2.3. LESA as a novel methodology for profiling PA QS-related molecules 219
5.2.4. LESA-MS technology and equipment 220
5.2.5. Research objective 222
5.3. Materials and Methods 222
5.3.1. Extraction solvents 223
5.3.2. Preparation of standard mixtures 227
5.3.3. Preparation of growth media 231
5.3.4. Preparation of bacterial extracts 235
5.4. Results and Discussion 238
5.4.1. Screening and detection in PAO1-L, PA14 and PAO1-L mutants using LESA-MS 230

Chapter 6. General Conclusions and Future Directions 243

Bibliography 250

Annexes 292

A1.1. Synergistic effects of GP QS-inhibiting compounds in PAO1-L CTX::P_{Km}-*luxCDABE* after double exposure 292
A1.2. Synergistic effects of GP QS-inhibiting compounds in PAO1-L after triple exposure 295
A1.3. Synergistic effects of GP QS-inhibiting compounds in PAO1-L after quadruple exposure 299
A1.4. Synergistic effects of GP QS-inhibiting compounds in PA14 302
A1.5. Synergistic effects in PAO1-N *lecA/lecB* after triple exposure 303
A1.6. Effect of mixtures of GP QSIs on pyocyanin production 305

A1.7. Ligand receptor binding and docking affinity of the GP QSIs to the PqsR protein …….. 306

List of Figures

Chapter 1. Introduction

Figure 1.1. *Pseudomonas aeruginosa* AHL quorum sensing signalling hierarchy 18

Figure 1.2. *Pseudomonas aeruginosa* PQS biosynthesis 21

Figure 1.3. Overview of some of the non-antibiotic approaches currently being developed to treat PA infections 34

Figure 1.4. Crystal Structure of the PqsRCBD 47

Chapter 2. Materials and Methods

Figure 2.1. Molecular structures of compounds used 80

Figure 2.2. Prosolia cell culture Omni slide™ 87

Chapter 3. Highthroughput screening for identifying novel potent PqsR inhibitors

Figure 3.1. Process of preliminary highthroughput screening 106

Figure 3.2. Summary of bioluminescence results in PAO1-L CTX*::*P_{pqsA}-*luxCDABE* exposed to the 15 GreenPharma PqsR inhibitory compounds 110

Figure 3.3. Summary of bioluminescence in PAO1-L CTX*::*P_{Km}-*luxCDABE* exposed to 15 putative GreenPharma Quorum sensing inhibiting compounds 111

Figure 3.4. Biofilm production by PAO1-L::mCherry exposed to 2% DMSO 128

Figure 3.5. Biofilm production by PAO1-L::mCherry exposed to 395 nM GPZ002966 128

Figure 3.6. Biofilm production by PAO1-L::mCherry exposed to 88 nM GPZ004927 129

Figure 3.7. Biofilm production by PAO1-L::mCherry exposed to 70 nM GPZ824390 129

Figure 3.8. Biofilm production by PAO1-L::mCherry exposed to 55 nM GPZ273902 130

Figure 3.9. Effect of a range of concentrations of GP QS-inhibitor GPZ273902 on biofilm biomass (left) and surface area (right) of a PAO1-L::mCherry biofilm 131

Figure 3.10. Effect of a log curve of concentrations of GP QS-inhibitor GPZ273902 on biofilm biomass (left) and surface area (right) of PAO1-L::mCherry 132

Figure 3.11. Effect of a range of concentrations of GP QS-inhibitor GPZ824390 on biofilm biomass (left) and surface area (right) of PAO1-L::mCherry 133

Figure 3.12. Effect of a log curve of concentrations of GP QS-inhibitor GPZ273902 on biofilm biomass (left) and surface area (right) of PAO1-L::mCherry 134

Figure 3.13. Effect of GP PqsR inhibitors on AQ molecules in PAO1-N 137

Figure 3.14. Effect of GP PqsR inhibitors on AQ molecules in PA14 137

Figure 3.15. Fluorescence of Jurkat cells at different DMSO concentrations 139

Figure 3.16. Fluorescence of Jurkat cells at different DMSO concentrations after 1 hour incubation with Alamar Blue 141

Figure 3.17. Fluorescence generated by exposure to GPZ002966 incubation with Alamar Blue 142

Figure 3.18a. Summary of structure and inhibition kinetics of the top four PA QSI candidates 148

Figure 3.18b. Perspective views representative of the binding between the best QSI molecules and the PqsR protein 149

Figure 3.19. Lowest IC_{50} scores for the top 4 PA QS inhibiting candidate molecules 150

Chapter 4. Engineering of a *pqsA-pqsR lux*-based biosensor in *E. coli*

Figure 4.1. Overview of the engineered PQS-based biosensor 176

Figure 4.2. Functional elements of the integrated heterologous AQ-based biosensor reporter 177

Figure 4.3. Cloning of the *pqsA* promoter (P_{pqsA}) in pBluescript to produce pIL001 179

Figure 4.4. Construction of pIL002 180

Figure 4.5. Construction of pIL003 181

Figure 4.6. – Control digestions to intermediate plasmids towards pIL005 182

Figure 4.7. – Linear plasmid map of pIL004 183

Figure 4.8 – Linear map of plasmid pIL005 184

Figure 4.9. - Verification of successful chromosomal integration of the mini-Tn7 biosensor element in ECIL02 185

Figure 4.10. - Verification of successful chromosomal integration in ECIL02 (fusion between transposition elements) 186

Figure 4.11. - Bioluminescence production in PAIL001 [PAO1-N *ΔpqsA ΔpqsR* miniTn*7, lacI*^{q}, P_{tac}-*pqsR*, P_{pqsA}-*luxCDABE*] 190

Figure 4.12. - Bioluminescence production in PAIL001 [PAO1-N *ΔpqsA ΔpqsR* miniTn*7, lacI*^{Q}, P_{tac}-*pqsR*, P_{pqsA}-*luxCDABE*] 192

Figure 4.13 - Bioluminescence production in PAIL003 [PAO1-N *ΔlasR miniTn7, lacI*^{Q}, P_{tac}-*pqsR*, P_{pqsA}-*luxCDABE*] 194

Figure 4.14 - Bioluminescence production in PAIL004 [PAO1-N *ΔrhlR miniTn7, lacI*^{Q}, P_{tac}-*pqsR*, P_{pqsA}-*luxCDABE*] under varying IPTG and C_7-PQS conditions 196

Figure 4.15. - Bioluminescence production in PAIL004 [PAO1-N *ΔrhlR miniTn7, lacI*^{Q}, P_{tac}-*pqsR*, P_{pqsA}-*luxCDABE*] after overnight exposure to 1 mM IPTG 198

Figure 4.16. - Bioluminescence production in *E. coli S17-λ1pir* pUC18R6K miniTn7T::pIL007 (P_{pqsA}-*luxCDABE*, *lacI*^{Q}, P_{tac}-*pqsR)* 202

Figure 4.17. - Bioluminescence production in *E. coli S17-λ1pir* pUC18R6K miniTn7T::pIL008 (P_{pqsA}-*luxCDABE*, *lacI*^{Q}, *Em7-pqsR)* 203

Chapter 5. Optimisation of liquid extraction surface analysis (LESA) as a new methodology for rapid screening of quorum sensing moelecules in *ex vivo* PA bacterial extracts

Figure 5.1. Composing parts of the Advion Mode 3 LESA® Triversa NanoMate bioanalyser 220

Figure 5.2. Advion Electrospray Injection Mode 1 221

Figure 5.3. Injection tips, sampling plate and culture slide 221

Figure 5.4. Standard mixture calibration curve using 80% LB plus 20% methanol sample 226

Figure 5.5. Standard mixture calibration curve using a 100% methanol sample 226

Figure 5.6. Effect of solvent composition in LESA extractions of a standard calibration mixture at a concentration of 80 µM 228

Figure 5.7. Standard mixture calibration curve in LB medium 232

Figure 5.8. Standard mixture calibration curve in M9 medium 232

Figure 5.9. Re-extractions of a 10 µM standard calibration mixture in 100% methanol 237

Figure 5.10. Liquid extraction surface analysis of PAO1-L wild-type and mutant strains 239

List of Tables

Chapter 1. Introduction

Table 1.1. Major virulence factors in PA and associated induced virulence mechanism 7

Table 1.2. List of some revelant non-antibiotic approaches developed against MDR PA over the past two decades 35

Table 1.3. List of selected inhibitors identified to interact with LasR ligand binding site of PA QS receptors 49

Table 1.4. List of selected inhibitors identified to interact with RhlR ligand binding site of PA QS receptors 52

Chapter 2. Material and Methods

Table 2.1. List of bacterial strains 55

Table 2.2. List of plasmids 56

Table 2.3. Oligonucleotide primers used in this study 58

Table 2.4. List of individual analytes, and their precursor and product ions, used to set up the LC-MS analysis 73

Table 2.5. List of compounds and respective analytical ionic specificities 79

Chapter 3. Highthroughput screening for identifying novel potent PqsR inhibitors

Table 3.1. List of selected inhibitors identified to interact with PqsR ligand binding site of PA QS receptors 100

Table 3.2. Summary of bioluminescence in PAO1-L CTX::P_{pqsA}/P_{Km}-*luxCDABE* after individual exposure to 15 GreenPharma compounds 108

Table 3.3. Summary of IC_{50} scores in PAO1-L/PA14 CTX::P_{pqsA}-*luxCDABE* 109

Table 3.4. Summary of compound synergistic effects in PAO1-L CTX::P_{pqsA}-*luxCDABE* after double exposure (vertical columns combined with horizontal column) 113

Table 3.5. Summary of bioluminescence in PAO1-N *CTX*::P_{lecA}-*luxCDABE* after individual exposure to pre-selected *pqsA*-inhbiting GreenPharma compounds 118
Table 3.6. Summary of bioluminescence in PAO1-N *CTX*::P_{lecB}-*luxCDABE* after individual exposure to selected GreenPharma compounds 119
Table 3.7. Summary of percentage of remaining activity of *lecA* after double combinatory exposures to selected GreenPharma inhibitors 121
Table 3.8. Summary of percentage of remaining activity of *lecB* after double combinatory exposures to selected GreenPharma inhibitors 123
Table 3.9. Effect of GP QS-inhibiting compounds on pyocyanin production 125
Table 3.10. Summary of biomass and surface area in biofilms exposed to the top 4 PqsR inhibitors 127
Table 3.11. Cytotoxicity of GPZ824390 tested against T-lymphocyte Jurkat cells 144
Table 3.12. Cytotoxicity of GPZ273902 tested against T-lymphocyte Jurkat cells 145
Table 3.13. Cytotoxicity of GPZ004927 tested against T-lymphocyte Jurkat cells 146
Table 3.14. Cytotoxicity of GPZ002966 tested against T-lymphocyte Jurkat cells 147
Table 3.15. Summary of QSI profiles of the top four GP candidate compounds studied 151

Chapter 4. Engineering of a *pqsA-pqsR lux*-based biosensor in *E. coli*

Table 4.1. – Summary of luminescence scores generated by the different mutant strains carrying the PQS−based biosensor 188

Chapter 5. Optimisation of liquid extraction surface analysis (LESA) as a new methodology for rapid screening of quorum sensing moelecules in *ex vivo* PA bacterial extracts

Table 5.1. Average MS response (NL counts) of QS molecules produced at two different solvent mixtures 224

Table 5.2. Summary of standards mixture calibration curves and minimum limit of detection by means of LESA-MS 225

Table 5.3. Summary of LOD and LOQ for standard mixture calibration solutions in LB and M9 media 233

Abbreviations

2-AA - 2-amino acetophenone

ABS – Activation binding site

ACP – Acyl carrier protein

AHL – Acyl homoserine lactones

AI - Autoinducer

AQNO - 2-alkyl-4-hydroxyquinoline *N*-oxide

AQ – Alkyl quinolone

Ap - Ampillicin

AMR – Antimicrobial drug resistance

AprA - Alkaline protease

BSA - Bovine serum albumin (BSA)

C9-PQS - 2-nonyl-3-hydroxy-4-quinolone

CAS - Chrome azurol S

Cb - Carbenicillin

CE – Collision energy

CF – Cystic fibrosis

CBD – Co-inducer binding domain

DHQ – 2,4-dihydroxyquinoline

eDNA – Extracellular DNA

EEA - European Economic Area

EGCG - epigallocatechin gallate

ESI – Electrospray ionisation mass-spectrometry

FabH - β-ketoacyl-ACP synthase

FAD - Flavin adenine dinucleotide

HAQ - 4-hydroxy-2-alkylquinoline

HHQ - 2-heptyl-4-quinolone

HQNO - 2-heptyl-4-hydroxyquinoline *N*-oxide

Kc - Kanamycin

K_D - Equilibrium dissociation constant

KHL - Keyhole limpet hemocyanin

MRSA - Methicillin-resistant *Staphylococcus aureus*

MDR – Multi drug resistance

MIC - Minimum inhibitory concentration

MS – Mass spectrometer

LB – Luria Bertani

LC – Liquid chromatography

LPS - Lipopolysaccharide

LTTRs - LysR family of transcriptional regulators

MPD - 2-methyl-2,4-pentanediol

MPQS - 3-hydroxy-2-methyl-4(1H)- quinolone

MS - Mass spectrometry

NHQ - 2-nonyl-4-hydroxyquinoline

NQNO - 2-nonyl-4-hydroxyquinoline *N*-oxide

PA – *Pseudomonas aeruginosa*

PA-IL – Galactophilic lectin LecA

PA-IIL – Fucose-specific lectin LecB

PBS – Phosphate buffered saline

PCN - Pyocyanin

PQS – *Pseudomonas* quinolone signal (2-heptyl-3-hydroxy-4(1*H*)-quinolone)

QQ – Quorum quenching

QS – Quorum sensing

QscR - Quorum-sensing control repressor

QSI – Quorum sensing inhibitors

QSSM - Quorum sensing signalling molecules

QZN – Quinazolinone

RBS – Regulatory binding site

RCF - Relative centrifugal force

SAR – Structure activity relationship

sRNA – Small ribonucleic acid

SB-VS - Structure-based virtual screening

SCV - Small colony variant

Sm – Streptomycin

Sp - Spectinomycin

SP – Surfactant proteins

Tc - Tetracycline

UHQ - 2-undecyl-4-hydroxyquinoline

UK – United Kingdom

UTR - Untranslated region

UQNO - 2-undecyl-4-hydroxyquinoline *N*-oxide

USA – United States of America

This thesis abides to the Vancouver style of referencing.

Abstract

Pseudomonas aeruginosa (PA), a Gram-negative opportunistic rod with ubiquitous presence in a panoply of different environments, secretes a wide array of virulence determinants that have established it as one of the leading nosocomial pathogens. Many of these virulence factors are regulated by the quorum sensing (QS) system that responds to environmental cell density variations. PA can ultimately trigger the onset of severe acute and chronic infections, especially in immunosuppressed subjects.

The QS network in PA is comprised of at least four multi-layered interconnected subsystems with hierarchical organisation. From these, three (las, rhl and pqs) play a pivotal role in the production of virulence factors (e.g., lectins and pyocyanin) with relevant participation in the development and maintenance of biofilm matrices. The QS network is divided in two major signaling pathways, the one driven by N-acylhomoserine lactone signals and the one driven by 2-alkyl-4-quinolone molecules. Two alkyl quinolones of core importance exist in PA, the 2-heptyl-3-hydroxy-4(1H)quinolone, typically recognised as the "*Pseudomonas* quinolone signal" (PQS) and its precursor 2-heptyl-4(1H)-quinolone (HHQ). In addition to the regulatory involvement of the *las* and *rhl* quorum sensing systems, the biosynthesis of PQS production is also positively regulated by PqsR-dependent transcription of the *pqsABCDE* operon (a multivirulence factor regulator also known as MvfR). For that reason, the alkyl quinolone (AQ) signalling pathway, and more specifically its major regulator PqsR, are widely seen as promising targets for novel antimicrobial approaches.

Because of the growing presence of multidrug resistant PA in the clinical setting, representing both an immediate menace to immunocompromised patients and a heavy burden on hospital budgets, the development of more

rapid and affordable screening strategies for detection of the pathogen are required. Thus, new screening strategies adapted to clinical samples and successful novel synthetic small PqsR antagonists can lead the way to a new Era in the battle against hyper-virulent/-resistant PA strains.

Primarily focusing on the AQ system, this research project investigated three inter-related areas, namely: (a) the highthroughput screening of novel synthetic small molecule antagonists of the PqsR protein, designed for suppression of virulence-associated phenotypes, (b) the development of a luminescent PQS-based screening bioreporter to be applied in the clinical setting, and finally (c) the optimisation of a methodology combining liquid extraction surface analysis (LESA) and mass spectrometry (MS) for screening PQS-related AQs from *in vivo* bacterial extracts, and also intended for future screening of a variety of clinical samples (e.g., blood plasma, urine and saliva).

A large number of synthetic small molecules with putative PqsR antagonism were obtained from our French partner GreenPharma, and studied for their capacity to interfere with expression of the key player of the pqs system, PqsR. By applying a rational selection strategy, based on the inhibitory effects on *pqsA* expression, assessment of metabolical exertion, and assay studies on the ultimate repression of key virulence-associated phenotypes (lectins LecA and LecB, pyocyanin, PQS-associated AQs) and impact on biolfilm formation, a final selection comprised of the four best antagonists was obtained. Compounds GPZ002966, GPZ004927, GPZ824390 and GPZ273902 had their cytotoxicity subsequently studied keeping in mind their applicability in pre-clinical studies.

Overall, these PqsR antagonists promoted very strong inhibition of *pqsA* and *lecA* expression, strongly reduced production of pyocyanin and PQS-related AQs (HHQ, HQNO and C_7-PQS itself), showed a strong degree of biofilm inhibition, with IC_{50} scores sitting at the nanomolar level, and no signs of metabolical arrest was reported by the test strains used. Some explanations,

focusing on the functional and structural organisation/composition of these compounds are also offered based on a comparative analysis against a number of the most prolific PqsR antagonists recently developed.

The bioluminescent PQS-based biosensor for the detection of PA was engineered to respond to the presence of exogenous PQS that forms a complex with the regulatory PqsR protein, ultimately stimulating the expression of a *luxCDABE*-fused *pqsA* promoter. The biosensor was subsequently inserted in a non-pathogenic *E. coli* recipient by means of chromosomal integration, devoid of the *sdiA* LuxR homolog that could potentially interfere with the recognition of PqsR. A silent reporter was observed when in *E. coli*, but further assessments to its genetic integrity did not reveal any single nucleotide polymorphisms (SNP). In addition, after further testings to its activity in different established PA mutants, devoid of genes that constituted the bioreporting system or to it directly associated, a fully functional bioreporter was confirmed. Finally, a few possible explanations as to what might be in the origin of a defective bioreporter in *E. coli* are discussed.

Lastly, a new LESA-MS protocol based on the surface sampling of dried bacterial extracts, envisaging its potentialities as a rapid and cheap screening method for detection of AQs, was designed and optimised. Even though the method has been widely used in a variety of research scenarios, this is the first time LESA-MS is applied as a screening methodology in the context of bacterial extract screening. Overall, the optimisation process showed that LESA-MS is an approach with numerous potentialities and immediate advantages, where one emphasises sampling simplicity, fast delivering of results, sensitivity to AQs at the nanomolar level (especially for C_7-PQS and the precursor HHQ). But simultaneously, this methodology also revealed limitations inherent to its setting up that constrain an effective screening. The most emphatic ones being the volatility of the preparations to intra-sampling variability, and to a certain degree, an unexpected insensitivity to important QS N-acyl homoserine lactones (AHLs), namely C_4-HSL and 3-oxo-C_{12}-HSL. Nevertheless, such

limitations do not present themselves as an insurmountable barrier, and based on results from available studies making use of the LESA-MS a number of possibilities to work around these are also presented.

Chapter 1 - Introduction

1. *Pseudomonas aeruginosa*

PA is a ubiquitous Gram-negative aerobic bacillus frequently associated with nosocomial infections. As a highly versatile organism it is adapted to survive in a widespread variety of environmental conditions ranging from animals to water and soil. This opportunistic pathogen generally infects those individuals with impaired mucosal defences, severely burned and immunocompromised. Patients with compromised immune systems typically present neutropenia and hence are prone to infection. This is the case for hospitalised patients subjected to iatrogenic procedures, such as, invasive intravenous cannulas, urinary catheters, or even endotracheal tubes (1).

Hence, PA is considered as one of the most challenging Gram-negative bacteria in modern hospital environments, and has been the lead cause of mortality in those dwelling with severe respiratory infections such as chronic lung infections in cystic fibrosis (CF) patients (2) (3).

PA also has a high genomic plasticity which has resulted in the emergence of strains with increased levels of resistance to multiple antibiotics (4). Outbreaks of multi-resistant PA have been reported in hospital settings (5). This organism also produces a large armoury of virulence factors (6) including proteases, lipases, exotoxins (7) and secondary metabolites (e.g. cyanide) (8) which are released in response to changes in population densities and environmental signals. PA uses a biofilm mode of growth during chronic infections, making it more difficult to eradicate by both host defences and antibiotic treatment (9) (10).

1.1. *P. aeruginosa* as a nosocomial threat and a financial burden

With the increasing numbers of hospitalised patients, nosocomial infections have been a strong promoter of morbidity and mortality over the last decades. As one of the most common Gram-negative nosocomial bacterium, especially in the intensive care units of Europe and the USA (11, 12), PA represents a high health risk putting serious financial pressure onto health services. At the beginning of the millennium and in the UK alone, PA affected an estimated 10,000 cases each year (13, 14).

The pathogen was identified as the sixth most frequently occurring one, second in ventilator-associated pneumonia and seventh commonest reason for catheter-related bloodstream infection (NHSN) (15). Sepsis originated by PA bloodstream infections has been reported to result in more than 20% death cases, especially among those inappropriately medicated with an initial course of antimicrobial drugs (16).

Many studies demonstrate that an inefficient antimicrobial approach to eradicating PA bloodstream infection in hospitals is linked to enhanced mortality (17-19). However, it is also known that altering antimicrobial treatment after an initial outburst, by applying a more adequate therapy regimen, is frequently inefficient. The initial antimicrobial drug treatment approach is the key step to drastically improve statistical data on mortality associated to nosocomial PA (20).

1.2. *P. aeruginosa* virulence

Bacterial virulence factors are traits produced by bacteria which contribute to the pathogenicity of the organism. They can be present on the surface of the bacteria or be secreted and their production is tightly controlled. Virulence factors play important roles in bacterial survival aiding colonisation

and the successful establishment of the infection. Two main types of virulence factors in PA are known (Table 1.1), those participating in the onset of acute infections (such as those secreted by Type II and III secretion systems) (21), and those mainly involved in the development of chronic infections like the ones driving biofilm formation. Due to their importance in establishing the level of pathogenicity of different bacteria, virulence factors are seen as crucial targets for novel antimicrobial therapeutic strategies.

The biological roles of the most important virulence factors produced by PA are described in the following sections.

Table 1.1. Major virulence factors in PA and associated induced virulence mechanism.

Virulence Factor	Biochemical definition	Induced virulence mechanism
Alginate	Polysaccharide	Protects bacteria from environmental adversities due to its mucoid properties (22); increases bonding to solid surfaces (23); promotes resistance to phagocytosis and antibiotics (10)
Alkaline protease (AprA)	Proteolytic enzyme	Participates in the disruption of complement-mediated lysis of erythrocytes; blocks complement-dependent neutrophil functions (24); important role in the cornea infection (25)
Elastases (LasA and LasB)	LasA is an extracellular protease LasB is an elastase	Cause haemorraghing and tissue necrosis (25); participate in the degradation of elastin in tissues (26)
Exotoxin A (ToxA)	Extracellular enzyme	Binds to specific receptors on animal cells allowing endocytosis of the toxin (27); promotes apoptosis and tissue necrosis (28)
Exoenzyme S	Extracellular ADP-ribosyltransferase Type III secretion effector	Antiphagocytic factor, disrupts the cytoskeleton (29); destroys

		immunoglobulin A and G, drives to depolymerisation of actin filaments (30); inhibits elongation factor-2 (31)
Exoenzyme U	Phospholipase	Antiphagocytic; causes lesions to the epithelial cells (29); responsible for bacterimia towards septic shock (32)
Flagella	Flagellin filaments	Responsible for motility and chemotaxis (33); ligand for clearance by phagocytic cells (34)
Lectins	Soluble lectins	Induce respiratory pathogenicity by inhibiting ciliary beating (35); involved in acute and chronic lung infections (36); promote biofilm formation (37)
Lipopolysaccharide (LPS)	Lipoglycan and endotoxin	Mediates host responses to infection (38); induces production of cytokines (39); promotes shock (40)
Pili	Appendage for bacterial conjugation	Adherence to respiratory epithelia to facilitate respiratory infection (41); mecanochemical regulation of virulence factors (42)
Phospholipase C	Heat-hemolysin	Local cytolysis effects (43); pulmonary atelectasis (44); participates in acute and chronic infection (45); supresses neutrophil respiratory activity (46)
Pyocyanin	Phenazine	Targets multiple cellular functions contributing to acute and chronic infections; causes tissue damage by endogenous proteases (47); suppresses lymphocyte proliferation (48); inactivates protease inhibitors; damages epithelial cells due to production of hydroxyl radicals (49);
Pyoverdin and Pyochelin	Major siderophores	Pyoverdin starts a signaling cascade responsible for

		generating several virulence factors, including exotoxin A (ToxA) (50); Pyochelin stimulates the persistence of avirulent bacteria and increase lethality associated to virulent bacteria by promoting their growth (51)
Rhamnolipids	Glycolipids	Surfactant hydrolysis (52); disrupt epithelia and promote paracellular invasion (53)

1.2.1. Pyocyanin

Pyocyanin (PCN) (5-*N*-methyl-1-hydroxyphenazine) is a phenazine redox-active secondary metabolite that is responsible for the blue/green coloration of PA. PCN can penetrate biological membranes and is toxic to bacterial and eukaryotic cells as it generates reactive oxygen intermediates (54). It is present in large quantities in sputum and ear secretion samples of CF patients infected by PA. Hence it has been valuable as an indicative infection marker for PA infection. *In vitro* studies have shown that PCN is involved in the interference with multiple cellular functions, such as suppression of lymphocyte proliferation (55), damaging of epithelial cells as a result of hydroxyl radical formation (56) (57), inactivation of protease inhibitors (49), overexpression of airway mucins in mice (58), induction of IL-8 secretion and mRNA expression in PMA-differentiated U937 cells (59) and disruption of eukaryotic cellular pathways (60). PCN is thus one of the major virulence factors in this pathogen, with involvement in both acute and chronic infections.

PCN is synthesised through modification of chorismic acid to phenazine-1-carboxylic acid using a number of steps involving the products of the *phzABCDEFG1* and *phzABCDEFG2* operons. Further modification of this

precursor by the *phzM* and *phzS* gene products results in the generation of PCN (Mavrodi, Bonsall (61)).

PCN can also work as a signal molecule during the stationary growth phase (62). The PCN stimulon comprises different genes including those coding for the *mexGHI-opmD* efflux pump and the monooxygenase gene PA2274, as well as genes involved in iron-acquisition (63).

1.2.2. Exoproteases

PA produces multiple exoproteases including LasA, LasB, alkaline protease encoded by *aprA* and Protease IV (encoded by *piv*) which are key for tissue invasion and the survival of this organism during infection (64) (65).

1.2.2.1. Elastases A and B

Elastase A or staphylolysin (LasA) is a 20 kDa extracellular zinc metalloprotease (66) and one of the most profuse of the PA-secreted endopeptidases. After being produced, LasA is secreted alongside its 40 KDa propeptide by means of the Xcp (type II) machinery (67) (68) becoming an active agent only when present in the extracellular environment.

Both exoproteases LasA and LasB are reported as key players in invasion for some PA strains (69) (70) (66) (71). There are a few substancial differences between metabolism and activity of these two elastases, but one of the most relevant ones is that, contrarily to LasB, the LasA propetide does not undergo autoproteolysis (72), ultimately being processed by endopeptidases (LasB and LysC) and protease IV (73) (74). Additionally, LasA participates in enhancing LasB elastolytic capacity (by promoting conformational changes in elastase) and is a virulence effector on epithelial cells (75). In fact, *in vitro* inactivation of

either LasA or LasB vastly reduces the ability of PA to infect epithelial cells, as it has been suggested that these two elastases are somehow involved in the toxic role of ExoS and ExoT, thus resulting in a decrease in invasive potential by PA colonies (71).

In terms of specificity functions, LasA has low elastolytic and high staphylolytic activities, also breaking a broad spectrum of glycine-containing proteins, including the human leukocyte and neutrophil elastases (26) (66).

1.2.2.2. Protease IV

Protease IV is a 26 kDa iron-regulated serine protease and lysyl endopeptidase observed in PA extracts (76) that is produced intracellularly in the shape of a 48 KDa pre-proenzyme. Protease IV is thought to be secreted by the type II secretion machinery and translocated across the outermembrane, at least when expressed in *Pseudomonas putida* (77).

Protease IV is known to degrade important host proteins such as the glycoprotein fibrinogen, that intervenes in the formation of blood clots resulting in haemorrhaging, plasminogen and immunoglobulin G (76) (78).

Just as with elastase B, protease IV is also capable of degrading a range of surfactant proteins (SP), like the SP-A/B/D (79) and damage SP-B in bronchoalveolar lavage fluid devoid of cells. Indeed, SP-D plays a role in the inflammation of the cornea of the eye (keratitis) (80).

1.2.2.3. Alkaline protease (AprA)

The alkaline protease (AprA), also named aeruginolysin, is one of the PA secreted zinc-dependent metalloproteinases with endopeptidase functions

that is encoded by the *aprA* gene. AprA has been shown to metabolise *in vitro* a wide range of substrates including laminin from the basal lamina of the epithelia. Laminin degradation enables PA to penetrate into deeper tissues causing tissue damage and necrosis.

LasB and AprA act together in PA infections, for example through the inactivation of γ-interferon (81), resulting in the onset of autoimmune diseases, and the degradation of factor-α (82), deregulation of the immune system enabling systemic inflammation. In addition, they can interfere with the neutrophil functions (83) allowing the pathogen to evade phagocytic surveillance by reducing the phagocytic activity of leukocytes (84). They can also cleave surface receptors that will ultimately repress the complex established by effector and targeted cell (85), and can impact on the normal human lymphocyte functioning by degrading IL-2.

1.2.3. Rhamnolipids

PA secretes glycolipid surfactants that contain rhamnose, known as rhamnolipids. Their production relies on several metabolic pathways such as those involving the biosynthesis of fatty acids and the alginate exopolyssacharide (86).

PA grown *in vitro* is known to secrete two main types of rhamnolipids (87): rhamnosil-β-hydroxidecanoil-β-hydroxydecanoate (also known as mono-rhamnolipid) and rhamnosyl-rhamnosyl-β-hydroxydecanoyl-β-hydroxydecanoate (also known as di-rhamnolipid) (88).

Even though the full role played by rhamnolipids is still to be completely unveiled, they are virulence factors *per se* (89), have antimicrobial activity (90), are involved in biofilm formation and in particular the generation of water channels (91), and are essential for swarming motility (92) (93).

1.2.4. Type IV pili

Type IV pili are extracellular structures involved with several functions including twitching motility, docking onto host cells (94), cellular aggregation in biofilms (95), phage transduction, and uptake of genetic material. The type IV pili subunits (pilins) are produced from their precursors prepilins by enzymatic cleavage (peptidase encoded by the *pilD* gene) of the hydrophilic peptide. Regarding the length of their final mature protein and leader peptide, these can be grouped into two classifications: Type IVa and Type IVb.

In PA type IV pili production is regulated by a range of signalling molecules, including cAMP and c-di-GMP (96) (97).

1.2.5. Flagella

PA flagella are highly complex motility organelles important for the establishment of respiratory tract infections. Flagella play a key role in virulence as they are not only involved in motility but also have a highly immunogenic nature (98). Together with eDNA and type IV pili they are also involved in the formation of biofilm mushrooms under certain growth conditions (99) (100). In addition, both flagella and type IV pili have also been shown to play a role in the dispersal of mature biofilms (101). Flagella deficient PA are less invasive in a mouse burn infection model (102).

1.2.6. Lectins

PA synthesises two surface associated lectins LecA and LecB (formerly known as PA-IL and PA-IIL respectively) (36).

LecA is a homotetrameric cytotoxic lectin expressed by PA in biofilms and has high affinity for galactosides. LecA causes permeability defects in the intestinal epithelium, resulting in increased absorption of exotoxin A. It also plays an important role in the adhesion of PA to enteral epithelial cells (gut-derived sepsis in mice) (103). Expression of the *lecA* gene can be induced by the presence of interferon-γ enabling PA to recognise changes in the host immune system (104).

LecB is a 11.73 kDa protein also present as a homotetramer (105) with high specificity for L-fucose and its derivatives (Gilboa-Garber et al., 2000; Garber et al., 1987), and lower affinity for D-mannose. The protein is abundant in the bacterial outer-membrane fraction and has been reported to reduce, *in vitro*, the ciliary beat frequency of the airway epithelium resulting in the interference with human lung defences (106, 107) and to be involved in pilus biogenesis and protease IV activity (108) contributing significantly towards chronic respiratory PA infections (36).

LecA and LecB have been reported to contribute to biofilm development in *PA*. LecA has also been shown to play an important role in biofilm formation in PA (109) (37). Addition of exogenous sugars specific for LecA or LecB either free or bound to a glycopeptide dendrimer inhibited biofilm formation (109) (110) (111).

1.2.7. Biofilm determinants

PA produces three major exopolysaccharides psl, pel and alginate, however mainly psl and pel have been found to play a key role in biofilm formation (112) (113) (114) (115).

1.2.7.1. Pel

Pel is an exopolysaccharide composed of cationic aminoacid sugars secreted by PA. The relevance of Pel in the production of competent biofilms depends on the strain. Pel operates as a structural skeleton in biofilm matrixes by preserving intercellular interactions in PA14 biofilm complexes and by increasing resistance to aminoglycoside antibiotics in biofilms (116). On the other hand, in biofilms of the common lab strain PAO1, Pel can be found cooperating with different types of exopolysaccharydes, but does not assume in this strain the primary role assumed by Psl (117) (116) (115).

Pellicle-deficient mutants lack on the trigger for biofilm formation and adherence power between clusters of cells to a surface (118) and resistance to some aminoglycoside antibiotics (116). On the other hand, an overexpression of Pel is related to wrinkle-type colony phenotypes (119).

1.2.7.2. Psl

The exopolysaccharide Psl is a cellulose-like polymer, rich in galactose and mannose, with fairly reduced levels of glucose and xylose in its composition, with known role in biofilm surface attachment and formation of small colonies. This exoproduct is secreted as planktonic development occurs, mediating attachment to surfaces and contributing to microcolony formation (120) (114). The Psl agglomerate responsible for the synthesis of Psl comprises fifteen genes (from *pslA* to *pslO* and also PA2231-2245), but only part of the cluster (11 of the 15 genes to be more precise) are actually necessary for Psl production in Psl-dependent matrices (121). In PA14 *pslA*- and *pslD*- deletions result in absence of Psl polysaccharide and compromised biofilms (122). Finally, in fully developed biofilms, Psl is linked to the formation of mushroom-like microcolonies, with an additional outlying 'web' covering the cap region (123) (114).

1.2.7.3. Extracellular DNA (eDNA)

Extracellular DNA (eDNA) has been shown to have an involvement in biofilm matrix sustainability (124) (125).

This eDNA is made of random chromosomal DNA, constituting yet another pivotal interconnecting element in PA biofilm matrix and cell-to-cell interactions (126) (124) (125). It is mostly visible in the stalk portion of microcolonies and spatially distant from Psl, where Psl sits on the sideline of the biofilm and eDNA in 'all' remaining space where Psl is not found (114). Degradation of eDNA by DNase treatment in early stages of biofilm formation interferes with the maturation of the biofilm matrix but does not affect the overall biofilm architecture (126). The presence of eDNA in biofilm matrices has been observed not only in lab strains but also in clinical isolates Whitchurch et al (2002) (126).

1.3. Role of quorum sensing in the virulence of *P. aeruginosa*

Quorum sensing (QS) is widely described in bacteria and responsible for controlling multiple gene expression in a population-dependent manner, using small signal molecules also known as autoinducers. PA produces two main families of QS signal molecules (QSSM): *N*-acylhomoserine lactones (AHLs) and alkylquinolones (AQs).

1.3.1. *N*-acylhomoserine lactone quorum sensing signalling

The first QS systems described in PA are those driven by AHLs (figure 1.1). There are two AHL QS interrelated systems in this organism. The first of these, known as the *las* system, uses as a cognate signal molecule *N*-(3-oxododecanoyl)-L-homoserine lactone (3-oxo-C_{12}-HSL) synthesized by LasI

which upon binding to the transcriptional regulator LasR triggers the expression of multiple virulence genes including those coding for elastase (*lasB*), pyoverdin, exotoxins etc. In turn, activated LasR is also capable of activating the second AHL-driven QS system, known as the *rhl* system. The *rhl* system uses the *N*-butanoyl-L-homoserine lactone (C_4-HSL) synthesised by RhlI which binds to the transcriptional regulator RhlR activating it. Activated RhlR switches on the expression of a wide range of virulence genes, including *lecA* and *lecB* lectins, the rhamnolipid biosynthetic genes *rhlAB*, the genes responsible for pyocyanin production, etc.

It is widely recognised that PA AHLs are vital for the success of the infection process in a range of hosts and human tissues (127). PA mutants in *lasI*, *lasR* and *rhlR* showed reduced virulence in keratitis mice models (128) (129), in mice lung infection models upon intratracheal PA infection that resulted in the presence of AHLs in severely compromised lung tissue (130), in urinary tract C_4-HSL and 3-oxo-C_{12}-HSL negative isolates (131) in mouse models of burn wound infection and pneumonia, and recently in a more indirect pathogenic regulation by increasing lethality in the slow-killing nematode model *Caenorhabditis elegans* (132) (133), just to name a few from a vast list.

Even though the QS *las* and *rhl* systems operate in parallel, there are partial mutation studies where one of the effectors has been silenced, revealing an increadible feature by this versatile network - the vicarious functioning of the *lasR/rhlR* regulation (134) with impact on the production of virulence factors, such as PCN (135), elastase and rhamnolipid production (136).

Most QS *luxR* homologue genes are located adjacent to their cognate *luxI* homologues but in certain instances these genes are not directly linked to a cognate *luxI*-type gene and their gene products have been named as LuxR orphans or LuxR solos (137) (138). PA has one of these in its genome which has been named QscR (139) and modulates the *las* and *rhl* QS circuits, although it also has its own regulon (140).

Interestingly, Fuqua (2006) (141) states that both QscR and RhlR are under the spell of the LasR regulator as the genetic expression of *rhlR* expression is activated by LasR, and LasI activates QscR. On the other hand, QscR influences negatively the *rhl* and the *las* systems (142).

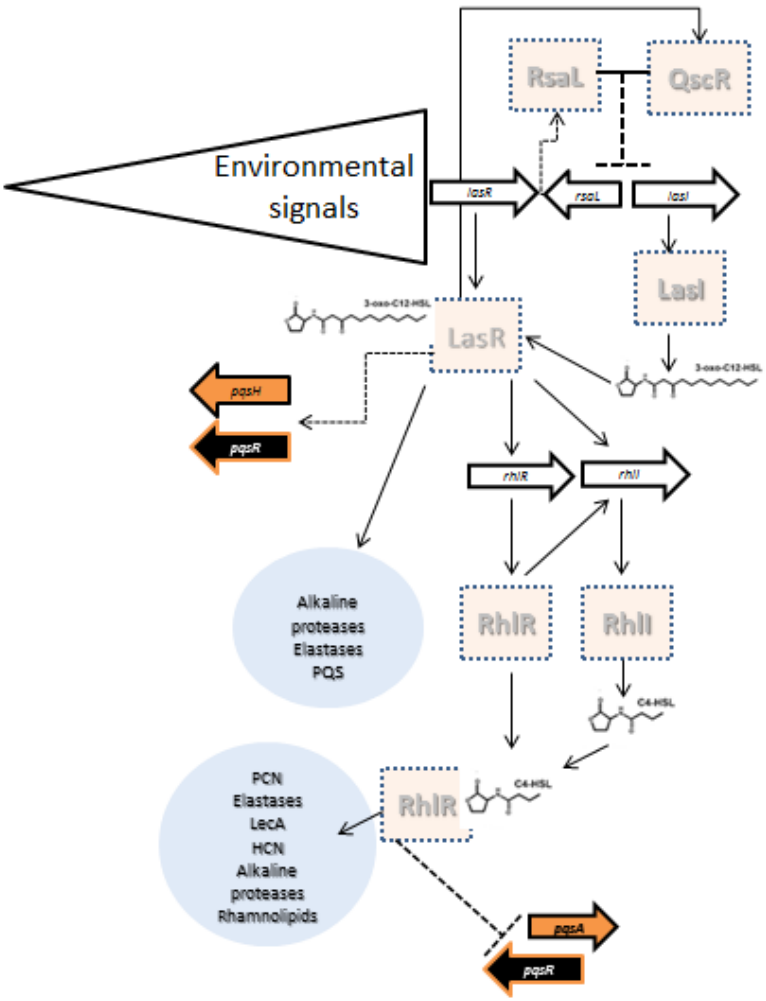


Figure 1.1. *Pseudomonas aeruginosa* AHL quorum sensing signalling hierarchy. At the top of the hierarchy sits LasR which directly exerts transcriptional regulation over the RhlR and QscR regulons. Dotted squares represent the individual regulons, full arrows stand for activation and inverted T arrow indicates inhibition. The molecular structures overlaying dotted squares represent a formed complex, whereas full circles indicate virulence-associated products.

1.3.2. Alkyl quinolone quorum sensing system

In PA there is a third QS system using 2-alkyl-4(1*H*)-quinolones (AQs) as the signal molecules (143). The primary AQ QS signal molecules are 2-heptyl-3-hydroxy-4(1*H*)-quinolone (generically known as *Pseudomonas* quinolone signal [PQS]) and 2-heptyl-4-hydroxyquinoline (HHQ) which through the interaction with the lysR-type regulator PqsR (also known as MvfR) can activate both the expression of the AQ biosynthetic genes and the gene encoding the virulence effector protein PqsE. There are more than 50 different AQs produced at different levels by the pqs biosynthetic genes and although only PQS and HHQ have been shown as signals, some of the other AQs also have certain biological roles during infection (144) (145).

1.3.2.1. Biosynthesis of alkylquinolones

The biosynthesis of AQs requires the *pqsABCD*, *phnAB*, *pqsH* and *pqsL* genes (146). There are more than 50 different AQs generated during this process although the biological role of most of them remains to be understood (144).

The first step in the biosynthesis of PQS (figure 1.2) is the production of anthranilate by *phnAB* which is then used by the anthranilate-coenzyme A (CoA) ligase PqsA to produce anthraniloyl-CoA (147). And even though PA shows several processes that are capable of producing anthranilate, the *pqsR*-controlled *phnAB* operon sitting in the vicinity of the *pqsABCDE* one, is the primary source of anthranilate (148). Although these two operons were originally thought to correspond to two independent transcriptional units, they have recently been shown to be co-transcribed under certain growth conditions (149).

PqsD through a condensation reaction has been proposed to form 2-aminobenzoylacetyl-CoA (2-ABA-CoA) from anthraniloyl-CoA and malonyl-CoA (150). The next step is catalised by PqsBC which are responsible for coupling 2-aminobenzoylacetate (2-ABA) to an octanoyl moiety to produce HHQ (151). Two secondary metabolites produced during these reactions are 2-aminoacetophenone (2-AA) and 2,4-dihydroxyquinoline (DHQ). The formation of DHQ has been shown to require PqsA and PqsD (Zhang et al., 2008), whereas 2-AA is thought to result from decarboxylation of 2-ABA (Dulcey et al., 2013). PqsE has recently been shown to work as a thioesterase guiding 2-ABA-CoA towards the synthesis of HHQ and suppressing DHQ formation (152). The mono-oxygenase gene *pqsH* converts HHQ into PQS as a PA strain devoid of the *pqsH* gene is unable to make 3-hydroxy-4(1*H*)-quinolones (153). The *pqsL* encodes a putative mono-oxygenase required for the synthesis of HQNO and associated *N*-oxides. A PA *pqsL* mutant shows increased levels of PQS but is unable to produce AQNOs (154) (155).

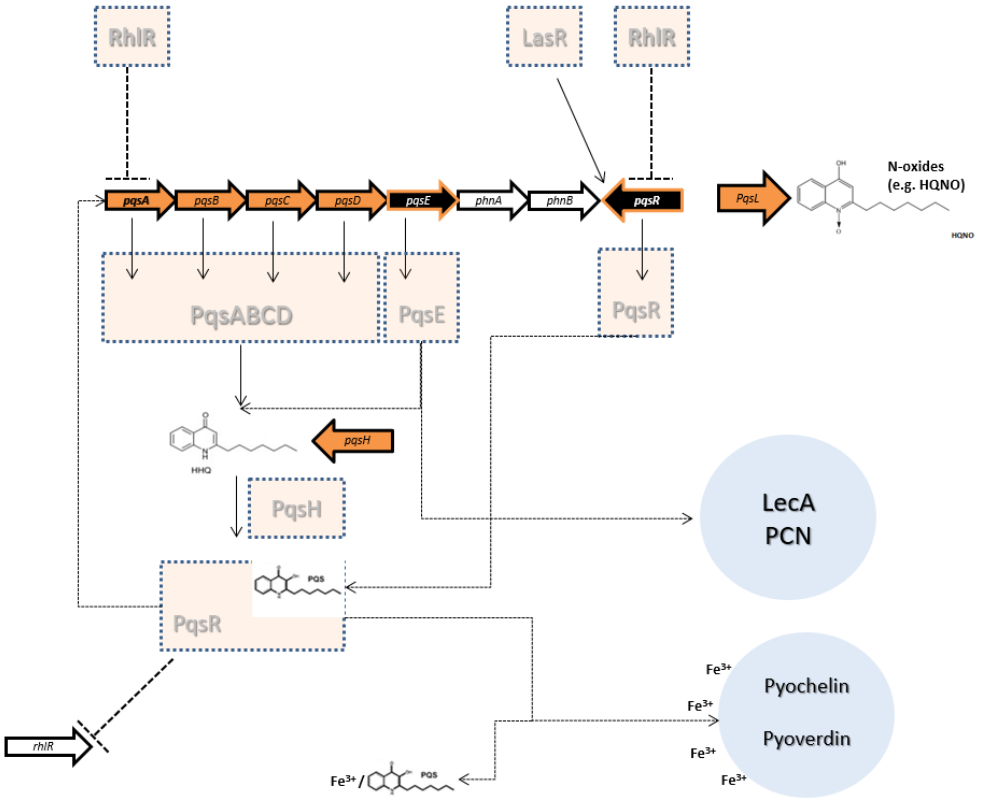


Figure 1.2. *Pseudomonas aeruginosa* PQS biosynthesis. Full horizontal arrows indicate participating gene, dotted thin arrows indicate subsequent attachment, ininterrupted thin arrows indicate immediate product, molecular structure overlaying box indicates complex formation, full circles stand for virulence-associated products, and inverted T arrow stands for repression or negative feedback. The diagram presented accounts only for the PQS biosynthesis through the involvement of the *pqsABCDE* operon, and the involvement of both *pqsH* and *pqsL* genes.

1.4. Role of AQs in the regulation of gene expression

The main virulence traits controlled by the *pqs* system result from the participation of the transcriptional regulator *pqsR*. This regulator affects the production of multiple virulence factors as well as the biosynthesis of 4-hydroxy-2-alkylquinolines (HAQs), where the Pseudomonas Quinolone Signal (PQS) is found. Even though the role of PQS is yet to be fully unveiled, it is known to control a large number of virulence genes, namely those associated to the *rhl* regulon, as the stationary phase of development is initiated. It affects the production of exoproducts, lectins, elastases (156), pyocyanin (PCN) and interferes with the biofilm formation (157). PQS acts as an intercellular

signalling molecule, an intermediate in the cell-to-cell communication pathway (158).

Some of the PQS-controlled genes are known to be related to iron scavenging. This has been explained by the fact that PQS has a 3-hydroxyl moiety which is typically present in some iron chelators. This moiety is not present in its precursor HHQ. Indeed, PQS has been found to bind iron in chrome azurol S (CAS) assays as well as in spectrophotometric titration assays (153). Also, addition of PQS to PA cultures reduced free iron levels (159), suggesting that PQS can trigger an iron starvation response in this organism.

PQS has been shown to control virulence and iron-mediated gene expression using two pathways: 1) via the virulence effector protein PqsE, through the activation of the *pqsABCDE* operon upon binding to PqsR (see section below), and 2) via the chelating properties of PQS (160).

PQS also shows a secondary role as iron entrapper in siderophore-mediated iron transfering. These findings revealed that in opposition to what is known for AHLs, exogenous supplying of PQS results in additional exoproducts (157) that go beyond the population-dependent threshold levels. The authors showed that exogenous PQS can impact on *lasB* expression resulting in additional virulent LasB elastase and upregulation of the PA QS rhl subsystem, but the inability to produce PQS will most likely impact on the immediate rhl-dependent phenotypes. They also suggest that PQS may even be able to deliver iron to siderophores. McKnight *et al* (2000) (156) theorise that the regulatory bridge between PA *las* and *rhl* subsystems in the QS system is possibly explained by PQS inducing *lasB* in a way that does not require *lasR* (157). The putative bridge established by PQS between the AHL and the AQ PA QS systems is reinforced by the fact that the *pqsR* gene is regulated by *lasR* (positive feedback) and *rhlR* (negative feedback), revealing an interdependent duality. In addition, DNA mobility shift assays certify of the PQS role as PqsR coinducer by revealing that PqsR binding increases when PQS is present (161) (162).

PqsE has also been shown to work as a virulence effector protein controlling the expression of virulence target genes through the QS Rhl pathway (163). Furthermore, mutations in either of the *pqsA* or *pqsE* genes results in reduced PA pathogenicity in both plant and animal disease models (164) (160). Moreover, *pqsE* mutants are associated to altered PCN, lectins and hydrogen cyanide production, but their AQ production is not affected. In addition, *pqsE* has a primordial role in activating a range of virulence phenotypes, such as PCN production, *phzA1* expression, lectin production, elastase production and rhamnolipid levels.

The role of AQs in virulence has already been proven in a range of disease models mutations in the *pqs* genes. These mutations resulted in reduced pathogenicity by PA14 infections in different organisms, from plants (*Arabidopsis thaliana*), to rodents (mouse full-thickness skin burn model) (165), to nematodes (*Caenorhabditis elegans*) (166), to insects (larvae of *Galleria mellonella*) (167), or with PA *pqsR* mutants causing reduced mortality rates in thermally injured rodents infected with 10^5 mvfR$^-$ bacterial cells (162) (162), or with single *pqsH* and double *pqsA/pqsH* mutants that are devoid of PQS (146) or have a lesser potent PQS rate (162). In these examples, the receptor PqsR arises as an immediate target protein when developing strategies to search for QSIs with disruptive role of the PQS-related gene expression. In these examples, the receptor PqsR arises as an immediate target protein when developing strategies to search for quorum sensing inhibitors with a disruptive role of the PQS-related gene expression.

1.4.1. Regulation of the *pqs* genes and relationships with the AHL-QS systems

The activation/regulation of the *pqsA* promoter does not involve direct interaction with the LasR and RhlR systems. The mapping of the transcriptional

start site for *pqsR* by Wade *et al* (2005) (161) helped understand that *pqsA* transcription is, however, controlled positively by the *las* system. By revealing that the participation of the protein LasR and the signalling AHL 3-oxo-C_{12}-HSL are required for endogenous *pqsR* induction in *E. coli*, and that the rhl QS subsystem represses the transcription of *pqsA*, McGrath *et al* (2004) (168) have pointed towards a direct +/- action of these elements on *pqsR*. Two presumed QS operator sequences located upstream from the *pqsA* promoter (168) have been suggested as having determinant roles in the regulation by LasR and RhlR. Competition between these subsystems is likely to occur in said region and Brouwer *et al* (2014) (169) even debates about the possibility that the repression of PqsA production occurs posttranscriptionally through the participation of RhlR.

PqsR is indeed the protein that binds the *pqsA* promoter in a reaction highly enhanced by the presence of the PqsR coinducer, PQS. The PqsR-PQS complex binds to two different locations in the *pqsA* promoter region to activate the transcription of the *pqsABCDE* operon. PqsR interaction with the *pqsA* promoter needs the participation of the transcriptional regulator *pqsR* for the synthesis of PQS (146). HHQ (the PQS precursor) is also capable of binding to PqsR inducing a conformational change on this protein, and also capable of enhancing PqsR binding to the *pqsA* promoter. Thus, neither LasR nor RhlR or even their associated signalling molecules, do interact with the *pqsA* promoter (164). However, it has been implied by Wade *et al* (2005) (161) that these QS AHL-associated regulators may be related to the control of other regulator(s) that ultimately interfere with the *pqsA* promoter, among which the *pqsR* transcriptional regulator is found.

The *pqsR* gene is homologous to elements seen in the family of LysR-type transcriptional regulators where several LysR-type transcriptional activators are known to possess two important structural features: 1) conserved DNA binding domains and, 2) a variable coinducer binding domain. These transcription activators characteristically connect to the promoter region

when there is no coinducer present, attaching to an adjacent site when the coinducer is available.

Typically, the LysR-type transcriptional activators family, to which PqsR belongs, possess a well conserved DNA binding domain and a variable one, usually showing a dual binding behaviour [access (170) for a review on the matter]. Overall, PqsR ultimately regulates PQS production, and the established PqsR-PQS complex formed is known to bind to diverse locations in the *pqsA* promoter region. The interaction established by PqsR and the *phnAB* promoter is processed positively by *pqsR* regulation over *phnAB* when the coinducer is not available (170). Finally, PqsR has been shown to have a balancing role by complementing PQS availability in a *lasR* mutant (161) and a PA *pqsR* mutation does not at all impact on the transcription of both *lasR* and *rhlR* (171).

In terms of *pqsR* regulation it is possible that it is very likely the result of a regulatory chain that involves the QS AHL regulons and where *pqsR* influences its own expression, by means of operating over the *pqsABCDE* operon, thus impacting on the production of PQS. In regards to *pqsR* transcription, there are two primary start sites (190 and 278 bp upstream from its ATG start codon). A basal expression of *pqsR* determines that the protein is constantly being produced at a background level. A study by Dötsch *et al* (2012) (172) using PA and focusing on the qualitative analysis of RNA has shown the presence of three possible transcriptional start sites in the *pqsABCDE* operon. Two of these are specifically located in the *pqsA* promoter region.

The *pqsA* transcriptional start site is thought to be located -71 base pairs upstream of the *pqsA* start codon. Moreover, the *pqsA* promoter is assumed to contain a LysR-type box (a crucial *pqsABCDE* regulatory element) with a symmetrical pair of -45 base pairs before the *pqsA* transcription initiation site. Studies involving point mutation of the putative LysR box present in the *pqsA* promoter show strong fallout in *pqsA* expression with null expression if the aforementioned symmetry is affected (173). PqsR-PQS binds to the LysR box in

order to upregulate the *pqsABCDE* operon, a feature not observed in *pqsR* mutants. Nonetheless, PQS is not the only AQ capable of upregulating AQ expression via PqsR.

Even though the *pqsR* gene is located adjacent to the PQS synthetic operons, the *pqsABCDE* operon and the *phnAB* operon, its putative operator sequence is believed to be located far from the *pqsR* transcriptional start sites. The controlling of the QS processes under the influence of the *pqsR* gene is hypothesised by Wade *et al* (2005) (161) to be through either one of two options, i.e., through the aforementioned potential operator site or through a less conserved operator still to be identified.

PqsR plays a fundamental pathogenicity role in PA virulence as debated by Kozak (174) and supported by the novel regulatory players known to interact with *pqsR*. These agents impact on the production of different virulent phenotypes and such inference is usually determined by small RNA fragments binding to target mRNA molecules or by the formation of secondary structures in the mRNA. It is here that a simplest form of riboswitches, the RNA thermosensors, gains relevance. The riboswitch is an important regulatory RNA agent located in the noncoding region of the mRNA; involved in genetic expression dependent on the folding of the initiation region of the mRNA (175). RNA thermosensors are a broadly researched example of this conformational-dependent regulatory process, and the PA heat-shock protein IbpA was recognised has being under the regulation of a dyad of temperature-sensitive hairpin structures sitting in 5' untranslated region (UTR) of the source gene *ibpA* (176). A similar conformational repression effect has recently been shown by Krajewski *et al* (2013) (176) in which PQS biosynthesis is inhibited in PA by RhlR, because of an obstruction of the translation initiation site of the *pqsABCDE* transcript when RhlR seeks transcription of *pqsABCDE* from an alternative transcriptional start site. This strategy ends up in long 5' UTR structural folding that ultimately delays the binding of the 30S ribosomal subunit with the mRNA, an effect that blocks translation initiation.

To confirm previous assumptions by Dötsch *et al* (2012) (172) describing transcriptional repression effects exerted by RhlR on *pqsR*, the induction of transcription start site *pqsA*-339 and the induction of *pqsA*-71 (PqsR-dependent), Brouwer *et al* (2014) (169) generated *luxCDABE* promoter fusions containing *pqsA*-339 and *pqsA*-71 transcription initiation sites of the *pqsABCDE* operon. The results obtained revealed that expression of *lux* in the parental strain of the highly virulent PA14 bacteria, and also in the derived *rhlR* and *pqsR* mutants, agreeded with what Brouwer *et al* (2014) (169) reported on the repression of the region containing sites *pqsA*-339 and *pqsA*-71. In fact, transcriptional start site *pqsA*-339 luminescence was noticed predominantly in the PA14 *pqsR* mutant strain and silent in the RhlR mutant strain; on the other hand, *pqsA*-71 was luminescing in the PA14 *rhlR* mutant strain but no light was generated with the *pqsR* mutant. And additional findings revealed RhlR inducing transcription of the pqs operon by promoting transcription of *pqsA*, as it concurrently inhibits PQS production in a double active *pqsA*-71 fusion in the *ΔrhlR* strain, in comparison to the wild-type bacteria.

1.5. Novel regulatory pathways influence PA virulence phenotypes

More recently two agents emerged as impacting on the production of virulent PA phenotypes, namely ANR and RpoN. Sonnleitner *et al* (2011) (177) showed that under conditions of limited availability to oxygen, the oxygen-responsive regulator Anr controls the expression of the small RNA (sRNA) PhrS, which in turn activates PqsR translation, resulting in an indirect stimulation of the AQ regulatory cascade. This activation that takes place through a PhrS-driven base-pairing process, to stimulate an open reading frame translationally coupled to *pqsR* gene, supports the active role of LasR in the regulation of *pqsH*. The PQS biosynthetic pathway delivers at some point its precursor HHQ that is later converted to PQS by the LasR-dependent monooxygenase PqsH in a process that does not involve oxygen-dependent enzymes (162). This enzymatic conversion process depends on the availability of oxygen, and its

rate decreases when in hypoxia (178), a feature typical of anaerobic biomes. When at limiting levels of oxygen, ANR-regulated sRNA PhrS induces *pqsR* translation as population increases. This PhrS-induced expression of PqsR operates as a response to the low levels of produced PQS when the system is oxygen-deprived. The above mentioned effect is not obligatory when in stationary phase as PQS synthesis can take place even in the absence of LasR (157) and *pqsH* mutants (incapable of generating PQS) still can sinthesise HHQ in a PqsR-dependent synthesis.

In addition, Cai *et al* (2015) (179) showed that RpoN, a sigma factor known to regulate several cellular functions, is also involved in the regulation of *pqsR*. The authors unveiled its effects on *pqsR* whilst using *ΔrpoN* mutants that were unable to produce normal levels of PCN. In fact, *rpoN*-deficient PA haplotypes usually appear in chronically infected cystic fibrosis (CF) patients. Actually, a study by Heurlier *et al* (2003) (180) on repression of QS by means of controlling RpoN showed that *rpoN* mutants are capable of synthesising HHQ but uncapable of activating PqsR. Consequently, their associated levels of PQS are ultimately linked to the very low levels of PCN produced, the incapacity to generate anti-staphylococcal effectors, the overexpressing of AHL-associated signalling molecules, elastases LasB and LasA, rhamnolipds and hydrogen cyanide.

Very recently, Farrow *et al* (2015) (181) elaborated on findings regarding the functions of CysB, a protein with predominant regulatory role on sulphur uptake regulation on intercellular communication in PA. CysB regulates cysteine synthesis and *pqsR* expression (by repressing it), and consequently resulting in the inhibition of PQS production. The authors have also revealed its capacity to neutralize LasR influence on *pqsR*. Nevertheless, having cysteine at disposal does not affect expression of *pqsR*.

In addition, a vicarious action of co-regulated genes is likely to operate in the QS system, at least in what concerns the rhl regulon and those genes

under the influence of *pqsR* that do not overlap with the former, as stated by Déziel *et al* (2005) (164). That was shown by means of *rhlR* mutants where virulence was not suppressed, but on the other hand *pqsA* and *pqsE* mutations fully reveal an attenuated virulence phenotype. This reduction in virulence potential has also been reported in single *lasR*, *lasI* and *rhlI* mutants, as well as in double *lasI*/*rhlI* ones. The somewhat expected reduction in virulence capacity in *rhlR/I*-devoid strains is likely to be linked to the fact that the RhlR protein possibly exerts its repressing action when there is unavailability of the *rhlR*-associated autoinducer C_4-HSL, as debated by Medina *et al* (2003) (182).

1.6. Impact of QS molecules in infection

QS molecules have been found in samples from CF patients infected with PA. AHLs were originally found in sputum from CF patients infected with either PA or *Burkhoderia cepacia* (183); and so were AQs (184). The presence of QS molecules in samples from infected patients is yet another evidence of the importance of these molecules in infection. The next two sections provide an overview of the impact of these molecules in the interaction between polymicrobial communities and the host.

1.6.1 Effect on interaction between polymicrobial communities

Bacteria live in polymicrobial communities and hence are subjected to a wide range of interactions including cross-talk using QSSMs. One of the most revealing studies on the implications of exogenous AHLs has been uncovered through the interactions between PA and *S. aureus* (the two most prevalent pathogens in airway infections of CF patients). One of these studies showed that 3-oxo-C_{12}-HSL from PA affects the growth of *S. aureus* at high concentrations. However, at low concentrations, resembling those found during infection, this AHL could activate the production of adhesins such as

fibronectin-binding proteins, and inhibit the production of toxins like the toxic shock syndrome toxin TSST-1. These traits are controlled by the *S. aureus* agr QS system. Interestingly, 3-oxo-C_{12}-HSL was found to directly inhibit this system although the mechanism behind this inhibition remains to be elucidated (185).

But regardless of this dual presence where *S. aureus* and PA coexist, not much is known about the real implications of polymicrobial colonisation/infections. However, in the past decade it has been unveiled that also AQs secreted by PA have an effect on other bacterial populations, such as *S. aureus*, especially those factors deriving from QS-related pathways such as elastase LasA, PCN, HCN and HQNOs. This had been suggested in the beginning of the 90s by Machan *et al* (1992) (186) and followed later on in studies by Hoffman *et al* (2006) (187) and Goerke *et al* (2010) (188). The latter reported that when the pathogen is exposed, for a prolonged period of time and to physiological concentrations of PA 4-hydroxy-2-heptylquinoline-*N*-oxide (HQNO), subpopulational growth arrest occurs and respiratory-deficient small colony variants (SCVs) are generated (187).

Stimulation of *S. aureus* biofilm formation and production of SCVs have also been reported by Fugère *et al* (2014) (189) as the result of exposure to PA AQ products, HQNO and PQS. The authors demonstrated that under HQNO exposure, activation of the sigma factor B takes place, hence resulting in higher expression of the cell surface bound adhesin fibronectin-binding protein A and higher expression of s*arA* genes (associated to biofilm development) in isolates from CF patients. The effect was confirmed *in vitro* by exposing *S. aureus* to supernatants from PA mutants incapable of secreting HQNO as this rendered *S. aureus* unable to generate a biofilm.

But the above-mentioned impact is not exclusive to *S. aureus* since the role of 3-oxo-C_{12}-HSL on the eukaryotic dimorphic fungus *Candida albicans* has also been getting attention from the scientific community. *C. albicans* is usually found in polymicrobial infections alongside PA, particularly in lungs of

immunosuppressed CF patients. It produces tyrosol and farnesol, two QS molecules (190) capable of accelerating (tyrosol) and inhibiting (farnesol) germ tube formation as morphological conversion from yeasts to hyphae take place.

It was later that a study by Cugini *et al* (2007) (191) reported on the dose-dependent inhibitory effects (not impacting on bacterial growth) of farnesol over PA PQS and its associated product, the virulence factor PCN. The authors showed that these two exoproducts released by *C. albicans* increase PQS, phenazine and C_4-HSL levels in PA *lasR* mutants (192) in a process that is thought to be the result of a cascade reaction triggered by reactive oxygen species.

There is yet another relevant QS molecule secreted by *C. albicans* and affecting PA virulence, tyrosol, an aromatic tyrosine derivative antibacterial alcohol capable of reducing the lag phase of growth in low-density cultures, stimulate germ tubing in yeast cells (193), stimulate hyphae formation in the early stage of biofilm production (194), and yet again without any implications on bacterial growth. Tyrosol has been suggested by Hassan *et al* (2015) (195) to exert a strong repression on the produced levels of PA hemolysin and protease.

1.6.2 Effects on bacterial host-cell interactions

In healthy people, PA is very rarely in the origin of infection. Its pathogenic efficiency is however potentiated in immunosuppressed patients. PA-associated morbidity and mortality derives from imbalanced pathogen–host interactions with consequences on gene expression, as microarray studies by Ichikawa *et al* (2000) (196) have identified. The authors used high-density DNA microarrays, comprising slightly over 1,500 human cDNA clones, and verified how differential gene expression was activated in the A549 lung pneumocyte cell line during exposure to PA. Host genes requiring interaction

with PA and expression of virulent factors (e.g., type IV pili major subunit PilA) were consequently identified.

Since PA interactions with the human compromised airway systems are usually associated with scarring of connective tissue (fibrosis), as a result of physical disruption; inflammation induced by PA results from direct release of immunogenic agents into the airway epithelium. Nevertheless, it is yet to be understood if the rather extreme inflammation typical of CF results just from exogenous bacterial stimulus or an extreme inflammatory response. Several human studies (197) (198) (27) suggest an increased risk of mortality (6-fold higher) in acute infections linked to expression of the type III secretory proteins. Other studies (199) (200) focusing on mice models of infection, debate on the capacity to compete for iron (e.g., with transferrin or lactoferrin) from host tissue, in order to promote successful virulent phenotypes (201).

Finally, from the plethora of novel hints in the host-pathogen interaction studies in PA infection, hypoxia emerges as a relevant factor. For example, hypoxia is a common feature of infected tissue areas, oxygen deprivation is typical of inflammation, genetic expression is related to innate immunity by means of the hypoxia-inducible factor and nuclear factor kappaB pathways (controlled by oxygen-dependent prolyl-hydroxylases), hypoxia affects virulence and resistance to antibiotics in bacteria, etc. But even though a lot is yet to be unveiled in what concerns the impact of hypoxia on host-pathogen adhesion and infection, *in vitro* studies combining human leukocytes and immunomodulatory effects of the 3-oxo-C_{12}-HSL have already demonstrated that the AHL signalling molecule was capable of repressing lymphocyte proliferation and stimulate downregulation of TNF-α and IL-12 production (202). In addition, 3-oxo-C_{12}-HSL has been observed *in vivo* to activate T lymphocytes, and thus stimulating host cells to prepare inflammation gamma-interferons (203), consequently unleashing a probable Th2-regulated response that can end up causing tissue damage and enhancing inflammatory progression.

1.7. Approaches to treat PA infections

1.7.1. MDR PA and the need for alternative therapeutic approaches

Antibiotic resistance in PA has been escalating over the years. In the USA and over a period of 3 years (1997 to 2000) the proportion of multiple drug resistant PA (ceftazidime, piperacillin, imipenem, ciprofloxacin, gentamicin and amikacin) increased from 12.8% to 20.8% (1). In 2001, PA strains with acquired resistances to antibiotics and antiseptics were responsible in France for 16.8% of nosocomial infections resistant, for example, to a third generation cephalosporin and Ceftazidim (a ß-lactam antibiotic). Indeed multidrug resistant PA has reached such a level of severity, as reported by centers for disease control all over the globe, that in some situations patients are being administered Colistin (also known as polymyxin E) as a last resort (204), regardless of its associated toxic side effects on kidneys and the nervous system.

The scientific community in synergy with the pharmaceutical industry have been producing a portfolio of new approaches to tackle the increasing inefficacy of traditional antibiotics in treating PA. New antibiotics, novel antibiotic combinations, but also the identification of alternative therapeutic routes (figure 1.3) devoid of antibiotic identity are being researched nowadays. There are nonetheless financial investment restrictions that have significantly slowed down progress in this field (205).

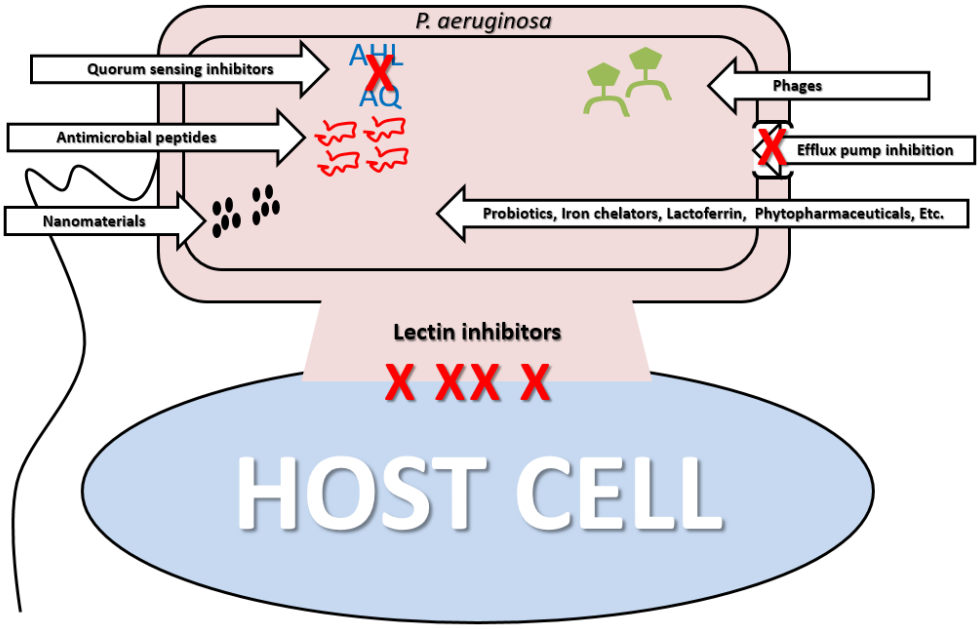


Figure 1.3. Overview of some of the non-antibiotic approaches currently being developed to treat PA infections. Quorum sensing inhibitors interfere with QS regulatory pathways and signalling molecules, ultimately repressing virulence factor production and disrupting biofilm formation; Antimicrobial peptides cross into the cytoplasmic membrane to activate bacterial murein hydrolases; Nanoparticles stimulate indirect activity against microbes; Phages propagate within the cell and then kill it; Efflux pump inhibitors with implications on the excretion of antibiotic molecules, organic solvents, biocides, etc.; Probiotics that enhance host innate defences; Iron Chelators interfere with iron acquisition essential for biofilm, pyocyanin and pyochelin production; Lectin inhibitors affect adhesion to epithelial host cells; Lactoferrin-hypothiocyanite combination therapy generate H_2O_2 and subsequent ROS; Traditional medicine and phytochemicals to reinforce the immune system.

Quorum sensing inhibitors promote degradation of AHL signalling molecules in QS proficient bacterial populations. These AHL-based QS antagonists are known to be narrow spectrum, but what might seem to be a disadvantage actually operates as an advantage for their specificity attenuates only the pathogens in polymicrobial populations typical of nosocomial infections. Table 1.2 provides a brief summary of the most relevant non-antibiotic approaches that have been recently reported in the battle against MDR PA; from antimicrobial peptides, to iron chelators, going through the efflux pumps, lactoferrin and hypothiocyanite combinations, to lectin inhibitors, nanoparticles, phage therapy, probiotics, vaccines, and finally to the latest advances in traditional medicine whenever possible combined with modern synthetic biology approaches.

Table 1.2. List of some relevant non-antibiotic approaches developed against MDR PA over the past two decades.

Group and primary function	Clinical advantages	Promising agents
Antimicrobial peptides [Cross the cytoplasmic membrane to activate bacterial murein hydrolases that damage peptidoglycan of host cells]	Selectivity, speed of action, difficult to gain resistances against, some already clinically available (e.g., nisin, polymyxin B, E1 and gramicidin S). Direct activity even against mucoid and antibiotic-resistant PA.	• Cecropin P1 (206), • Protegrin-1 (207), • LL-37 (208), • Indolicidin/Nisin/Ranalexin (209), • Magainin II (210), • Elafin/trappin-2 (211)
Iron Chelators [disturbance of iron acquisition essential for biofilm, pyocyanin and pyochelin production]	Direct interference with virulence. Disruption of bacterial iron metabolism.	• Gallium (212) (213) • Desferrioxamine (214) • Deferasirox (215)
Lactoferrin-hypothiocyanite combination therapy [Produced in the airways by the immune system and have the ability to generate H_2O_2]	Effect on biofilm formation but no action over established biofilm matrices.	• Combinations of hypothiocyanite and lactoferrin along with tobramycin and aztreonam (216)
Lectin Inhibitors [Affecting adhesion to epithelial host cells through recognition of sugar receptors and disruption of biofilms through interference with lectin-bacterial cell interactions]	Receptor blockage of LecA/B binding to fucose-/galactose-specific receptors	• Reduction in sputum PA colonies after using fucose/galactose inhalation therapy (217) (218)
Nanoparticles	Produce successful	• Zinc oxide (219),

[Ultra-small solid lipidic nanoparticles that penetrate mucus and improve delivery of anti-virulence novel QS antagonists]	therapeutic actions against a range of microbes (PA included). Particular interest on metallic nanoparticles for penetrating bacterial membrane.	Copper oxide, Iron (III) oxide, Titanium dioxide (220) • Silver:Gold alloy (221) Etc.
Phage therapy [Some display lytic activity and alginate degrading activity, show synergetic applications with streptomycin resulting in growth inhibition, potential destruction of biofilm]	Phages allow genetic alteration for reducing host inflammatory responses as treatment progresses. Effective against PA biofilm formation. Numerous advantages over antibiotic usage, for example, phages increase in number over the course of treatment, cause minimal disruption of gut flora, effective against both antibiotic-sensitive/resistant bacteria, low associated toxicity.	• E79, JG024, LUZ7, M4, MPK1, MPK6, PaP1, PAK-P1, PIK with anti-PA activity (222) (223) (224)
Probiotics [Enhance host immune system potential; enhance natural protection against enteric pathogens (acid secretion, bacteriocins, growth repressing, etc.)]	Well-studied gastrointestinal bacteria. Additional health promoting results.	• Lactobacillus plantarum inhibit PA pathogenicity (225) (226) • Lactobacillus fermentum secrete elastin, growth, biofilm formation and cytotoxins inhibitors (227)

Efflux pump inhibitors [Lower outtermembrane permeability and the extruding of antibiotics, biocides, detergents, organic solvents and other antibacterial agents present outside the bacterial cell]	Difficult to develop bacterial resistance against efflux pump inhibitors.	• Phenyl-arginine--naphthylamide can inhibit PA efflux pumps, hence enhancing sensitivity towards fluoroquinolones (228) (229) (230)
Traditional medicine and phytochemicals [Ayurvedic medicines to reinforce the immune system]	Readily available. A few show promising effects under *in vitro* conditions.	• Triphala Churna with antibacterial properties (231) • Antimicrobial components present in a range of plants (e.g., protocatechuic acid, gallic acid, ellagic acid, rutin, myricetin, berberine, etc.) (232) • Combinations including phytochemicals potentiate antimicrobial activity (232)
Vaccines [Reduce bacterial adherence and neutralise activity of exotoxin A, whilst generating antigen-specific antibodies]	Several candidate formulations display promising effects (increase survival and raise LD_{50} of treated models]	• PopB, type IV pilin-exotoxin A toxoid (233) • 3-oxo-C_{12}-HSL-carrier protein conjugates (234) • Mutated toxAm and pcrV genes inserted into the eukaryotic pIRES plasmid (235)

1.7.2. Quorum sensing inhibition

As a central chemical communication mechanism controlling the virulence of PA and its interactions with the host, QS has been considered an important alternative target for antimicrobial development. The process of interfering and disrupting QS signalling is known as quorum quenching (QQ) and although this strategy will not kill PA, it would attenuate virulence and can be used as an adjuvant therapy, especially in immunocompromised patients (236) (237).

Since QS-mediated communication requires emitter and receiver cells, QQ strategies aim at blocking this process in three primary ways: (i) interfering with the emitting cell, (ii) interfering with the receiver cell, (iii) and finally, targeting the signal molecules. It is important to understand that QSSM inhibitors (QSIs) are not antimicrobials and do not replicate antibiotic effects.

The properties of the researched molecules are of vital importance in the highthroughput screening process that will lead to isolation and identification of QS inhibitors (QSIs). These are relevant only for the use of compounds, where they should preferably be: of low-molecular-weight (the activity of which causes a significant reduction in the expression of QS-controlled genes) (238), highly specific (directed at a known QS regulator) (239), non-toxic to both prokaryotic and eukaryotic cells (no interference with RNA and protein synthesis related to basal metabolic pathways of the bacteria), with minimal selective pressure (240), and the molecules need to be chemically stable, resistant to metabolism (241), and at a later stage after the obligatory clinical testing, be easily excretable by the higher host organism.

1.7.2.1 Signal biosynthesis Inhibitors

1.7.2.1.1. Targeting AHLs

In silico studies by Yang *et al* (2010) (242) combining molecular dynamics simulation with wet experiments, enabled the efficacy of two putative QQ molecules to be assessed, namely triclosan (a known antibacterial and antifungal agent) and epigallocatechin gallate (EGCG) (catechin found in green tea leaves). The authors were able to show their ability to interfere with AHL production through the inhibition of the enoyl-acyl carrier protein reductase (FabI) of the bacterial type II fatty acid synthesis pathway. This pathway is involved in the biosynthesis of AHLs 'delivering' these to the acyl chain to be used by the LuxI-type AHL biosynthesis protein (243), proposing a

QQ role for EGCG due to binding strongly and more effectively to the enoyl-acyl reductase of PA. This disruptive role for EGCG is shown by their studies as being capable of virulence attenuation and repression of biofilm production in PA.

1.7.2.1.2. Targeting AQs

One of the key enzymes involved in the first steps of PQS and HHQ biosynthesis is PqsD, as described in section 1.3.2.1. By studying the participation of the CoA-PqsD complex in the condensation and cyclisation reactions using several β-ketodecanoic acid species *in vitro*, Storz *et al* (2012) (244) identified a number of nonbactericidal PqsD inhibitors. PqsD structurally resembles the β-ketoacyl-ACP synthase (FabH) which has also been considered by Pistorius *et al* (2011) (245) also a potential target to interfere with AQ production. Likewisedebated by Storz *et al* (2012) (244) whether FabH inhibitors would have potential impact on the protein PqsD. When these compounds were tested they showed moderate activity against PqsD *in vitro*, although their *in vivo* action on PA has not yet been fully investigated. Such biochemical similarity has been functionally verified by Weidel *et al* (2013) (246) when showing that the sulfonamide substituted 2-benzamidobenzoic acids (recognised FabH inhibitors) do actually inhibit PqsD activity.

More recent studies by Sahner *et al* (2013) (247) and Storz *et al* (2013) (248) have shown significant efforts in the discovering of potent PqsD inhibitors with the finding of the PqsD-inhibitory potential of 2-nitrophenyl derivatives. One of the most active compounds was able to decrease HHQ and PQS production levels and the volume of biofilm generated by the PA strain PA14, with no impact to the bacterial cell viability. The disruption of the catalysis of the transitory CoA-PqsD complex, by means of adding (2-aminophenyl)methanol (a transition state analog of the reaction established between PqsD and its primary substrate anthraniloylCoA) was a partially successful strategy explored by Storz *et al* (2013) (248) for inhibiting PqsD.

More recently, Allegretta *et al* (2015) (Allegretta, Weidel et al. 2015) assessed, using Surface Plasmon Resonance, a new class of PqsD inhibitors with IC_{50} values in the micromolar region. These molecules have a catechol structure and have been recognised as hits for the inhibition of PqsD activity.

1.7.2.2. Signal molecule scavengers

There are two main strategies used to remove free active QSSMs from the environment and hence quench QS-mediated virulence. These involve the use of 1) signal degrading enzymes, and/or 2) removal of QSSM by different means including antibodies and polymers.

1.7.2.2.1. Signal degrading enzymes

1.7.2.2.2. Degradation of AHLs

There are two main classes of AHL degrading enzymes described in the literature: acylases (cleave the acyl chain of AHL) and lactonases (hydrolyse the lactone ring of AHL). Lactonases are metalloenzymes with AHL QQ activity shown in several bacterial species. Migiyama *et al* (2013) (249) engineered a PAO1 strain by expressing the AHL-lactonase AiiM in intratracheally infested mouse model of acute pneumonia. The resulting strain reduced AHL accumulation (C_4-/C_6-HSL and 3-oxo-C_{12}-HSL) in comparison to the wild-type strain, as visualized with the AHL reporter strains *C. violaceum* CV026 and Vir07, for short and long-chain AHL reporting, respectively. The same strain was tested against human lung epithelial cells and showed reduced toxicity 24h post-infection. In the mice infection models, an increase in survival rates associated to the expression of *aiiM* was observed. In addition, proinflammatory cytokines and myeloperoxidase activity in bronchoalveolar

lavage fluid was remarkably reduced in mice infected with the PAO1 strain expressing *aiiM* in comparison to those infected with the parental counterpart.

Also, the *aiiA* gene obtained from *Bacillus thuringiensis* was cloned and transformed into PAO1 and its expression fully degraded C_4-HSL and 3-oxo-C_{12}-HSL, resulting in reduced expression of elastase and PCN, affecting bacterial swarming motility and biofilm formation/dispersion (250). Later on, Rajesh *et al* (2014) (251), using cell-free lysate containing AHL lactonase (as specified by isolation and amplification of the gene (*aiiA*)) obtained from the endophytic bacteria *Bacillus firmus* PT18 and *Enterobacter asburiae* PT39, showed its strong AHL degrading capacity. Whilst inhibiting around 80% of the violacein production in a biosensor strain, the cell-free lysate applied to PAO1 and PAO1-JP2 biofilm, induced inhibition. Recently, the use of yet another lactonase was assessed by Hraiech *et al* (2014) (252); SsoPox-I is another successful case promoting the lowering of mortality rates in PA pneumonia-diseased rats by more than 50%. SsoPox-I was capable of decreasing PAO1 *lasB* virulence, reducing production of PCN and repressing proteolytic activity, as well as affecting the formation of biofilm.

Interestingly, the human host also produces enzymes with lactonase activity which can degrade AHLs. These are the human serum paraoxonases which are hydrolytic enzymes operating over a wide range of possible substrates: Aybey and Demirkan (2016) (253) assessed the capacity of purified human serum paraoxonase 1 (hPON1) to hydrolyse bacterial AHLs. Using purified hPON1 at different concentrations, reduction of a range of virulence factors (PCN, rhamnolipids, elastases and proteases) was accomplished.

The second main family of AHL degrading enzymes are acylases which catalyse the hydrolysis of the amide bond of AHLs in PA. For example, PvdQ acylase is necessary for the biosynthesis of pyoverdine and its deletion affects pyoverdine synthesis. PA devoid of PvdQ do not express an infectious phenotype, and that particular inhibitory molecule was unveiled by Theriault *et*

al (2013) (254) and applied by Wurst et al (2014) (255) to disrupt siderophore production through PvdQ inhibition.

1.7.2.2.3 Degradation of AQs

The search for AQ degrading enzymes is more limited due to the fact that these molecules are mainly produced by PA, unlike AHLs. Pustelny *et al* (2009) (256) identified a 2,4-dioxygenase enzyme named HoD (3-hydroxy-2-methyl-4(1H)-quinolone 2,4-dioxygenase) from the *Arthrobacter nitroguajacolicus* strain Rü61a. Hod catalised the conversion of PQS to two immediate substrates, N-octanoylanthranilic acid and carbon monoxide. Regardless of a far less catalytic effectiveness when compared to its natural substrate 3-hydroxy-2-methyl-4(1H)-quinolone (MPQS). Even though Hod was susceptible to PA exoproteases, to competitive inhibition by HHQ, and to sequestration of PQS, the enzyme was in fact a strong reducer of the expression of important PA virulence factors, growth arrest and tissue impairment in a plant leaf infection model. The authors reported that addition of exogenous purified Hod to PAO1 cultures reduced the expression of *pqsA*, *lecA* and the production of PCN and rhamnolipids. In addition, it also reduced the virulence of PA in a lettuce disease model.

More recently, genetic involvement hypothesised in the metabolism of HHQ involving hydroxylation towards the product PQS, with subsequent dioxygenolytic cleavage of the heterocyclic ring and hydrolysis of the consequential *N*-octanoylanthranilate, was put to testing by Müller *et al* (2015) (257). They observed that the *Rhodococcus erythropolis* BG43 is also capable of metabolising PQS and its precursor HHQ, whilst producing anthranilic acid. The candidate gene clusters *aqdA1B1C1* and *aqdA2B2C2* were transfered in a plasmid into strain BG43 and transcription of these operons seem to be upregulated by PQS. The observed results point towards the possibility that the

assessed candidate clusters might be involved in the production of enzymes participating in AQ-specific catabolism.

1.7.2.2.4. Antibodies

QQ by antibody interference on PA is also being investigated as a therapeutic strategy including its usage in vaccination strategies (see Table 1.2). These approaches focus prominently on the use of AHL analogues which can be used in vaccination against PA infections (133) (258). The conservation of the basic AHL backbone molecule and the fact that these molecules are present in the extracellular milieu increase the chances of success of this type of approach. The way these immunisation strategies generally work is by promoting the blocking of the autoinducer molecules, 3-oxo-C_{12}-HSL and C_4-HSL. Two possible approaches have been used: (i) Passive immunisation where there is a transfer of specific active humoral immunity (the antibodies) and (ii) Active immunisation where vaccines are administered to promote memory recognition (e.g., antibodies, memory B cells) against AHLs.

By developing a small molecule attached to a protein carrier that together elicit an immune response, Kaufmann *et al* (2006) (259) validated their hapten construction strategy to further collect specific monoclonal antibodies against AHLs. The authors intended to understand the anti-AHL dynamics by exposing the immune system to an AHL-like molecule with a carboxylic acid overhang designed to allow carrier proteins like bovine serum albumin (BSA) or keyhole limpet hemocyanin (KHL) to form conjugates. About a couple dozen haptens were produced per carrier protein, and mice were immunised with the KHL immunoconjugates for hybridoma production. From those obtained, the monoclonal antibody RS2-1G9 was the one displaying best potential to inhibit signalling by 3-oxo-C_{12}-AHL participation. This analog showed strong inhibition of the AHL and also a visible reduction of PCN in the PA strains tested, contrarily to weak or inexistent inhibitory capacity observed with other tested analogues.

In addition, this was the first reported antibody to show inhibition of QS signalling in PA strains.

Another example of immunisation against 3-oxo-C_{12}-HSL was reported by Miyairi *et al* (2006) (234). In their study the effects of yet another carrier-conjugated AHL was analysed for protection against PA lung infection using a mouse disease model. By administering 3-oxo-C_{12}-HSL–BSA subcutaneously with boosters for the immune system, namely Freund's complete adjuvant (an immunopotentiator comprised of antigen in mineral oil) and also incomplete adjuvant, serum of mice treated solely with the adjuvant did not show intensification in antibody titring against 3-oxo-C_{12}-HSL when compared to the control mice serum. Alternatively, immunisation with the full 3-oxo-C_{12}-HSL–BSA conjugate showed over 100-fold induction in specific antibody production in the tested acute pulmonary infection subjects. Mice were challenged with PAO1 and their survival rates compared with the uninfected controls. The population that did not undergo full 3-oxo-C_{12}-HSL–BSA conjugate immunisation died by day 2 post PAO1 challenge, whereas only 36% of the immunised population did not survive. In addition, apoptosis and necrosis studies showed that 50 mM of 3-oxo-C_{12}-HSL decreased cellular viability to as low as 10%. However, full immunisation resulted in preserved full cellular viability after treatment with a 1% immune serum solution.

The first indications in the direction of an anti-AHL immunisation in humans are within reach, especially after very recent studies by Golpasha *et al* (2015) (260). The authors studied the type III secretion system that permits straight delivery of a range of toxic proteins into the cytoplasmic environment eukaryotic cells by focusing on the PcrV protein (or V antigen) that is a vital part of the translocation pore system in PA host-cell interactions (261). With their prophylatic bivalent antigenic mixture (PcrV protein plus 3-oxo-C_{12}-HSL) they have realised that this conjugate composition can be used as a preventive vaccine against PA in burn wound infection models. They tested its capacity to promote immune responses against PA in conjugate form and in standalone

recombinant PcrV protein (r-PcrV). Both survival rate and PA presence in skin, liver and spleen were quantified 25 hours after burn wound infection. Immunization with the conjugate 3-oxo-C_{12}-HSL-r-PcrV did significantly enhance total IgG and individual specific antibodies (IgG1, IgG2a, IgG2b, and IgM) in the serum of two of the test groups compared to the control group. The present study proposed two-component vaccine to inhibit *Pseudomonas* infections in burned mice.

1.7.2.2.5. Polymers

Another area of QQ by signal scavenging that has been explored in the recent years involves the *in silico* engineering of molecules that interfere with QS-related molecules. Piletska *et al* (2011) (262) have shown the design of engineered polymers capable of inhibiting PA biofilm formation by scavenging the 3-oxo-C_{12}-AHL signalling molecule. The tested polymer and respective analogue reduced biofilm formation and attenuated the production of QS-regulated traits.

1.7.3. Receptor antagonists

In silico advances in the modelling and engineering of compounds capable of blocking QS signal transduction have revealed a field of opportunities for highthroughput screening of receptor antagonist molecules, at least for those capable of competing with native signal binding sites in the LuxR-type receptors. The engineering of novel synthetic small molecules invests on introducing, changing or substituting the acyl side chain, whilst maintaining the lactone ring unaltered. Tables 1.3 and 1.4 and 3.1 provide a summary of the most successful examples in the recent years in the identification of QS receptor antagonists in PA. The next section will focus on

antagonists of the PqsR regulatory protein in line with the work presented in this thesis.

1.7.3.1. PqsR inhibition

Although the search for inhibitors of the AHL QS system started a long time back, the search for inhibitors of the AQ-driven QS system in PA is a more recent occurrence. Since 2012, a number of molecules have been described to be able to antagonise PqsR (MvfR). The increasing understanding of the PqsR structure function has played a key role in the design and identification of these antagonists.

PqsR belongs to the LysR family of transcriptional regulators (LTTRs) that are prevalent in bacteria (263) where PA is found to possess a wide range of them (264). Proteins in the LTTR group usually hold a highly conserved *N*-terminal helix-turn-helix DNA-binding domain, and non-conserved highly distinctive co-inducer binding domain (CBD), binding low molecular weight molecules (figure 1.4). This protein structure is likely to confer PqsR not only with a stabilisation coupling (to agonists), by means of hydrophobic interactions, but also holds target-receptor pockets accessible to antagonists that can successfully compete for its occupancy.

In addition, these LTTRs can have distinct roles as stimulators or inhibitors of specific feedback loops in which the co-inducer ligand assumes pivotal participation in transcriptional control functions. As a LysR-type regulator, PqsR is predicted to form dimers associated into tetramers (dimer of dimers) (265) (266) (267) in which recognition and attachment to multiple binding sites, located in areas of the promoter and/or the operator region of different target genes, take place. These areas are the regulatory binding site (RBS), the LTTR box (consensus T-N_{11}-A) and the activation binding site (ABS).

Binding of the tetramer to these loci results in DNA bending and transcriptional initiation through interactions with the RNA polymerase) (263).

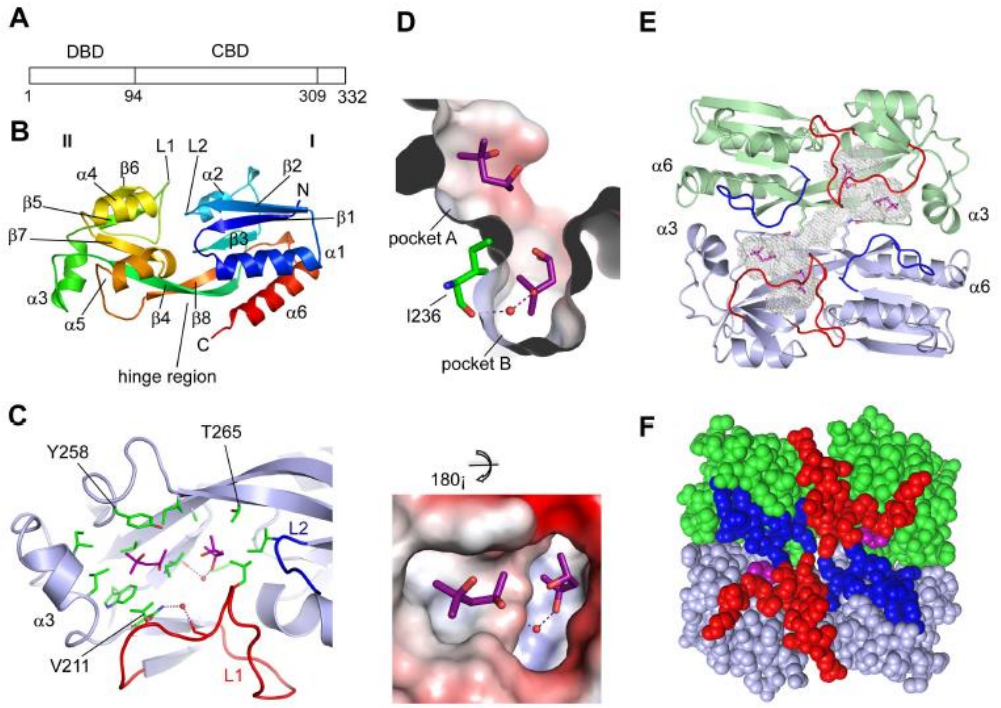


Figure 1.4. Crystal Structure of the PqsRCBD. (A) Diagrammatic representation of the linear PqsR protein showing the positions of the DNA-binding (DBD) and co-inducer-binding (CBD) domains; (B) Topology diagram of the PqsRCBD monomer consisting of two sub-domains and a hinge region; (C) PqsRCBD hydrophobic ligand-binding pocket with two bound 2-methyl-2,4-pentanediol (MPD) molecules shown as purple sticks; (D) Charged surface representation of the A and B pockets shown as two views related by a 180u rotation. Hydrogen bonds are shown as dotted lines and water molecules as red spheres; (E) The PqsRCBD dimer shown as a topology diagram with bound MPD molecules shown as sticks. Loops forming a lid are coloured red and blue. The Lys266 and Glu259 residues are shown as sticks with the salt bridge shown as a purple dotted line. The pocket shape is shown as a white mesh. (F) The PqsRCBD dimer shown as solid spheres with the same colour scheme.
Source: Ilangovan *et al* (2013) (268).

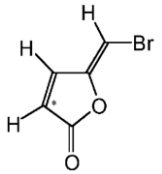
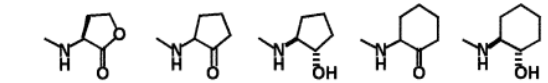
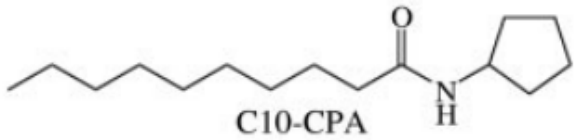
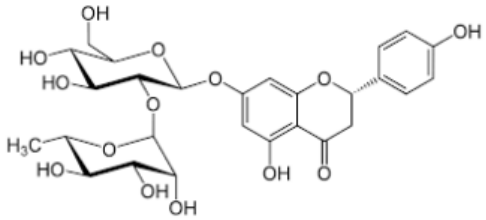
As a crucial element of the AQ-associated QS in PA, PqsR is critical for activation of genes responsible for the PQS biosynthesis, of its precursor HHQ and even activation of genes responsible for the biosynthesis of several C_9/NHQ-quinolones.

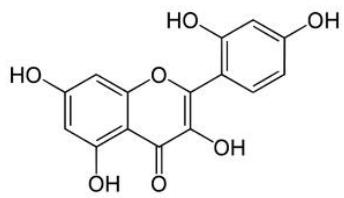
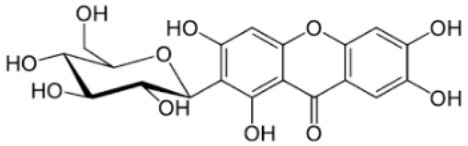
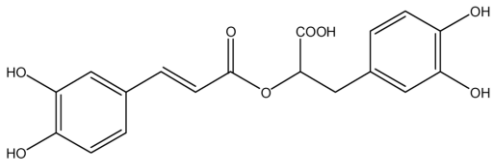
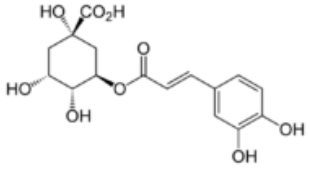
The PQS system plays a pivotal role in inducing and controlling virulence and consequently the pathogenicity of PA. Such assumption is based on

reportings linking management of PQS production and reduced virulence. For example where the mutated PQS-controlled virulence genes resulted in reduced pathogenicity by PA14 infections in different organisms (from plants, to nematodes, to insects) (167), or with PA *pqsR* mutants showing reduced mortality rate in thermally injured rodent models infected with 10^5 $mvfR^-$ bacterial cells (162), just to name a few. In these examples, the receptor PqsR arises as an immediate target protein when developing strategies to search for QSIs with disruptive role of the PQS-related gene expression.

For that matter, PqsR (the receptor of the PA-specific PQS QS system) is seen as the most enticing target to develop QSIs, to measure the effect of PqsR antagonists, and to understand the link between these novel drugs and a limited pathogenicity level. Details of the work carried out up to know in the development of PqsR antagonists are described in Chapter 3.

Table 1.3. List of selected inhibitors identified to interact with LasR ligand binding site of PA QS receptors. Since there is a vast literature available on LasR inhibitors, this selection focuses on compounds from synthesised molecules to natural products demonstrating specific inhibition of LasR.

QS inhibiting molecule	Target receptor	Activity	Source
Furanone 56 	Specific to PA las QS subsystem Represses *lasB*	Reduced elastase and chitinase activity Reduced stability of LasR	(269) (270)
3-oxo-C_{12}-(2-aminocyclopentanol)  X^1 = AI1 **1** **2** **3** **4** X^2 = AI2 **5** **6** **7** **8**	Probably unable to interact with RhlR	Inhibited *lasI*	(271)
N-Decanoyl cyclopentylamide 	Probably playing a role as effective competitor of autoinducer binding to LasR	Inhibition of *lasI/B* and *rhlA* inhibited production of virulence factors, including elastase, pyocyanin, rhamnolipid and biofilm formation without affecting growth	(272)
Naringin 	Docking to LasR and RhlR	All except mangiferin showed significant protease, elastase and hemolysin inhibition. All five compounds probably inhibit biofilm producing phenotypes.	(273)

Morin  **Mangiferin**  **Rosmarinic acid**  **Chlorogenic acid** 			

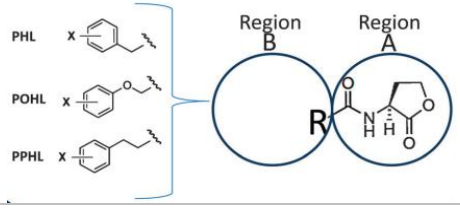
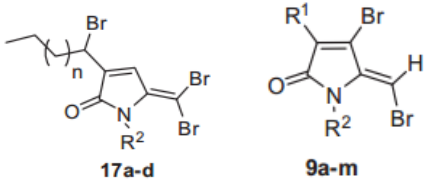
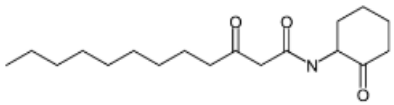
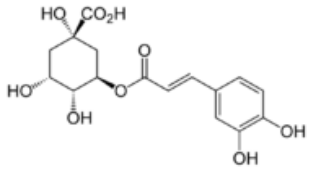
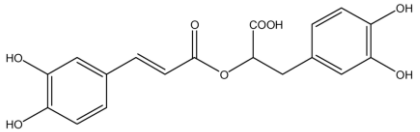
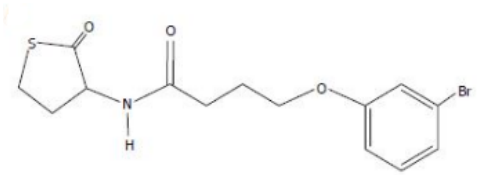
PHL, POHL and PPHL groups of active AHL analogs 	Pharmacophore pattern in region A is necessary for molecular recognition by the recipient LasR prior to folding process	POHL group with moderate antagonist activity	(274)
1,5-dihydropyrrol-2-one analogs [Compounds 17a and 9c]  **17a-d** **9a-m**	Both 17a and 9c dock to LasR: 17a directs its N-phenyl substituent into the pocket of LasR; 9c with a shallower positioning of the dihydropyrrol-one moiety, more approximate to the location occupied by the lactone part of 3-oxo-C_{12}-HSL.	17a very active (immediately followed by 9c) against *E. coli* AHL-monitor strain JB357 gfp that expresses *luxR-PluxI-gfp* in the presence of the AHL signalling molecule 3-oxohexanoyl-HSL.	(275)

Table 1.4. List of selected inhibitors identified to interact with RhlR ligand binding site of PA QS receptors. Since there is a vast literature available on LasR inhibitors, this selection focuses on compounds from synthesised molecules to natural products demonstrating specific inhibition of RhlR.

QS inhibiting molecule	Target receptor	Activity	Source
3-oxo-C_{12}-(2-aminocyclohexanone) 	Probably binds RhlR and stops C_4-HSL binding	Inhibited *lasI* and *rhlI*, pyocyanin, elastase and biofilm.	(271)
Chlorogenic acid  **Rosmarinic acid** 	Docking with RhlR	Chlorogenic acid inhibited protease (68%), LasB (65%) and biofilm production; Rosmarinic acid inhibited protease (87%), LasB (67%), hemolysin (60%) and biofilm production	(273)
Meta-bromo-thiolactone 	Attach to and inhibit RHlR receptors Induces conformational changes in LuxR-type receptors impairing their capacity to interact with RNA polymerase resulting in a reduction of the transcription activation rate	Inhibits PCN and biofilm formation mostly by means of partial repression of RhlR	(276)

1.8. Objectives

This thesis is divided in three interrelated investigations on the development of new PA detection tools, and on the efficacy of novel synthetic PqsR antagonists for repressing PA-associated virulent phenotypes.

The first objective of this thesis was the identification of novel inhibitors of the PqsR QS regulator. To accomplish it, *in silico* engineered small synthetic inhibitors were obtained from an industrial partner and assessed for PqsR antagonism in order to understand: a) their target interactions with QS-signalling pathways, b) the impact on the expression of virulence pathways that comprise the crux of pathogenic dynamics, c) the functional characterisation towards hit optimisation, by learning the potential of these PqsR antagonists as clinical antimicrobial drug candidates, d) their cytotoxicity towards model eukaryotic immune system T-lymphocyte cells, e) the value of synergistic interactions, and finally f) their thermodynamic binding signatures, established in the ligand-receptor interactions.

The second objective was the engineering of a PQS-based biosensor to be established in *E. coli* for the detection of PQS as a signature biomarker of early PA infections. Thus, representing a powerful tool for the rapid screening of clinical samples (sputum, plasma, urine, etc). The assembling of the biosensor accounted for two functional subsystems, an inducible one to regulate the production of PqsR, and a bioreporting one. The construct was intended to work as a single copy in the chromosome of *E. coli* using its natural replication and enhanced transcriptional control.

The third and final objective was the optimisation of the LESA-MS analytical technique as a rapid and highly specific means for screening PA QS-related molecules in dry bacterial extracts. A LESA-MS protocol was developed and implemented for detecting five pre-defined molecules from crude PA

extracts, namely *N*-butyryl-L-homoserine lactone (C_4-HSL), 2-heptyl-4-quinolone (C_7-HHQ), 4-hydroxy-2-heptylquinoline *N*-oxide (C_7-*N*-Oxide), C_7-PQS and *N*-(3-oxododecanoyl)-L-homoserine lactone (3-oxo-C_{12}-HSL).

Chapter 2
Materials and Methods

2.1. Bacterial strains

The bacterial strains used in this study are listed in Table 2.1.

Table 2.1. List of bacterial strains.

Strain	Properties	Reference source
Escherichia coli		
ECKR	*E. coli ΔsdiA, ΔlacI, Km^R, Amp^R*	Lab collection
ECKR02	*E. coli ΔsdiA, ΔlacI, Km^R, Amp^R* (clones number 369 and 370)	Lab collection
ECIL01	*E. coli ΔsdiA, ΔlacI, Amp^R*	This study
E. coli S17-λ1pir	*thi*, *pro*, *hsdR*, *hsdM+*, RP4-2-Tc::Mu-Km::Tn7, *λpir*	Simon *et al.*, 1983 (277)
E. coli DH5α	F-, φ80d*lacZΔM15*, Δ(*lacZYA-argF*)U169, *deoR*, *recA1*, *endA1*, *phoA*, *hsdR17*(rK-, mK+), *supE44*, *thi-1*, *gyrA96*, *relA1*	GibcoBRL, Life Technologies
Pseudomonas aeruginosa		
PAO1-N	PAO1 wild-type, Nottingham strain	Holloway collection
PAO1-L	PAO1 wild-type, Lausanne strain	ATCC 15692
PAO1-N pMiniCTX::P*pqsA-lux*)	*pqsA* promoter *lux*-based reporter fusion in PAO1; TcR	Ilangovan *et al.*, 2013 (278)
PAO1-N Δ*pqsH*	In-frame chromosomal deletion of *pqsH* in PAO1	Fletcher *et al.*, 2007 [205]
PAO1-N Δ*pqsE*	In-frame chromosomal deletion of *pqsE* in PAO1	Rampioni *et al.*, 2010 [104]
PAO1-N Δ*lasI*	In-frame chromosomal deletion of *lasI* in PAO1	Giordano Rampioni, unpublished
PAO1-N Δ*lasR*	In-frame chromosomal deletion of *lasR* in PAO1	Steven Higgins, unpublished
PAO1-N Δ*rhlI*	In-frame chromosomal deletion of *rhlI* in PAO1	Giordano Rampioni, unpublished
PAO1-N Δ*rhlR*	In-frame chromosomal deletion of *rhlR* in PAO1	Rampioni *et al.*, 2010 [104]

PA14	Clinical isolate UCBPP-PA14	Rahme *et al*., 1995 (165)
PAO1-N *lecA::lux*	*lecA::luxCDABE* genomic reporter fusion in PAO1	Winzer *et al*., 2000 (279)
PAO1-N *lecB::lux*	*lecB::luxCDABE* genomic	Lab collection
PAO1-N *pqsE*ind	PAO1 with *pqsE* under the control of a P*tac* promoter	Rampioni, *et al*., 2010 (160)
PAO1-N *ΔpqsA ΔpqsR*	Double *pqsA pqsR* inframe deletion mutant derived from PAO1	Lab collection
SED2-LES	Isolate LES (Liverpool Epidemic Strain) is one of the 44 haplotypes of PA isolated from a chronically infected CF patient. It is also the laboratory reference isolate for the (LES) analysis conducted by Sophie e. Darch.	Kindly provided by Sophie Darch) for more information access Darch *et al*, 2015 (280)
PAO1-N *pKm::CTX-luxCDABE*	Kanamycin promoter fused to a *lux* reporter	Lab collection
PAO1-L *mCherry::luxCDABE*	*mCherry* fusion to a *lux* reporter	Lab collection

2.2 Plasmids

All plasmids used in this study are listed in Table 2.2.

Table 2.2. List of plasmids.

Name	Description	Reference source
***pminiCTX::ppqsA-lux* fusion**	Plasmid from *E. coli S17-λ1pir* containing a *miniCTX-lux::PpqsA* fusion used in generating pIL001 by ligation of fragment of interest to a pBluescript backbone	Lab collection
pFLP2	FRT recombination plasmid with ß-lactam selection and SacB counterselection	Hoang *et al*, 1998 (281)
pIL001	*E. coli* DH5α::pIL001 (*PpqsA*) [pBluescript backbone]	This study
pCR3	Plasmid pCR3 is a 5.06 Kb parental mammalian expression vector for TA cloning of PCR products. Based on pUC6S. Contains *lacI^{q}*, *Ptac* and *pqsR* for generating pIL002.	Lab collection
pIL002	*E. coli* DH5α::pIL002 (*lacI^{Q}*, *Ptac-pqsR*)	This study

	[The background plasmid consists of a fusion between pCR3 and pUC6S]	
pBS	pBluescript II KS (+) cloning vector; ColE1 replicon; ApR	Stratagene
pBluelux	Cloning vector containing luxCDABE: Ap^R	Atkinson *et al.*, 2008 (282)
pUC18R6KT mini-Tn7T-Tc (mini-Tn7)	Plasmid obtained from *E. coli S17-λ1-pir* (strain 211)	Choi *et al.*, 2005 (283)
pIL003L	*E. coli* DH5α::pIL003 (*lacI*^{Q}, *Ptac-pqsR*, P*pqsA-luxCDABE*) [A small 22bp linker containing SalI restriction site inserted right after the *PpqsA*] Cb, Ap	This study
pHP45Ω	Source of the omega cassette with transcription and translation termination signals, $Sm^R/Sp^R/Cb^R$	Prentki and Krisch, 1984 (284)
pIL004	*lacI*^{Q}*, Ptac-pqsR, PpqsA-luxCDABE* [there is a Km^R-omega transcription terminator between *lacI*^{q} and *PpqsA*)	This study
pTNS2	*Ap*^{R}*, R6K* replicon, plasmid expressing *tnsABCD* from *Plac*	Choi *et al.*, 2005 (285)
pIL005	(*lacI*^{Q}, *Ptac-pqsR*, *PpqsA-luxCDABE*) [there is a Km^R-omega transcription terminator between *lacI*^{Q} and *PpqsA*)	This study
pMiniCTX-lux	Promoter-probe vector containing the *luxCDABE* operon; Tc^R	Becher and Schweizer, 2000 (286)
pMiniCTX::pqsA-lux	Reporter plasmid containing the *pqsA* promoter region fused to the *lux* reporter; Tc^R	Diggle *et al.*, 2007 (153)
pUCP18	pUC18-derivative containing a stabilising fragment for maintenance in *Pseudomonas;* Ap^R, *E.coli*/Cb^R, *P. aeruginosa*	Schweizer, 1991 (287)
pME6032	Cloning and expression vector derived from pVS1, containing the *Ptac* promoter (Tc^R)	Heeb et al., 2002 (288)
pBluescript-II KS+	pBluescript KS cloning vector; ColE1 replicon (Ap^R)	Stratagene

2.3 Oligonucleotide primers

Oligonucleotide primers were synthesised by Sigma (UK) and Eurofins (UK). Where necessary, restriction sites were incorporated into the 5' end of

the primer to aid cloning of the PCR product. Primer sequences are listed in Table 2.3.

Table 2.3. Oligonucleotide primers used in this study.

Primer	Sequence (5' to 3')	Function
FW lacI	GCGGTATGGCATGATAGCG	Forward primer to amplify the *lacI* fragment
RV lacI	AAGCCTGGGGTGCCTAATG	Reverse primer to amplify the *lacI* fragment
IL-PPQSAFw	TATAAGCTTAGTACTTACGC AATGGGATTTCAACA	Forward amplification of ppqsA from *E. coli S17-λ1pir::mini CTX-lux::PpqsA*
IL-PPQSARv	TATCTGCAGTCAGCGATAT GCATCCGGAT	Reverse amplification of ppqsA from *E. coli S17-λ1pir::mini CTX-lux::PpqsA*
Forward linker PTc	CTTCTCATGTTTGACAGCTT ATCATCGATAAGCTTTAATG CGGTAGTTTATCACAGTTA AATTGCTAACGCAGTCAGG CACCGTGTAGGAGGCCGC	Oligo containing a SalI restriction site in its sequence to combine with the reverse linker
Reverse linker PTc	GGCCTCCTACACGGTGCCT GACTGCGTTAGCAATTTAA CTGTGATAAACTACCGCATT AAAGCTTATCGATGATAAG CTGTCAAACATGAGAAGAG CT	Oligo containing a SalI restriction site in its sequence to combine with the forward linker
Newomegfor-xhoI	AGACCTCGAGCCGGGGATC CGGTGATTGAT	Ω bidirectional termination fragment Forward primer
Newomegrev-xhoI	AGACCTCGAGCCCGGGGAT CCGGTGATTGA	Ω bidirectional termination fragment Reverse primer
MauBIPmeIEm7pqsR FW	ACGAACGCGCGCGGTTTAA ACCACGTGTTGACAATTAA TCATCGGCATAGTATATCG	Forward primer of the oligos designed to add the Em7 constitutive promoter

	GCATAGTATAATACGACTC ACTATAGGAGGAGGGCCA CCATGCCTATTCATAACCTG AATC	
SFilEm7pqsRT7term Rv	AGCAGGGCCTTGCAGGCCC CTGCAGGTAGCATAACCCC CTACTCTGGTGCGGCGCGC TGG	Reverse primer of the oligos designed to add the Em7 constitutive promoter
pTac FW	TTGACAATTAATCATCGGCT CGTAT	Forward primer of the oligos designed to verify the presence of the *pTac/pqsR* fusion
pqsR FW	ATGCCTATTCATAACCTGAA TCACG	Forward primer of the oligos designed to verify the presence of the *pqsR/Tn7L* fragment
pqsR RV	CTACTCTGGTGCGGCGCGC TGGCGG	Reverse primer of the oligos designed to verify the presence of the *pTac/pqsR* fusion
luxC FW	TATAGGGAAAATAATGAAT AAATGT	Forward primer of the oligos designed to verify the presence of the *luxC/pqsA* fusion
pqsA RV	TCAGCGATATGCATCCGGA TCAGGA	Reverse primer of the oligos designed to verify the presence of the *luxC/pqsA* fusion
glmS	TGCGACGTCGAAATCGCC	Forward primer of the oligos designed to verify the presence of the *glmS/Tn7R* fragment
phoS	CAGACCGATCGGCCATTTT AC	Forward primer of the oligos designed to verify the presence of the *phoS/Tn7L* fragment
Tn7L	ATTAGCTTACGACGCTACA CCC	Reverse primer of the oligos designed to verify the presence of the *phoS/Tn7L* and *pqsR/Tn7L* fragments
Tn7R	CACAGCATAACTGGACTGA TTTC	Reverse primer of the oligos designed to verify the presence of the *glmS/Tn7R* fragment

2.4. General Chemicals

All general chemicals were obtained from Sigma (UK) unless otherwise stated.

2.4.1. Antibiotics and IPTG

Stock solution of antibiotics were prepared according to Sambrook (1989) (289) and stored at -20°C. The ampillicin (Ap) and carbenicillin (Cb) antibiotics were used from 50 mg/ml stock solutions prepared in 50% (v/v) EtOH, tetracycline (Tc) was used from either 50 mg/ml or 10 mg/ml solutions that were prepared in MeOH, kanamycin (Km), streptomycin (Sm) and spectinomycin (Sp) from 50 mg/ml solutions made in dH2O.

The work concentrations in growth media of antibiotics used for selection and maintenance of bacterial plasmids were as follows: Ap 100 µg/ml (*E. coli*); Cb 400 µg/ml (*P. aeruginosa*); Tc 10 µg/ml (*E. coli*) and 125 µg/ml (*P. aeruginosa*); Sm 100 µg/ml (*E. coli*); Sp 100 µg/ml (*E. coli*).

For inducing expression of genes under the control of the *tac* promoter, isopropylthio-β-D-galactosidase (IPTG) was added to growth media at a final concentration of 0.1 mM, from a 10 mM stock solution made in dH2O, unless stated otherwise in specific studies.

All reagents were filter-sterilised before use by means of passin them through 0.22 µM Sartorius Minisart filters.

2.4.2. Synthetic AHLs and AQs

Synthetic AHLs and AQs were supplied by Alex Truman and Siri Ram Chhabra from the School of Pharmaceutical Sciences, University of Nottingham. Compounds were kept as 10 mM stocks in MeOH as described by Pesci *et al* (1999) (143) and Chhabra *et al* (2003) (290) and stored at -20°C.

2.5. General procedures

2.5.1. Growth media preparation

Unless otherwise stated, growth media was prepared using dH_2O previously autoclaved at 121°C for a period of 20 minutes and at a pressure of 15 p.s.i.

2.5.1.1. Luria Bertani (LB) medium

LB broth medium was prepared as follows: tryptone (Bacto) 10 g/L, yeast extract (Oxoid) 5 g/L and sodium chloride 10 g/L in distilled water prepared as described in Sambrook (1989) (289) (Sambrook *et al*., 1989).

LB agar medium was prepared by adding 1.5 % (w/v) Technical Agar No. 3 (Oxoid) to LB broth.

2.5.1.2. M9 minimal medium

M9 minimal media was prepared as follows: 200 ml of 1 x M9 salts (0.3 % (w/v) potassium phosphate monobasic, 0.6 % (w/v) disodium phosphate monohydrate, and 0.05 % (w/v) sodium chloride were supplemented with 2 ml of ammonium chloride (1.87 M), calcium chloride (20 µM), magnesium sulphate (202.72 mM), glucose (2 M) and adjusted to pH 7.2. Glucose or succinate was supplemented as carbon source at 10 mM and 1 mM, respectively.

2.5.1.3. RPMI-1640-based cell culture media (CCM)

For a total volume of 50 ml of CCM the following steps were taken: 500 µl of a penicillin/streptomycin mixture were added to 500 µl of L-glutamine and 5 mL of foetal calf bovine serum. The whole mixture was made up to 50 ml with the addition of L-glutamine free RPMI-1640 medium.

2.5.2. Growth and storage of bacterial strains

All strains were routinely grown in LB broth or on LB agar unless stated otherwise.

Liquid cultures were grown in LB broth with agitation at 200 rpm in a Gallenkamp static incubator (Gallenkamp Ltd., UK) at 37 °C unless otherwise stated. Growth of bacterial cultures was monitored by absorbance at a wavelength of 600 nm (optical density, OD_{600}) using a Novospec II visible spectrophotometer (Pharmacia LKB Ltd., Cambridge, UK).

2.5.2.1. Small and large scale growth of bacterial strains

Bacterial cultures were routinely grown in LB in a 37°C shaking incubator, with agitation at 200 rpm unless otherwise stated. Growth of bacterial cultures was monitored by means of measuring absorbance at a wavelength of 600 nm (optical density; OD_{600}) using a Novaspec II Visible Spectrometer (Pharmacia LKB Ltd, Cambridge, UK), or an automated luminometer-spectrometer (Tecan Infinite 200).

Bacteria developed in larger culture volumes was grown in sterile Erlenmeyer flasks, with the volumes of culture being at a maximum of 10 % of the total volume of the flask (for adequate culture aeration) and a standard bacterial culture inoculum of OD_{600} equal to 0.01, unless otherwise stated. Small scale bacterial cultures developed in UV-sterilised microtitre plates were set up using 200 µl total culture volumes and an initial bacterial inoculum of OD_{600} equal to 0.01 or 0.05 (according to individual assay specifications). Both large and small cultures were incubated statically at 37°C, unless otherwise stated.

2.5.2.2. Long-term storage and revival of bacterial strains

All bacterial strains were stored in 2 ml microtubes (Sarstedt, Germany) as a cryo-preserved sample at -80°C in LB medium containing 50% (v/v) glycerol, and revived by streaking onto LB agar [15% (w/v) Oxoid technical agar No3 in LB] with posterior overnight incubation at 37°C.

2.5.3. DNA qualitation and quantification

The Nanodrop ND-1000 (Nanodrop Technologies) was used to measure DNA concentrations and purity rate by testing 1 µl liquid samples.

2.5.4. DNA manipulation

2.5.4.1. Isolation of chromosomal DNA

Genomic DNA was isolated with the use of the Wizard Genomic DNA Purification Kit (Promega, UK) as described in the manufacturer's guidelines and briefly summarized as follows: Pelleted bacterial cells from a 1 ml overnight culture were lysed after being thoroughly resuspended in 600 µl nuclei lysis solution and incubated at 80°C for 5 min. After cooling to room temperature, 3 µl RNase solution was added and the samples were incubated at 37°C for 1 hour. 200 µl protein precipitation solution was added and the samples were incubated on ice for 5 min, then the precipitated proteins were pelleted out of solution via centrifugation in a microcentrifuge (Heraeus Pico Biofuge) at 16,060 x g for 3 min. The supernatant was mixed with 600 µl of isopropanol, to precipitate the DNA, and was centrifuged at 16,060 x g for 3 min and the resulting supernatant was subsequently discarded. 600 µl of 70 % (v/v) ethanol was added for washing the remaining pellet and was centrifuged at 16,060 x g for 2 min; the supernatant was then removed and the pellet was left to dry. 100 µl of rehydration solution was added to the resulting DNA pellet and was incubated at 65°C for 1 hour.

2.5.4.2. Isolation of plasmid DNA

High-copy number plasmid DNA was isolated using the Qiagen Miniprep Kit (Qiagen, UK) as briefly summarized as follows: Pelleted bacterial cells from 5 ml overnight cultures were thoroughly resuspended in 250 µl Buffer P1. 250 µl of Buffer P2 was added to lyse the cells under alkali conditions and then the subsequent lysate was neutralised with 350 µl of Buffer N3. Centrifugation at 16,060 x g for 10 min separated the cell debris. The lysate was then applied to a silica gel membrane to which the plasmid DNA bound in high-salt conditions. The membrane was washed with 500 µl Buffer PB to ensure plasmid stability,

then with 750 µl of Buffer PE to allow the removal of salts. The plasmid DNA was eluted using RNase-free distilled water (Fischer-Scientific, UK). On occasion, the GenElute Plasmid Miniprep Kit (Sigma Aldrich, UK) was also used to isolate plasmid DNA using the same alkaline-lysis and silica membrane isolation procedure.

Low-copy number plasmid DNA was isolated as described in the manufacturer's instructions with the Qiagen Plasmid Midi Kit (Qiagen, UK). This method uses a similar modified alkaline lysis procedure followed by membrane DNA isolation under low salt conditions and elution of the DNA under high salt conditions.

2.5.4.3. DNA ligation

PCR products were purified and digested (if required) before being ligated into the appropriate vectors. Ligations were routinely performed using 1:2 or 1:3 ratios of vector to insert concentrations. The manufacturer's guidelines were followed when using the pGEM-t easy vector system (Promega, UK), with ligations carried out in a total volume of 10 µl and with samples incubated on melting ice overnight. Other ligation reactions were prepared in a total volume of 20 µl, containing 0.5 µl T4 DNA ligase (3 u/µl Promega, UK or NEB, USA) and 2 µl 10x T4 ligation buffer. Samples were incubated on melting ice, overnight.

2.5.4.3.1. DNA restriction enzymes

Restriction enzymes (Promega, UK) were used according to the manufacturer's instructions. The digestion reactions were set up in a total volume of 20 µl with contents including 0.5-1 µg of DNA, 0.5-1 µl restriction enzyme, 2 µl of the appropriate restriction buffer, with the remaining volume

made up with nuclease-free water. Samples were incubated at 37°C for 1-4 hours before being analysed on 0.5-1 % (w/v) agarose gels prior to gel extraction using the Qiagen Gel Extraction Kit (Qiagen, UK).

2.5.5. DNA agarose gel electrophoresis

DNA loading buffer was added to the DNA samples that were run on 0.5-1 % (w/v) agarose gels in horizontal gel apparatus (Biorad, UK). The gels were prepared according to the methodology described in Sambrook (1989) (289), using analytical grade agarose (Sigma Aldrich, UK) in 1x TAE buffer and with a final concentration of 10 µg/ml ethidium bromide. The gels were run in TAE buffer at voltage of 100-120 V. DNA bands were observed using a UV-transilluminator (UVP, USA), and when DNA fragments were required for subsequent applications, the corresponding bands were extracted from the agarose gels using the Qiagen Gel Extraction Kit (Qiagen, UK).

2.5.5.1. DNA molecular weight markers

To determine and establish the sizes of DNA fragments on agarose gels, 1 µg of DNA ladder solution was mixed with DNA loading buffer. The markers used were 1 kb DNA ladder (Promega, UK), 1 kb DNA ladder (New England Biolabs, UK), 100 bp DNA ladder (Promega, UK) and the 20 Kb HindIII-lambda DNA marker.

2.5.5.2. Extraction and purification of DNA from agarose gels

DNA products were excised from agarose gels and purified according to the manufacturer's guidelines using the Qiagen Gel Extraction Kit (Qiagen, UK) as briefly summarized as follows: 3 gel volumes of Buffer QG were added to 1

agarose gel volume slice and were incubated at 50°C for 10 min to allow the gel to melt. 1 gel volume of isopropanol was subsequently added. The reaction mixture was applied to the silica membrane of a QIAquick column and centrifuged at 16,060 x g for 1 min. Wash steps were undertaken with 500 µl Buffer QG and 750 µl Buffer PE with centrifugation at 16,060 x g for 1 min, before the DNA was eluted with 30-50 µl RNase-free sterile water (Fischer-Scientific, UK).

2.5.6. Polymerase Chain Reaction (PCR) amplification

PCR amplifications were carried out in final 50 µl volumes and as described by Saiki *et al* (1988) (291). General PCR reactions contained 0.5 µl *Taq* polymerase (5 u/µl) in 10 µl of 5x Flexi Buffer (Promega, UK), 2 mM MgCl2, 1 µM of each oligo primer, 50 µM dNTPs, and DNA template. The DNA template consisted of a final concentration of 0.04 % (v/v) genomic DNA or whole bacterial cells transferred from a fresh colony. The PCR reactions were carried out in a Progene PCR Thermal Cycler (Techne) for a total of 30 cycles. Briefly, the DNA was denatured at 94°C for 5-10 min, followed by 30 cycles of denaturation at 94°C for 30 s, annealing at 55-58°C for 30 s and elongation at 72°C for 0.5-6 min depending on the length of DNA to be amplified (~1 kb per min). The annealing temperature was adjusted depending on the nature of the primers used. PCR reaction mixes were subsequently cooled to 4°C until needed.

2.5.5.7. Purification of PCR products

PCR products were purified with the use of DNA agarose gel electrophoresis and extractions with the Qiagen Gel Extraction Kit (Qiagen, UK), or via the use of the Qiagen PCR Purification Kit (Qiagen, UK). Manufacturer's guidelines were followed and are hereby briefly summarised: 5 volumes of

Buffer PB were added to the PCR reaction mixes. Samples were loaded onto QIAquick silica membrane columns and were centrifuged at 16,060 x g for 1 min. The column was washed with 750 µl Buffer PE, with the PCR products being eluted with 30-50 µl RNase-free sterile water.

2.5.5.8. Cloning of PCR products

Purified PCR products were digested overnight at 37°C with the relevant restriction enzyme(s) and using the appropriate buffer. The digested PCR fragments were ligated into an appropriate vector and electroporated into *E. coli* DH5α. Transformants containing recombinant clones were identified by 1) antibiotic resistance screening on LB agar plates containing the appropriate antibiotics, and 2) restriction digestion of their minipreped plasmids.

2.5.5.8.1. DNA sequencing

2.5.5.8.1.1. Obtaining DNA sequence data

Routine DNA sequencing was performed by the DNA Sequencing Laboratory, at the Queen's Medical Centre, University of Nottingham, using the Applied Biosystems BigDye® Terminator v3.1 Cycle Sequencing Kit and 3130xl Genetic Analyzer.

2.5.5.8.1.2. DNA sequencing analysis

Sequencing data was analysed using BLAST programs available on the NCBI website (http://www.ncbi.nlm.nih.gov/). *Pseudomonas* sequences were also analysed using information on the Pseudomonas Genome Sequence Database (http://www.pseudomonas.com/).

2.5.5.9. Transformation

2.5.5.9.1. Preparation of electrocompetent *E. coli* cells

To prepare competent cells of *E. coli*, a 1 % (v/v) inoculum from an overnight *E. coli* culture was added to 100 ml of sterile Nutrient Yeast Broth (2.5 % (w/v) Nutrient broth No.1, 0.5 % (w/v) Yeast Extract) in a 1 L conical flask and grown at 37 °C, 200 rpm to an OD_{600} of 0.4-0.8 (approx 6 h). Cells were harvested by centrifugation at 5500 rpm (JA-14, Beckman) for 10 min at 4°C and washed four times in sterile ice cold along with 10% (v/v) glycerol containing 1 mM MOPS (4-morpholinepropanesulfonic acid) before being resuspended in 1 ml of the same buffer. Cells were aliquoted into 50 µl samples, flash frozen in liquid nitrogen and stored at -80°C in microcentrifuge tubes.

2.5.5.9.2. Electroporation of *E. coli* cells

For electroporation of DNA into *E. coli* cells, salts were firstly removed from the DNA solution by filter dialysis using 0.025 µm millipore filters (Millipore Corporation, USA) for at least 20 min. Electroporation was then performed in 0.2 cm electrode gap Gene Pulser cuvettes (BioRad, UK) containing 50 µl of competent cells and 2-3 µl dialysed DNA. An electroporation pulse of 2.5 kV was delivered using the BioRad Gene Pulsar connected to a BioRad pulse controller (BioRad, UK). A 1 ml aliquot of pre-warmed (37 °C) LB broth was added to the cells which were then incubated at 37°C for 1 h in the absence of antibiotics. Aliquots of cells were subsequently plated onto LB agar plates containing appropriate antibiotics to select for transformants, and grown overnight at 37°C. Controls of electroporated cells (containing no plasmid and transformed separately with undigested plasmid) were prepared in a similar manner.

2.5.5.9.3. Preparation of electrocompetent *Pseudomonas aeruginosa* cells

For the preparation of PA electrocompetent cells, 1 ml of bacterial overnight culture was pelleted at 16,060 x g for 1 min. The cells were washed 3 times with 1 ml of 10 % (v/v) glycerol, and consequently resuspended in a final volume of 50 µl 10 % (v/v) glycerol. Whenever found necessary, the cells were flash-frozen in liquid nitrogen before being stored at -80°C.

2.5.5.9.4. Electroporation of electrocompetent PA cells

Transformation of plasmid DNA into PA electrocompetent cells was performed as described in section 2.5.5.10.2.

2.6. Quorum sensing signaling molecules (QSSM) analysis

2.6.1. QSSM extractions from bacterial supernatants

To assess strains for the production of AQ and AHL QSSMs, flask cultures containing LB broth were inoculated with 1 in 100 dilutions of OD_{600} equal to 1.0 and cultures grown overnight with incubation at 37°C and agitation at 200 rpm. At appropriate time points (8 h and 24 h unless otherwise stated) fractions of the cultures were taken and pelleted by centrifugation at 9,838 x g, 4°C for 10 min. The supernatants were filter-sterilised into clean tubes via passing them through 0.22 µM Sartorius Minisart filters. Supernatants were then acidified to pH 2.0 using HCl, filter-sterilised again and were incubated at 37°C, 200 rpm, for 24 hours (unless otherwise stated). Acidified ethyl acetate was

then added to the supernatants, a volume equal to that of the supernatant used. The mixtures were then vigorously vortexed for 30-120 seconds before being centrifuged to separate the organic and aqueous phases. The organic phase was subsequently transferred into clean glass jars. The supernatants were subjected to 3 extractions, after which the obtained extracts were evaporated to dryness using a centrifugal evaporator (RCT 1022, Jouan). 1.2 ml of MeOH was then added to the samples which were transferred to sterile eppendorf tubes and evaporated to dryness once again.

The samples were reconstituted in 50 µl MeOH for subsequent analysis via liquid chromatography-mass spectrometry (LC-MS). Blank growth media was also extracted to be used as a negative control. Unless otherwise stated, 1 ml of culture supernatants was extracted for LC-MS analysis. Samples quantified via LC-MS analysis were supplemented with known amounts of internal standard compounds (5 µl of 10 µM deuterated PQS and 5 µl of 10 µM deuterated *N*-pentanoyl-L-homoserine lactone) prior to the extraction procedure to verify extraction efficiency and calculate loss of analytes during the procedure.

2.6.2. Liquid chromatography-mass spectrometry for detection of QSSM

LC-MS analysis was performed using a method developed by (292) on QSSM extracts from various PA wild type and mutant cultures. Three QSSM extracts from separately grown bacterial cultures were analysed for each strain. Reverse phase liquid chromatography (RP-HPLC) using a Phenomenex Gemini (C18, 5 µM, 250 x 2.00 mM) column was coupled with MS (Applied Biosystems 4000 Q-TRAP) and eluted with a 10- 99 % (v/v) (acetonitrile + 0.1 % (v/v) formic acid)/ (H_2O + 0.1 % (v/v) formic acid + 200 µM EDTA) gradient. The fragmentation ions of each of the anticipated alkyl quinolones (AQs) were recorded using Multiple Reaction Monitoring Triggered Traps (MRMTT).

Calibration curves from extracted spiked media containing 0.2-500 µM of stock QSSMs were performed for each molecule, allowing accurate quantification of the levels of QSSM in the extracted culture samples by comparison.

Analysis to quantify AQs in bacterial supernatant extracts using LC-MS/MS

Samples were sequentially injected into the HPLC and undergone a chromatographic separation. The MS was set up in MRM mode to constantly screen the eluent from the LC column for all the HSL and AQ analytes of interest.

1. For analysis, 5 µl of each prepared sample was injected into the LC system flowing at a constant 450 µl/min. A mobile phase gradient was applied. The initial 1 min after injection is an isocratic flow of 10% B, followed by a linear gradient to 50% B over the next 0.5 min. The linear gradient continues to 99% B over 4 min and is maintained at this composition for 1.5 min. The column was then re-equilibriated for 2.9 min at the initial starting composition. The column oven is maintained throughout the run at 50°C. The LC flow is diverted away from the MS at all times other than the period from 1 to 7 min.

2. Parameters that the MS was set to are: curtain gas 20, nebuliser gas (GS1) 30 and turbo gas (GS2) 10. The ion source potential is held at 5 KV and the temperature is set at 450°C. The declustering potential and collision energies are analytical parameters that are unique to each analyte. A list of these, along with the precursor and product ions used to set up an MRM for each individual analyte is contained in Table 2.4.

3. During data analysis Analyst software was used for automatic peak identification and integration. For each analyte a calibration line was constructed by calculating a mean peak area/IS ratio for the three replicate calibrants and plotting this value against concentration. The observed results

for the quality control standards can be used to ensure that the overall quantitative process provides a result that is suitably accurate and precise. Quantitative results for PAO1 supernatant samples are determined from the calculated peak area/IS ratio for each observed analyte, and the known slope and intercept of the corresponding straight line calibration graph.

Table 2.4. List of individual analytes, and their precursor and product ions, used to set up the LC-MS analysis.

Analyte	Precursor Ion (m/z)	Product Ion (m/z)	Declustering Potential (V)	Collision Energy (eV)
C_4-HSL	172.1	102.1	26	15
HHQ	244.1	159.1	31	20
HQNO	260.1	159.1	71	32
C_7-PQS	260.1	175.1	71	22
3-oxo-C_{12}-HSL	300.1	102.1	35	19
C_5-HSL-d_9[a]	195.1	103.1	40	15
PQS-d_4[a]	264.1	179.1	80	42
[a] Internal standards				

2.7. Virulence phenotype assays

2.7.1. Determination of bioluminescence and optical density of *lux* bioreporter strains using microtitre plate

Bioluminescence and optical density were monitored simultaneously in 96 well microtitre plates using the Tecan Infinite 200 microplate reader. Unless stated otherwise, the usual OD_{600} ranged from 0.05 to 1.0 where the bacterial overnight cultures were diluted in growth media and the assays were performed at 37°C. The software program measured optical density at 600 nm

and luminescence in relative light units (RLU) individually from all wells, for periods of 30 min during 24 h, unless stated otherwise.

2.7.2. Quantification of Pyocyanin in overnight bacterial extracts

Pyocyanin was prepared from late stationary phase cultures of PA grown in LB broth based on protocols established in Chang and Blackwood (1969) (293) and Ingledew and Campbell (1969) (294). Overnight bacterial cultures were standardised to OD_{600} of 1.0 before being diluted 1 in 100 in 50 ml LB broth and grown in either 200 or 500 ml flasks at 37°C, with shaking at 200 rpm, for 24 h. A 4.5 ml volume of chloroform was added to 7.5 ml filter sterilised culture supernatant and was vortexed for 10 seconds. 3 ml of the resulting blue coloured chloroform layer was transferred to a fresh tube and mixed with 1.5 ml of 0.2 M HCl. After vortexing for 10 seconds, the sample was centrifuged at 9,383 x g, at 4°C for 2 min and the top pink layer (containing 0.2 M HCl) was removed for subsequent absorption reading at 520 nm using a spectrophotometer (Novaspec II; Pharmacia). Pyocyanin levels were measured using an assay based on the method by Essar *et al* (1990) (295) where pyocyanin concentration (µg/ml) was calculated by multiplying the previously obtained absorption value by 17.072 and then again by 1.5 (as only 3 ml out of a possible 4.5 ml of chloroform were taken and used in the experiments). Assays were repeated in triplicate and error values represent 1 x standard deviation from the mean (95% Confidence Interval).

2.7.3. Biofilm assay using glass chamber slides

Overnight bacterial cultures were standardised to OD_{600} of 1.0 with LB broth and inoculates of 500 µl were presented to test concentrations of QSIs. These were subsequently incubated in Thermo Scientific™ Nunc™ Lab-Tek™ II Chamber Slides with shaking at 200 rpm, at 37°C for 48 hours. After the

incubation period the liquid remaining in the chamber slides was carefully removed for posterior analysis. The chamber slides were examined for biofilm growth using a Zeiss LSM 700 confocal laser scanning microscope (Carl Zeiss, Ltd, Welwyn, UK), with a laser wavelength of 405 nm and using the 40x objective, water immersion and the rhodamine filter, with the pinhole diameter, gain and laser detection settings (465-700 nm) adjusted for each individual image in order to optimise the sharpness and focus. ImageJ software and Microsoft Excel were used to analyse the images.

It is important to bear in mind that in Chapter 3 some of the technical concepts concerning the biofilm inhibition are based on Comstat2.1, the software used in analysing the obtained data; thus a short definition of their meaning is hereby provided. By biofilm is understood the collected voxels containing biomass. The biomass is presented as volume per area ($\mu m^3/\mu m^2$) and designates the voxels with a grey level above the threshold. In calculating the biomass the connected volume filtering (filtering of the biomass containing voxels that have a physical connection to the substratum) is applied automatically by means of Otsu's Method (296). The connected volume filtering only considers being biofilm the biomass connected to the substratum. Thus, interstitial layers detached from the substratum are therefore ignored by the automatic calculations. This is in correlation to what is desired from the compounds, i.e., a disintegrative effect of the biofilm matrix hence producing a ruptured structure.

Even though the software used in analysing the biofilm formation, Comstat2, can analyse several channels from a single stack of images, no correlation between the channels is actually performed by the program. Thus, contradictory results may appear, for example, when biomass is recorded in more than one channel due to fluorescence cross-talk. Then, the total number of biomass filled pixels in some slices may exceed the number of pixels available if summing/adding up all read channels. In this analysis and whenever possible,

a minimum of three and a maximum of five readings per biofilm were produced.

2.8. Cytotoxicity assays

2.8.1. Alamar Blue lymphocyte proliferation assay

100 µL of the individual treatments were added to the tissue cultures distributed in a 96 well plate. The 100x Alamar Blue was diluted to a 10x solution with 1M phosphate buffer and 10µL of the 10x Alamar Blue/Phosphate buffered saline (PBS) solution was transferred to each well and incubated at 5% CO_2 and 37°C. The incubation period used was of 24 h but a minimum of 12 h incubation should be respected. After incubation small volumes of the samples were transferred to a micrititer plate and two absorbance readings were established: 1) the culture absorbance was read at 570 nm and the obtained value subtracted by the 2) absorbance read at 600 nm that provides the background noise reading. Another optional way is to measure the fluorescence with an excitation of 530 nm and an emission wavelength of 590 nm. Note that for a kinetic protocol, a plate reader that can incorporate a lid is necessary, whereas for an endpoint protocol a standard microtitre plate reader is acceptable. For quality control purposes, a blank without the addition of Alamar Blue was used for working out if there was any absorbance interference from the culture media.

2.8.2. Flow Cytometry cytotoxicity assay

1 ml of an $8x10^5$ Jurkat cells/mL solution prepared in CCM media was transferred to each individual well of a 24 well plate and treated with the GreenPharma (GP) candidate QSIs to the desired concentrations. In the mean time, all wells containing the GP compound treatments were corrected for percentage of DMSO (the vehicle solvent). The 24 well microtitre plate was

then incubated at 37°C for 20 hours before cells can be stained with 7-aminoactinomycin-D (7-AAD).

Staining cells with 7-AAD

After incubation, the content of each well was gently mixed before a volume of 2 ml was transferred to Falcon tubes for three consecutive washing steps. Each washing step consisted of centrifugation at 300 relative centrifugal force (rcf) at 4°C for 10 minutes, removal of the formed supernatant and washing of the remaining pellet with 1 ml of ice cold PBS. After the final wash the pellet was mixed with 200 µL of ice cold PBS. Stain each individual tube containing the respective cellular treatments with 5 µl of a 1 mg/ml 7-AAD solution prepared in ice cold PBS. Incubate the stained samples protected from light for a period of 10 min after which 300 µl of ice cold PBS are added to the individual samples before cellular integrity is measured by means of a flow cytometer.

Note: After addition of 7-AAD and whenever possible the samples shall be operated within a Styrofoam ice box and protected from light.

2.9. Ligand-Receptor affinity prediction

2.9.1. Protein preparation

The X-ray structure of PqsR – QZN complex (PDB ID: 4JVI) was used as a protein template. Hydrogen atoms were added to the model using Maestro interface (version 10.5; Schrodinger LLC, New York) based on an explicit all atom model. The multistep Schrodinger's protein preparation tool (PrePrep) was used for the final preparation of the protein.

2.9.2. Ligand preparation

The chemical structures of the inhibitors were sketched using ChemDraw (Version 14) and were converted to SDF files. LigPrep software was used for the final preparation of the ligands for the docking predictive analysis. LigPrep is a utility of Schrodinger software suit that combines tools for generating 3D structures from 1D (Smiles) and 2D (SDF) representation, searching for tautomers and steric isomers and performing a geometry minimization of the ligand. Ligprep utility produces a number of structures from each input structure with various ionisation states, tautomers, stereo chemistries, and ring conformations. The program retained the present stereochemistry for each ligand. Furthermore, a unique low-energy ring conformation for each stereoisomer with correct chirality was generated with the help of Ligprep. The partial atomic charges were assigned to the molecular structures using the 2005 implementation of the OPLS-AA force field. The energy minimised structures were used for Glide (grid-based ligand docking with energetic) docking.

2.9.3. Molecular Docking

The “Extra Precision” (XP) mode of Glide docking has been used to perform all docking calculations using the OPLS-AA 2005 force field. The grid box of size 10 Å ×10 Å ×10 Å was defined in the PqsR protein and centred between the following residues: (Ala102, Pro129, Ile149, Thr166, Ala 168, Val 170, Ile186, Ile189, Gln194, Ser196, Leu196, Leu197, Leu207, Leu208, Pro210, Val211, Trp234, Gly235, Pro238, Ser255). The scale factor of 0.8 for van der Waals radii was applied to atoms of protein with absolute partial charges less than or equal to 0.15. The number of poses per ligand was set to five after energy minimisation. The best docked structure was chosen using a Glide Score (Gscore) function.

2.9.4. Extraction solvents

All extractions were performed with solvents acetonitrile and methanol (Fisher International HPLC gradient grade) and 0.1% formic acid (Fisher International LC-MS grade).

2.9.5. Preparation of standard mixtures

The compounds used (Table 2.5 and Figure 2.1) in producing calibration solution mixtures contained the duly aliquoted target molecules C_7-PQS, 3-oxo-C_{12}-HSL, *N*-butanoyl-l-homoserine lactone (C_4-HSL), C_7-HHQ and C_7-N-Oxide.

Table 2.5. List of compounds and respective analytical ionic specificities. It is important to bear in mind that for the listed compounds a collision cell exit potential of 10V is normally used for LC-MS/MS analysis. The declustering potential is a voltage applied to the orifice that helps prevent ions from clustering back together. The collision energy (CE) refers to the rate of acceleration as the ions enter the fragmentation quadrupole; the higher the collision energy, the greater the fragmentation. However, setting the CE too high or too low can cause too much fragmentation or reduced sensitivity of the multiple reaction monitoring method, respectively.

Analyte	Precursor Ion (*m/z*)	Product Ion (*m/z*)	Declustering Potential (V)	Collision Energy (eV)
C_4-HSL	172.1	102.1	26	15
HHQ	244.1	159.1	31	20
HQNO	260.1	159.1	71	32
C_7-PQS	260.1	175.1	71	22
3-OXO-C_{12}-HSL	298.1	102.1	30	19
C_5-HSL-d_9[a]	195.1	103.1	40	15
PQS-d_4[a]	264.1	179.1	80	42

[a] Internal standards

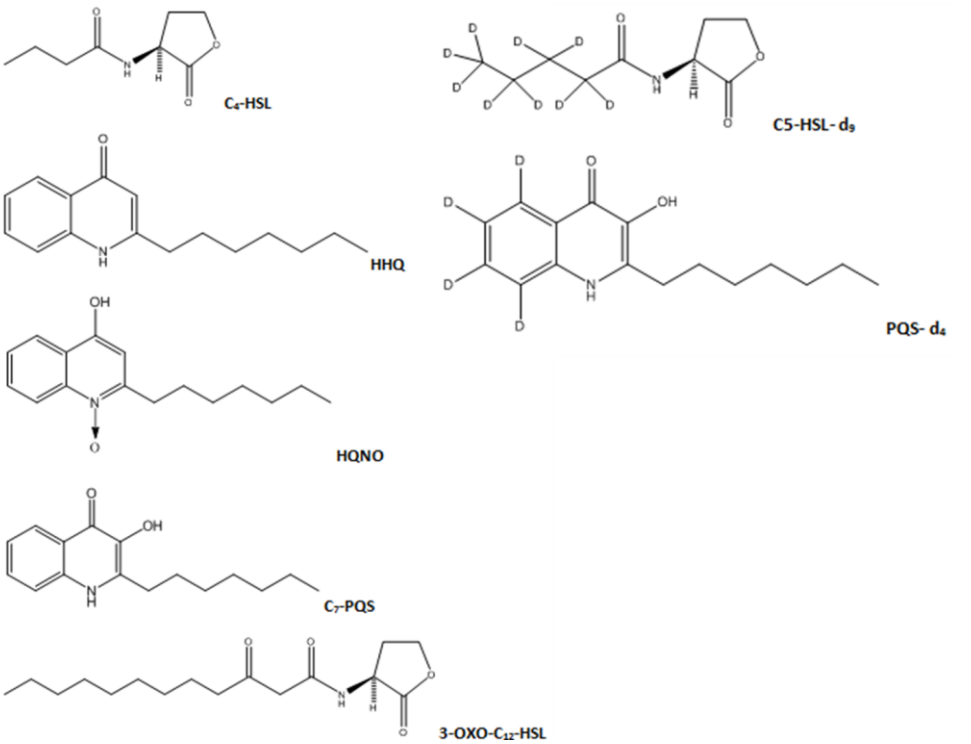


Figure 2.1. Molecular structures of compounds used. Left) AHLs and AQs screened for, Right) Deuterated compounds used as internal standards.
Source: Images kindly provided by Alex Trumman and Ram Chhabra.

To make synthetic standard stock solutions each individual HSL and AQ were prepared to 1.0 mg/ml solution in methanol and stored at -20°C. Consequently, stock solutions of the long chain HSLs require re-solvating (after warming of samples to room temperature) by rapid vortexing, thus counteracting precipitation after freezer storage.

To make the internal standard (IS) mixture, synthetic standard stock solutions of C_5-HSL-d_9 and PQS-d_4 were combined and diluted to a final 10 µM solution of both internal standards, in methanol with subsequent freeze storage at -20°C prior to use.

Calibration standards and stock solutions were prepared using the following procedures: (1) Synthetic standard stock solutions of individual HSLs and AQs were diluted resulting in 1 mM methanol solutions for each analyte. (2) 1 mM stocks were combined and diluted to prepare calibration standard

mixture samples in methanol corresponding to concentrations of 1, 10, 20, 50, 75, 100, 200 and 300 µM. (3) Quality control standard mixture samples were prepared in a manner similar to step 2, but reduced to only two final concentrations of 10 and 200 µM. (4) In preparing the calibration mixture each of the individual calibrants was spiked (1 ml of sterile LB medium with 50 µl of the calibration standard mix prepared in step 2), followed by 5.0 µl of the IS mix. (5) The quality control samples were prepared in a procedure similar to step 4, i.e., by spiking 1 ml aliquots of sterile LB medium with the quality control standard mixes prepared in step 3.

2.9.6. Preparation of growth media

All media was prepared using distilled H_2O autoclaved at 121°C for a period of 20 min at 15 psi unless otherwise stated.

2.9.6.1 Luria Bertani media

Luria Bertani (LB) broth was prepared as described bySambrook (1989) (289) and consisted of 10 g tryptone, 5 g yeast extract and 10 g NaCl. LB agar was prepared by addition of 0.8 % (w/v) Technical Agar No. 3 (Oxoid) to LB broth. All PA strains were routinely grown in LB broth unless otherwise stated.

2.9.6.2. Long term storage of bacterial strains

For long term storage of bacterial strains, 0.75 ml of an overnight bacterial culture was added to 0.75 ml of a sterile solution of 50 % (v/v) glycerol and mixed. The suspension of cells and glycerol was transferred into 2 ml micro tubes (Sarstedt, Germany) and flash frozen in liquid nitrogen before storage at -80 °C.

2.9.6.3. Bacterial growth conditions

Liquid cultures were grown in LB broth with agitation at 200 rpm in a Gallenkamp static incubator (Gallenkamp Ltd., UK) at 37°C, unless otherwise stated. Growth of bacterial cultures was monitored by absorbance at a wavelength of 600 nm (optical density, OD600) using a Novospec II visible spectrophotometer (Pharmacia LKB Ltd., Cambridge, UK), or at OD495 using an Anthos LUCYI combined spectrophotometer/luminometer (Anthos, Austria). When performing growth curves, strains were grown in identical 1 L flasks containing 100 ml LB broth.

2.9.6.4. Preparation of bacterial extracts

LESA-MS profiling was used to caracterise bacterial species (wild-type strains and mutants) in regards to their QS molecules content. Samples were obtained directly from overnight culture extracts through the steps mentioned below:

For the wild-type extracts, the growth of strains was initially carried out in 50 ml volumes of LB broth medium (Falkon tubes) at 37°C and shaking of 200 rpm. LB broth medium is prepared by combining tryptone (Bacto) 10 g/l, yeast extract (Oxoid) 5 g/l and sodium chloride 10 g/l in distilled water. Strains were stored as cryo-preserved (-80°C) samples in LB broth containing 10% (v/v) glycerol, and revived by streaking onto LB agar (1.5% w/v Oxoid technical agar No. 3 in LB). Then subsequently standardised to OD_{600} of 1.0 and regrown in triplicates of 250 ml (conical flasks) for 20 hours in a shaker-incubator (Kuhner, Switzerland) at 37°C and shaking of 200 rpm. Finally, the cultures were centrifuged for 10 min at 10,300 g to remove the pellet residue, filter-sterilised with a Minisart® 2 µm filter membrane and the obtained liquid extract was freezer-stocked at -20°C. Prior to screening the stocked extracts were thawed

at room temperature and characterised by LESA-MS in a combined mixture constituted of 80% LB broth culture and 20% methanol/water.

For obtaining bacterial exctracts the following strains were used:

a) PAO1-L (wild-type strain),
b) PAO1-L *ΔlasI* (*lasI* mutant),
c) PAO1-L *ΔrhlI* (*rhlI* mutant),
d) PAO1-L *ΔpqsA* (*pqsA* mutant),
e) PAO1-L *ΔpqsH* (*pqsH* mutant),
f) PA14 (wild-type strain).

2.10. LESA-MS Infusion optimisation methodology

The flow injection system directly injects samples from a previously cooled (4°C) automatic sampling system. 10 µl sample injection was analysed in a flow of 300 µl/min of 0.1% formic acid for half a minute. The Triversa NanoMate (Advion BioSciences, USA) coupled to the ion trap MS (LTQ Velos, Thermo Scientific) was applied for both chip-based infusion and LESA-MS. Regarding the chip-based infusion, a sample volume of 3-5 µl was infused from a 96-well plate into the MS device. When in the LESA-MS section, the injected volume of 10 µl of 0.1% formic acid in 7:3 methanol:water was used to extract analytes from 1 µl of dry bacterial extract spots sampled on Prosolia cell culture Omni Slides™. The NanoESI spraying conditions made use of nitrogen gas at a head pressure of 0.7 psi and 1.5 kV (ESI+) and 1.8 kV (ESI-) spraying voltage controlled by the Chipsoft Manager software (version 8.3.3, Advion BioSciences, USA). The dry bacterial extract spots had their positions mapped for subsequent LESA-MS analysis by means of the LESA-Points software (version 1.1, Advion BioSciences, USA).

All samples analysed were prepared in a mixture of growth medium, methanol and water to fraction percentages (V/V) specific to each individual optimisation step (see the results section). Individual samples of each treatment were collected from a 96-well plate in triplicate or sextuple, as mentioned in the particular steps. Optimised mass spectrometry data acquisition was performed for a minimum of 1 minute each replicate. A negative pressure was applied to aspirate the organic solvent containing the analyte molecules into the pipette. The aspirated sample was then sprayed into the ESI chip matrix. Since the infusion flow rate of the sample sits between 100 and 200 nL/min, it allows a volume from 1 to 3 µL each sample to be sprayed for several minutes, if that is desired.

2.10.1. LESA-MS optimisation methodology

LESA microextraction experiments were performed using the TriVersa Nanomate platform (Advion Biosciences Inc. Ithaca, NY, USA). To perform the automatic microextraction of standard calibrants or QS molecules from bacterial extracts, several modifications were made on the system. The specific setting up of the automatic methods for QS molecules extraction was produced using the Advanced User Interface (AUI) of the Chipsoft software (version 8.3.3, Advion BioSciences, USA). A description of the different methods is detailed in the relevant subsections where the different extraction solutions tested are also described.

Volumes of 1 µl of the different liquid samples were spotted onto a Prosolia cell culture Omni Slide™ and dried at room temperature for around 30 minutes. The arm robot collected the organic solvent mixture to produce 3-5 µl droplets at each individual spot prepared for analysis. A negative pressure was applied to aspirate the organic solvent containing the analyte molecules into the pipette. Analyte molecules were extracted into the organic solvent and dispensed from the pipette onto the ESI chip matrix. The procedure was

repeated for a minimum of 3 and a maximum of 6 replicates per treatment condition (see individual conditions in the results section). Chromatographic screening of the analytes was performed by mass spectrometry as described in the section below.

For a better understanding of the sequence of events that comprised the optimisation process, it is important to clearly explain and define the mentioned operational sets beforehand:

The infusion part sits inside the Triversa Nanomate and is undertaken by a robot arm prepared with a pipette tip. This arm will aspirate, from a user pre-defined sampling sequence of wells (from a 96-well sampling plate), the targeted sample preparation that is squirted towards the chip after the tip engages with the back of the ESI chip. The targeted fraction is infused and when the high voltage is applied to the pipette tip, the nanoelectrospraying is initiated with the ions being sprayed into the the mass spectrometer. The idea behind the use of infusion is actually to further optimise the mass spec.

The LESA-MS part also starts with the robot arm set with a pipette tip, but this time and contrarily to infusion, the TriVersa Nanomate robot collects the extraction solvent from the reservoir into the pipette tip prior to moving to the sample slide. The solvent is then carefully dispensed from the pipette tip and held in contact with a preprogrammed (software-set by the user) position on the surface spot that is to be analysed. The analytes are directly extracted from the surface into the solvent and the solution extract is withdrawn into the pipette tip. As mentioned before the tip engages with the back of the ESI Chip for the subsequent high voltage ionization and electrospraying into the mass spec.

The LESA-MS technique is also known as ambient mass spectrometry (uses direct sampling and ionization at ambient conditions). It can be defined as a mass spectrometric analysis with minimal or even inexistent effort in

regards to sample preparation. For the sake of proper understanding, it is important to clarify that ambient MS is not the same as atmospheric pressure ionization, used in techniques such as atmospheric pressure MALDI-MS or ESI-MS. Contrarily to these techniques, where there is need for the sample to be mixed and co-crystallized with a matrix, or dissoluted of the sample, no desalting steps are necessary.

After simultaneous fraction collection in sample plate (infusion) or slide spots (LESA) take place, the samples are fractionated by the ESI chip and transferred to the mass spectrometer (MS) for producing the chromatographic peaks. The user can therefore analyse the fractions of interest.

Finally, the Accessories section concerns optimisation of minor component parts and machinery settings, bacterial growth media, solutions not directly related to either infusion or LESA, and which optimisation is relevant to improving reliability of the mass spec. The accessories hereby covered are: the substrate sampling surface or slide surface, the bacterial growth media, pre-air space and the reading delay.

2.10.2. Optimisation of surface for sample analysis

The present research study also analysed from two possible surfaces the best slide surface for sampling onto, Glass and PTFE Printed Slides (figure 2.2). The PTFE (polytetrafluoroethylene) slide surface is extremely hydrophobic, resistant to acetone and chemicals, but autoclavable. These slides are adequate for controlling cross-contamination in staining, immunolabeling and immunofluorescence tests. On the other hand, the glass slide is known to be hydrophilic due to its polar ionic nature. All printed slides are precleaned, frost-ended and designed for one time use only. The spotting surface is 100% wettable, hence providing for better cell attachment whilst

augmenting spreading of sample within the spot. The slide undergoes a bioadhesive surface treatment to enhance cell and tissue attachment.



Figure 2.2. Prosolia cell culture Omni Slide™. Microtiter format sampling slides with hydrophobic and hydrophilic coating arrays designed for DESI.
Source: (297).

Chapter 3

3.1 Highthroughput screening for identifying novel potent PqsR inhibitors

3.1.1. Development of PqsR antagonists

The search for novel small molecules with antagonic specificity to PqsR is not new, but the most successful molecules targeting PA transcriptional regulator, responsible for the production of a panoply of virulence factors, is definitely a recent chapter. Table 3.1 lists a personal selection of the most potent PqsR antagonists found to date and that can establish a promising starting point to further optimisation of PqsR inhibitors.

Successful work by Lesic *et al* (2007) (298) where the authors identified halogenated anthranilic acid analogs specifically repressing HAQ biosynthesis and disrupting PqsR-dependent gene expression gave the motivation for the engineering advances on selective PqsR antagonists. Mainly because the found molecules tested *in vivo* on mice models, thermally injured, infected with PA14, and then individually intravenously injected with each analog (6h post-infection), limited PA systemic diffusion and reduced PA-associated mortality. The compounds tested did not disturb the pathogen viability and inhibited osmoprotection [for more information on osmoprotection see Messmer (2007) (299)], and did in fact significantly delay the kinetics of mortality in the treated mice, pointing towards a possible future inactivated immunisation.

The anthranilic acid analogs tested were capable of reformatting genetic expression in PA14 and ultimately indirectly inhibiting the transcriptional regulator *pqsR*, by means of direct action on HHQ and PQS coligand synthesis that in the end deters PqsR activation. Thus, a number of

positively regulated loci driving the HAQ synthesis were repressed, and with these the associated virulent phenotype. A total of 144 PA14 genes are regulated by PqsR (122 are upregulated and 22 downregulated) (164); from these 111 were differentially expressed by at least one of the developed anthranilic analogs. Individually speaking, the most active analogs were 6FABA, 6CABA and 4CABA (for a summary see Table 3.1), affecting the expression of 54, 89 and 102 PqsR-dependent loci, respectively. Of the associated genes some were known for their pathogenicity, and their repression impacted on the expression of biosynthetic and some virulence-related operons, such as *pqsA*, *pqsE*, the phenazine operon, *hcnABC*, *chiC*, *lecA*, *lecB* and *lasB*. The result was a decrease in production of PCN, hydrogen cyanide, chitinase, lectins, and elastase, verified by means of functional assays.

Around the same time the above mentioned anthranilic acid analogs were unveiled by Cugini *et al* (2007) (191) who was studying the quick action of Farnesol, a sesquiterpene present in many organisms including the *Candida albicans* fungus, on PA. Farnesol establishes a non-productive collaboration between PqsR and the *pqsA* promoter, as development of PA grown amidst *C. albicans* revealed. The result is a reduction in PQS and PCN levels. An *E. coli* strain producing PqsR as well as bearing a *pqsA* promoter fused to *lacZ* was used to demonstrate that farnesol displayed a quick inhibitory action on *pqsA* transcription at low concentrations whilst not affecting regulation of the transcriptional regulator *pqsR*. Electromobility shift assay (EMSA) analysis indicated a stimulation of the PqsR interaction with the *pqsA* promoter in the LysR-type protein recognition region where the PqsR-PQS binding is established, i.e., -45 bp in relation to the *pqsA* transcriptional initiation site.

The farnesol findings supported the idea that other similar molecules (structurally and functionally speaking), found in the environment or with the potential to be chemically engineered, could have the same type of modulatory effects on PA virulence. Thus, pointing towards *in silico* predictions for future chemical analogs with PqsR-inhibitory effects or natural molecules from

environmental sources, or even self-regulatory molecules in PA. The latter was actually the successful strategy used by Kesarwani *et al* (2011) (300) when the authors identified for the first time a self-regulatory QS molecule, the 2-aminoacetophenone (2-AA). 2-AA is a low molecular weight volatile compound secreted by PA and known to operate by means of a negative feedback loop exerted on PqsR-regulated loci, hence potentiating virulent phenotypes in subjects with chronic lung infections if the associated virulence expression is not silenced. 2-AA is known to reduce bacterial virulence *in vivo* in subjects like the *Drosophila melanogaster* fly and in an acute mouse infection model, organisms that share numerous similarities with mammalian innate immunity and physiology.

Even though, 2-AA synthesis is regulated by PqsR, it is not necessary for the activation of the transcriptional regulator *pqsR*. PqsR is suggested by the authors to activate and inactivate cells whilst switching on and off a bistable phenotype where cells respond to 2-AA concentrations. This dual response was observed by measuring the levels of HHQ in 2-AA treated cells where it was detected that HHQ production happened to be inhibited by 2-AA in a dose-dependent fashion. In addition, the study also showed that 2-AA was responsible for reducing production of PqsR-associated virulence factors, PCN and pyoverdin.

2-AA also downregulated the *pqsABCDE* operon expression through direct action on PqsR and by interfering with the biosynthesis of HAQ enzymes. Probably one of the most noteworthy facts suggested by the discovery of how 2-AA operates is that 2-AA strongly induced bacteraemia in the PA14 infected mice, a complication that is also significantly observed in human patients dealing with PA infections. Hence, 'killing' the PqsR participation in the regulatory process of virulence is part of the answer in avoiding systemic diffusion of PA cells, even though virulence attenuation does not directly result from controlling dissemination.

Advances towards the discovery of PqsR antagonists were facilitated by studies developed since the early 2010s in two main research areas. One focusing on finding small molecules with potential to inhibit PqsR (301-303) and another one aiming towards structural studies of the PqsR protein, and the impact of its kinetics/thermodynamics on inhibition effectiveness (304) (267) (278). In regards to the first line of research, successful studies emerged from the efforts of the Hartmann group, even providing initial pointers that later on helped improve the findings by the second branch of research.

Lu *et al* (2012) (303) used a reporter gene assay in *E. coli* to discover the first (allegedly) PqsR antagonists with competitive performance and capable of reducing PCN production in PA14 bacterial cells. In addition, the authors also offered further understanding of the PqsR ligand-receptor interaction that helped pave the road towards subsequent *in silico* drug engineering studies.

In order to accomplish the prime compound 19 (a PqsR antagonist with IC_{50} and $Kd_{,app}$ scores in the low nanomolar range) the authors had to develop a ligand-based drug design methodology where a group of HHQ and PQS analogs were engineered. The approach accounted for side chain variations and introduction of substituents into the carbocyclic region of the quinolone structure, these were subsequently assessed *in vitro* by means of a β-galactosidase reporter gene assay in *E. coli*. Antagonic properties were studied based on natural agonists and supported by the scaffold axiom explored by Hartman *et al* (1980) (305) premising that antagonists can be acquired by structurally altering the original agonists, which in a structural perspective makes perfect sense.

The structural engineering process through which compound 20 was obtained accounted for many observations that offered a reduced PqsR activity: 1) an elongation of the side chain by one carbon (in compound 5), the introduction of a 3-phenylpropyl side chain (in compound 7), the introduction of electron donating and withdrawing groups into the benzene part of the HHQ

molecule, until two compounds were structurally combined (compounds 10 and 19) to generate a more active antagonist (compound 21). At this point the authors had to retract for the resulting agent was less effective than its best predecessor (compound 19), regardless of its higher antagonistic potency. It was then that surface plasmon resonance biosensor assays provided indications on the binding capacity of compound 18 to PqsR and the best three final antagonist molecules resulted, namely compounds 18, 19 and 20.

With competitive trials in PA14, the impact of two of the lead selected PqsR antagonists, specifically compounds 18 and 19, had their inhibitory efficacy studied on the production of PCN (control-compared to compounds 15 and 17). The PqsR antagonists 18, 19, and 20 did not display antibacterial properties against *E. coli tolC* (an outter membrane protein linked to the functioning of several efflux systems) and did not induce natural selection pressure in PA14 at concentrations as high as 5 mM.

It was finally compound 19 that emerged successful with its IC_{50} and $Kd_{,app}$ values sitting in the low nanomolar range, whilst reducing PCN production by 74% in PA14 at a concentration of 3 mM. However, a poor aqueous solubility problem was still affecting this compound as it had to undergo further structural modifications to amend its antagonistic properties. It resulted in an improved antagonist of PqsR, since aqueous solubility is an essential pharmacokinetic property for any candidate compound to make its break through as a potential drug (306, 307) .

After structural modifications performed to the previous antagonist 2 (for the easy synthetic accessibility of the nitro compounds) four classes of novel quinolone-based compounds were created. The compounds were studied for their structure-activity relationships and their surface plasmon resonance was constantly assessed throughout the whole process of optimisation. Consequently, and pointing to the improvement of the poor aqueous solubility index, a series of alterations were effected: 1) a methyl

group was introduced to block H bonding between the NH group at 1-position and the carbonyl group at 4-position (likely to contribute to the poor solubility index) resulting in the class 1 compounds; secondly, oxygen was added into the alkyl side chain producing compounds in class 2, as with a polar or ionisable element hydrophilicity is increased; thirdly, the 3-position was substituted with e.g., amide, amino, carboxylic or hydroxamic acid groups producing compounds in class 3; and the benzene moiety was replaced (by means of electron withdrawing groups) by a pyridine to finally generate compounds in class 4.

The best eigth compounds were then chosen for determination of PqsR antagonistic properties and calculation of logP values, from which compound 16 emerged as presenting not only good aqueous solubility as well as repression of virulent phenotype in PA14. Structurally this research provided with insights as to how a mere substitution at position 3 takes such an important part in the whole ligand-receptor relationship, in terms of functionality; and the carbonyl group at position 4 is shown to be essential for the interactions between ligand and protein. These results provided a very promising opening to the studies later developed on the structural characterisation of the PqsR protein receptors and putative ligands with antagonistic objectives.

But a somewhat surprising and unexpected *in vivo* functional inversion of a QS receptor antagonist into an agonist by PA, drove the Hartmann group to produce a much more potent PqsR inhibitor, in consequence. It happened when antagonist 1 (a compound based on the scaffold of HHQ) with a reported high activity for PqsR (IC_{50} in *E. coli* of 51 nm and inhibition in PA of 60% at 10 µM), obtained with an *E. coli* reporter gene assay (303), caused a very mild reduction of PCN production. When profiling antagonist 1 the authors found that its antagonistic behaviour respected a dose-dependent agonistic activity in PA, not at all seen in *E. coli*. These opposing responses established by two different bacterial species immediately proposed a possible biotransformation

of the molecule taking place in PA. They speculatively suggested that PqsH-related enzymes responsible for the conversion of HHQ into PQS may be responsible for such biochemical alterations, due to the similarities between the antagonist 1 and HHQ, and due to the fact that several PQS analogs display agonistic activity on PqsR (303) (308).

The debated hypothesis was thoroughly investigated and validated with the use of adequate animal models. To validate the strong antivirulent protective role of the antagonist 3, *C. elegans* that is sensitive to PCN, was studied against a PA14 infection in the presence of the antagonist 3. Its survival sat at 94%, but when tested without the antagonist 3 (control) the survival rate fell to 47% within 6 hours. Moreover, support to the idea that QS signalling disruption is more advantageous than genetic deletion came with the results obtained with PA14-contaminated *C. elegans* larvae. Those treated with the antagonist 3 had increased survival rates in comparison to those infected with PA mutants deficient in PQS, due to silenced *pqsA* and *pqsR* genes.

A simple hydroxylation was able to return the antagonist properties to compound 1, that had suffered a complete loss of its inhibitory potential and even reinforced the agonism into the ligand. In fact, either in cell-based assays or under *in vivo* conditions numerous times are these inhibitory compounds prone to inefficiency, due to the excretion by the efflux systems. The work by the Hartmann group shows that knowing the ins and outs of the structural relationships, and considering slight structural alterations alongside an understading of the enzymatic conversion of the candidate molecules, can indeed potentiate crucial advances in the production of very strong PqsR inhibition molecules.

The influence of structural properties and the understanding of its manipulation set the premise for very important QS inhibitory achievements, hereby discussed as part of the second branch of research on QSIs targeting the PA transcriptional regulator PqsR. Studies by Klein *et al* (2012) (on hit

selection optimisation) (304), Xu *et al* (2012) (on preliminary crystal structure analysis of the ligand-binding domain) (267) and by Ilangovan *et al* (2013) (on the structural basis for synthetic inhibitor recognition) (278) are to the best of my knowledge the most relevant published to date.

With a hit optimisation strategy Klein *et al* (2012) generated small molecules binding to the PqsR protein, determined their thermodynamic binding signatures and characterised their functioning in *E. coli*. The resulting product was a promising potent hydroxamic acid-derived PqsR antagonist 11 (IC_{50} = 12.5 μM in *E. coli* and IC_{50} = 23.6 μM in PA) with strong repression on PCN production. The unveiled antagonists were used as scaffolds for subsequent molecules derived from the former.

The best PqsR antagonist developed by the authors was the κ-opioid receptor agonist 1 [(±)-trans-U50488] for it stimulated transcription of the *pqsABCDE* operon in PAO1 suggesting that it possibly operates through PqsR binding. This scaffold was the original one selected for further optimisation by breaking it into smaller fragments and analogs. It resulted in a less potent inhibitor of PqsR, but due to its low molecular weight one with a high potential for future optimisation. In terms of its biochemistry, thermodynamic analysis and site-directed mutagenesis allowed the authors to reveal that the only polar aminoacid residue in the PQS-binding pocket Gln194 (probably through hydrogen bonding) and aminoacid Phe221 (probably through CH/π interactions) are involved in the ligand binding. For more information on the CH/π interactions in proteins read (309).

The PqsR-mediated transcriptional effect can be 'measured' with a heterologous reporter gene assay in *E. coli*, allowing a profiling of the functionality of PqsR ligands without interferences from the remainder of the PA pqs system. Its application delivered rather surprising results, i.e., antagonist 1 did not stimulate the transcription of *pqsABCDE*, actually acting as a weak PqsR antagonist. On the other hand, 4 promoted a substantial decrease

in PqsR production and was then chosen for subsequent optimisation efforts by means of structural alterations, some previously attempted for with success by other research groups: 1) alkyl chain length variation in PQS (310) (308), and 2) alkyl chain length variation in HHQ and derivatives.

The variation of the length of the alkyl chain revealed that both agonist and antagonist activities depend to a certain extent on the length of the alkyl chain. The introduction of alkyl chains ranging from 1 to 4 carbon atoms in the para-position (i.e., the one where two same functional groups are linked to a benzene ring in positions 1 and 4) produced antagonists 6 to 10. The modification resulted in better binding affinity (29-fold higher than antagonist 4). In the meanwhile, as they attempted a constitutive alteration from a tertiary butyl configuration to an isobutyl one, the affinity index suffered an immediate reduction.

When swaping the amide by a hydroxamic acid group, in the ligand that had shown the best affinity score, the produced antagonist 11 delivered a 4.6-fold reduction in the affinity to PqsR, a consequence of a decrease in the enthalpy of the established binding system. However, two surprising effects were generated, a) a rather enhanced antagonistic strength, and 2) the extinction of the agonistic functioning. And further investigations clearly helped understand the role of certain structural modifications on the overall agonism/antagonism of the formed compounds. For example, the replacement of the amide by a hydroxamic acid usually produced antagonists from former agonists, replacing the Cl-substituent in para-position by alkyl-residues created agonists from former antagonists.

Thus, by means of serial biophysical alterations the allegedly first small-molecule PqsR ligands were generated and their inherent antagonistic properties evaluated to the best optimised compound (antagonist 11 - a potent hydroxamic acid-derived PqsR antagonist). This study helped understand that improving the engineering of PqsR inhibitors demands structural perception of

the PqsR protein. Insight that was taken to an upper level with the work by Xu *et al* (2012) (267) where the hexagonal crystal form assumed by the ligand-binding domain of PqsR was disclosed, alongside its recombinant production and crystallisation.

Focusing their analysis on the residues unique to PqsR, i.e., those in the region where the ligand binding domain without the C-terminal structural element can be found (residues 320 to 332), the study was capable of unveiling a series of important structural findings: 1) electron density analysis revealed the existence of a five-stranded β sheet, typical of the ligand-binding domain in LysR-type transcription factors, 2) the asymmetric unit [meaning the smallest portion of a crystal that when worked by crystal symmetry operations produces the unit cell of the former] has only one protein chain, 3) the dimer of the PqsR residue region (comprised by residues from 91 to 319), and also its arrangement, are responsible for solvent-filled channels through the c axis of the unit cell [meaning the smallest fraction of a crystal that when duplicated and translated generates the entire crystal structure).

These findings were important for the groundbreaking work by Ilangovan *et al* (2013) (278) on the impact of the QZN system (sterically associated to the natural AQ ligands) on AQ biosynthesis, virulence phenotyping and biofilm progression. By means of a ligand-based design strategy, 50 AQ and novel quinazolinone (QZN) analogs were engineered and subsequently assessed. Again, simple alterations exerted on the molecular structure of the candidate molecules were essential to define for the first time an LTTR-antagonist complex.

These alterations consisted on investigating the molecular basis of PqsR ligand recognition by determining its crystal structure. The crystal matrix was inspected and a large dimer interface revealed two CBDII pockets sitting on the same surface. In addition, the pocket in each monomer is found to link through the dimer interface in a thin mesh-like channel. Furthermore, the recognition

of naturally occurring AQ co-inducers by the $PqsR^{CBD}$ revealed an interesting aspect of the protein structure, i.e., the interactions are all hydrophobic apart from those in hydrogen bonds or electrostatic interactions to the NHQ carbonyl oxygen or NH group of the bicyclic ring. Even though the interactions established with NHQ are purely hydrophobic, altering the hydroxyl group in the PqsR co-inducer, PQS, shows that this group might hypothetically establish a supplementary interaction by means of a hydrogen bonding ligation to a carbonyl group of Leu207.

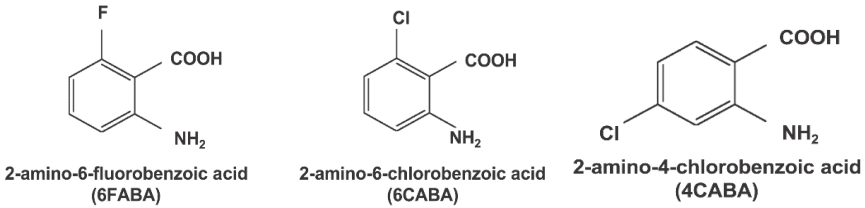
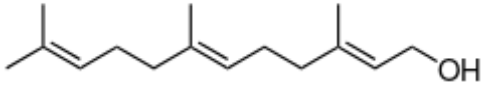
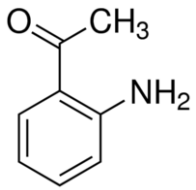
In fact, whilst probing the participation of crucial $PqsR^{CBD}$ amino acid residues involved in binding to AQs, both Leu207 and Phe were mutated and provided significant results. Phe mutation was expected to disrupt the binding, for it would alter the binding pocket and increase its inherent volume; and Leu207 (Leu207Ala and Leu207Glu) expected to interact with NHQ at the junction between the alkyl chain and the bicyclic ring over its terminal side chain atom. In comparison to the wild-type strain, the mutated organisms produced an approximate 10% response, meaning that the transformed size and electrical charge do interfere in the ligand-receptor binding. In addition, mutations to Ile149, Phe221, Tyr258, Ile263 end up in total activity loss. Another important observed feature was the precipitation of the $PqsR^{CBD}$ protein when in the presence of its highly hydrophobic ligands even at diluted protein concentrations, a finding also noted by Xiao *et al* (2006) (162) and an aspect that complicates biophysical manipulating of the system.

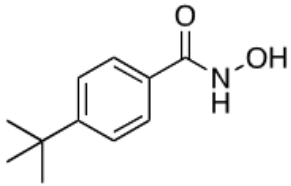
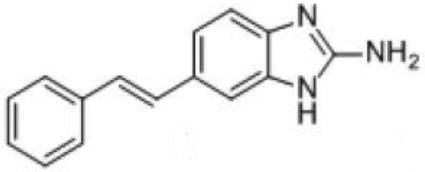
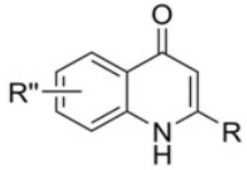
The synthesis and assessment of the putative antagonists knew several steps. By swapping two isosteres (OH for NH_2) they transformed a QZN agonist into an antagonist whilst affecting the underlying virulence factor production. Systematic variations to the nature and size of the substituents, located at positions 2 and 3 in the heterocyclic ring and positions 6 and 7 in the carbocyclic ring of the QZN structure, produced a spectrum of analogs with molecular features that ideally hold the desired stereo-electronic properties to enhance ligand recognition and enhance associated antagonism. The resulting QZN

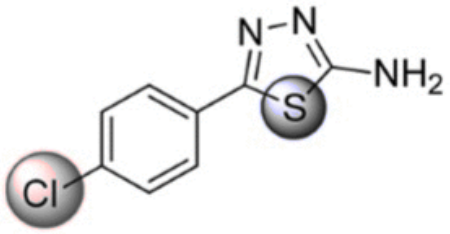
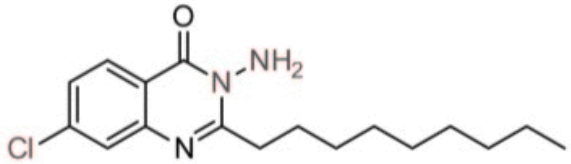
compounds, after being assessed by means of whole bacterial cell assays of PqsR activity, were placed in two separate groups: a) a group constituted by the 3-OH QZNs (where compounds were expected to behave as agonists), and b) a group composed by the 3-NH_2 QZNs (where compounds are expected to behave as competitive antagonists).

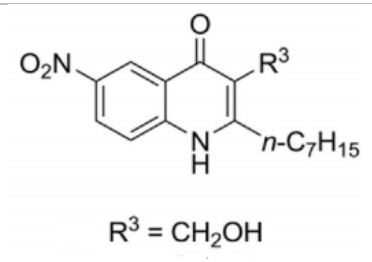
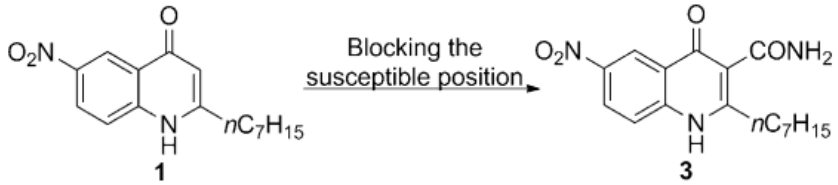
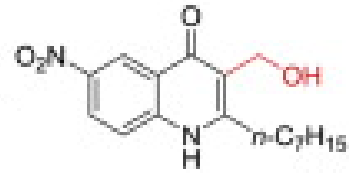
Moreover, both groups of compounds have their activity enhanced when an alkyl chain of 9 carbons at the second carbon in the heterocyclic ring and a halogen at the seventh carbon in the carbocyclic ring are present. The study revealed compounds 3NH_2-7Cl-C_9-QZN (IC_{50} 5.0 mM), 3-NH_2-7F-C_9-QZN (IC_{50} 4.3 mM) and 3-NH_2-6F,7F-C_9-QZN (IC_{50} 1.7 mM) as the strongest synthesised antagonists.

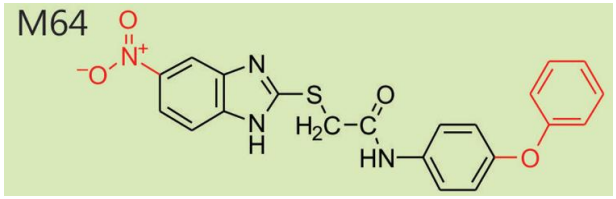
Table 3.1. List of selected inhibitors identified to interact with PqsR ligand binding site of PA QS receptors. This selection focused on compounds from synthesised molecules to natural products, demonstrating specific inhibition of PqsR, where hypothesised antagonism is not based on purely speculative assumptions and functional inhibition but by a direct inference on the PqsR protein.

QS inhibiting molecule	Target receptor	Activity	Source
6FABA, 6CABA and 4CABA  2-amino-6-fluorobenzoic acid (6FABA) 2-amino-6-chlorobenzoic acid (6CABA) 2-amino-4-chlorobenzoic acid (4CABA)	Direct action on HHQ and PQS coligand synthesis	No disturbance of the pathogen viability Inhibition of osmoprotection Delaying of the kinetics of mortality in treated mice	(298)
Farnesol 	Stimulation of the PqsR interaction with the *pqsA* promoter (-45 bp in relation to the *pqsA* transcriptional initiation site)	Quick inhibitory action on *pqsA* transcription at low concentrations of PQS No effects on *pqsR* transcriptional regulation Reduction of PCN and PQS levels	(191)
2-aminoacetophenone 	Probable negative feedback loop exerted on PqsR-regulated loci Interference with the biosynthesis of HAQ enzymes	Inhibition of HHQ production in a dose-dependent manner Reduction of PCN and pyoverdin levels Stimulation of strong bacteraemia	(300)

Antagonist 11 [Hydroxamic acid-derivative with less antagonistic potential but higher optimisation potential due to low molecular weight and action over PA] 	Probably binding to PqsR	Reduction of PCN production at 87.2 µM PqsR antagonistic activity IC_{50} of 23.6 µM Stimulation of transcription of the *pqsABCDE* operon in PAO1	(304)
2-Aminobenzimidazole stilbene derivative 1 	Unknown, but possibly through PqsR binding	Inhibition of the growth of and dispersing of preformed biofilms	(311)
Antagonist 19 [HHQ analog with trifluoromethyl and nitro functional groups in position 6] 	Binding to PqsR	Reduction of PCN production in 74% PqsR antagonistic activity IC_{50} of 54±23 nM PqsR stimulation induced by 10 mM test compound compared to 50 nM PQS (= 1.00) of 0.00 Inhibition of PqsR stimulation induced by 1 mM HHQ in the presence of 10 mM test compound (Full Inhibition = 1.00) of 0.95 Water solubility < 5 µM	(303)

Oxadiazole-2-amine [Antagonist 37] CF_3 derivative 	Competitive binding to PqsR	Reduction of production of PCN in *pqsH* mutants Antagonist activity of EC_{50} = 38.5 µM Reduction effects on HQNO (43±3% at 250 µM) Inexisting *in silico* predicted toxicological concerns	(312)
QZN antagonists of PqsR: 3-NH2-7Cl-C_9-QZN (image below), 3-NH_2-7F-C_9-QZN, 3-NH_2-6F and 7F-C_9-QZN 	Competitive binding to PqsR	3-NH_2-7Cl-C_9-QZN (IC_{50} 5.0 mM) antagonises AQ biosynthesis, virulence gene expression, PCN production and biofilm formation; 3-NH_2-7F-C_9-QZN (IC_{50} = 4.3 mM) 3-NH_2-6F and 7F-C_9-QZN (IC_{50} = 1.7 mM)	(278)
Antagonist 16 [HHQ analog synthesised based on analog 2 with a subsequent substitution in position 3 with amino or ionisable groups, as previously described in (303)]	Binding to PqsR	PqsR antagonistic activity IC_{50} of 72± nM PCN production reduction of 83% at 15 µM [IC_{50} = 3.8 µM] PQS production reduction of 33% at 15 µM Solubility in 2% DMSO = 9.4 µM	(302)

		clogP of 6.94/4.67,	
Antagonist 3 [a carbomaxide derived from antagonist 1 obtained after dwelling on an unexpected inversion from antagonistic to agonist behaviour promoted by PqsH occurred with 1 due to its HHQ scaffolding] 	Binding to PqsR	93% survival rate in *G. mellonella* PA14-infected larvae Strong reduction in HHQ (50%) and PQS (30%) levels at 15 µM IC_{50} PCN reduction at 2 µM	(301)
HHQ synthesised as previously described in Lu *et al* (2012) (303) with a subsequent substitution in position 3 with amino or ionisable groups 	Binding to PqsR	IC_{50} for PCN of 3.8 mM Repression of biosynthesis of PCN and PQS PqsR antagonistic activity IC_{50} of 72 nM	(302)

M64 [potent benzamide-benzimidazole derivatives] 	Blocks synthesis of both pro-persistence and pro-acute PqsR-dependent signalling molecules Targets PqsR rather than upstream regulatory components Blocks PqsR binding to *pqsA* promoter in PA14	Prevention of synthesis and cell accumulation of 2-aminoacetophenone [antibiotic-tolerant cell formation in humans] Restriction of formation of antibiotic-tolerant persisters to quinolones Inhibition of PCN production K_D = 5.4 nM Reduction of PA14 infection and persistence in murine burn and lung infection models	(313)

3.1.1.1. Preliminary studies towards final pool of QS inhibiting candidates

In PA, amid the 2-alkyl-4-quinolone (AQs) molecules produced is PQS. The process hereby described of researching on putative QS inhibitors for attenuation of virulence in PA, accounted for PqsR-interfering candidate molecules directly or indirectly interfering with the PQS biosynthesis pathway.

The preliminary highthroughput screening process (figure 3.1.) that gave way to the group of candidate molecules assessed in this study, used a chemically diverse initial pool of 6960 natural and synthetic compounds (based on more than 150,000 structures). These were previously evaluated by means of biosensor activity testing using a chromosomal CTX::P*pqsA-luxCDABE* transcriptional fusion in *P. aeruginosa* towards the identification of molecules inhibiting this PqsR-controlled fusion and hence displaying downstream repression of virulence potential (pyocyanin production and biofilm formation) in PA.

From the preliminary studies two compounds were selected for their ability to inhibit *pqsA* expression: GPZ273902 (IC_{50} = 6.6µM) and GPZ377445 (IC_{50} = 7.2 µM). A subsequent set of 49 molecules derived from candidates GPZ273902 and GPZ377445 were consequently evaluated during SAR (structure activity relationship) analysis for their ability to inhibit PQS production. This resulted in the identification of the PqsR antagonists GPZ824390, GPZ002966 and GPZ004927. These compounds could strongly inhibit *pqsA* expression with IC_{50} scores of 0.75 µM, 1.9 µM and 3.9 µM, respectively and were the basis of the SAR analysis presented in this chapter and which resulted in the testing of a pool of 15 compounds targeting inhibition of PqsR activity.

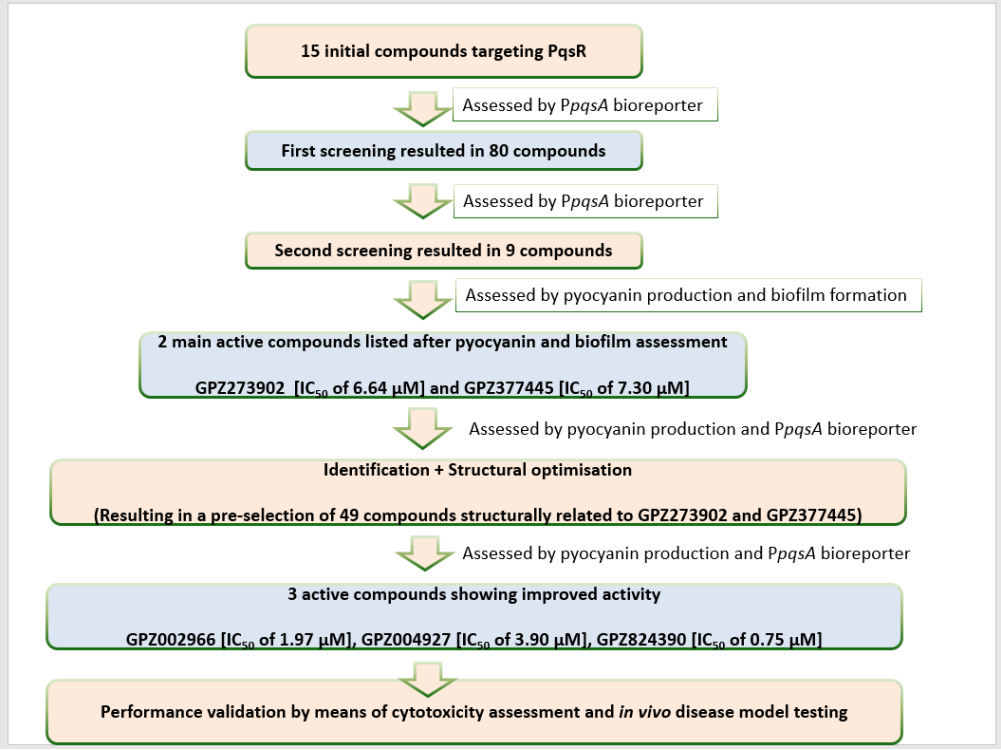


Figure 3.1. Process of preliminary highthroughput screening. From a total of 6960 natural and synthetic molecules, a series of assessments on the capacity to inhibit *pqsA* was performed, and a subsequent list of 9 compounds produced. Consequently, after assessing their effects on reduction of pyocyanin and biofilm formation, 2 final active compounds were lined up for identification and structural optimisation. The resulting 49 identified and optimised molecules delivered a group of 3 main active compounds that served as the base group for a performance validation that assessed their further clinical application potential.

3.2 Hit optimisation of PqsR inhibitors in *Pseudomonas aeruginosa*

With the objective of assessing their potential to inhibit and undertake further optimisation of their structural design in order to improve repression of the PqsR protein, the 15 synthetic small molecules obtained from GreenPharma Ltd. (GP) were lined up for screening. The compounds were initially tested on strain PAO1-L for their inhibitory effects on *pqsA* expression (by means of a CTX::P_{pqsA}-*luxCDABE* -based biosensor) using as a control the *luxCDABE* genes expressed from the P_{Km} constitutive promoter (CTX::P_{Km}-*luxCDABE*) to account for any effect of compounds on the activity of the reporter genes themselves. The screening was mostly conducted on strain

PAO1-L, but whenever found pertinent references to other PA strains differing in virulence were used as indicated throughout the results section.

3.2.1. Effect of the GP QS-inhibiting compounds on the activity of *pqsA* and P_{Km}.

The bacterial PAO1-L bioreporter strain was incubated with concentrations of 10 and 100 µM of each individual GP PqsR inhibitor (Table 3.2 and Figures 3.2 and 3.3). Two controls were also applied, 1) the bacterial culture in LB medium without compound, and 2) bacterial culture with the equivalent percentage of DMSO (vehicle solvent in which compounds were reconstituted), i.e., 0.1% for the 10 µM compound concentration and 1% for the 100 µM compound concentration. These controls take into account the reduction in luminescence derived from the effects associated to the presence of DMSO, thus enabling data normalisation and the elimination of false positives. The percentage of remaining activity upon exposure to the smallest concentration (10 µM) and the IC_{50} scores produced (Table 3.2) were used for pre-selecting the best four candidate molecules, namely GPZ002966, GPZ004927, GPZ824390 and GPZ273902.

As there was no prior indication of the range of concentrations to be used, the first IC_{50} assessment was just an estimate (Table 3.2) of where the real IC_{50} scores would likely to be found when refined and optimised. This crude assessment was then used to select the best PqsR inhibitors for further analysis. For this subsequent analysis three separate assays were carried out on two strains differing in pathogenicity: PAO1-L and PA14 harbouring the same biosensors (Table 3.3).

Table 3.2. Summary of bioluminescence in PAO1-L CTX*::*P_{pqsA}/P_{Km}-*luxCDABE* after individual exposure to 15 GreenPharma compounds. Bold green values stand for inhibitory effects with percentage of remaining activity of *pqsA* below 33% (100 µM) and 45% (10 µM). AUC = area under curve. Compounds in green were selected for IC_{50} optimisation with both PAO1-L/PA14 CTX*::*P_{pqsA}-*luxCDABE*. Values are the result of three replicates.

Compound	% of remaining activity (100µM) CTX::P_{pqsA}-*lux*	% of remaining activity (10µM) CTX::P_{pqsA}-*lux*	% of remaining/ increased activity (100µM) CTX::P_{Km}-*lux*	% of remaining/increased activity (10µM) CTX::P_{Km}-*lux*	Optimised IC_{50} Nr. Analysed points R square
Average 0% DMSO	-	-	-	-	-
Average 0.1% DMSO	-	86	-	117	-
Average 1% DMSO	65	-	80	-	-
GPZ002966	11	9	73	103	394.8 nM 23 points 0.9292
GPZ004927	22	29	80	101	88.14 nM 19 points 0.9303
GPZ406918	41	76	**138**	**107**	-
GPZ244801	43	69	74	68	-
GPZ738715	37	83	68	83	-
GPZ850128	34	85	**101**	89	-
GPZ349236	42	86	**108**	96	-
GPZ961685	46	87	**113**	85	-
GPZ683975	**31**	74	**109**	84	-
GPZ555169	44	82	**115**	96	-
GPZ535307	49	87	**115**	90	-
GPZ687738	42	57	**106**	90	-
GPZ870387	**27**	58	74	86	-
GPZ775924	50	80	**110**	89	-
GPZ481832	**33**	**42**	**100**	97	-
GPZ824390	15	12	73	103	70.32 24 points 0.8877
GPZ273902	13	9	67	100	56.88 nM 22 points 0.9217

Table 3.3. Summary of IC_{50} scores in PAO1-L/PA14 CTX::P_{pqsA}-*luxCDABE*. Strains were grown overnight at 37°C and 200 rpm, optimised to OD_{600} of 0.05 on the following day, exposed to 24 concentrations ranging from 0.60 nM to slightly over 500 µM, and their luminescence read at 37°C for 24h with no shaking. Experiment done in triplicate.

Compound	PAO1-L CTX::P_{pqsA}-*luxCDABE* 1st Optimised IC_{50} Nr. Analysed points R square	PAO1-L CTX::P_{pqsA}-*luxCDABE* 2nd Optimised IC_{50} Nr. Analysed points R square	PAO1-L CTX::P_{pqsA}-*luxCDABE* 3rd Optimised IC_{50} Nr. Analysed points R square	PA14 CTX::P_{pqsA}-*luxCDABE* 1st Optimised IC_{50} Nr. Analysed points R square	PA14 CTX::P_{pqsA}-*luxCDABE* 2nd Optimised IC_{50} Nr. Analysed points R square	PA14 CTX::P_{pqsA}-*luxCDABE* 3rd Optimised IC_{50} Nr. Analysed points R square
GPZ002966	**394.8 nM** 23 points 0.9292	**29.11 nM** 22 points 0.9024	**3.692 nM** 21 points 0.9333	**1.359 µM** 22 points 0.9080	**202.3 nM** 24 points 0.8163	**1.763 µM** 24 points 0.8557
GPZ004927	**88.14 nM** 19 points 0.9303	**179.1 nM** 20 points 0.9164	**1.188 µM** 20 points 0.8582	**466.0 nM** 25 points 0.9469	**2.481 nM** 18 points 0.7663	N/A
GPZ824390	**96.76 nM** 19 points 0.9017	**28.61 nM** 23 points 0.9578	**131.4 nM** 24 points 0.9550	**209.9 nM** 21 points 0.9091	**69.48 nM** 24 points 0.9296	**116.5 nM** 22 points 0.8716
GPZ273902	**56.88 nM** 22 points 0.9217	**130.2 nM** 22 points 0.9005	**299.2 nM** **21 points** 0.8289	**47.324 µM** 23 points 0.8910	**1.934 µM** 24 points 0.9069	**520.7 nM** 24 points 0.8672

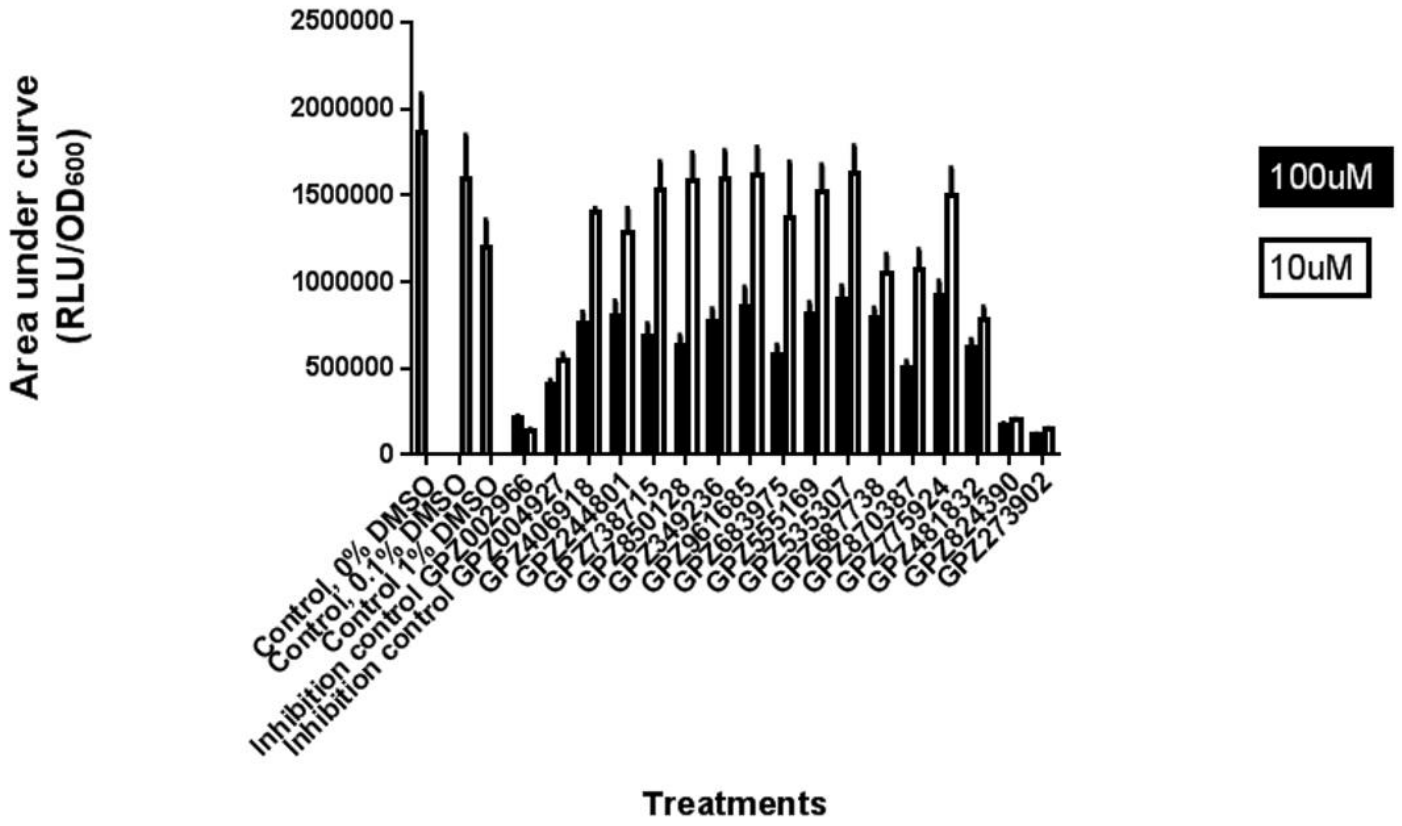


Figure 3.2. Summary of bioluminescence results in PAO1-L CTX*::*P_{pqsA}-*luxCDABE* exposed to the 15 GreenPharma PqsR inhibitory compounds. The bacterial strain was grown at 37°C overnight and exposed individually to two concentrations of each compound, 10 µM and 100 µM. Luminescence was read in cycles of 30 minutes for a period of 24 hours. Initial OD_{600} equals to 0.05. Experiment done in triplicate. Vertical lines above the individual columns correspond to standard deviation values.

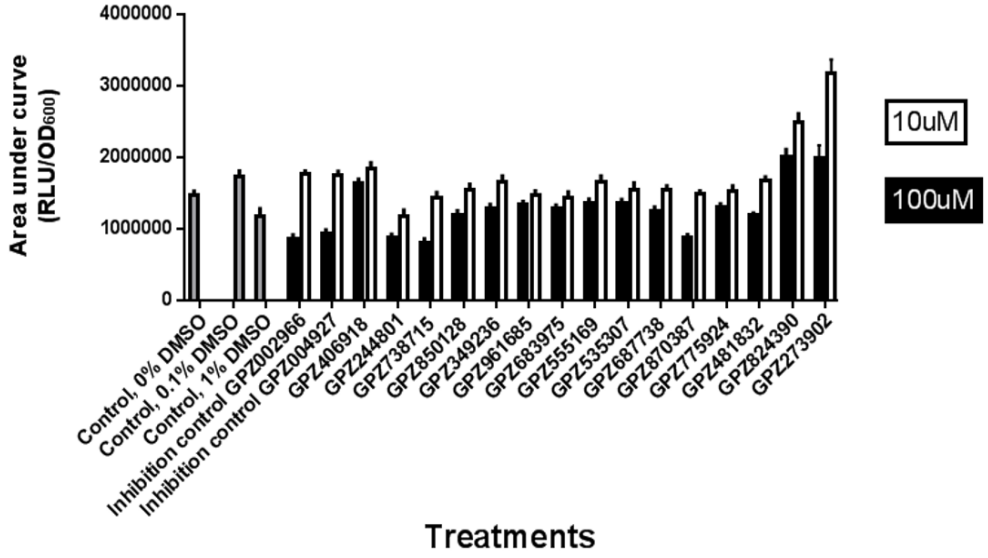


Figure 3.3. Summary of bioluminescence in PAO1-L CTX*::P_{Km}-luxCDABE* exposed to 15 putative GreenPharma Quorum sensing inhibiting compounds. The bacterial strain was grown at 37°C overnight and exposed individually to two concentrations of each compound, 10 µM and 100 µM. Luminescence was read in cycles of 30 minutes for a period of 24 hours. Initial OD_{600} equals to 0.05. Experiment done in triplicate

3.2.2. Synergistic effect of the PqsR inhibitors on CTX::P_{pqsA}-*luxCDABE*

In order to assess the possibility of synergistic effects between the different PqsR inhibitors, the biosensor strains were exposed to 25 µM of double combinations of the 15 inhibitors (Table 3.4). The results obtained with the *pqsA* biosensor revealed that some combinations have an upregulatory effect on *pqsA* expression, but a few showed increased inhibition when compared to the use of 100 µM individual concentrations. Thus, for a number of double combinations, a quarter of the individual concentration initially tested improved on the QS-inhibitory effects measured by repression of *pqsA* expression. These observations suggest that the improved inhibitory effects may be a result of a possible synergistic effect. In addition, the impact of these compounds on the expression of the control CTX::P_{Km}-*luxCDABE* reporter were also tested in PAO1-L and some combinations also in PA14 in double, triple and

quadruple combinations (see Tables A1.1 to A1.3 in the Annexes section) with considerable inhibitory effects.

Table 3.4. Summary of compound synergistic effects in PAO1-L CTX*::*P_{pqsA}-*luxCDABE* after double exposure (vertical columns combined with horizontal column – 25 µM of each compound). Green stands for percentage of remaining activity lower than the best individual inhibitory compounds, and red for percentage of remaining activity above the worst of the two individual inhibitors combined. Black stands for irrelevant variations. The last vertical and horizontal lines present the values corresponding to the exposure of the PAO1-L CTX*::*P_{pqsA}-*lux* to the compound individually. Percentages were obtained by comparing the AUC of the different double ombinations to the 1% DMSO control (DMSO percentage in the 100 µM exposure). Initial OD_{600} equals to 0.05. Values in brackets stand for standard deviation values in relative luminescence units.

PAO1-L CTX::P_{pqsA}-*lux*CDABE VS. 25µM each	GPZ406918	GPZ244801	GPZ738715	GPZ850128	GPZ349236	GPZ961685	GPZ683975	GPZ555169	GPZ535307	GPZ687738	GPZ870387	GPZ775924	GPZ481832	GPZ824390	GPZ002966	GPZ004927	GPZ273902	Individual variation (% of remaining activity @ 100 µM)
GPZ406918	X	989358 (82%) [115114]	794474 (66%) [58139]	889172 (74%) [58842]	1255102 (104%) [63418]	848321 (71%) [57445]	1348843 (112%) [118115]	2111178 (176%) [147022]	695547 (58%) [43897]	1897177 (158%) [131091]	1888638 (157%) [124447]	2315272 (193%) [165017]	655275 (54%) [26353]	477779 (40%) [16928]	183416 (15%) [8903]	506087 (42%) [24150]	97848 (8%) [10425]	758305 (41%) [65807]
GPZ244801	X	X	705919 (59%) [86587]	753352 (63%) [84814]	1035668 (86%) [129695]	1049322 (87%) [125140]	835735 (70%) [103492]	649530 (54%) [68685	422517 (35%) [47994]	437176 (36%) [47844]	251709 (21%) [19861]	1076624 (90%) [145461]	555108 (35%) [73921]	101309 (8%) [6680]	94877 (8%) [6520]	445805 (37%) [32103]	103199 (14%) [9817]	806782 (43%) [82260]
GPZ738715	X	X	X	1088756 (91%) [102760]	1160332 (97%) [114517]	849871 (71%) [87700]	685013 (57%) [75028]	1069136 (89%) [100866]	1097703 (91%) [101061]	733345 (61%) [73332]	465197 (39%) [36948]	1034097 (86%) [100783]	452526 (38%) [36317]	156660 (10%) [8118]	339253 (28%) [11016]	342550 (22%) [23213]	99447 (13%) [10481]	684566 (37%) [73693]
GPZ850128	X	X	X	X	1524730 (127%) [134388]	1264860 (105%) [123457]	746182 (62%) [75980]	874695 (73%) [79848]	2330196 (194%) [163966]	2003606 (167%) [143394]	1845729 (154%) [142808]	2226060 (185%) [166226]	874200 (73%) [86938]	417951 (35%) [15814]	382488 (32%) [9307]	552628 (46%) [34706]	100450 (8%) [9505]	627413 (34%) [63573]
GPZ349236	X	X	X	X	X	1212523 (101%) [117703]	700148 (58%) [71668]	1481457 (123%) [120739]	1472527 (122%) [127358]	1246222 (104%) [102754]	1246882 (104%) [104469]	1421811 (118%) [123245]	896469 (75%) [87711]	181884 (15%) [8148]	372878 (31%) [10144]	652949 (54%) [43722]	113574 (9%) [10952]	774976 (42%) [66829]
GPZ961685	X	X	X	X	X	X	565044 (47%) [54402]	1157172 (96%) [106798]	1618524 (135%) [124774]	859016 (71%) [90422]	1733033 (144%) [22812]	1184508 (99%) [118301]	594230 (49%) [48273]	182340 (15%) [7847]	379894 (32%) [9445]	723663 (60%) [47491]	108706 (9%) [10790]	859270 (46%) [110080]
GPZ683975	X	X	X	X	X	X	X	731679 (61%) [73373]	668183 (56%) [64724]	1099484 (91%) [87958]	419587 (35%) [32862]	748115 (62%) [76692]	403326 (34%) [32063]	171205 (14%) [8761]	325062 (27%) [9130]	461105 (38%) [32342]	121456 (10%) [11140]	582272 (31%) [54297]
GPZ555169	X	X	X	X	X	X	X	X	2175266 (181%) [148330]	1797522 (149%) [116585]	1733033 (144%) [117386]	2153350 (179%) [155765]	828569 (69%) [78099]	338516 (28%) [14090]	344677 (29%) [9543]	694161 (58%) [50915]	115301 (10%) [11031]	810298 (44%) [69735]
GPZ535307	X	X	X	X	X	X	X	X	X	988771 (82%) [71493]	1271841 (106%) [97466	755599 (63%) [71730]	645438 (54%) [50875]	182901 (15%) [8051]	134006 (11%) [6549]	618075 (51%) [42851]	114167 (9%) [10764]	902189 (49%) [74368]
GPZ687738	X	X	X	X	X	X	X	X	X	X	1357187 (113%) [96013]	1634025 (136%) [118853]	319549 (27%) [22220]	160608 (13%) [7623]	107941 (9%) [6995]	400389 (33%) [23529]	117392 (10%) [10979]	787063 (42%) [60127]
GPZ870387	X	X	X	X	X	X	X	X	X	X	X	307933 (26%) [24027]	213860 (18%) [10734]	145568 (12%) [7692]	302252 (25%) [7128]	400389 (33%) [31565]	104169 (9%) [11058]	502986 (27%) [38185]
GPZ775924	X	X	X	X	X	X	X	X	X	X	X	X	798506 (66%) [65458]	165362 (14%) [8064]	158849 (13%) [7491]	430213 (36%) [25903]	97724 (8%) [9292]	924766 (50%) [77991]

PAO1-L CTX::P_{pqsA}-*lux*CDABE VS. 25µM each	GPZ406918	GPZ244801	GPZ738715	GPZ850128	GPZ349236	GPZ961685	GPZ683975	GPZ555169	GPZ535307	GPZ687738	GPZ870387	GPZ775924	GPZ481832	GPZ824390	GPZ002966	GPZ004927	GPZ273902	Individual variation (% of remaining activity @ 100 µM)
GPZ481832	X	X	X	X	X	X	X	X	X	X	X	X	X	199092 (17%) [9420]	151334 (13%) [6995]	436854 (36%) [14453]	106953 (9%) [10934]	620287 (33%) [47961]
GPZ824390	X	X	X	X	X	X	X	X	X	X	X	X	X	X	178719 (15%) [8503]	201189 (17%) [7166]	106326 (9%) [7386]	175954 (15%) [7088]
GPZ002966	X	X	X	X	X	X	X	X	X	X	X	X	X	X	X	139215 (12%) [10429]	106676 (9%) [10388]	209697 (11%) [15617]
GPZ004927	X	X	X	X	X	X	X	X	X	X	X	X	X	X	X	X	119604 (10%) [12063]	407207 (22%) [25960]
GPZ273902	X	X	X	X	X	X	X	X	X	X	X	X	X	X	X	X	X	150193 (13%) [6001]
0% DMSO	X	X	X	X	X	X	X	X	X	X	X	X	X	X	X	X	X	X
1% DMSO	X	X	X	X	X	X	X	X	X	X	X	X	X	X	X	X	X	X
Individual variation (% of remaining activity @ 100 µM)	758305 (41%) [65807]	806782 (43%) [82260]	684566 (37%) [73693]	627413 (34%) [62573]	774976 (42%) [66829]	859270 (46%) [110080]	582272 (31%) [54297]	810298 (44%) [69735]	902189 (49%) [74368]	787063 (42%) [60127]	502986 (27%) [38185]	924766 (50%) [77991]	620287 (33%) [47961]	175954 (15%) [7088]	209697 (11%) [15617]	407207 (22%) [25960]	150193 (13%) [6001]	X

In terms of double combinations of GP QS-inhibiting compounds that result in an improved *pqsA* inhibition with just a quarter (25 µM) of the initial concentration (100µM), six out of fifteen compounds can be highlighted for their potential synergy in combinations, namely: GPZ273902 (14 combinations), GPZ824390 (7 combinations), GPZ244801 (5 combinations), GPZ687738 (5 combinations), GPZ870387 (5 combinations), GPZ002966 (3 combinations). It is important to observe that one of the best inhibitors, GPZ004927, does not add to the inhibitory synergistic effects, acting as a much better inhibitor when applied on its own.

GPZ273902 on its own was already a strong inhibitor, resulting in only 13% of remaining activity in *pqsA*-lux exposed to 100 µM and only in two combinations failing to deliver an improved inhibition. GPZ002966 initially identified as an inhibition control due to its inhibitory potency, only showed potential synergism in three combinations. The synergistic effect was also manifested with combinations of weaker inhibitors, when used individually, such as GPZ870387 and GPZ687738. In addition, compounds that individually at 100 µM responded halfway in the inhibiting spectrum strength produced an unexpected upregulatory effects on *pqsA* expression. However, when combined with a potent inhibitor they still show a negative effect on *pqsA* transcription. The latter is the case, for example, for GPZ406918 combined with GPZ273902 (8% remaining *pqsA* activity when combined) and GPZ738715 combined to GPZ824390 (10% remaining *pqsA* activity when combined).

Even though these results are just a crude evaluation of the synergistic capacity of these compounds, as there is no statistical analysis of their combinatory profiles, it is reasonable to suggest that when looking at inhibition of PqsR, combination of inhibitors leads to better inhibitory effects, in some cases.

3.3. Effect of PqsR inhibitors on AQ-dependent virulence factor production

After initial assessment of the capacity of the molecules mentioned above, in inhibiting *pqsA* expression, assessment of their effects on three key virulent phenotypes controlled by the AQ system was conducted in PA. These were lectin and PCN production as well as biofilm formation. The primary strain used was PAO1, but to ensure the effect observed was not strain specific, PA14 and SED2-LES were also used.

In addition, synergistic effects of double combinations were also tested in some of these phenotypes. Data using triple and quadruple compound combinations is shown in the Annexes section (Tables A1.1 to A1.3).

3.3.1. QSIs effects on the production of lectins

Lectin-mediated bacterium-cell recognition and adhesion are critical steps in initiating PA pathogenesis. In PA, adhesion is mediated by a glycanic recognition pattern involving several adhesins, including lectins, where LecA and LecB are protein products present mainly on the surface of the bacterium. These two lectins are regulated by both QS and the alternative sigma factor RpoS, suggesting that they are parts of the numerous systems involved in PA virulence playing a major role in lung injury (36). Both LecA and LecB participate in the adhesion of the bacteria to endothelial cells, are involved in pilus biogenesis and are important for complementation.

Two chromosomal bioreporters, PAO1-N CTX::P_{lecA}-*lux* and PAO1-N CTX::P_{lecB}-*lux*, were tested for luminescence production to assess the effect of pre-selected GreenPharma compounds on LecA and LecB production. Assays included individual exposures to the best 8 of a total of 15 candidate *pqsA*-

inhibiting compounds at an individual concentration of 10 and 100 µM (Table 3.5), as well as assessment of synergistic double combinations (individual exposures to 50 µM), triple combinations at individual exposures to 50 µM (Tables A1.6 in the Annexes section) and quadruple combinations at individual exposures to 25 µM) of the referred compounds (data not shown).

Whilst 6 out of 8 compounds repressed *lecA* activity at 10 µM that was not at all the case for *lecB* (Table 3.6), as there was only one compound (GPZ273902) capable of that, and at both 10 and 100 µM concentrations. GPZ273902 seems again to be the compound that more efficiently inhibits virulence (see Table 3.4).

Table 3.5. Summary of bioluminescence in PAO1-N CTX::P$_{lecA}$-*luxCDABE* after individual exposure to pre-selected *pqsA*-inhbiting GreenPharma compounds. Strains were grown overnight at 37°C in LB medium and exposed to two individual concentrations of 10 µM and 100 µM. Bold values stand for inhibitory effects with percentage of remaining activity of *lecA* below 33% (100µM) and 45% (10µM). AUC = area under curve. Initial OD_{600} equals to 0.05. Values in brackets stand for standard deviation values in relative luminescence units.

GP QS-inhibiting compound	Bioluminescence at 10 µM (AUC)	Percentage of remaining activity at 10 µM	Bioluminescence at 100 µM (AUC)	Percentage of remaining activity at 100 µM
GPZ824390	1070605 [89424]	**34%**	1034178 [81715]	46%
GPZ002966	807198 [64675]	**26%**	739829 [58558]	**33%**
GPZ004927	777874 [54524]	**25%**	1129226 113088]	51%
GPZ244801	1310024 [180501]	**42%**	1079732 [182917]	48%
GPZ687738	3344142 [382127]	**107%**	1452204 [237801]	65%
GPZ870387	2843583 [314926]	91%	1538483 [232042]	69%
GPZ481832	1079732 [182917]	**34%**	1823619 [162818]	82%
GPZ273902	1199320 [167091]	**38%**	1021920 [145769]	46%
Average of 0% DMSO	2914770 [323819]	-	2914770 [323819]	-
Average of 0.1% DMSO	3135185 [357637]	-	-	-
Average of 1% DMSO	-	-	2229706 [295194]	-

Contrarily to *lecA*, *lecB* expression was not repressed much by the compounds at both concentrations used with one exception, GPZ273902. Five of the compounds tested showed increased expression of this lectin, but the reasons behind this remain to be investigated.

Table 3.6. Summary of bioluminescence in PAO1-N CTX::P_{lecB}-*luxCDABE* after individual exposure to selected GreenPharma compounds. Strains were grown overnight at 37°C in LB medium and exposed to two individual concentrations of 10 µM and 100 µM. Green bold values stand for inhibitory effects with percentage of remaining activity of *lecB* below 33% (100µM) and 45% (10µM). Red bold values stand for upregulation of *lecB*. AUC = area under curve. Initial OD_{600} equals to 0.05. Values in brackets stand for standard deviation values in relative luminescence units.

GP QS-inhibiting compound	Bioluminescence at 10 µM (AUC)	Percentage of remaining activity at 10 µM	Bioluminescence at 100 µM (AUC)	Percentage of remaining activity at 100 µM
GPZ824390	507194 [10943]	77%	285851 [9122]	81%
GPZ002966	574114 [10922]	88%	328469 [9211]	94%
GPZ004927	658109 [11312]	100%	492181 [9700]	**140%**
GPZ244801	1308722 [20492]	**200%**	515228 [9185]	**147%**
GPZ687738	1174990 [17083]	**179%**	268617 [8849]	76%
GPZ870387	1182076 [17068]	**180%**	627305 [12164]	**179%**
GPZ481832	1228477 [21022]	**187%**	445916 [8996]	**127%**
GPZ273902	89958 [7303]	**14%**	76902 [6453]	**22%**
Average of 0% DMSO	655740 [18276]	-	655740 [18276]	-
Average of 0.1% DMSO	550001 [14938]	-	-	-
Average of 1% DMSO	-	-	351194 [10679]	-

3.3.1.1. Synergistic effects on *lecA/lecB* expression in PAO1-N after double exposure to PqsR inhibitors

Some of the compound combinations used to test synergism on the repression of the *pqsA* and P_{Km} reporters were used to test the expression of the *lecA* (Table 3.7) and *lecB* (Table 3.8) reporters. Results obtained are very

promising since they delivered a reduction in the percentage of remaining activity even when using lower concentrations of the QS-inhibiting agents.

Table 3.7. Summary of percentage of remaining activity of *lecA* after double combinatory exposures to selected GreenPharma inhibitors. Strain was grown overnight at 37°C in LB medium and exposed to quadruple combinations of GP QS-inhibiting compounds at an individual concentration of 25 µM. Luminescence was read every 30 minutes for a period of 24 hours. Green stands for percentage of remaining activity lower than the better of the two individual compounds combined, and red for percentage of remaining activity above the worst of the two individual compounds combined. Black stands for inert combinations. Percentages were obtained by comparing the AUC of the different triple combinations to the 1% DMSO control (DMSO percentage in the 100 µM exposure). Initial OD_{600} was of 0.05. Values in brackets stand for standard deviation values in relative luminescence units.

PAO1-L CTX::P_{lecA}-*lux* VS. 25 µM each	GPZ824390	GPZ002966	GPZ004927	GPZ244801	GPZ687738	GPZ870387	GPZ481832	GPZ273902	Percentage of remaining activity at 100 µM
GPZ824390	*	976557 (43%) [83460]	904672 (28%) [71723]	577078 (18%) [63118]	369416 (16%) [29249]	1141077 (50%) [75950]	876499 (27%) [71951]	477086 (45%) [69555]	1034178 (42%) [81715]
GPZ002966	*	*	908231 (28%) [73349]	670875 (21%) [72121]	685579 (30%) [52411]	923649 (41%) [69513]	1546261 (68%) [125060]	437427 (41%) [63158]	739829 (30%) [58558]
GPZ004927	*	*	*	1757270 (77%) [231798]	1062827 (47%) [80651]	883527 (39%) [65361]	1180595 (36%) [90642]	534609 (50%) [58071]	1129226 (46%) [113088]
GPZ244801	*	*	*	*	2065344 (124%) [275868]	1652876 (99%) [182112]	1602222 (63%) [177780]	409915 (38%) [46654]	1079732 (44%) [182917]
GPZ687738	*	*	*	*	*	2481153 (34%) [271238]	824773 (41%) [80439]	785783 (28%) [36271]	1452204 (91%) [237801]
GPZ870387	*	*	*	*	*	*	815396 (47%) [77191]	785783 (28%) [26551]	1538483 (97%) [232042]
GPZ481832	*	*	*	*	*	*	*	940806 (31%) [91538]	1823619 (56%) [162818]
GPZ273902	*	*	*	*	*	*	*	*	1021920 (33%) [145769]
Percentage of remaining activity at 100 µM	1034178 (42%) [81715]	739829 (30%) [58558]	1129226 (46%) [113088]	1079732 (44%) [182917]	1452204 (91%) [237801]	1538483 (97%) [232042]	1823619 (56%) [162818]	1021920 (33%) [145769]	*

All double combinations using the top 8 compounds from the initial pool of 15 reduced *lecA* expression, but not all improve *lecA* inhibition, i.e., the obtained *lecA* expression levels when the two most active compounds were added individually were higher than when combined together. The most remarkable inhibiting effects observed on *lecA* expression were those by the GPZ824390/GPZ687738 combination that reduced remaining activity to a mere 16%, when the best of their individual effect was at 42% (at 100 µM). Another effective combination is the one produced by GPZ824390/GPZ244801 reducing *lecA* expression to 18% improving on the better of their individual participations by a 24% reduction. Contrarily to what could be expected, double-combining the four best *pqsA* inhibitors (GPZ824390, GPZ273902, GPZ002966 and GPZ004927) did not correspond to improved inhibition effects on *lecA*, except when GPZ004927 is present. GPZ004927 shows good synergistic effects on most of its double combinatory participations, but does not respond properly when combined to GPZ273902. Overall GPZ824390 and GPZ481832 are the compounds that effectively produce the most number of *lecA* inhibiting double combinations. Their double combination would be expected to repress *lecA* expression and indeed it did reduce *lecA* activity to remaining activity of 27%, 15% less than what is achieved with GPZ824390 at an individual participating concentration of 100 µM. Noteworthy that also for *lecA*, the role of GPZ244801 as the worse of the selected inhibitors is reinforced by the obtained data.

In regards to synergistic effects using *lecB*, once again a more robust capacity to counteract the QS-inhibiting potency of the tested agents is observed. However, whenever a double combination includes GPZ273902 the result is often a strong repression resulting in low percentages of remaining *lecB* expression. Both GPZ273902 and GPZ481832 have delivered the best results when combined to the other compounds, especially for GPZ273902/GPZ870387 constraining the gene expression to only 37% of remaining *lecB* activity.

Table 3.8. Summary of percentage of remaining activity of *lecB* after double combinatory exposures to selected GreenPharma inhibitors. Strain was grown overnight at 37°C in LB medium and exposed to quadruple combinations of GP QS-inhibiting compounds at an individual concentration of 25 µM. Luminescence was read every 30 minutes for a period of 24 hours. Green stands for percentage of remaining activity lower than the better of the two individual compounds combined, and red for percentage of remaining activity above the worst of the two individual compounds combined. Black stands for inert combinations. Percentages were obtained by comparing the AUC of the different triple combinations to the 1% DMSO control (DMSO percentage in the 100 µM exposure). Initial OD_{600} was of 0.05. Values in brackets stand for standard deviation values in relative luminescence units.

QS-inhibitor at an individual concentration of 25 µM	GPZ824390	GPZ002966	GPZ004927	GPZ244801	GPZ687738	GPZ870387	GPZ481832	GPZ273902	Percentage of remaining activity with Individual exposure of 100µM
GPZ824390	*	432463 (55%) [10896]	313112 (61%) [15868]	267788 (62%) [7574]	**296557 (57%) 14931**	294444 (68%) [7511]	305701 (71%) [7849]	252044 (58%) [6776]	285851 (48%) [9122]
GPZ002966	*	*	301710 (58%) [13034]	303767 (70%) [8467]	**300497 (69%) [8387]**	278524 (64%) [8322]	**230229 (53%) [6684]**	272624 (63%) [7487]	328469 (56%) [9211]
GPZ004927	*	*	*	**239747 (46%) [11870]**	309768 (60%) [14365]	**94371 (59%) [7803]**	**284747 (55%) [13095]**	**86848 (55%) [7030]**	492181 (83%) [9700]
GPZ244801	*	*	*	*	**535203 (103%) [52477]**	**488235 (94%) [48080]**	**520682 (81%) [38544]**	**208896 (40%) [9144]**	515228 (87%) [9185]
GPZ687738	*	*	*	*	*	**493302 (95%) [46921]**	389026 (75%) [32904]	**220619 (43%) [9717]**	268617 (46%) [8849]
GPZ870387	*	*	*	*	*	*	**96485 (61%) [7865]**	**192430 (37%) [9717]**	627305 (76%) [12164]
GPZ481832	*	*	*	*	*	*	*	**86388 (54%) [6982]**	445916 (106%) [8996]
GPZ273902	*	*	*	*	*	*	*	*	76902 (68%) [6453]
Percentage of remaining activity with Individual exposure of 100µM	48%	56%	83%	87%	46%	76%	106%	68%	*

3.3.2. Effect of PqsR inhibitors on pyocyanin production

To understand how the PqsR inhibitors affected the production of the AQ-controlled PCN in different strains (with differing virulence potentials), the effect of these compounds were tested on PAO1-N, PA14 and SED2-LES (Table 3.9).

Table 3.9. Effect of GP QS-inhibiting compounds on pyocyanin production. Strains were grown overnight at 37°C and then standardised to an OD_{600} of 1.0 to be exposed to the GP QS-inhibiting compounds whilst reincubating at 37°C and 200 rpm for 18 hours. Compounds were added to individual concentrations of 10 µM, 100 µM and IC_{50} values (57 nM GPZ273902, 74 nM GPZ004927, 97 nM GPZ824390, 395 nM GPZ002966). Whenever possible the samples were exposed to IC_{10}, IC_{70} and IC_{90} values. Three replicates of each treatment were analysed. Green and red bold values stand for percentage of remaining activity at least 20% below and above control, respectively.

PAO1-N	Mean [Pyocyanin] µg/ml	Remaining Pyocyanin Production %	Standard deviation ± 95% confidence (µg/ml)
10 µM GPZ824390	0.058	**1.2%**	0.40 ± 0.02
10 µM GPZ244801	4.43	92%	26.00 ±1.3
14.5 nM GPZ824390 (IC_{10})	7.16	84.5%	8.40 ±0.42
747 nM GPZ824390 (IC_{70})	1.70	**27.4%**	2.00 ±0.10
1.2 µM GPZ824390 (IC_{90})	0.55	**8.9%**	0.80 ±0.04
57 nM GPZ273902 (IC_{50})	14.22	**35%**	1.87 ± 0.09
74 nM GPZ004927 (IC_{50})	27.26	**246%**	5.05 ± 0.25
97 nM GPZ824390 (IC_{50})	6.05	119%	1.52 ± 0.08
395 nM GPZ002966 (IC_{50})	14.12	**34%**	8.40 ± 0.42
PA14	**Mean [Pyocyanin] µg/ml**	**Remaining Pyocyanin Production %**	**Standard deviation ± 95% confidence (µg/ml)**
10 µM GPZ002966	6.726	**57%**	2.00 ±0.10
10 µM GPZ824390	1.383	**12%**	1.00 ±0.05
10 µM GPZ481832	7.230	**63%**	0.60 ±0.03
10 µM GPZ244801	11.23	98%	2.80 ±0.14
10 µM GPZ870387	11.78	85%	1.60 ±0.08
10 µM GPZ273902	28.10	**125%**	5.00 ±0.25
10 µM GPZ004927	3.107	**11%**	0.60 ±0.03
10 µM GPZ687738	11.90	94%	0.40 ±0.02
57 nM GPZ273902 (IC_{50})	7.085	**33%**	0.88 ± 0.04
74 nM GPZ004927 (IC_{50})	27.55	119%	4.22 ± 0.21
97 nM GPZ824390 (IC_{50})	6.940	**77%**	0.53 ± 0.03
395 nM GPZ002966 (IC_{50})	3.730	**44%**	0.98 ± 0.05
PA SED2-LES	**Mean [Pyocyanin] µg/ml**	**Remaining Pyocyanin Production %**	**Standard deviation ± 95% confidence (µg/ml)**
10 µM GPZ961685	30.52	105%	4.80 ±0.24
10 µM GPZ687738	16.43	**46%**	2.60 ±0.13
10 µM GPZ870387	29.27	96%	3.60 ±0.18
10 µM GPZ481832	26.71	88%	5.00 ±0.25
10 µM GPZ002966	10.93	**28%**	2.20 ±0.11
10 µM GPZ824390	6.385	**17%**	1.20 ±0.06
10 µM GPZ004927	13.19	**35%**	1.60 ±0.08
10 µM GPZ244801	36.03	87%	3.20 ±0.16
10 µM GPZ273902	26.98	**65%**	3.00 ±0.15
10 µM GPZ683975	25.94	**75%**	4.40 ±0.22
10 µM GPZ824390	19.56	**38%**	4.36 ±0.22
100 µM GPZ961685	24.17	85%	N/A
100 µM GPZ555169	24.39	85%	3.00 ±0.15
100 µM GPZ870387	20.84	**73%**	N/A
57 nM GPZ273902 (IC_{50})	38.93	89%	2.60 ±0.13
74 nM GPZ004927 (IC_{50})	48.08	110%	3.88 ±0.19
97 nM GPZ824390 (IC_{50})	44.11	86%	3.12 ±0.16
395 nM GPZ002966 (IC_{50})	43.11	98%	6.40 ±0.32
747 nM GPZ824390 (IC_{70})	18.36	**71%**	0.80 ±0.04
2.077 µM GPZ002966 (IC_{70})	8.869	**55%**	5.00 ±0.25
8.025 µM GPZ004927 (IC_{90})	15.17	94%	3.00 ±0.15

The results initially obtained suggested that only the top four QS-inhibitting compounds had enough strength to reduce PCN production at IC_{50} values. Further testing indicated that GPZ824390 at a concentration of 10 µM is the best PCN production inhibitor available. Reduction caused by its action ranges from 17% in SED2-LES (the most virulent strain) to 1.2% in PAO1-N (the least virulent strain). Nevertheless, as an example of all the top compounds tested its capacity to reduce PCN production decreases with the increase in pathogenicity of the tested strain. GPZ002966 also shows strong inhibiting virulence repression by reducing remaining activity strongly at 10 µM in PA14 (57%) and to 28% in SED2-LES. However, the most surprising results emerging from the PCN measurements were the ones produced by both GPZ004927 and GPZ273902 with both showing contradictory effects; GPZ004927 at its IC_{50} is not capable of inhibiting PCN formation and it even promotes its production in the least virulent strain (246% of remaining activity in PAO1-N). GPZ273902 at 10 µM induces expression of PCN in PA14 but reduces it to 65% remaining activity in SED2-LES; nonetheless at its IC_{50} it does show its strength by reducing PCN production in PA14 to 33% remaining activity, but is not able to produce better than an 11% decrease in remaining activity on the most virulent strain SED2-LES by reducing it to 89% remaining activity.

Synergistic effects were also measured in terms of PCN production and showed relevant inhibition even when using compounds outside the top four listing (Table A1.7 in the Annexes section). Nevertheless, not many combinations were tested, but results obtained sustain the idea brought from previous experiments with *pqsA*, *PKm*, *lecA* and *lecB*. This meaning that at smaller individual concentrations, a combination of GP QS-inhibiting compounds will operate on PqsR delivering reduced levels of virulence than when exposed to their individual counterparts at a higher concentration.

3.3.3. Effect of PqsR on biofilm formation

To understand the impact of the PqsR-inhibiting molecules on the formation of biofilm, this research study analysed their effect on PAO1-L::mCherry. Initially, the subject strain was exposed to the four best PqsR inhibitors at their IC_{50} concentrations with the DMSO controls (figures 3.4 to 3.8). The analysis to the biofilm produced was based on two direct parameters, biomass (providing an idea of matrix growth) and surface area (providing an idea of matrix spreading). Consequently, the biofilm formation was analysed when PAO1-L::mCherry was exposed to a range of concentrations of GPZ824390 and GPZ273902 to up to 100 nM (figures 3.9 and 3.11). Finally, two individual log curves ranging from 2 nM to 2 mM were produced for GP QS-inhibiting compounds GPZ824390 and GPZ273902 (figures 3.10 and 3.12). Biomass and surface area results are summarised in Table 3.10.

Table 3.10. Summary of biomass and surface area in biofilms exposed to the top 4 PqsR inhibitors. The concentrations used at the time of the assay were those belived at the time to be the IC50 values of the corresponding QSI compounds. Values in green represent the best biofilm inhibition produced whilst using less QSI compound, hence GPZ0002966 at 395 nM is not considered the best biofilm repressor.

[QSI Compound]	Biomass ($\mu m^3/\mu m^2$)	Surface Area (μm^2)
Control (2% DMSO)	62.3	$9.5x10^6$
395 nM GPZ002966	36.0	$4.2x10^6$
88 nM GPZ004927	37.1	$4.5x10^6$
70 nM GPZ824390	48.8	$8.1x10^6$
55 nM GPZ273902	56.1	5.8

3.3.3.1. Images of PAO1-L::mCherry biofilm formation after exposure to the top four GP QS-inhibiting compounds at their IC_{50}s

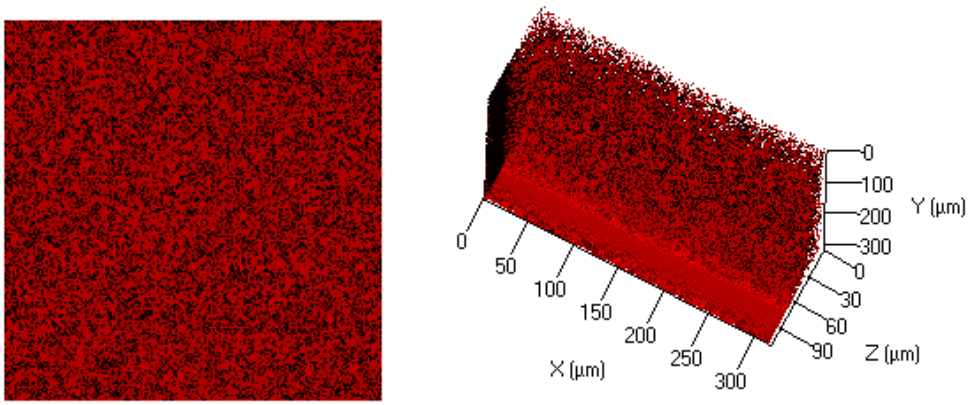


Figure 3.4. Biofilm production by PAO1-L::mCherry exposed to 2% DMSO - Left) 2D surface perspective, **Right) 3D perspective.** Strain was grown at 37°C overnight in LB medium with 200 rpm shaking and then diluted to OD_{600} of 1.0 for subsequent static overnight growth (20 hours) at 37°C in RPMI medium. Biofilm formation observed by confocal microscopy and analysed with Comstat2. **Biomass = 62.3 µm³/µm² and surface area = 9.5E6 µm²** (data obtained by analysis of channel T–PMT).

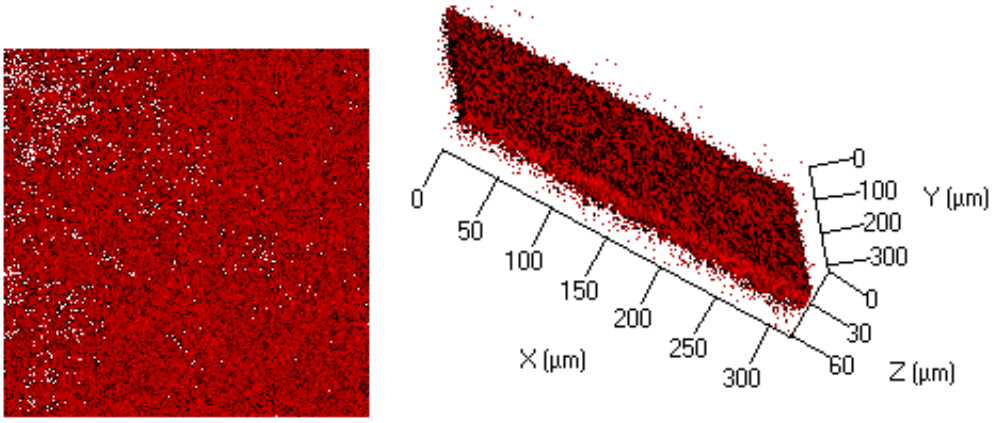


Figure 3.5. Biofilm production by PAO1-L::mCherry exposed to 395 nM GPZ002966 - Left) 2D surface perspective, **Right) 3D perspective.** Strain was grown at 37°C overnight in LB medium with 200 rpm shaking and then diluted to OD_{600} of 1.0 for subsequent static overnight growth (20 hours) at 37°C in RPMI medium. Biofilm formation observed by confocal microscopy and analysed with Comstat2. **Biomass = 36.0 µm³/µm² and surface area = 4.2E6 µm²** (data obtained by analysis of channel T–PMT).

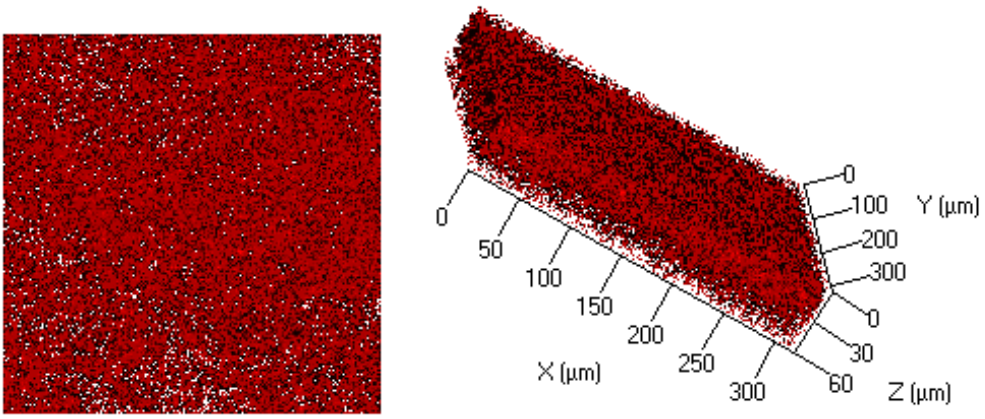


Figure 3.6. Biofilm production by PAO1-L::mCherry exposed to 88 nM GPZ004927 - Left) 2D surface perspective, **Right) 3D perspective.** Strain was grown at 37°C overnight in LB medium with 200 rpm shaking and then diluted to OD_{600} of 1.0 for subsequent static overnight growth (20 hours) at 37°C in RPMI medium. Biofilm formation observed by confocal microscopy and analysed with Comstat2. **Biomass = 37.1 µm³/µm² and surface area = 4.5E6 µm²** (data obtained by analysis of channel T–PMT).

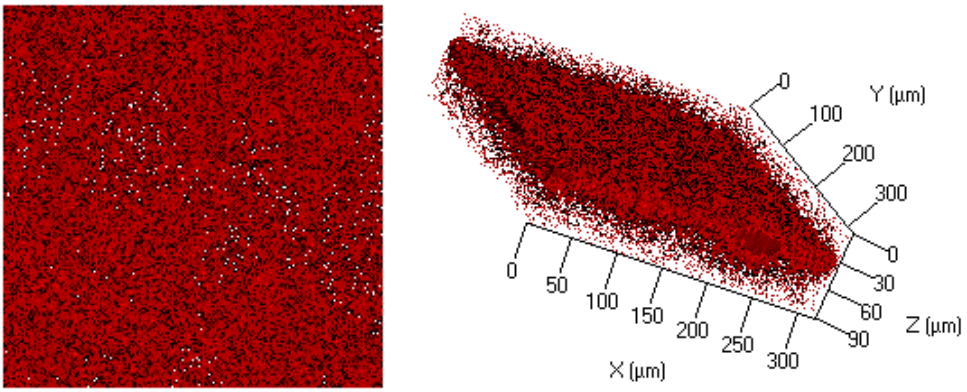


Figure 3.7. Biofilm production by PAO1-L::mCherry exposed to 70 nM GPZ824390 - Left) 2D surface perspective, **Right) 3D perspective.** Strain was grown at 37°C overnight in LB medium with 200 rpm shaking and then diluted to OD_{600} of 1.0 for subsequent static overnight growth (20 hours) at 37°C in RPMI medium. Biofilm formation observed by confocal microscopy and analysed with Comstat2. **Biomass = 48.9 µm³/µm² and surface area = 8.1E6 µm²** (data obtained by analysis of channel T–PMT).

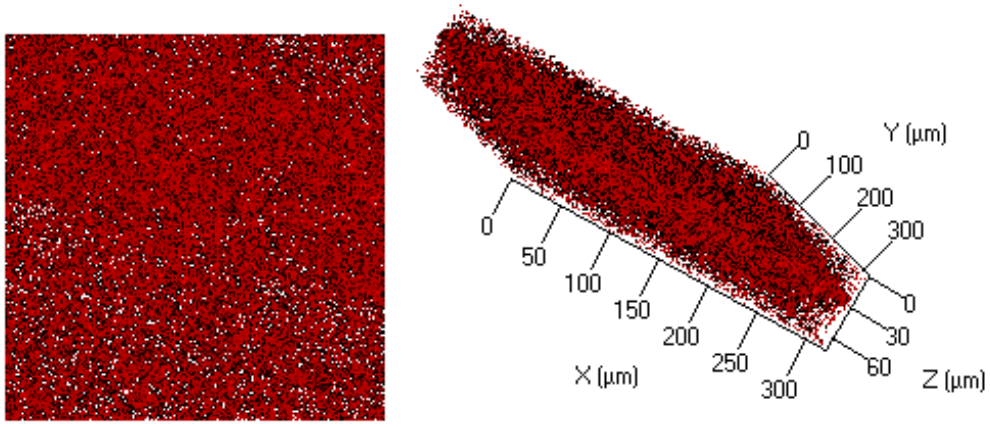


Figure 3.8. Biofilm production by PAO1-L::mCherry exposed to 55 nM GPZ273902 - Left) 2D surface perspective, **Right) 3D perspective.** Strain was grown at 37°C overnight in LB medium with 200 rpm shaking and then diluted to OD_{600} of 1.0 for subsequent static overnight growth (20 hours) at 37°C in RPMI medium. Biofilm formation observed by confocal microscopy and analysed with Comstat2. **Biomass = 36.1 $\mu m^3/\mu m^2$ and surface area = 5.8E6 μm^2** (data obtained by analysis of channel T–PMT).

3.3.3.2. Analysis of a PAO1-L::mCherry putative dual behaviour response

The biofilm reduction accomplished with the top four PqsR-inhibitors at IC_{50} concentrations prompted to testing if the effect of these compounds on biofilm formation was dose-dependent. Consequently, a range of concentrations ranging from 3.12 nM to 100 nM were used and expected lighter phenotypic pressure, and another one of expected stronger inhibitory effects ranging from 2 nM to 2 mM. In that sense, PAO1-L::mCherry was individually exposed to GPZ273902 (figure 3.9 and 3.10) and GPZ824390 (figure 3.11 and 3.12) and the produced biomass and surface area of the corresponding formed biofilms were assessed.

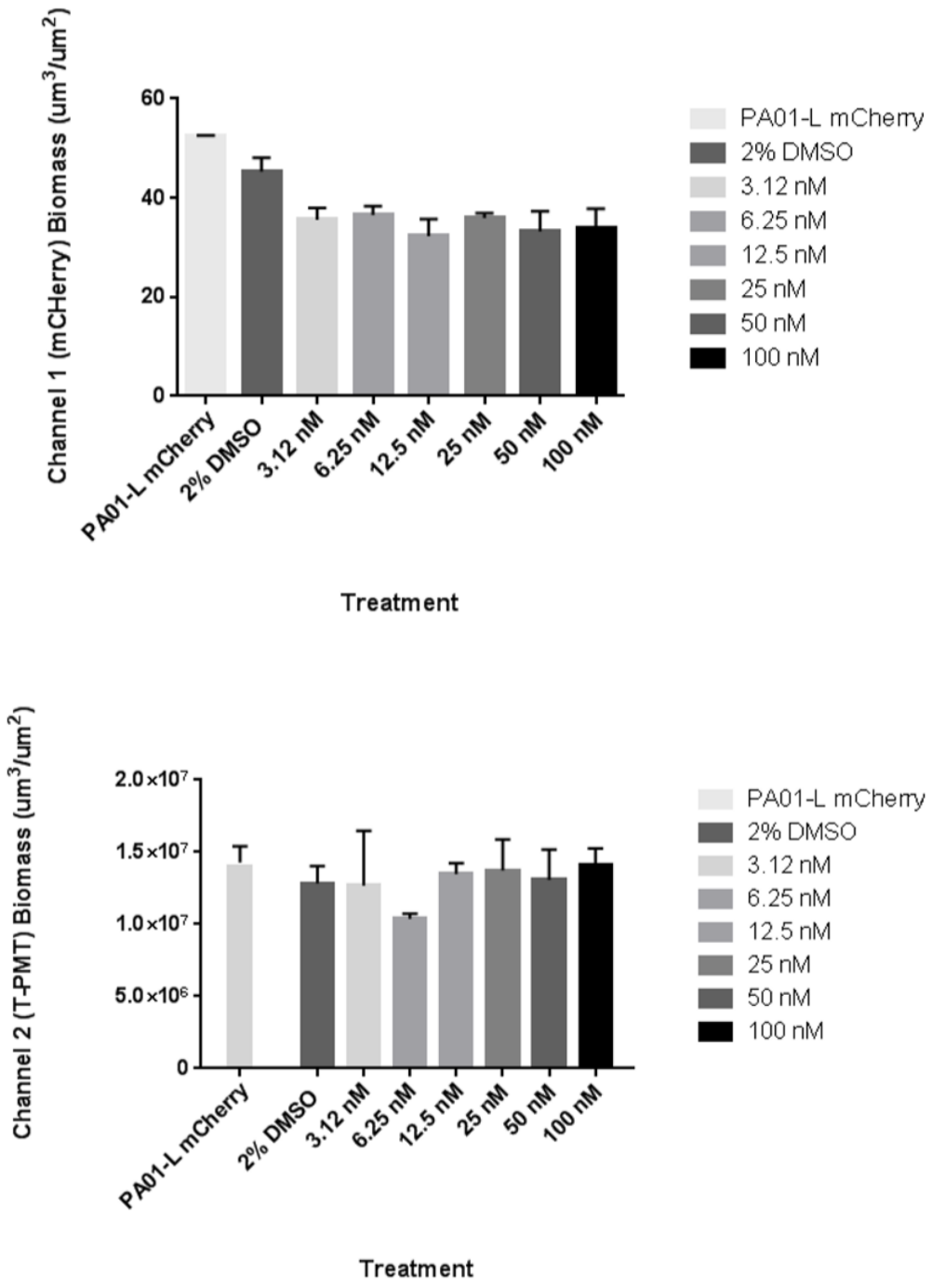


Figure 3.9. Effect of a range of concentrations of GP QS-inhibitor GPZ273902 on biofilm biomass (up) and surface area (down) of a PAO1-L::mCherry biofilm. Strain was grown at 37°C overnight in LB medium with 200 rpm shaking and then diluted to OD_{600} of 1.0 for subsequent static overnight growth (48 hours) at 37°C in RPMI medium without glutamine. Data corresponding to 5 replicates. Vertical bars correspond to standard deviation.

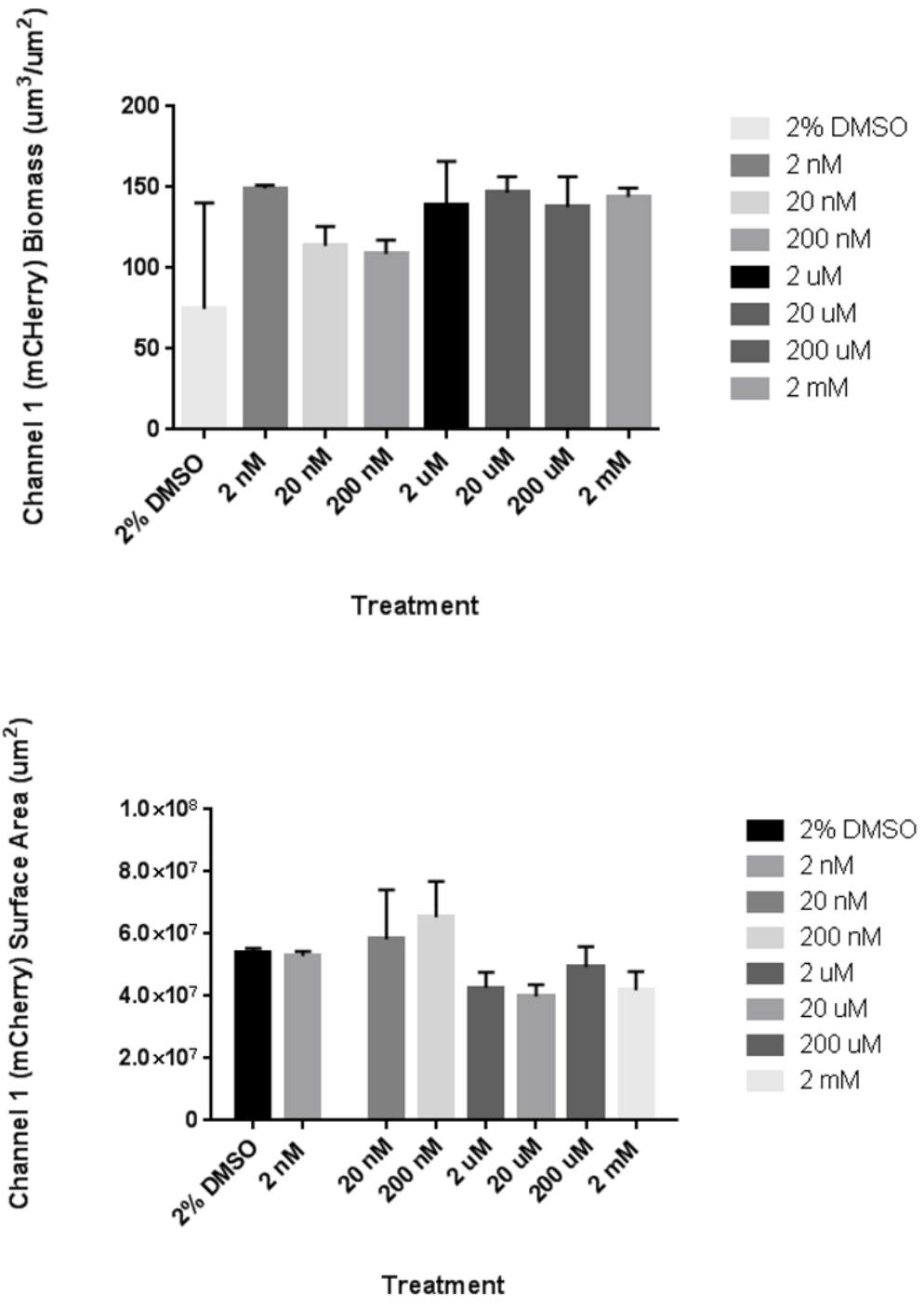


Figure 3.10. Effect of a log curve of concentrations of GP QS-inhibitor GPZ273902 on biofilm biomass (up) and surface area (down) of PAO1-L::mCherry. Strain was grown at 37°C overnight in LB medium with 200 rpm shaking and then diluted to OD_{600} of 1.0 for subsequent static overnight growth (24 hours) at 37°C RPMI medium without glutamine. Data corresponding to 5 replicates. Vertical bars correspond to standard deviation.

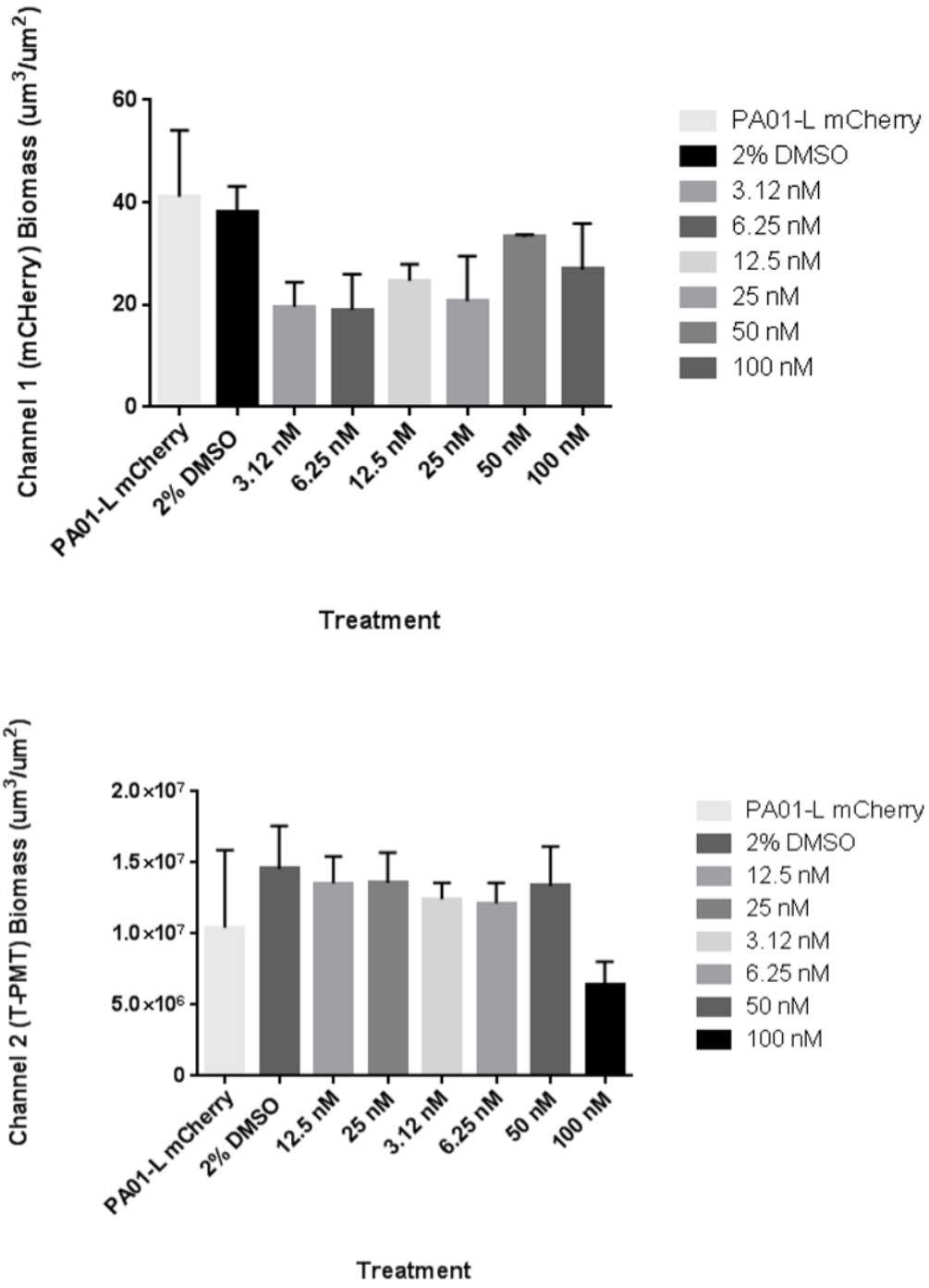


Figure 3.11. Effect of a range of concentrations of GP QS-inhibitor GPZ824390 on biofilm biomass (up) and surface area (down) of PAO1-L::mCherry. Strain was grown at 37°C overnight in LB medium with 200 rpm shaking and then diluted to OD_{600} of 1.0 for subsequent static overnight growth (48 hours) at 37°C in RPMI medium without glutamine. Data corresponding to 5 replicates. Vertical bars correspond to standard deviation.

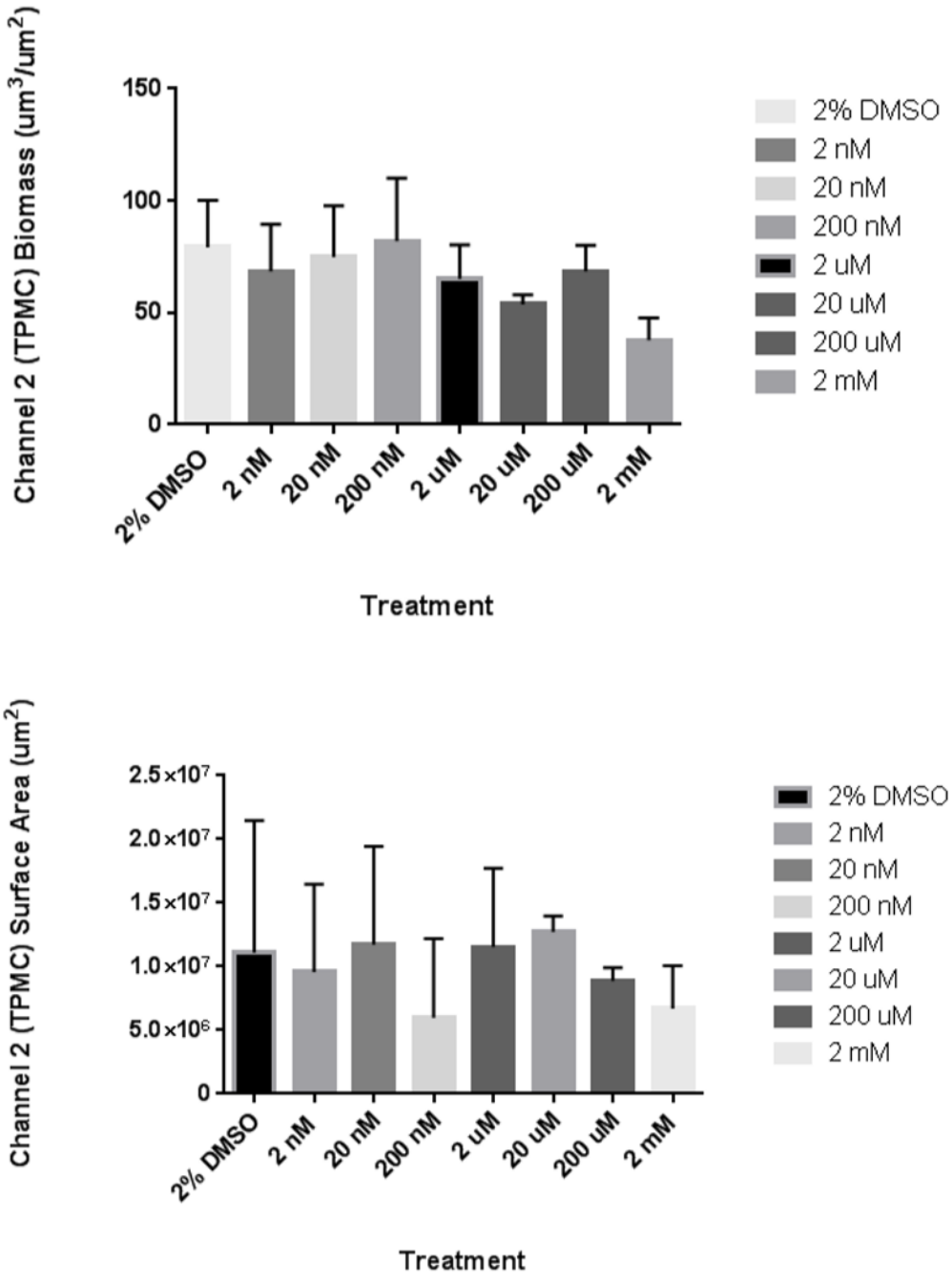


Figure 3.12. Effect of a log curve of concentrations of GP QS-inhibitor GPZ273902 on biofilm biomass (up) and surface area (down) of PAO1-L::mCherry. Strain was grown at 37°C overnight in LB medium with 200 rpm shaking and then diluted to OD_{600} of 1.0 for subsequent static overnight growth (24 hours) at 37°C in RPMI medium without glutamine. Data cprresponding to 5 replicates. Vertical bars correspond to standard deviation.

With regards to the biofilm formed in the presence of GPZ273902, it is easily observed that a slight reduction in biomass is produced up to 200 nM.

But after 200 nM no effects on biomass production are found, however a reduction in biofilm surface area is suggested after such concentration of GPZ273902. On the other hand, and concerning GPZ824390, there is a repressive effect on biomass production visible from the very first tested concentrations and up to 2 mM of compound, whilst the surface area seems to be only affected after a concentration of over 100 nM of compound.

Even though there is a high level of variability between these experiements, the results suggest two possible outcomes: 1) GPZ824390 shows a likely stronger inhibitory potential of biomass production at low concentrations with surface area inhibition occurring after 100 nM of compound; and 2) GPZ273902 also induces repression of biofilm biomass production in early concentration points of the tested scale, but soon (~200 nM) the biomass production remains unaltered giving way to repression effects seen on the surface area of the formed biofilm.

3.4. Impact of PqsR inhibitors on AQs biosynthesis

In order to identify and allow further quantification of the effects of the GP PqsR inhibitors on a number of AQs (e.g., HHQ, HQNO and PQS), two strains differing in virulence potential (PAO1-N and PA14) were exposed to IC_{50} values of the previously selected top compounds, namely: 57 nM GPZ273902, 74 nM GPZ004927, 97 nM GPZ824390 and 395 nM GPZ002966. The results produced by exposures to the referred QS-inhibiting molecules (figures 3.13 and 3.14) were analysed by LC-MS/MS and compared to control exposures, at equivalent percentage volumes of solvent (DMSO) in which these compounds had been reconstituted. In addition, a deuterated internal standard, d4-PQS, was used for calibration and control purposes. Overall the best inhibitor of AQs production is GPZ824390 in PAO1-N. A contradictory effect is seen in PAO1-N

and PA14 for GPZ273902 when upregulatory effects are observed, but due to inherent reinforced virulence are not so much felt in the latter strain.

Individually speaking, GPZ273902 at IC_{50} concentration only produced a slight increase in all tested molecules in PAO1-N. On the other hand, GPZ273902 effects over a more virulent PA14 generated a slight increase of HHQ and PQS, whilst maintaining the levels of HQNO.

GPZ004927 at 74 nM generates a slight increase in the levels of HHQ and PQS, whilst reducing the levels of produced HQNO. In PA14 a slight reduction in HHQ and HQNO can be observed whilst the levels of PQS are maintained.

GPZ002966 at 395 nM has possibly generated in PAO1-N a slight increase of HQNO and PQS, but maintained unnafected the levels of HHQ. On the other hand, in PA14 a slight reduction in HQNO and PQS were unaffected whilst the levels of produced HHQ were maintained.

A concentration of 97 nM of GPZ824390 reduced the levels of all three tested QS molecules in PAO1-N, especially impacting on the levels of HQNO in this strain. On the other hand, in PA14 this compound did not result in strong repression of the produced QS molecules.

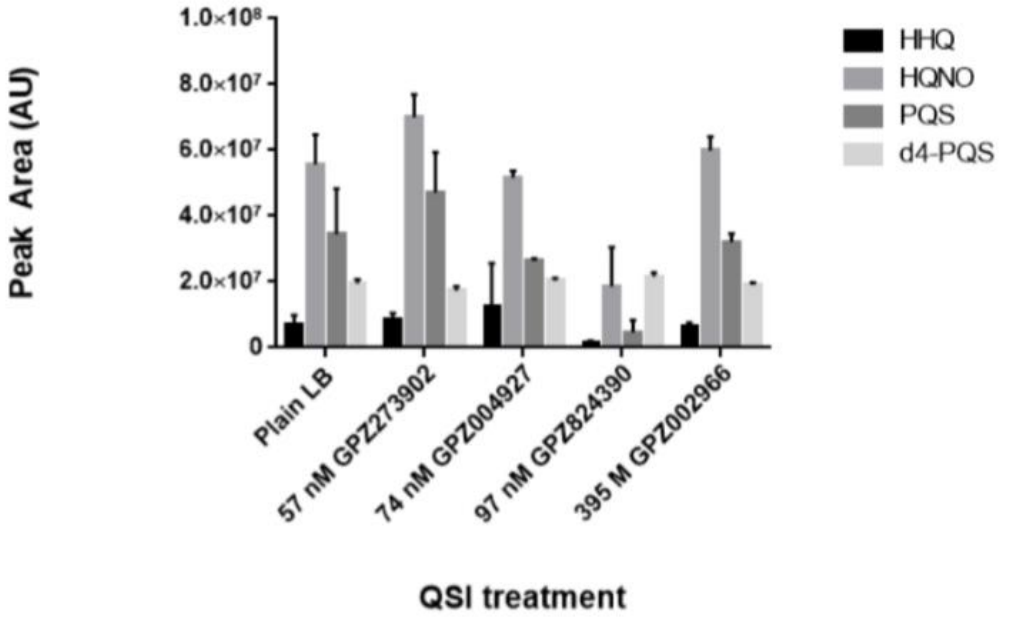


Figure 3.13. Effect of GP PqsR inhibitors on AQ molecules in PAO1-N. 100 µL of each filter sterilised supernatant sample was diluted with 400 µL of fresh LB and spiked with 10 µL of internal standard. Supernatant samples were extracted (x3) with 0.5 mL of EtOAc. Combined extracts were dried under vacuum (Speedvac) and stored at -20°C prior to analysis. For analysis, dried extracts were re-dissolved in 100 µL of MeOH. Deuterated d4-PQS was used as internal standard. The effect of DMSO has been accounted for (added or subtracted) in the plotting of all QSI treatments. Vertical bars correspond to standard deviation.

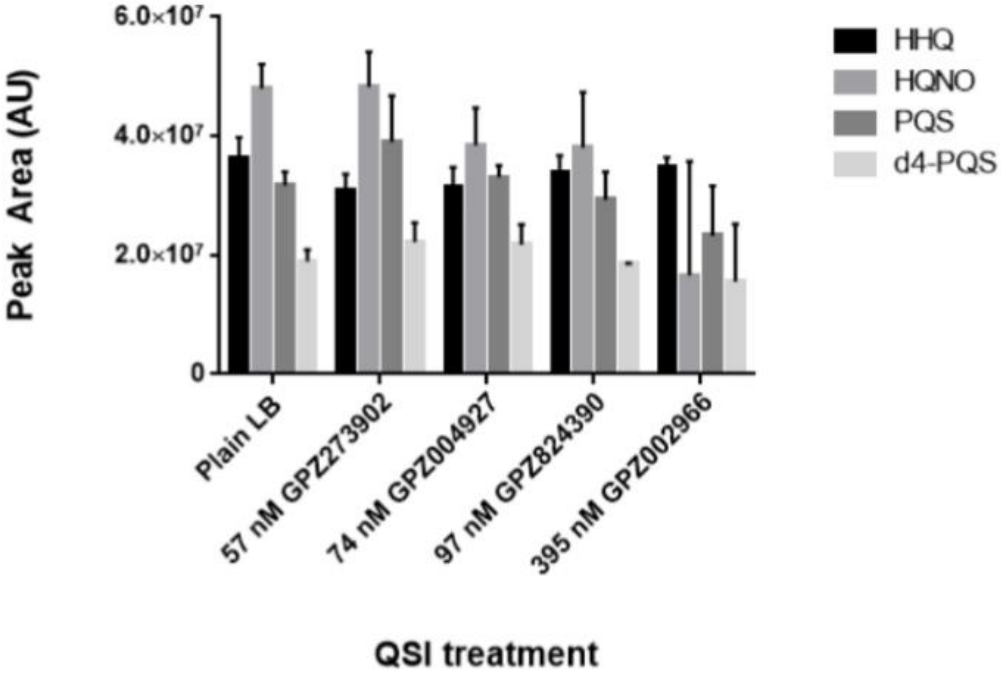


Figure 3.14. Effect of GP PqsR inhibitors on AQ molecules in PA14. 100 µL of each filter sterilised supernatant samples were diluted with 400 µL of fresh LB and spiked with 10 µL of

internal standard. Supernatant samples were extracted (x3) with 0.5 mL of EtOAc. Combined extracts were dried under vacuum (Speedvac) and stored at -20°C prior to analysis. For analysis, dried extracts were re-dissolved in 100 µL of MeOH. Deuterated d4-PQS was used as internal standard. The effect of DMSO has been accounted for (added or subtracted) in the plotting of all QSI treatments. Vertical bars correspond to standard deviation.

3.5. Cytotoxic effect of PqsR inhibitors on eukaryotic cells

3.5.1. Previous assays towards an optimised cytotoxicity protocol

Considering the potential use of the selected GP PqsR-inhibiting compounds or any future lead derived from them in animal models or even human clinical trials, an understanding of their cytotoxic potential was necessary. For pre-clinical assays to be even considered, the top four QS-inhibitors had their cytotoxicity tested against eukaryotic cells, in a process that started with the optimisation of the assay itself. Jurkat T-lymphocite cells (an IL-2 producing T lymphocyte cell line) (314) were the subjects selected for cytotoxic measurements as these cells are commonly used to study T cell signalling for their easiness to culture and rapid growth. In addition, these cells express readily detectable levels of STAT1, STAT3 and STAT5, and so are useful for analysis of cytokine signaling. Jurkat cells are also useful for looking at stress-mediated pathways, including p38 MAPK, JNK signaling, and NF-kappaB signaling.

The initial steps taken identified the level of interference generated by toxicity due to the vehicle solvent (DMSO). Fluorescence measured using Alamar blue as a dye reported on the cytotoxicity of DMSO at a range of concentrations (Figure 3.15), showing that DMSO concentrations up to 2% did not affect Jurkat cells.

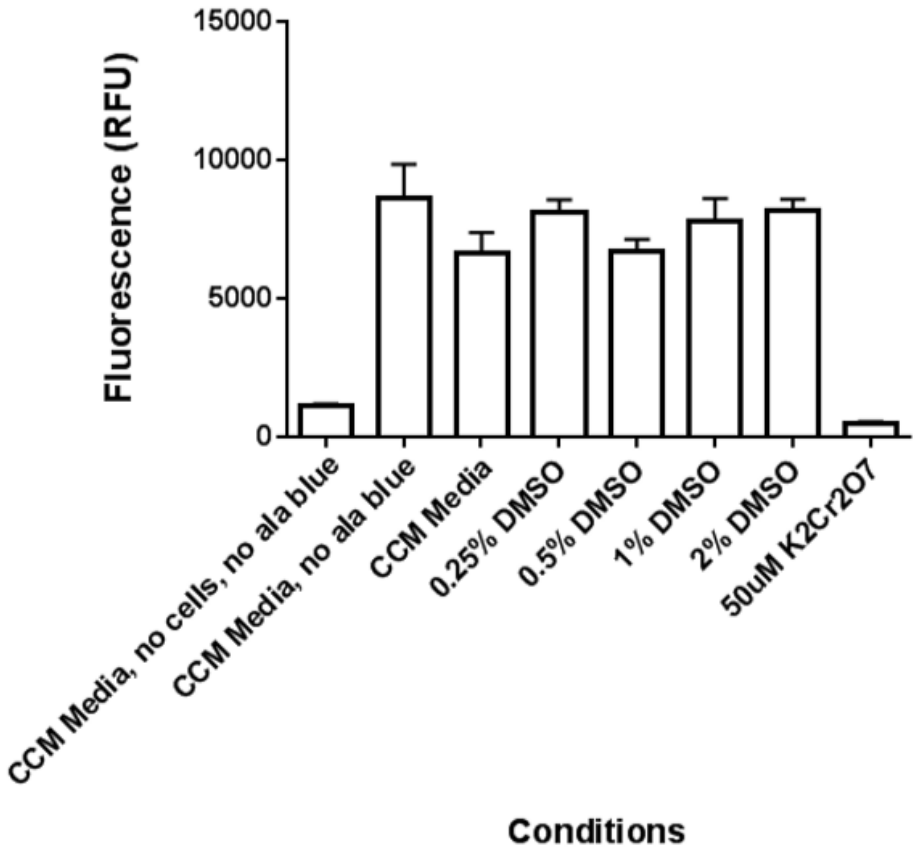
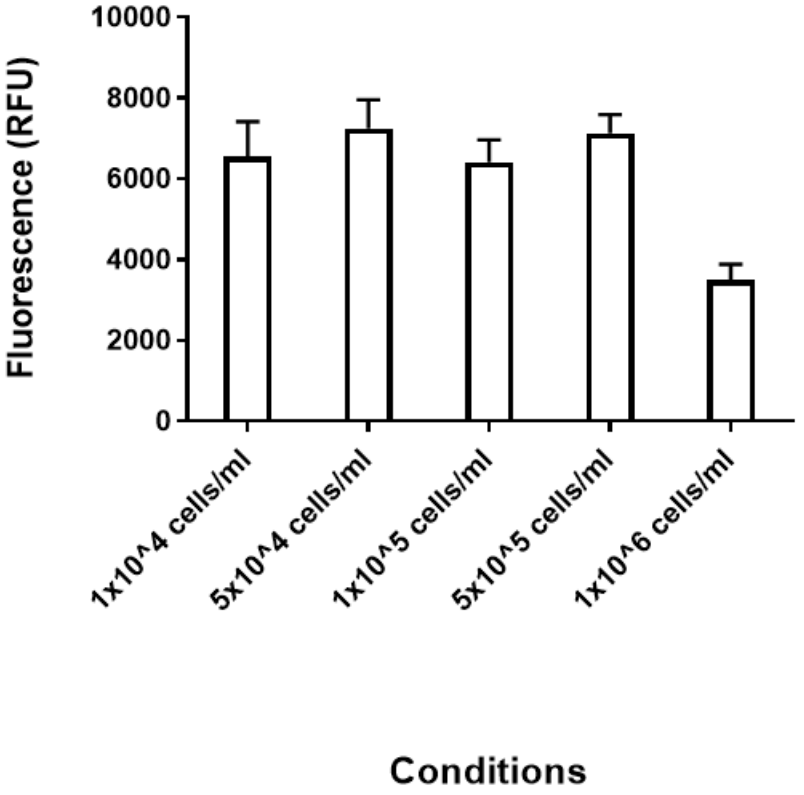


Figure 3.15. Fluorescence of Jurkat cells at different DMSO concentrations. Cells were grown overnight for 20 hours incubating at 37°C and subsequently exposed to four concentrations of DMSO (0.25%, 0.5%, 1% and 2%). Samples contain $1x10^6$ cells/ml and are exposed to 1X Alamar Blue for 1 hour. Negative control corresponds to potassium dichromate at a concentration of 50 µM. Fluorescence readings correspond to an optimal analysis of 56 gain with 1 hour exposure to Alamar Blue. Vertical bars correspond to standard deviation.

Another important feature to consider was the optimum concentration of Jurkat cells to use in the cytotoxicity assay (Figure 3.16). Our results showed that whilst $5x10^5$ cells/mL is the optimum concentration, $1x10^6$ cells/mL reduces fluorescent output. In addition, an exposure longer than 1 hour to 1X Alamar Blue responds with fluorescence rates that decrease as cellular concentration increases. Consequently, a final concentration of $8x10^5$ cells/mL was decided for the final cytotoxicity assays using this cell line.


Fluorescence (RFU)
10000
8000
6000
4000
2000
0
1x10^4 cells/ml
5x10^4 cells/ml
1x10^5 cells/ml
5x10^5 cells/ml
1x10^6 cells/ml
Conditions

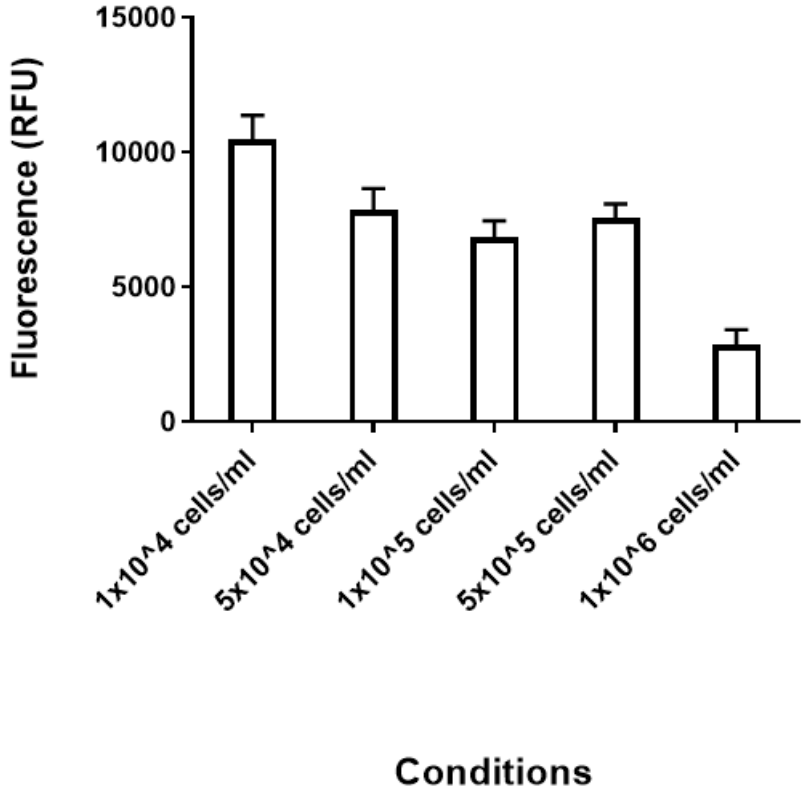
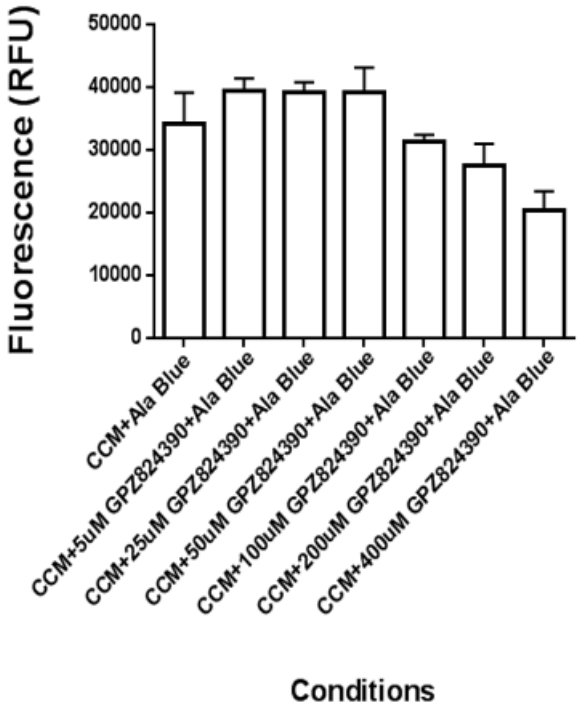

Fluorescence (RFU)
15000
10000
5000
0
1x10^4 cells/ml
5x10^4 cells/ml
1x10^5 cells/ml
5x10^5 cells/ml
1x10^6 cells/ml
Conditions

Figure 3.16. Fluorescence of Jurkat cells at different cellular concentrations after 1 and 2 hours incubation with Alamar Blue. Cells were grown overnight for 20 hours incubating at 37°C and subsequently exposed to five Jurkat cellular concentrations ($1x10^4$, $5x10^4$, $1x10^5$, $5x10^5$ and $1x10^6$ cells/mL). All samples were exposed to 1X Alamar Blue for 1 hour (up) or 2 hours (down). Fluorescence readings correspond to an optimal analysis of 50 gain with a previous 1 hour exposure to Alamar Blue. Vertical bars correspond to standard deviation.

The final issues observed when optimising the cytotoxicity experiments concerned autofluorescence generated by exposing Jurkat cells to the top four QS-inhibiting compounds. In that sense, cells that were not exposed to 1X Alamar Blue were never affected in their fluorescence output, but those exposed to GPZ824390 saw this compound reacting with the dye from a concentration of 50 µM. Moreover, GPZ002966 reduced fluorescence when combined with 1X Alamar Blue (1 hour exposure) even at 5 µM, and GPZ004927 reacted strongly with Alamar Blue at all tested concentrations (Figure 3.17).



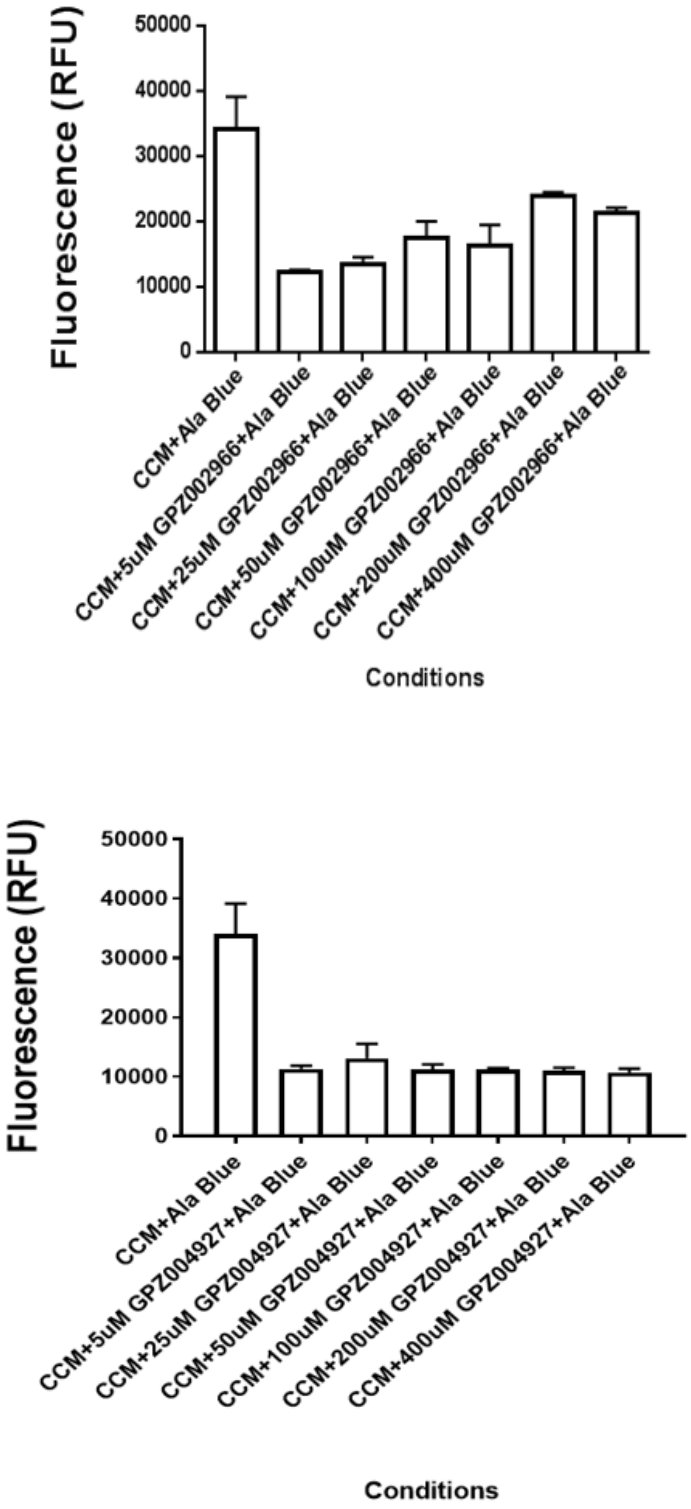


Figure 3.17. Fluorescence generated by exposure to GPZ002966, GPZ824390 and GPZ004927 incubated with Alamar Blue. No cells were used in this assay. CCM media was combined with 1X Alamar Blue and a range of concentrations of GPZ02966. Fluorescence readings correspond to an optimal analysis of 116 gain after 1 hour incubation with GPZ824390 (up), 1 hour incubation with GPZ002966 (middle) and 1 hour incubation with GPZ004927 (down) and exposure to 1X Alamar Blue. Vertical bars correspond to standard deviation.

Autofluorescence inherent to the nature of the tested compounds, in addition to fluorescence of the Alamar blue dye, resulted in altered fluorescence readings. A change of procedure was deemed necessary and the whole cell assay flow cytometry that uses the 7-AAD dye was the technique opted for measuring cytotoxicity of the GP QS-inhibiting compounds. In that sense, the selected top four compounds were then tested for their cytotoxicity (with a minimum of three replicates) in a range of 8 concentrations (1, 2, 5, 10, 25, 50, 75 and 100 µM).

3.5.2. Cytotoxic Effects of GP PqsR-inhibiting compounds on Eukaryotic cells (T Lymphocyte Jurkatt cells)

Overall, the results obtained indicate that GPZ824390 shows very low cytotoxicity even at a high concentration of 100 µM (Table 3.11) considering the 4 replicates tested. Compound GPZ273902 revealed a much more increased toxicity in Jurkat cells with the established cut-off at around 50 µM (Table 3.12). Compounds GPZ004927 and GPZ002966 display no apparent cytotoxicity for all concentrations tested resulted in no variation in percentage of cellular abnormalities (Tables 3.13 and 3.14, respectively).

Table 3.11. Cytotoxicity of GPZ824390 tested against T-lymphocyte Jurkat cells. Cells were grown for 20 hours at 37°C in 5% CO_2 and exposed to a range of 8 concentrations of GPZ824390 (1, 2, 5, 10, 25, 50, 75 and 100 µM). All controls used a cellular concentration of $8x10^5$ cells/mL except for the plain CCM medium where wells with and without cellular content were utilised. Control samples were constituted by 100 µM K_2Cr_2O7 (negative control), plain CCM medium and 1 % DMSO in CCM medium. Cytotoxicity was measured in an Astrios Flow Cytometer. Replicate 2 was measured approximately 30 minutes after replicate 1. Red bold values stand for cytotoxicity of tested compound 20% over the obtained with the 1% DMSO control. Percentages indicate rate of cellular abnormalities.

	1st trial		2nd Trial		3rd Trial		4th Trial	
Astrios GPZ824390 1st trial $8x10^5$ cells/ml	**Replicate 1**	**Replicate 2**	**Replicate 1**	**Replicate 2**	**Replicate 1**	**Replicate 2**	**Replicate 1**	**Replicate 2**
100 µM $K_2Cr_2O_7$	27%	35%	44%	42%	59%	56%	36%	38%
1% DMSO	7%	6%	12%	12%	4%	5%	6%	8%
CCM cells	6%	6%	10%	9%	5%	5%	6%	6%
100 µM	17%	17%	Faulty	Faulty	**29%**	**29%**	18%	**20%**
75 µM	15%	12%	**22%**	**25%**	13%	14%	11%	12%
50 µM	8%	7%	17%	17%	6%	8%	9%	7%
25 µM	8%	7%	12%	10%	6%	6%	10%	5%
10 µM	4%	5%	9%	9%	4%	8%	9%	8%
5 µM	8%	5%	8%	11%	6%	5%	5%	10%
2 µM	5%	5%	8%	15%	4%	6%	7%	4%
1 µM	4%	4%	12%	15%	3%	5%	5%	10%

Table 3.12. Cytotoxicity of GPZ273902 tested against T-lymphocyte Jurkat cells. Cells were grown for 20 hours at 37°C in 5% CO_2 and exposed to a range of concentrations of GPZ273902 (1, 2, 5, 10, 25, 50, 75, 100 µM, 250 µM and 300 µM). All controls used a cellular concentration of $8x10^5$ cells/mL except for the plain CCM medium where wells with and without cellular content were utilised. Control samples were constituted by 100 µM K_2Cr_2O7 (negative control), plain CCM medium and 1 % DMSO in CCM medium. Cytotoxicity was measured in an LSRII Flow Cytometer. Replicate 2 was measured approximately 30 minutes after replicate 1. Red bold values stand for cytotoxicity of tested compound 20% over the obtained with the 1% DMSO control. Percentages indicate rate of cellular abnormalities.

	1st trial		2nd Trial		3rd Trial		4th Trial		5th Trial	
LSRII GPZ273902 1st trial $8x10^5$ cells/ml	**Rep 1**	**Rep 2**	**Rep 1**	**Rep 2**	**Rep 1**	**Rep 2**	**Rep 1**	**Rep 2**	**Rep 1**	**Rep 2**
100 µM $K_2Cr_2O_7$	27%	35%	37%	39%	33%	37%	40%	31%	34%	39%
1% DMSO	7%	6%	2%	2%	3%	4%	2%	6%	3%	3%
CCM cells	6%	6%	3%	3%	5%	5%	4%	4%	4%	3%
300 µM	-	-	**37%**	**39%**	-	-	-	-	-	-
250 µM	-	-	**39%**	Faulty	-	-	-	-	-	-
100 µM	17%	17%	**25%**	10%	**48%**	**50%**	**47%**	**37%**	**50%**	**53%**
75 µM	15%	12%	14%	18%	**45%**	**44%**	**47%**	**49%**	**31%**	**28%**
50 µM	8%	7%	4%	4%	Faulty	**45%**	**49%**	**49%**	18%	15%
25 µM	8%	7%	3%	2%	5%	12%	11%	7%	4%	6%
10 µM	6%	5%	2%	3%	5%	4%	4%	5%	3%	3%
5 µM	8%	5%	2%	2%	4%	6%	3%	5%	3%	3%
2 µM	5%	5%	-	-	2%	3%	9%	5%	2%	4%
1 µM	4%	5%	-	-	4%	3%	5%	4%	5%	3%

Table 3.13. Cytotoxicity of GPZ004927 tested against T-lymphocyte Jurkat cells. Cells were grown for 20 hours at 37°C in 5% CO_2 and exposed to a range of 8 concentrations of GPZ004927 (1, 2, 5, 10, 25, 50, 75 and 100 µM). All controls used a cellular concentration of $8x10^5$ cells/mL (1st trial), $6x10^5$ cells/mL (2nd trial) and $3x10^5$ cells/mL (3rd trial), except for the plain CCM medium where wells with and without cellular content were utilised. Control samples were constituted by 100 µM K_2Cr_2O7 (negative control), plain CCM medium and 1 % DMSO in CCM medium. Cytotoxicity was measured in an LSRII Flow Cytometer. Replicate 2 was measured approximately 30 minutes after replicate 1. Red bold values stand for cytotoxicity of tested compound 20% over the obtained with the 1% DMSO control. Percentages indicate rate of cellular abnormalities.

	1st trial		2nd Trial		3rd Trial	
Astrios GPZ004927 1st trial $8x10^5$ cells/mL 2nd trial $6x10^5$ cells/mL 3rd trial $3x10^5$ cells/mL	**Replicate 1**	**Replicate 2**	**Replicate 1**	**Replicate 2**	**Replicate 1**	**Replicate 2**
100 µM $K_2Cr_2O_7$	34%	42%	37%	47%	32%	21%
1% DMSO	4%	4%	3%	2%	1%	1%
CCM cells	5%	3%	4%	2%	2%	2%
100 µM	5%	5%	2%	4%	1%	2%
75 µM	3%	5%	2%	2%	1%	2%
50 µM	4%	4%	2%	2%	1%	2%
25 µM	4%	3%	2%	3%	1%	2%
10 µM	3%	4%	2%	2%	1%	3%
5 µM	3%	4%	2%	2%	2%	1%
2 µM	3%	5%	2%	2%	1%	2%
1 µM	3%	2%	2%	2%	1%	0%

Table 3.14. Cytotoxicity of GPZ002966 tested against T-lymphocyte Jurkat cells. Cells were grown for 20 hours at 37°C in 5% CO_2 and exposed to a range of concentrations of GPZ002966 (1, 2, 5, 10, 25, 50, 75, 100 µM, 250 µM and 300 µM). All controls used a cellular concentration of $8x10^5$ cells/mL (1st and 3rd trial) and $3.2x10^5$ cells/mL (3rd trial), except for the plain CCM medium where wells with and without cellular content were utilised. Control samples were constituted by 100 µM K_2Cr_2O7 (negative control), plain CCM medium and 1 % DMSO in CCM medium. Cytotoxicity was measured in an LSRII Flow Cytometer. Replicate 2 was measured approximately 30 minutes after replicate 1. Red bold values stand for cytotoxicity of tested compound 20% over the obtained with the 1% DMSO control. Percentages indicate rate of cellular abnormalities.

	1st trial		2nd Trial		3rd Trial	
Astrios GPZ002966 1st trial $8x10^5$ cells/mL 2nd trial $3.2x10^5$ cells/mL 3rd trial $8x10^5$ cells/mL	**Replicate 1**	**Replicate 2**	**Replicate 1**	**Replicate 2**	**Replicate 1**	**Replicate 2**
100 µM $K_2Cr_2O_7$	52%	44%	53%	Faulty	40%	30%
1% DMSO	4%	5%	4%	Faulty	3%	3%
CCM cells	7%	7%	5%	6%	4%	4%
100 µM	7%	12%	11%	15%	6%	5%
75 µM	9%	13%	13%	12%	5%	5%
50 µM	11%	11%	7%	7%	5%	4%
25 µM	8%	11%	7%	5%	4%	6%
10 µM	8%	10%	6%	4%	3%	3%
5 µM	4%	8%	5%	4%	4%	6%
2 µM	5%	5%	4%	5%	Faulty	4%
1 µM	6%	10%	5%	6%	4%	4%

3.6. Summary of characterisation of PqsR-inhibitors

As previously mentioned, the present research study focused on a subset of 15 compounds selected after a preliminary screening of a long list of approximately 7,000 QSI candidate molecules from different origins. The synthetic compounds were obtained from the French pharmaceutical research partner GreenPharma Ltd. The selection of these compounds was based on their ability to inhibit CTX::P_{pqsA}-*luxCDABE* and CTX::P_{lecA}-*luxCDABE* chromosomal transcriptional fusions the first of which was used to determine their IC_{50} values. The final outcome was the indentification of four strong inhibitors of PqsR shown in Figure 3.18a. These compounds were shown to

dock into the PqsR ligand binding domain (Figure 3.18b) and the docking scores determined. The lowest of the obtained IC_{50} scores (three trials attempted) can be found in figure 3.19.

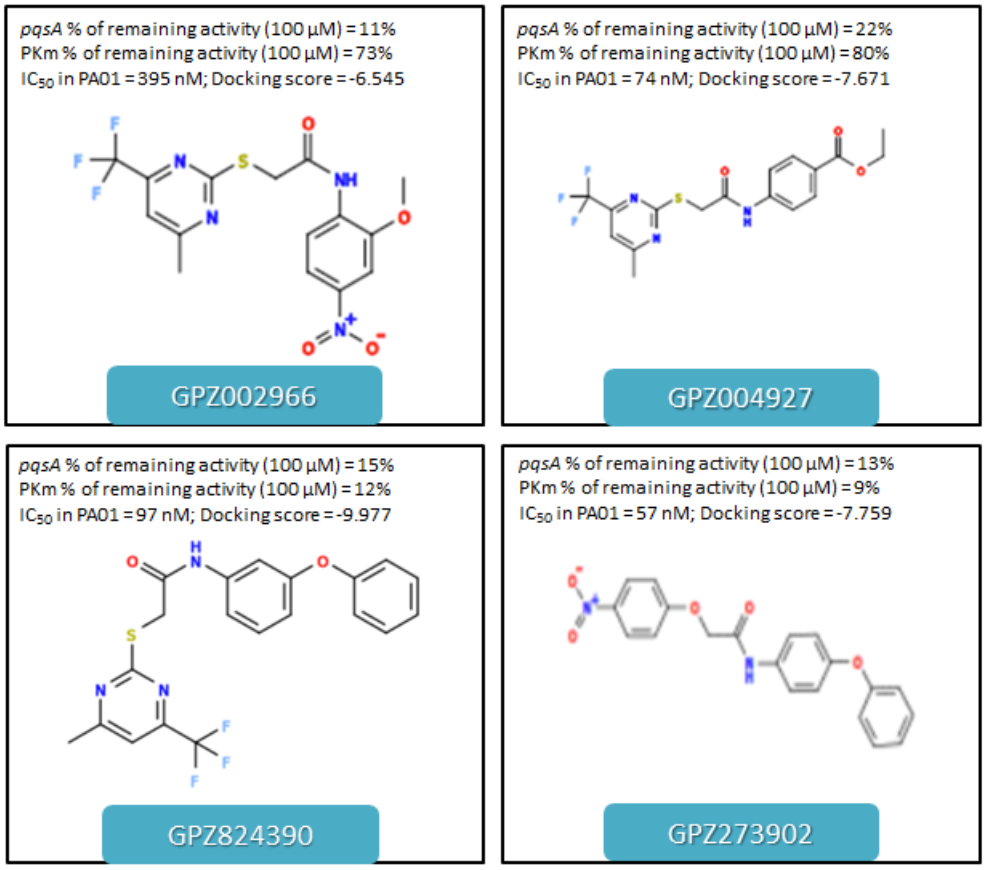


Figure 3.18a. Summary of structure and inhibition kinetics of the top four PA QSI candidates. The structures represented were selected from a group of 15 candidate molecules showing *pqsA*-inhibiting effects based on the IC_{50} scores obtained at the time of the assays. Docking scores were provided by Dr. Fadi Soukarieh and obtained with the software package Extra Precision (XP) mode of Glide docking, representing Gibbs free energy (ΔG) values where the more negative the value the better the binding force.
Source: Images adapted from originals by GreenPharma Ltd.

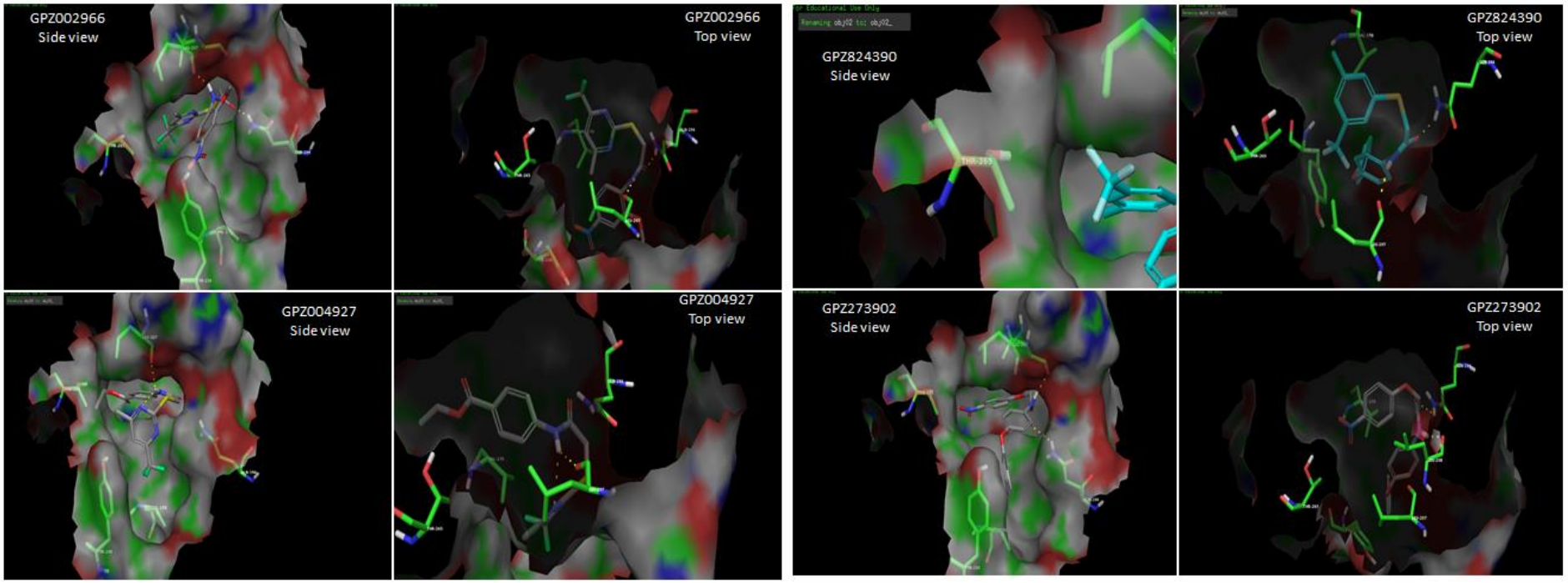


Figure 3.18b. Perspective views representative of the binding between the best QSI molecules and the PqsR protein. Two views are presented, side view and perspective from above. The inner bordered area appearing in the side view represents the pocket within the protein molecule where the antagonist attaches to. The pocket region is further explored with the top view perspective of the binding between inhibitor and protein. The ligation is represented by yellow dots where the number of dots is proportional to the approximation between structures. Aminoacids that normally interact with the QSI molecule are represented by their chemical structures, with their names in white, and whenever possible distinguishable by the colours of their composing atoms: for hydrogen atoms, **blue** for nitrogen atoms, **red** for oxygen atoms, **green** for fluoride atoms, **yellow** for sulphur atoms and **gray** for carbon atoms. The interactions predicted are theoretical approximations obtained by computer software under a precise application protocol, accounting for the many types of interactions established between protein (PqsR) and ligand (antagonist). The program software first uses the crystal structure and the antagonist structure to help predict the antagonism design, then alternatively replacing the antagonist, fiting the molecule in the binding pocket and rotating it to find the best possible temporary ligations. The images above can be found in larger formats in the Annexes section (Figures A1.1 to A 1.8).
Source: Images kindly provided by Fadi Soukarieh.

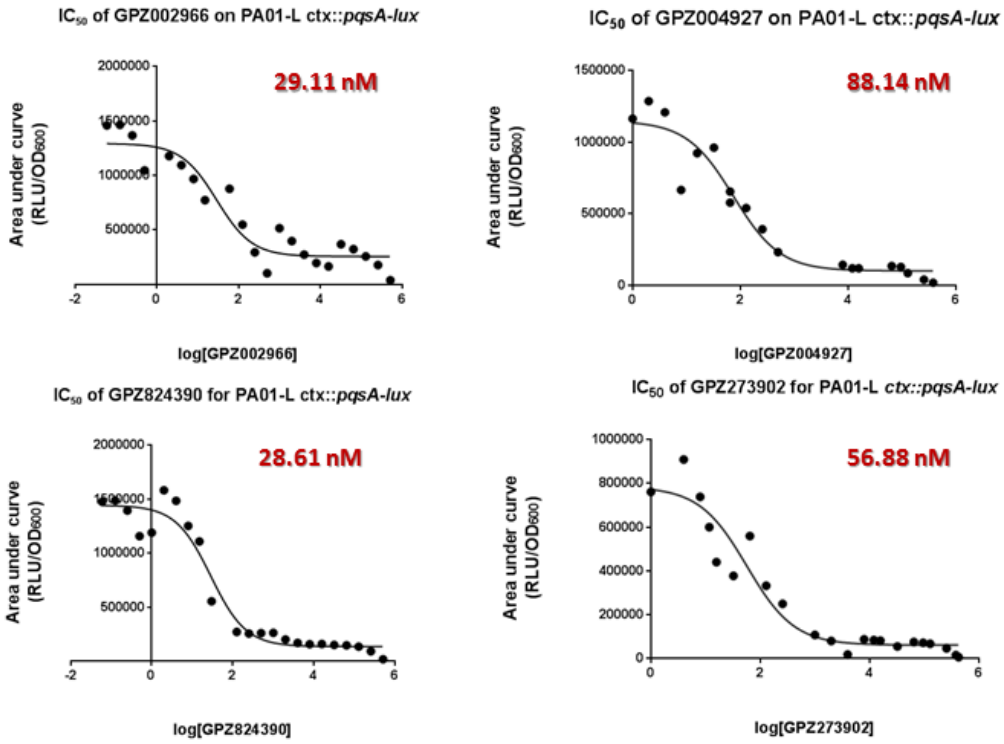


Figure 3.19. Lowest IC_{50} scores for the top 4 PA QS inhibiting candidate molecules. The IC_{50} curves were tested by reading luminescence for 24 h with the automated luminometer-spectrophotometer (TECAN GENios Pro™). Strains were grown overnight and optimised to an initial OD_{600} of 0.05 before being presented to compound concentrations ranging from 0.6 nM to 512 µM. The IC_{50} scores displayed represent the lowest ones obtained from 3 trials with individual R^2 curves above 0.9 and each trial consisting of a minimum of 19 to a maximum of 25 concentration points. Absent concentration points account for outlyers that were purposedly ignored.

The compounds were tested for their inhibitory potencial on major virulence pathways, as well as for their colonisation potencial and applicability in future clinical assays, as summarised in Table 3.15.

Table 3.15. Summary of QSI profiles of the top four GP candidate compounds studied. Results presented concern effects produced on strain PAO1 only.

QSI compound	Assays IC_{50} (*pqsA* expression)	% of remaining activity (P_{pqsA}) at 10 µM 100 µM	% of remaining activity (P_{Km}) at 10 µM 100 µM	% of remaining activity (P_{lecA}) at 10 µM 100 µM	% of remaining activity (P_{lecB}) at 10 µM 100 µM	% of remaining activity (PCN) at IC_{50}	Effect of tested IC_{50} on biofilm formation: Δ biomass Δ surface area	Effect on: HHQ HQNO PQS	Cytotoxic (up to 100 µM) resulting in >20% of cellular abnormalities in T lymphocytes
GPZ002966	395 nM	9% 11%	103% 73%	10% 33%	88% 94%	34%	<26.3 ($\mu m^3/\mu m^2$) <5.3 (μm^2)	Unaltered Increase Increase	No reported cytotoxicity
GPZ004927	74 nM	29% 22%	101% 80%	25% 51%	100% 140%	246%	<25.2 ($\mu m^3/\mu m^2$) <5.0 (μm^2)	Increase Reduction Increase	No reported cytotoxicity
GPZ824390	97 nM	12% 15%	103% 73%	34% 46%	77% 81%	119%	<13.5 ($\mu m^3/\mu m^2$) <1.4 (μm^2)	Reduction Reduction Reduction	≥75 µM
GPZ273902	57 nM	9% 13%	100% 67%	38% 46%	14% 22%	35%	<6.2 ($\mu m^3/\mu m^2$) <3.7 (μm^2)	Increase Increase Increase	≥50 µM

3.7. Discussion

The *pqs* system is pivotal for the expression of virulent phenotypes, that are themselves a hallmark of pathogenicity in PA. In that sense, the PqsR regulator has been seen as an important target protein for progress on inhibitors of the *pqs*-related gene expression. The fact that PQS is present at such high levels in the sputum of immunocompromised patients, like those suffering with CF (Collier et al., 2002), supported even further the assumption that targeting an upstream regulatory protein, ultimately responsible for the production of PQS in PA, can represent a clinical strategy for chronically infected patients. Many developments have been supporting this notion, for instance the reduced mortality that *pqsR* mutants report in mice infection models (Xiao et al., 2006), the reduced virulence that is displayed by strains mutated at *pqs*-associated regulatory points and that result in diminished pathogenicity in a range of different organisms (insects, nematodes, plants) (Mahajan-Miklos et al., 1999; Jander et al., 2000).

PqsR is the central point in acute, chronic and persistent infections, hence the in-depth analysis of synthetic PqsR inhibitors, which were assessed for their capacity to repress virulence and their potential for pre-clinical studies. The main purpose was to assess the inhibitory efficiency of a number of QSI molecules targeting PqsR by investigating their impact on the expression of PA *pqs*-related virulent phenotypes. The studied molecules were proven highly efficacious in interfering with the PqsR-dependent intercellular communication *in vitro*, attenuating virulence-associated PA phenotypes.

Relevance of specific structural groups on QSI potency

In the context of antimicrobial drug innovation, the key factor in the highthroughput screening of small molecules is defined by the binding affinity established in the ligand-receptor complex. An attribute that is summarised by the docking scores of the candidate molecules to the target protein. The candidate compounds assessed are improved hit-optimised PqsR inhibitors. Their docking scores derive from a virtual screening prediction of the ligand binding mode that must not be confused with predictive affinity (calculated as the binding energy of the ligand per heavy atom). Even though the results generated by the docking program are believed to be very valid approximations, they require further practical validation. Such validation is debated in this research project, specifically looking into how well repression of the PqsR protein nullified the pqs-associated virulence traits (PCN and biofilm production) and impacted on *pqsR* associated expression (on *pqsA*, *lecA* and *lecB*).

In addition, the synthetic engineering of fragments, based on agonist scaffolds, is a fruitful approach as it allows the tackling of specific key issues encountered throughout the developmental process. These can range in nature from undesirable physicochemical properties to issues related with effectiveness on specific target receptors. However, the screening of small simple molecules has the known disadvantage of a typical low binding affinity (315). But large libraries of complex molecular structures are less prone to deliver successful hits, in opposition to reduced libraries of smaller simpler structures. The latter allow a more direct view of the necessary alterations to apply to the synthetic assemble, so binding affinity to the receptor target is improved.

One of the most effective PqsR inhibitors to establish a comparison with the ones assessed in this project is the M64 molecule by Starkey *et al* (2014) (313). M64 is a very competent QSI targeting PqsR, capable of reducing

expression of the virulence traits that are also studied in this research project. In comparison to GreenPharma's best hits GPZ002966, GPZ004927, GPZ824390 and GPZ273902 (from now on referred as GP QSIs), the structure of M64 (Table 3.1) presents a few substantial differences that result in significant impact on the generating of virulence associated phenotypes. Structurally, M64 is composed of four aromatic rings, three benzene rings and a furan ring. The GP QSIs do not contain any furan ring in their making, with two possessing solely two benzene rings (GPZ002966 and GPZ004927) and the other two (GPZ824390 and GPZ273902) possessing only three benzene rings. Another important difference is that structurally M64 is divided into two functional domains separated by a thiol group, itself linked to several organic function groups like a carbonyl, an amine and a methylene group. The thiol group is also present in all GP QSIs structures except GPZ273902.

Zender *et al* (2013) (312) had introduced the thiol group in its inhibitor structure (oxadiazole-2-amine) and a chlorobenzene function, a feature also used in the most promising PqsR-targeting antagonists (298) (301-303). In fact, Lu *et al* (2012) used both chloride and fluoride as part of the QSIs derivatives, with a scaffold based on HHQ. In addition, Zender *et al* (2013) makes use of a nitrogen dioxide radical on the far end of the molecule where the benzene and furan rings domain sit. In the GP QSIs, only GPZ002966 and GPZ273902 hold such nitrogen dioxide groups.

A very significant difference that can be seen in three of the GP QSIs (GPZ273902 not included) and the M64 antagonist molecule is that the latter does not hold any fluoride elements. That is introduced in the antagonist molecules developed by Lesic *et al* (2007), Lu *et al* (2012) and Ilangovan *et al* (2013). In both the QZN antagonists and the HHQ derivatives, the presence of all the mentioned organic groups add substantially to the complexity of the active molecules; a feature not at all seen with the single aromatic ring benzoic acids developed by Lesic *et al* (2007).

It is thus easy to understand that the improvement in the inhibitory capacity of the most prominent PqsR-targeting antagonists gained from a similar application of active organic functions. Thus, even though the objective is to produce the smallest molecules possible, when considering the most effective antagonists, the more complex structures have surpassed the inhibitory strength of the fairly smaller and simplistic antagonists developed. It is actually with work by Frei *et al* (2012) (311), when developing the 2-Aminobenzimidazole derivative 1, that structures containing several aromatic rings [not to be confused with polycyclic aromatic hydrocarbons that are fairly metabolisable by PA (Bugg *et al*., 2000)] start reporting a PqsR IC_{50} shift from the micromolar to the nanomolar level. However, the repressing effect on PqsR by the antagonist 2-Aminobenzimidazole derivative 1, is not entirely sure to be exerted on the regulatory protein or in an indirect manner.

All of the above mentioned organic functional groups have a specific impact on the antagonistic properties of the molecule against PqsR. This is not only because of electrostatic conjugation, in itself a very important factor, but also due to the influence these specific elements have on several virulence factors and their metabolic pathways. For example, Persson *et al* (2005) (316) replaces a C-3 carbon by sulphur in the acyl side chain, an alteration responsible for converting the compound from one with an agonistic behaviour to another with an antagonistic behaviour (effective against expression in both LuxR-and LasR-regulated QS reporters). This effect might be exclusive to thiol groups placed amidst the main carbon skeleton as no QSI activity was reported by Schaefer *et al* (1996) (317) when one or more carbon, sulphur and nitrogen elements were added to the lactone ring. A similar effect was observed with the first reported garlic QSI, ajoene (318), a natural compound containing three sulphur atoms, a disulphide bridge and a sulphur monoxide group, all located in the main core chain of the antipathogenic compound.

It is actually quite remarkable that more sulphur-containing compounds are found to behave as antagonists of the QS system, not only in PA (303), but

also in *Vibrio harvei* (319) (320); or even in *E. coli* where sulphur metabolism that is regulated by *cysB* (also present in PA) interferes with biofilm production. In PA, CysB is the transcriptional regulator that controls sulphur uptake and cysteine biosynthesis. This regulator represses PqsR transcription and PQS production, interferes with PqsR transcription by LasR, thus influencing cell-to-cell signalling (181). These findings support the idea that QS inhibiting bioactivity may be firstly associated to the presence of a sulphoxide group or sulphur-containing organic functions in the QSIs structure, as it has been observed by Koch *et al* (2005) (321). The authors showed that replacing a carbonyl group with a sulphur atom in both 3-oxo-C_6-HSL and C_6-HSL altered the inherent bioactivity, shifting from an agonistic to an antagonistic behaviour.

Probably, one of the strongest examples that makes the case for the importance of sulphur in the QSIs structural composition, is the one provided by studies on indole. For instance, indole represses genes, such as *sbp*, *cysI* and *cysND*, that are involved in the degradation of sulphur in PA. In fact, the entire *ssuFBCDAE* locus was shown to have a crucial uptake activity in regards to organosulphur (322). Indole down regulates sulphur uptake in PA without affecting the transcriptional level of the RhlR/I, LasR/I and PqsR.

Finally, the presence of sulphur in the antagonist composition might be linked to imbalance in the oxidative phosphorylation, mainly because sulphur is sensitive to oxidative stress. And since iron-sulphur proteins have been related to involvement in protection against ROS (323) when PA infects the human host, one of the host defence strategies is to produce ROS to counteract bacterial progression. That is accomplished with, for example, the antibiotic azithromycin, that upregulates at both transcriptional and protein level *cysP* (a sulphate binding protein).

In addition to the explored effects supposedly produced by thiol groups in the depicting of the QS antagonism, the usage of halogens is also believed to be advantageous. Fewer cases have been documented, but bromide, fluoride

and chloride, have been reported to participate in the repressing of virulence in PA. For example, with the antagonist 7-fluoroindole identified by Lee *et al* (2012) (324), a compound with inhibiting potential over biofilm formation does not affect viability of PA. The value of halogens as part of the structure of PqsR antagonists is indirectly validated by the defensive mechanism bacteria employ when they use oxidised AHL signalling molecules like 3-oxo-C_{12}-HSL to attack oxidised halogen compounds (containing for example small number of chloride or bromide atoms). This strategy is actually quite dispersed through other realms as is the example of marine alga *Laminaria digitata*, an alga that produces and secretes oxidised halogen compounds known to affect QS-controlled gene expression of colonising bacteria (325). Another example is set by ammonium chloride, a drug able to penetrate the lysosomes of cells and inhibitors of the flow of virulence factors (326) that travel from the endosomal vesicles into the cell cytoplasm (327).

Even though n-oxides are more related to PA inhibition occurring enzymatically through *pqsD* expression, and protein interactions with the concomitant protein, these elements can also be relevant in the engineering of PqsR inhibitors. Such can be inferred from the results obtained by Rasmussen *et al* (2005) (328) on garlic extract and the 4-nitro-pyridine-N-oxide. These two substances target specifically the QS-regulated genes in PA and were shown to be able to significantly decrease biofilm resistance to the antibiotic tobramycin (without affecting cellular viability); observations also verified with the less virulent potential of PAO1 on the infected nematode model *C. elegans*. Interestingly, the authors studied *S*-phenyl-L-cysteine sulfoxide and its breakdown product, diphenyl disulphide (again a disulphide bridge unifying two aromatic rings) and were able to significantly reduce biofilm formation of PA to similar levels obtained with the 4-nitropyridine-*N*-oxide. Whether this inhibitory effect is potentiated by the presence of sulphur alone or synergistically reinforced by the *N*-oxide group in conjunction with sulphur elements, is yet to be unveiled. Furthermore, using the insect infection model *D. melanogaster*, both *S*-phenyl-L-cysteine sulphoxide and diphenyl disulphide

had significant impact on reducing PA presence (CFU/fly) 18h into recovery stage, even showing no lethal toxicity to the fly hosts (329).

Thiol-, chloride- and fluoride-rich compounds have been thoroughly used successfully for repressing QS in PA via the AHL-signalling pathway, through activity on QscR, and even in a panoply of other bacterial species. For example, the antagonists chlorolactone and chlorothiolactone (330), *D. pulchra* halogenated furanone (5*Z*)-4-bromo-5-(bromomethylene)-3-butyl-2(5*H*)-furanone, fully repressed AI-2-controlled swarming of *E. coli*, reduced the thickness of its biofilms by 55%, the presence of live bacterial cells in the biofilm matrix by 87%, and repressed both AHL-mediated as well as AI-2-mediated luminescence in *V. harveyi*. Finally, antagonists of the QscR using the synthetic B6 compound with a bromobenzene in its outermost end inhibited by 76% QscR at 180 nM (331).

The robust research work on the contribution of several functional organic elements in QSIs is also highlighted with the presence of bromide and chloride in derivatives of the (2-nitrophenyl)methanol scaffold, and their effect on PqsD (332). The authors also dwelled on the importance of the ortho positioning of the nitro group and how essential it turned out to be for *in vitro* PqsD inhibition, as well as the participation of the phenyl residue in improving inhibitory potency.

Overall, the above mentioned examples support the idea that optimising QSIs targeting bacterial intracellular QS signalling repression is a multi-parameter problematic. A lot more research on the roles of the functional groups in inhibitors is still required.

In regard to the GP QSIs, there is a strong binding affinity between ligands and receptor protein pockets, as revealed by the predicted docking values of the molecules to the PqsR protein. The predicted score values are very approximate to each other and the strongest binding affinity calculated are, as

described by Gibbs free-energy (ΔG) values, -9.977 Kj/K (GPZ824390), -7.759 Kj/K (GPZ273902), -6.545 Kj/K (GPZ004927) and -7.671 Kj/K (GPZ002966) demonstrating that the energy associated to the binding reaction is strong for the four PqsR antagonists. The more negative the ΔG values the higher the tendency for spontaneous reactions, favoured for both enthalpy (internal energy available and its effects in the overall spacing at constant pressure) and entropy (disorder or spatial arrangement inherent to the reaction), at standard conditions and at any temperature. Hence, there is a natural binding affinity that is strong for GPZ824390, but also for the remaining GP QSIs, as the discussion of the observed results will attest. The docking values suggest that the stoichiometry titration is high, i.e., there is a strong binding affinity to the protein by the antagonists, which in practical terms results in full protein availability for binding interactions with the ligand.

Effects on *pqsA* expression

When a PAO1 light reporter strain was exposed to two concentrations of 10 and 100 µM of each individual GP QSI candidate compound, the compounds caused a very strong inhibition of *pqsA* expression (Table 3.2 and figure 3.2). GPZ002966 was the best inhibitor of the *pqsA* promoter reducing its remaining activity to mere 9%, whereas GPZ004927 had the worst repressing effects (yet still substantially strong) with a percentage of remaining activity set at 29%, almost a third of the normal expectable expression. The *pqsA* promoter fusion reporter allowed the quantitative measuring, to a certain extent, of the specific targeting of the GP QSIs to PqsR. This specificity is direct, contrary to a few of the virulence-associated repressors found (operating indirectly towards an upstream effect with consequences on the production of PqsR). Examples of the latter are compounds 6FABA, 6CABA, 4CABA (298) that act on HHQ and the PQS coligand synthesis; farnesol, that interacts with the *pqsA* promoter at the vicinity of the *pqsA* transcriptional initiation site (191), and 2-aminoacetophenone (300) that interacts with a PqsR-regulated loci.

Other potent antagonists that bind directly to the PqsR protein are the HHQ analog antagonist 19 (303), the competitive binders oxadiazole-2-amine CF3 derivative antagonist 37 (312) and QZN antagonists of PqsR (278), the HHQ analog antagonist 16 (302), and finally the carbomaxide derivative antagonist 3 (301). Their capacity to reduce *pqsA* expression is definitely a good indicator of the preceding interaction that is established between PqsR and the *pqsA* promoter. Understanding how such binding affinity is structurally and metabolically affected, the nature of their productive/non-productive ligand-receptor interactions and the many enzymatic reactions involved, can help on both the screening and the structural design processes.

In that sense, it is important to analyse agents that participate effectively in competing with the primary ligand, by either mimicking the substrate or globally reducing the affinity of the primary interaction, that would therefore result in a non-productive interaction. Thus, when analysing the effectiveness of farnesol in repressing PqsR, and the results obtained by Cugini *et al* (2007) (191) when measuring PqsR-mediated transcription from the *pqsA* promoter by means of a *pqsA–lacZ* fusion in *E. coli*, two important scenarios emerged: 1) the undesirable one where farnesol promoted the binding of PqsR to the *pqsA* promoter, and 2) the desirable one where farnesol inhibited PQS-stimulated transcription by repressing the *pqs* operon in a dose-dependent manner.

At first, observations revealed by Cugini *et al* (2007) do not directly make a case for farnesol as a PqsR antagonist, but indeed add a very important aspect in the context of inhibition, i.e., the competitiveness between PQS and an additional element for the binding region of the *pqsA* promoter. Even though this repression occurs at the translational level (during synthesis of protein from mRNA) and not like with the GP QSIs at the actual protein level, it is however important to understand how a sesquiterpene was capable of competitive inhibition of PqsR without affecting overall growth kinetics (in *E.*

coli). The relevant aspect inferred from the results by Cugini *et al* (2007) that definitely can help shape future antagonistic structures is that: by causing a non-productive interaction with the *pqsA* promoter, that did not result in transcriptional activation of the *pqsABCDE* operon, farnesol was able to competitively inhibit PQS production at low PQS concentrations in a heterologous *E. coli* system. Whilst PQS stimulated transcription from the *pqsA* promoter at nanomolar concentrations (12 to 60 nM), 30 to 300 mM farnesol (~500-fold higher) were required for repression. Nonetheless, one needs to consider that *E. coli* may naturally have different *pqsR* expression levels and/or PQS uptaking, and different efflux pumping mechanisms in comparison with PA (an aspect also debated in section 4.4), as well as differently uptaking farnesol.

The GP QSIs produced very low IC_{50} scores in both PAO1 and PA14 strains (Table 3.3), and even though the PqsR binding to the *pqsA* promoter wasn't directly measured by quantitative PCR, the repressing of the *pqsA* promoter was attained at the nanomolar level with all four PqsR antagonists. Only a concentration of 10 µM of M64 was capable of full inhibition of the *pqsA* gene expression on PA14, with an IC_{50} at 1 µM (for 9 concentration points tested). Comparing to the GP QSI molecule with the best docking score and a structural composition closer to that of M64 (GPZ824390), in terms of *pqsA* promoter remaining activity on PA14, the IC_{50} is at 69.48 nM (R^2=0.9296 and 24 concentration points tested). That represents less than 14-fold the concentration of antagonist used by Starkey *et al* (2014) (313).

As it is the case for M64, the GP QSIs directly bind to PqsR (unknown stoichiometry). They inhibit the *pqs* operon expression by reducing the PqsR binding affinity to the *pqsA* promoter, as suggested by the IC_{50} scores on both PA01 and PA14. Starkey *et al* (2014) also used HTS to identify inhibitors of the PqsR protein regulon activity that would not disturb cell growth or affect cellular viability, thus accounting for specificity in terms of action. With 240±38 µM the PqsR binding to the *pqsA* promoter of PA14 was blocked by the antagonist M64 (expressed as the percentage of the overall input DNA), as

assessed by ChIP-qPCR and standardised to the norm by the *rpoD* promoter lacking on the PqsR binding site.

In addition, several other prominent PqsR antagonists were tested with the support of reporter gene assays for their IC_{50} scores (PqsR antagonism), however with remarkably less inhibitory capacity. That is the case for the hydroxamic acid-derivative (antagonist 11) with an IC_{50} of 23.6 µM (304), the oxadiazole-2-amine CF3 derivative (antagonist 37) with IC_{50} of 30.5 µM (312); both of fairly simplistic composition. But when scrutinising the antagonists developed by Lu *et al* (2012) where their PqsR antagonistic activity IC_{50} is sitting in the nanomolar level, it is possible that structurally conjugated benzene rings located in adjacent positions can in fact be behind better binding affinity to the PqsR protein. The HHQ analog with trifluoromethyl and nitro functional groups in position 6 (antagonist 19) showed an IC_{50} of 54 nM, whereas for the antagonist 16 is 72 nM. Since the nitro functional groups are maintained between these two molecular species, one can speculate that the lack of a trifluoromethyl in the antagonist 16 (that is present in the antagonist 19) does not favour the ligand-receptor affinity between antagonist molecule and the PqsR protein. The very low IC_{50} registered for the antagonist 19 is likely to be also attributable to the presence of fluoride (as debated previously), as part of the trifluoromethyl radical, in addition to the nitro functional group.

Overall, the results obtained with the GP QSIs and compared to the best PqsR antagonists recently developed show that this repression occurs primarily by means of either a productive/non-productive conformational change and four main factors affect the inhibitory capacity of a putative antagonist to repress ligand-receptor affinity:

1) the presence of halogens (especially Br^-, F^-, Cl^-),

2) the presence of multivalent non-metals (like S^{2-}) likely to be involved in the degradation of ROS,

3) the position at which these functional agents are added to or removed from,

4) their approximation to aromatic conjugations (like for example benzofurans).

These structures can affect PqsR production by inducing conformational changes in the receptor protein (affecting the ligand binding affinity) or by indirect repression of upstream gene expression. Either way, the equilibrium lies in the adequate stabilisation of the binding affinity with the molecular size of the antagonist.

Effects on the production of lectins

Lectins play a noticeable part in PA-triggered human infections, for their role in biofilm formation. Considering that lectin-mediated bacterium-cell recognition and adhesion are critical phases in initiating PA pathogenesis, and that PA adhesion happens to be mediated by a glycanic recognition pattern involving several adhesins, including the cytoplasmic lectin products LecA and LecB, their expression was measured by means of gene assay reporters. Two chromosomal bioreporters, PAO1-N CTX::P_{lecA}-*lux* and PAO1-N CTX::P_{lecB}-*lux*, were exposed to 10 and 100 µM concentrations (Tables 3.5 and 3.6) and it was revealed that the *lecA* reporter did not alter much, and *lecB* responded more sensitively to the 100 µM exposure. The different threshold levels to which lectins responded validate the partly differing roles these lectins have in the overall virulence array of PA. The reported inhibitory strength of the GP QSIs over *lecA* can be divided in two classes that go accordingly to their structural similarities: 1) those composed of two aromatic rings and that repressed *lecA* activity to a percentage of remaining activity around 25% (GPZ002966 and GPZ004927), and 2) those composed of three aromatic rings having repressed *lecA* to a percentage of remaining activity sitting between 34-38% (GPZ824390 and GPZ273902).

These antagonists are designed to interact with the PqsR protein, that do not entirely discard possible inhibitory 'side-effects' on, say lectin activity rather than just affecting expression. Any interferences from activity by the GP QSIs on lectins would have to be assessed with single and double *lecA*/*B* mutants exposed to the candidate molecules. However, LecA production depends on *pqsE* expression (160) which in turn needs the activation of the *pqsABCDE* operon (a PqsR-dependent operon). Thus any potential repressors of PqsR must be considered immediate repressors of the *lecA* expression, as it is shown by results obtained with these GP QSIs. Basically, for transcription of PqsE to take place there is a need for the formation of the PqsR/HHQ complex (in an initial stage) or the PqsR/PQS complex (in a later phase). But when its induction is not activated by PqsR, the repression of the *pqsABCDE* operon will determine a less virulent phenotype that not only results in lesser LecA, but also in lesser PCN (due to inactivation of the *phzA1* promoter).

Moreover, repression at the smallest concentration tested can be considered strong, especially for the GP QSIs that are made of only two aromatic rings (GPZ002966 and GPZ004927) and that once again go hand-in-hand in terms of inhibitory efficacy. Two-ring aromatic antagonists are possibly the better PqsR-inhibitors in suppressing *lecA* expression; and three-ring ones are more indicated to induce PqsR-mediated *lecB* repression. Nevertheless, *lecB* posed a much stronger barrier to repression, although it is not known whether this is exerted directly or indirectly by the GP QSIs.

LecA and LecB are ubiquitous carbohydrate-binding proteins that are seen throughout all known life forms. They bind to multivalent carbohydrates present on cell surfaces as is the case for glycoproteins and glycolipids. They arbitrate a wide spectrum of cellular and tissue adhesion mechanisms. And even though the carbohydrate-binding sites of LecA/B lectins are usually specific, they are known to be relatively weak, allowing for efficient ligand recognition to be established by means of a post-binding multivalency effect

(the cluster effect). Several authors have explored this particularity for generating synthetic ligands with very high affinity binding potential, directed towards glycoclusters (333), glycopolymers (334), and also towards glycodendrimers (335) (336) (337).

Effects on pyocyanin production

One of the most relevant virulence factors secreted by PA is the most-studied member of the phenazine family, the blue phenazine redox-active secondary metabolite PCN. Its presence and pathogenic specificity is invaluable for fast identification of the pathogen. As one of the major virulence factors in PA, screening will provide insight on the potential of any PA virulence inhibitor. In order to understand not only the indirect capacity for repressing PCN via PqsR-targeting, but also the role of these inhibitors in strains with different virulence machineries. The impact of the GP QSIs on production of PCN was studied using three different PA strains, namely PAO1-N, PA14 and SED2-LES.

Apart from GPZ004927, all the tested GP PqsR inhibitors repressed the levels of PCN of PA01-N, PA14 and SED2-LES at IC_{50} concentrations (Table 3.9), and even more effectively at 10 and 100 µM concentrations. Surprisingly, at IC_{50} concentrations, GPZ004927 was never able to induce any PCN inhibition, even resulting in an overproduction (percentage of remaining activity of 224%) in the least virulent strain PA01-N. In fact, only very high concentrations of GPZ004927 were seen to promote a considerable repressive effect; for example, on PA14 10 µM of the compound resulted in a percentage of remaining activity of 11% and SED2-LES exposed to 8 µM of the compound would result in an insignificant variation (reduction) of 6% to the overall SED2-LES PCN percentage of remaining activity. On the other hand, GPZ824390 was the most effective inhibitor of the GP QSI, basically abolishing any PCN production in PAO1-N at 10 µM (1.2% remaining activity), producing a strong repression in PA14 with exposure to 10 µM (12% remaining activity) and

reducing percentage of remaining activity to mere 38% of overall PCN production in the PA clinical haplotype SED2-LES.

Analysing the effectiveness of the different GP PqsR inhibitors in reducing both *pqsA* expression and PCN production, it is clear that they are unlikely to result from direct interaction with the ligand-PqsR protein receptor complex. This is especially true for GPZ002966 (11% *pqsA* remaining activity) and GPZ273902 (13% *pqsA* remaining activity). In regard to effects on PCN production, at 10 µM, GPZ002966 and GPZ273902 resulted in 57% and 125% in PA14, respectively. In addition, the same compounds resulted in 28% and 65% remaining PCN activity, respectively, in SED2-LES. These results suggest that there is a likely participation of the GP QSIs in secondary virulence pathways specific to each class of pathogenic PA subtype independently of PqsR. Another possible explanation indicates subtle functional differences arising from the distinct groups that are part of the structural construction of these inhibitors. This is also suggested by results obtained in many other PqsR-inhibition studies (191) (300, 304) (301, 303) (302, 312, 313).

Even though, the regulation of PCN production has been attributed to PqsR, via *pqsABCDE* control, some genes (e.g., *pqsA*, *pqsR*, *pqsH*) directly or indirectly associated to PQS production, are known to generate reduction or full inhibition of the PCN production. Biologically speaking, PCN is known to be toxic to mammalian and bacterial cells, whilst producing ROS by means of an active oxidation-reduction activity. These aspects make of PCN a fascinating agent, chemically speaking, due to its zwitterion structure (neutral molecule with opposing electrical charges) which represents more solubility and intermembrane penetration, but at the same time less permeability.

The PqsR antagonists hereby used for comparison to the GP QSIs can help establish an idea of how the structure of the antagonist impacts on PCN production. Those antagonists that do not directly target the binding pockets of PqsR have shown a poorer capacity to inhibit its production, revealed by the

need for higher QSI concentrations. For example, 250 mM farnesol resulted in a 72% decrease in PCN production in PAO1 and also reduced extracellular PCN production (95%) (191); moreover 200 μg/ml of 2-aminoacetophenone presented to PA14 reduced PCN production to around 50% (300). But as one moves towards antagonists that directly interfere with the protein binding capacity, less QSI is actually more effective in reducing PCN production, for example antagonist 11 (IC_{50} = 87.2 μM) (304) and antagonist 37 (reduced PCN levels in 46±9% at 250 μM). This is most likely related to the direct relationship between PqsR production and PQS levels, with the latter determining levels of PCN. However, the most remarkable alterations impacting on repression of PCN production is delivered by Ilangovan *et al* (2013) and Lu *et al* (2012) (antagonist 19 was able to decrease PCN production in PA14 by 74% at 3 μM) where one sees the introduction of adjacent benzenes into a dibenzene resulting in the loss of repression activity on PCN (303). In fact, the authors observed that a hydroxymethyl group at the 3-position repressed PQS production and consequently PCN levels, whereas those antagonists unsubstituted in position 3 resulted less active. The dibenzene structure is proven again important for repressing the levels of PCN for 3-NH_2-7Cl-C_9-QZN when reduces PCN levels substantially (~50%) (278). Again, a benzene ring adjacent to a furan ring may be associated to strong PCN repression for M64 reduced PCN production at an IC_{50} of 300 nM in several clinical isolates (313), a figure much closer to the results obtained with the GP QSIs.

M64 inhibits the *pqs* operon in a PQS-independent fashion and induces a non-productive conformational change in PqsR that will disturb an effective ligand-receptor attachment in regards to the native binding domain. Molecules targeting PqsR are not expected to affect production of HAQs (as is the case for M64). To the best of my knowledge no PqsD inhibitors have been successfully identified to date. Thus, the repression of the virulence regulator PqsR is seen as the most attractive target for controlling bacterial pathogenicity without promoting further AMR strategies. On the other hand, agents inhibiting the PqsB or PqsC enzymes are expected to augment DHQ secretion (produced by

both PqsA/D), repress the production of HHQ and consequently PQS, also affecting HQNO levels by means of a pathway that demands the enzymatic participation of PqsA/B/C/D.

Very recently, Miller *et al* (2013) (276) developed potent inhibitors of PCN production in PA, based on prior research and supported with information acquired by Galloway *et al* (2011) (338). The authors covered the engineering of inhibitors of LasR-type receptors constructed on the scaffold of native AHL signals, like the 3-oxo-C_{12}-HSL. The generated ligand was able to bind to and even stabilise the receptor, encouraged dimerisation, the binding of DNA and even genetic regulation. They investigated the 4-aminopyridine scaffold by introducing a variety of substituents about the pyridine ring, and subsequently scoped the influence of other related pyridines, the influence of indole and even of benzofuran motifs. Among less effective analogs in comparison to the parent molecule 4-aminopyridine that showed 63% inhibition capacity, the simple introduction of a fluoride at the 2-position accompanied by the removal of a ketone in the far end of the structure led to a compound that reduced PCN production by 70% (see entry 7), as well as the incorporation of a trifluoromethyl group (also present in the most potent GP QSI in terms of PCN repression) that completely eliminated PCN production (99%) (339).

Even though this is a repression of a virulence factor through AHL signalling pathways, LasR and the AHL 3-oxo-C_{12}-HSL are known to have a positive influence on *pqsR* expression. Based on this assumption the strong inhibitory activity of fluoride and the monoketone, in contrast to the weakened activity when the halogen is absent and a biketone is present, should definitely be further investigated.

Effects on biofilm formation

To understand the impact of the GP PqsR inhibitors on biofilm formation, the fluorescent PAO1-L::mCherry reporter was used in studying alterations in the matrix surface area and biofilm volume (biomass). All tested GP QSIs at IC_{50} concentrations repressed biofilms, especially GPZ004927 which produced biomass of PAO1-L::mCherry of 37.1 $\mu m^3/\mu m^2$ (< 25.2 $\mu m^3/\mu m^2$ that of the control) and surface area of $4.5x10^6$ μm^2 (<5 μm^2 of control) (figures 3.6 to 3.10). GPZ824390 showed a stronger inhibition of biomass production at low concentrations with surface area inhibition occurring after application of 100 nM; and GPZ273902 repressed biofilm biomass production at low concentration but above ~200 nM the biomass production remained unaltered whilst repression of the surface area of the biofilm remained evident.

The results obtained across QSI concentrations (figures 3.11 and 3.12) revealed what appears to be a strategy undertaken by the pathogen when pressure is being exerted to the limit of its innate resistance. PAO1 develops its biofilm matrix using a biphasic strategy: initially there is a clear investment on biomass to secure widespread infection to the detriment of enlarging its biofilm surface area, subsequently such efforts are then reverted to favouring of surface area when the biomass volume becomes limiting. This possibly indicates a pathogen tendency to supress the immunocompromised subject through spreading (favouring infection) which then is replaced by an approach where the gaining of nutrients is preferred by adopting larger surface area when facing dispersal arrest (favouring survival).

The presence of the amino group as a potentiator of biofilm inhibition has been touched on by some authors as a successful structure in the engineering of effective biofilm inhibitors (278, 311). Indeed, Frei *et al* (2012) dissected the stilbene antagonist 1, producing five sub-structures that were tested in PA for biofilm formation inhibition studies. In these, the removal of

the amino-group generated a full loss of inhibitory capacity, whereas the aryl function was shown pivotal for biofilm inhibition.

Effects on C_7-AQs production

In PA, secretion of a wide range of virulence and regulatory factors with roles on interspecies communication is controlled by the QS system in response to cell density. The molecules PQS and HHQ (among others responsible for the ultimate production of PCN, HCN extracellular proteases, etc.) are integral part of this regulatory network and operate in line with the expression of several genes. Identifying the consequences of PqsR direct inhibition of C_7-AQs of PA, like (e.g., HHQ, HQNO and PQS) in strains of 'differing virulence', can provide a solid idea of their quenching potential.

Interestingly, when observing the PAO1-N and PA14 control batches it is visible that the levels of endogenous HHQ and PQS show different rates in the different strains, i.e., in PAO1-N HHQ levels are far less than those of PQS (HHQ:PQS ratio of 0.2), and in PA14 HHQ levels are very close to those of PQS (ratio of 1.1) (figures 3.15 and 3.16). It is possible that in addition to the pathogenic islands in PA14 or as a consequence of its existence, higher virulence could also be a result of a constant availability of the precursor HHQ. By reducing the HHQ:PQS ratio, GPZ824390 and GPZ002966 might as well interfere with the stoichiometry of the HHQ conversion to PQS, an effect only observed in PA14 and therefore possibly linked to pathogenic-associated machinery that is not present in PAO1-N. The opposite effect, i.e., overproduction of PQS from its precursor HHQ, is seen with GPZ273902 in PA14. This undesirable effect is not seen with GPZ273902 in PAO1-N, possibly indicating that it might depend on the presence of virulence-associated elements that are not at all present in PAO1-N. This possibility presents just one out of many contributing factors, one that on its own does not explain increased virulence, especially when considering the multifactorial differences

between PAO1-N and PA14, and between different laboratory sublines of the same strain.

Nonetheless, in comparison to the best PqsR antagonists found in the literature available, the nanomolar concentrations used with the GP QSIs reveal a very promising antagonistic force. Farnesol inhibits PQS production in a dose-dependent manner where 25 mM reduced production of extracellular PQS levels in 39% and 250 mM in 85% (191). The antagonist 3 developed by Lu *et al* (2014) (301) and examined against PA14 resulted in a strong reduction of both HHQ (by 37%) and PQS (by 54%) at a concentration of 15 mM.

Synergistic effects

Therapeutically speaking, the application of molecules intended for bacterial biofilm control (operating in a nonmicrobicidal fashion) are expected to act synergistically when used alongside classic antibiotics. Combinatory synergistic cooperation represents an important advantage in the sense that it surpasses persister defences more easily, in comparison to monotherapeutics. Such assumption is acceptable because the pathogen is exposed to more than one suppressor (340). A combinatory approach can produce synergism and/or additive collaboration (positive effects) or on the other hand antagonist and/or toxic consequences (negative effects). It is important to measure relevant effectiveness of the different trialled combinations and to understand their *modus operandi* before assuming synergistic behaviour. Moreover, there are numerous reports on potential antimicrobials (from peptides to synthetic and semysynthetic molecules, etc.) used in conjunction with traditional antibiotic formulations with enhanced success on chronic lung bacterial infections (341) (342) (343) (344) (345). But few synergistic approaches combining synthetic PqsR antagonists and classic antimicrobial drugs are known to date.

Synergism is a difficult concept to validate in practical terms, especially if the different inhibitors composing the mixture act singularly as potent antagonists. In light of these interacting PqsR antagonists, a definition of synergism is hereby established as: the molecular potential to bind to distinct available ligand domains in the protein structure, forming a dimer-of-dimers with small conformational changes, increasing affinity to subsequent binding inhibitors that eventually attach to available ligand binding domains.

In that sense, the GP QSIs assessed here characterised were in double, triple (see annexes) and even quadruple combinations (data not presented) for their synergistic potential. These multiples were chosen due to the quaternary structure of the PqsR protein. Successful synergy was accepted whenever a combination reduced actively more than any individual antagonist applied. Likewise, for offering a clear idea of synergistic strength, the overall concentrations tested were reduced as the number of participating PqsR antagonists increased. The results obtained throughout the different combinations delivered very promising results. In terms of double combinations, improved *pqsA* inhibition was observed with just a quarter of the initial tested concentration (Table 3.3). However, GPZ004927 did not contribute to the inhibitory synergistic effects, acting as a much better inhibitor when applied on its own, not an alien result considering that the literature shows plenty of examples of single potent antagonists converted to weakened or innefective compounds when combined 'synergistically' (Tables 3.4, 3.7 and 3.8).

All double combinations that made use fo the best eight GP QSIs reduced *lecA* activities, but not all repressed *lecA* expression in comparison to the better of the two individual compounds. Nonetheless, these results show very strong repressive effects impacting on *lecA* expression at low concentrations, especially if the binding domains of the protein are exhausted by plentiful antagonists. The poor synergistic effects on *lecB* expression (Table 3.8) reinforced the idea that this genetic element is less volatile to repression

by PqsR-targetting antagonists. The results obtained on *lecB* also highligth the structural participation of GPZ273902, for whenever involved in a double combination it often generates robust repression resulting in low percentage of remaining activity.

Understanding the synergistic collaboration exerted on the tetrameric PqsR protein, and possibly even impacting on the homotetrameric lectin structure, requires the determination of binding curves against a range of concentrations of GP QSIs. The binding kinetics would reflect underlying conformational changes contributing to the complex dissociation kinetics, something that can be accomplished by, for example, stopped-flow spectrophotometry. In fact, this methodology has been successfully applied to the study of protein-protein interactions by Nissen *et al* (346). Stopped-flow spectrophotometry can help reveal the variation in affinity, if such variation is in its nature caused by an increase in the dissociation rate of the antagonist, allowing sequential comparison between dimeric, trimeric and tetrameric ligands. Actually, the authors propose that increased affinity of ligands is likely to result from reduced chance of concurrent dissociation of all existing binding moieties in the ligand-protein interaction. Thus, optimisation of the binding affinity of the GP QSIs could then be attempted by means of the aforementioned suggested strategies, such as, varying the core length of the antagonist, halogenic participation in their composition, proximity of functional groups to the aromatic rings, etc.

Another important aspect to consider concerns the ligand-receptor binding producing conformational changes with further dimerisation of the protein. These effects have been reported in the past by Qin *et al* (2000) (347) whilst researching the QS signal binding of the bacterial QS system activator TraR. An important aspect suggested by the authors is that when not bound to a ligand, the N-terminus of the protein is hiden from the aqueous environment, and the N-terminus exposure is reverted when the ligand is connected to the protein, meaning that the protein suffers a natural conformational change

upon ligand binding. Consequently, there is an alteration in the equilibrium-state favouring dimerisation. An acyl-HSL-induced alteration at the N-terminus region has been shown necessary for transcriptional activation (348). Possibly, such induced conformational change and subsequent dimerisations generated by the GP QSIs on the PqsR protein also result in a blockade to molecular access by the RNA polymerase.

In conclusion, with the disturbing reality that the usage of classical antibiotics is seriously limited in the face of the acquired resistances by nosocomial pathogens, research on new antimicrobial drugs is compulsory. The novel methodologies depend on developing synthetic antagonists of the PA QS system with potent efflux inhibitory capacity, and synergistically combine them with fluoroquinolones and/or fourth generation β-lactams. Fluoroquinolones, for example, have been extensively associated with enhanced antagonistic strength when used as part of their structural composition. Fluoroquinolones efficiently penetrate lung tissue, have minimal nephrotoxicity, are extremely active *in vitro*, effective on both Gram-positive as well as Gram-negative pathogens, and are pharmacokinetically adapted to a wide spectrum of infections.

Chapter 4

4.1. Engineering of a *pqsA-pqsR* lux-based biosensor in *E. coli*

The goal of this chapter is to engineer an *Escherichia coli* biosensor (figure 4.1) based on the detection of PQS for screening PA by making use of two subsystems: an inducible part composed of *lacI^q-Ptac-pqsR* to regulate the production of PqsR and a reporting one composed of the *luxCDABE* operon fused to the *PpqsA* promoter. This construct is designed to be inserted in single copy in the chromosome of *E. coli* by way of a mini-Tn7 element, allowing for its natural replication and enhanced transcriptional control. A perfectly functional system would then make use of the early detection of PQS production as a signature of PA infection, thus representing a powerful tool for the rapid screening of clinical samples such as sputum, blood plasma, urine and saliva.

4.1.1. General schematic of the construct

In regards to the design of the biosensor, the first genetic set or module is the *lacI^q* gene constitutively producing the LacI repressor, and the LacI-controlled *tac* promoter driving the expression of the *pqsR* gene encoding the transcriptional regulator PqsR, whereas the second set/module is composed of the *luxCDABE* operon transcribed from the *pqsA* promoter. To prevent interference between the two parts, these are separated by an omega interposon that terminates transcription in both directions.

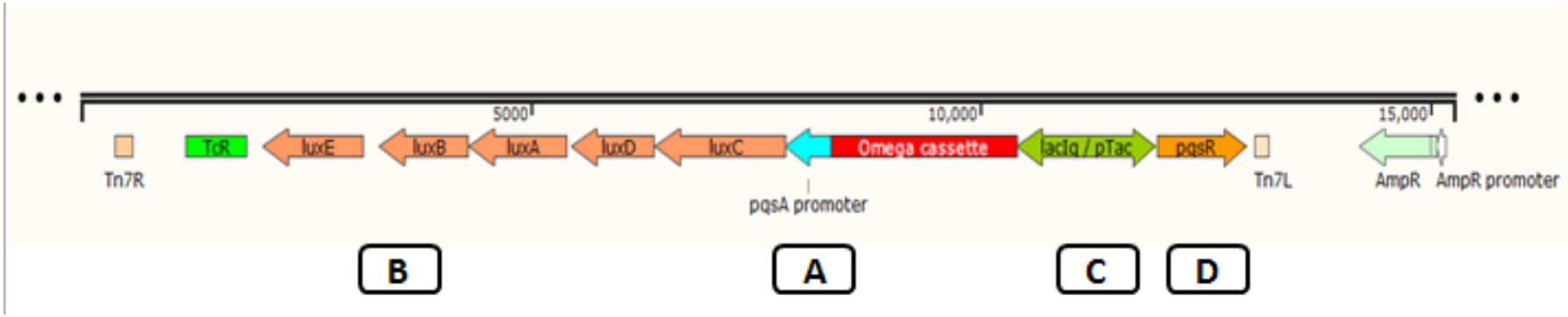


Figure 4.1. Overview of the engineered PQS-based biosensor. Constituting elements are the (A) Response promoter (*pqsA* promoter), (B) light reporter (*lux* cassette), (C) transcription terminator and (D) regulatory and inductive switch. Tn7R and Tn7L represent Tn7 right and left ends, respectively and are used to integrate the biosensor in the chromosome of *E. coli*. Amp^R stands for the β-lactam resistance gene from the mini-Tn7 delivery plasmid prior to chromosomal integration.

In general terms and in the absence of inducing alkyl quinolones the system is naturally shut off, but in the presence of PQS, PqsR will induce the *pqsA* promoter and therefore the production of light by expression of the contiguous *lux* operon. Isopropyl β-D-1-thiogalactopyranoside (IPTG) is used to induce the P_{tac} promoter which is otherwise repressed by LacI, in order to adjust the levels of PqsR in the system (figure 4.2).

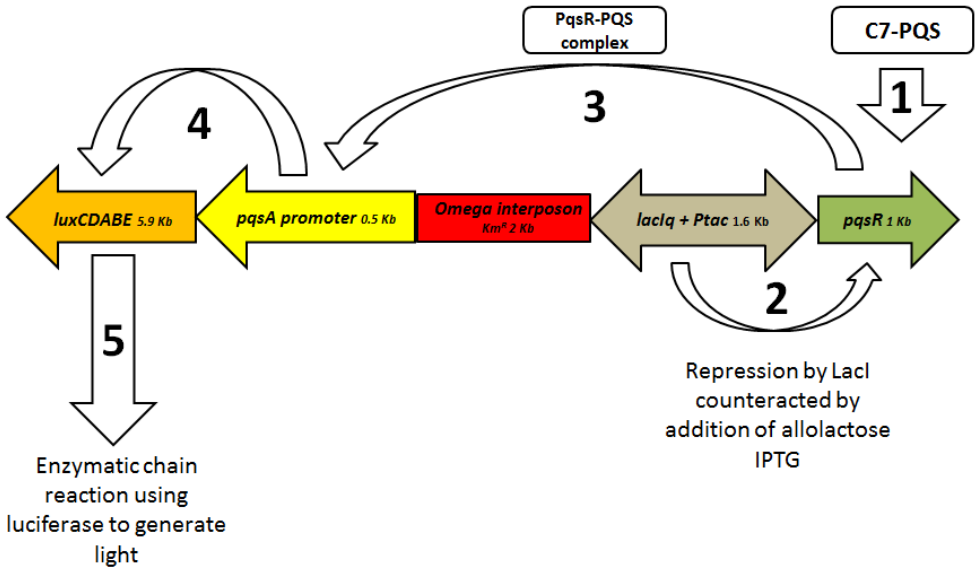


Figure 4.2. Functional elements of the integrated heterologous AQ-based biosensor reporter. The biosensor refers to a phenotypical reporter based on visible light generation as a response to inducing alkyl quinolones such as PQS. In this sense **(1)** C_7-PQS is the most common signalling molecule, but other molecules such as C_9-PQS and HHQ can also have the same role. The *E. coli*-based system represents a more direct assay of PqsR activity and the stimulation and repression sub-system that regulates *pqsR* is monitored by **(2)** the *lacI*^{q} gene coding for the lac repressor (LacI). In that sense, LacI binds in a sequence specific manner to the major groove of the operator sequence and blocks T7 RNA polymerase from binding to the promoter sequence. In the absence of IPTG the *lac* repressor binds to the operator sequence on DNA twisting it 40 degrees. This blocks access of T7 RNA polymerase to the promoter site and thus prevents leaky transcription of the gene before induction. When IPTG is present it binds to LacI inducing a conformational change in the protein structure that reduces its binding forces to the operator DNA sequence. Unlike lactose, IPTG is not part of any metabolic pathway and so will not be broken down or used by the cell. This guarantees that the concentration of IPTG added remains constant, making it a more useful inducer of the *lac* operon than lactose itself. **(3)** When *pqsR* is not repressed by LacI, C_7-PQS will activate the transcriptional regulator *pqsR* that ultimately secretes PqsR. This protein will form a complex with PQS that attaches to and **(4)** activates transcription of the *pqsA promoter*. Being fused to a *lux* reporter, P_{pqsA} activation ultimately **(5)** triggers an enzymatic reaction cascade regulated by the *lux* operon.

4.1.2. Implementation of the bioengineering strategy

ECKR02 is the recipient strain prepared to have the construct integrated in its chromosome, consequently giving origin to ECIL02 [*E. coli ΔsdiA*, *ΔlacI, miniTn7* (*lacI*^{q}, P$_{tac}$-*pqsR*, P$_{pqsA}$-*luxCDABE*)].

In order to generate an effective luminescent PQS-based bioreporter successfully integrated in the chromosome of *E. coli*, several cloning steps had to be engineered. The final construct plasmid pIL005 was obtained after constructing four intermediate plasmids, namely pIL001 (cloning of the *pqsA* promoter into pBluescript, figure 4.3), pIL002 (addition of the elements *lacI*^{q}, P$_{tac}$ and the transcriptional regulator *pqsR* to plasmid pIL001, figure 4.4), pIL003 (addition of the *lux* cassette to plasmid pIL002, figure 4.5) and pIL004 (addition of the Ω interposon to plasmid pIL003, figure 4.7). Figure 4.6 shows enzymatic digestion controls to the intermediate plasmids pIL003 and pIL004 and final pIL005. The biosensor construct was then integrated in the chromosome of *E. coli* ECKR02, producing strain ECIL02.

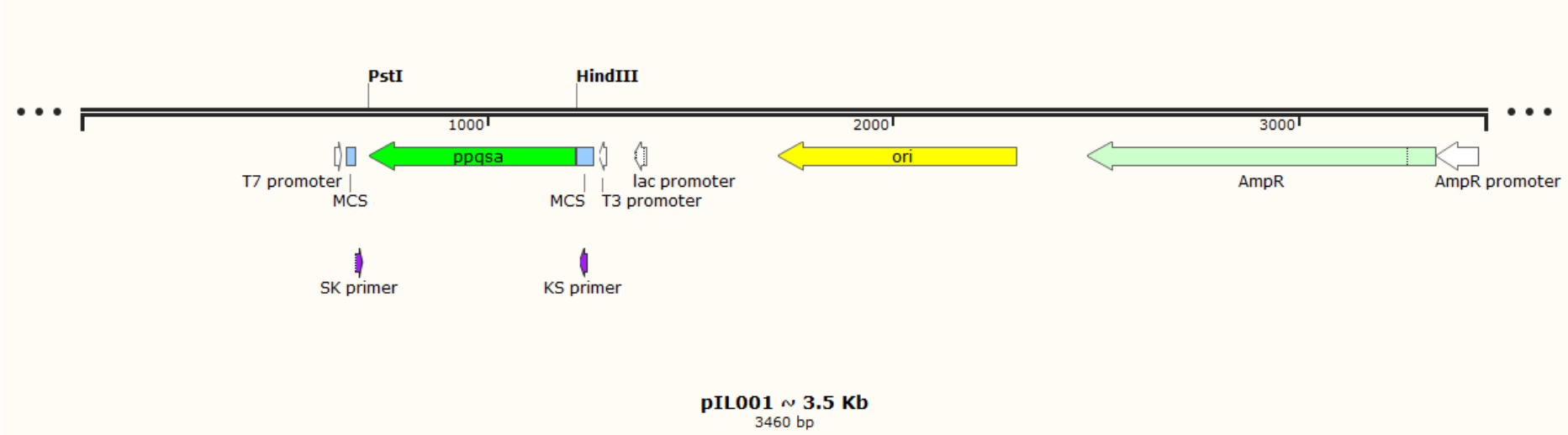


Figure 4.3. Cloning of the *pqsA* promoter (P_{pqsA}) in pBluescript to produce pIL001. A fragment corresponding to the 500 bp region upstream the ATG start codon of the *pqsA* gene was amplified by PCR from plasmid miniCTX::P_{pqsA}-lux. The oligonucleotide primers (see table in materials and methods) for PCR were engineered to contain a *HindIII* and *PstI* restriction sites. After digestion with *HindIII* and *PstI*, the *pqsA*-containing fragment was ligated into pBluescript digested with the same enzymes.

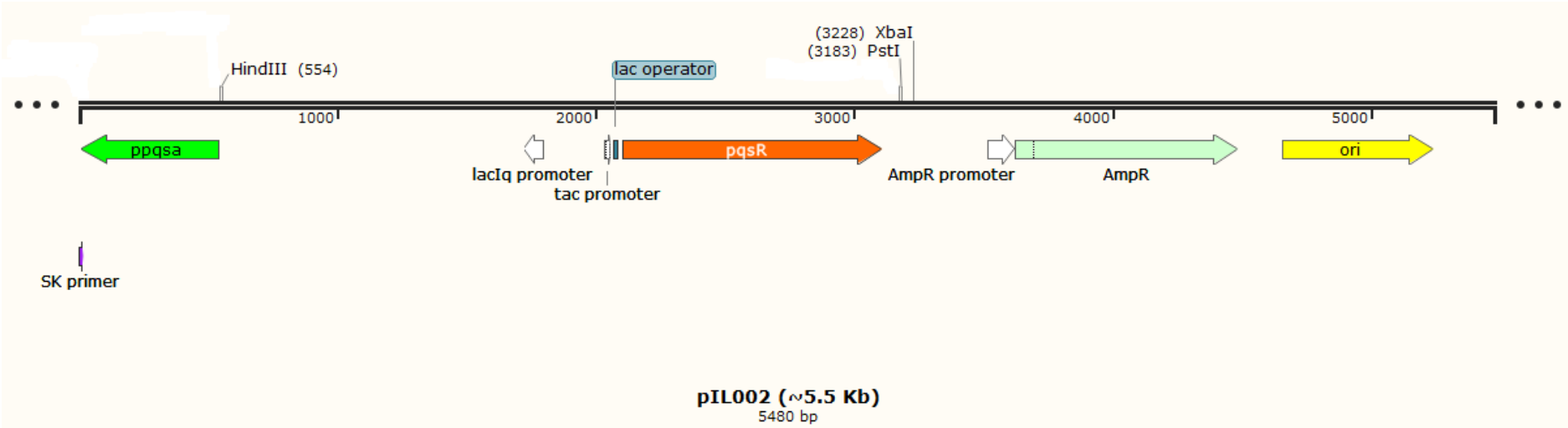


Figure 4.4. Construction of pIL002. This step involved adding *pqsR* and all the components that would regulate its expression to pIL001. The three elements were subcloned as a single ~2.5-Kb *HindIII-lacI*^{Q}-P$_{tac}$-*pqsR-PstI-XbaI* fragment from pCR3 into pIL001 digested with *XbaI* and *HindIII* producing plasmid pIL002. Black ellipses represent the pCR3-based backbone of the plasmid.

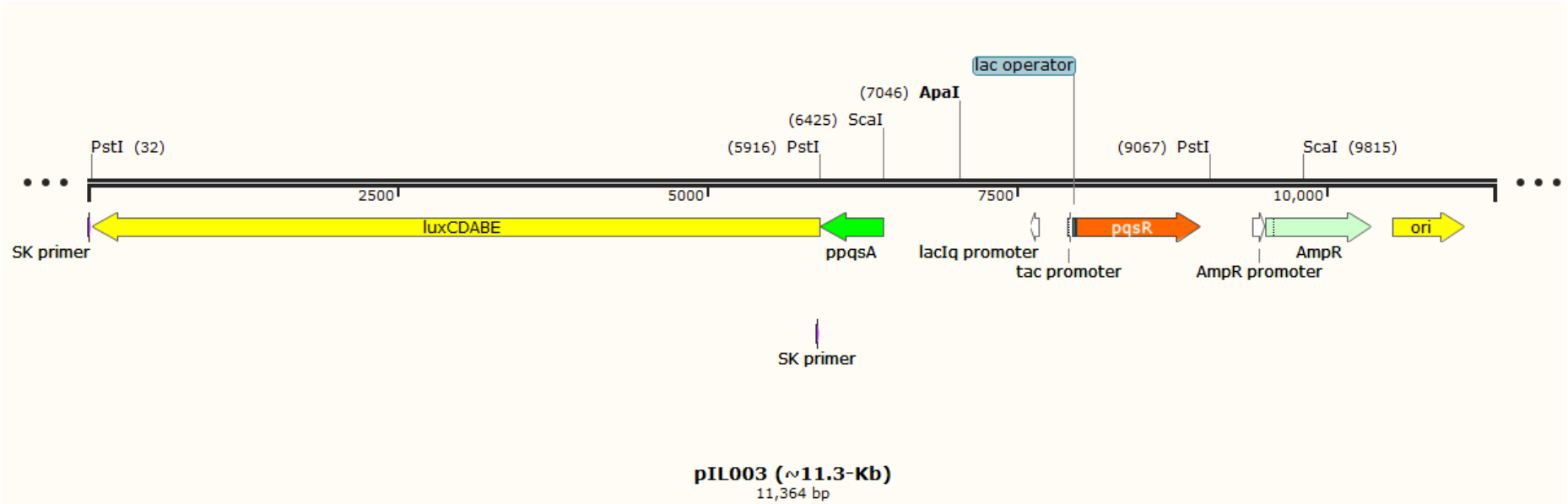


Figure 4.5. Construction of pIL003. In order to prepare plasmid pIL003, a 5.9-Kb *luxCDABE* reporter cassette was obtained by digestion of pBluelux with *PstI* and inserted in *PstI*-digested pIL002. Right orientation of the lux operon was verified by screening light producing colonies exposed to visible light in a dark camera. To enable the next step towards pIL004, a linker incorporating a SalI site was inserted in the ScaI site immediately after the *pqsA* promoter by performing a partial ScaI digestion of pIL003 to produce pIL003L. Successful insertion of the linker in pIL003L was confirmed by two digestions: 1) single digestion with *SalI* to verify its presence, 2) double digestion with *SalI* and *ScaI* to verify the presence of both linker and only one remaining *ScaI* restriction site.

Figure 4.6 shows an expected staircase pattern verifying the correct size excisions of pIL003, pIL004, pIL005 and pUC18R6KT miniTn7T-Tc.

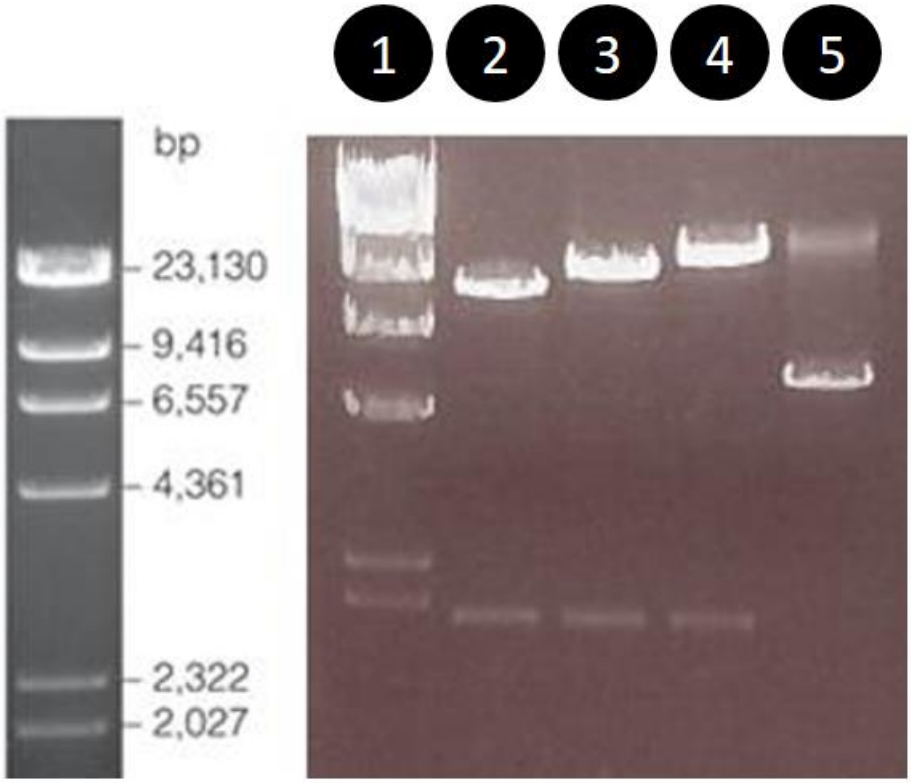


Figure 4.6. – Control digestions to intermediate plasmids towards pIL005. The digestion products are placed alongside. ApaI was the enzyme of choice for showing a link between the produced constructs as it single-cuts pCR3 (the backbone of the construct since plasmid pIL002). Apa digestion of the plasmids produce a small fragment trace seen in all the plasmids carrying the biosensor.
Lane 1 – λ-*HindIII* Promega DNA ladder.
Lane 2 – pIL003 (~1.9-Kb + ~9.4-Kb)
Lane 3 – pIL004 (~1.9-Kb + ~11.4-Kb)
Lane 4 – pIL005 (~1.9-Kb + ~14.6-Kb)
Lane 5 – *ApaI*-pUC18R6KT miniTn7T-Tc (linearised plasmid of ~4.8-Kb)

Plasmid pIL004 (figure 4.7) was generated after addition of a bidirectional transcriptional terminator (omega cassette Km^R) separating the inducible from the reporting parts. To allow subsequent chromosomal integration into ECKR02 the construct was cloned in the mini-Tn7 suicide delivery vector pUC18R6K-mini-Tn7T-Tet (Choi et al. 2005). The resulting plasmid generated was then pIL005 [pUC18R6K mini Tn7T::pIL005 (*lacI*^{Q}, P_{tac}-*pqsR*, ΩKm, P_{pqsA}-*luxCDABE*)] (figure 4.8), a plasmid that encompasses the final stage of the functioning construct.

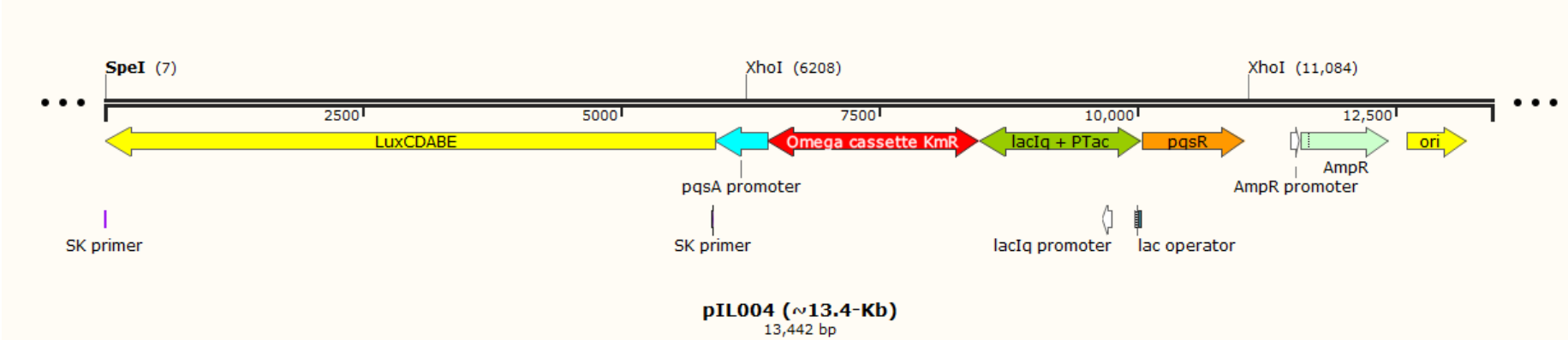


Figure 4.7. – Linear plasmid map of pIL004. The omega interposon was PCR-amplified from pHP45Ω with oligonucleotides incorporating XhoI (C'TCGAG) sites on both ends, compatible to the SalI (G'TCGAC) extremeties in pIL003. These DNA fragments were ligated and the resulting plasmids subsequently transformed in DH5α. Successful ligation was verified by digesting pIL004 with SpeI (linearises pIL004) and XhoI (XhoI generates two bands where the lower band is 2.0 Kb higher than pIL003+linker, i.e., corresponding to the inserted omega cassette).

Transposition of the mini-Tn7 element carrying the biosensor construct into the chromosome of *E. coli* ECKR02 was carried out as described in the materials and method section, by electroporating an optimised pTNS2:pIL005 DNA ratio of 1:2. The resulting strain was called *E. coli* ECIL02.

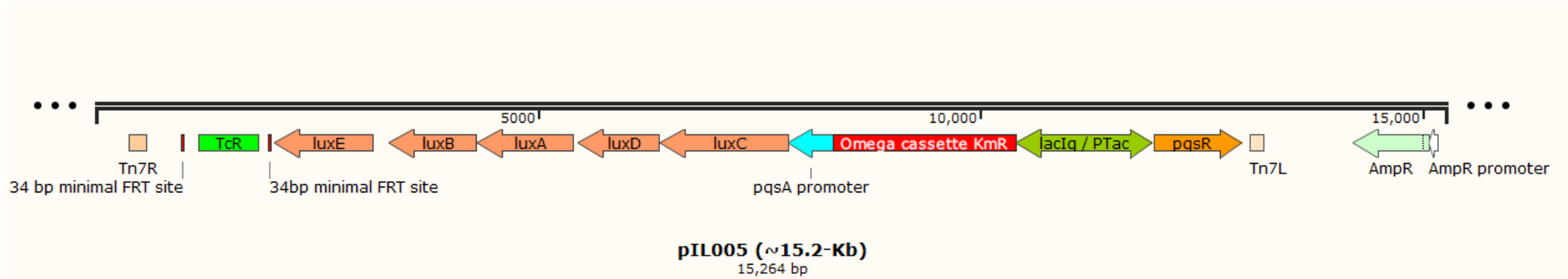


Figure 4.8 – Linear map of plasmid pIL005. The mini-transposon ends Tn7R and Tn7L are located on both left and right ends of the biosensor. To construct pIl005, plasmid pIL004 was partially digested with XhoI and then fully digested with SpeI to excise the biosensor part which was then subcloned in the pUC18R6KTminiTn7T plasmid double-digested with SpeI and XhoI. Plasmid pIL005 was therefore produced by ligating the previously digested fragments.

After chromosomal integration of the biosensor construct to produce ECIL02 by electroporation alongside the pTNS2 helper plasmid a confirmation of correct insertion was carried out. Making use of oligonucleotides directed at the *glmS* and the *pohS* genes, that flank the Tn7L and Tn7R sites after integration of the mini-Tn7 element into its attachment site in the chromosome, the obtained PCR products confirmed that the construct had been integrated in the right position. Two screening control strategies were applied: 1) minipreping of the resistant colonies identified colonies lacking plasmids (confirmed by nanodroping); 2) a PCR with primers that amplified fragments limited by the insertion genes (figure 4.9) and chromosomal recognition genes (*phoS* and *glmS*) located near the transposition sites, namely *phoS-Tn7L* (~1000-bp) and *glmS-Tn7R* (~997-bp) (figure 4.10).

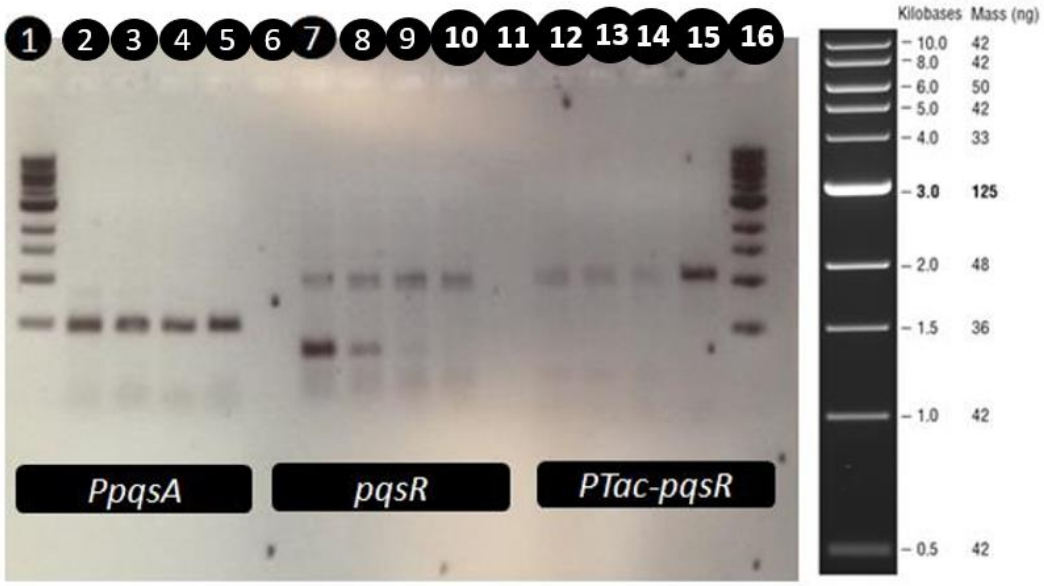


Figure 4.9. - Verification of successful chromosomal integration of the mini-Tn7 biosensor element in ECIL02. Genomic DNA was extracted from *E. coli* ECIL02 and primers for amplification of the genetic sets P_{pqsA} (~0.5-Kb), *pqsR* (~1-Kb) and P*tac-pqsR* (~1.25-Kb) were obtained by gradient PCR. The optimal temperature was found to be 57°C corresponding to the fourth lane of each genetic set, in contrast to the non-specific annealing seen with lower temperatures.
Lanes 1 and 16 – 1Kb NEB DNA ladder
Lanes 2 to 5 – P_{pqsA}
Lanes 7 to 10 – *pqsR*
Lanes 12 to 15 – P_{tac}*+pqsR*.

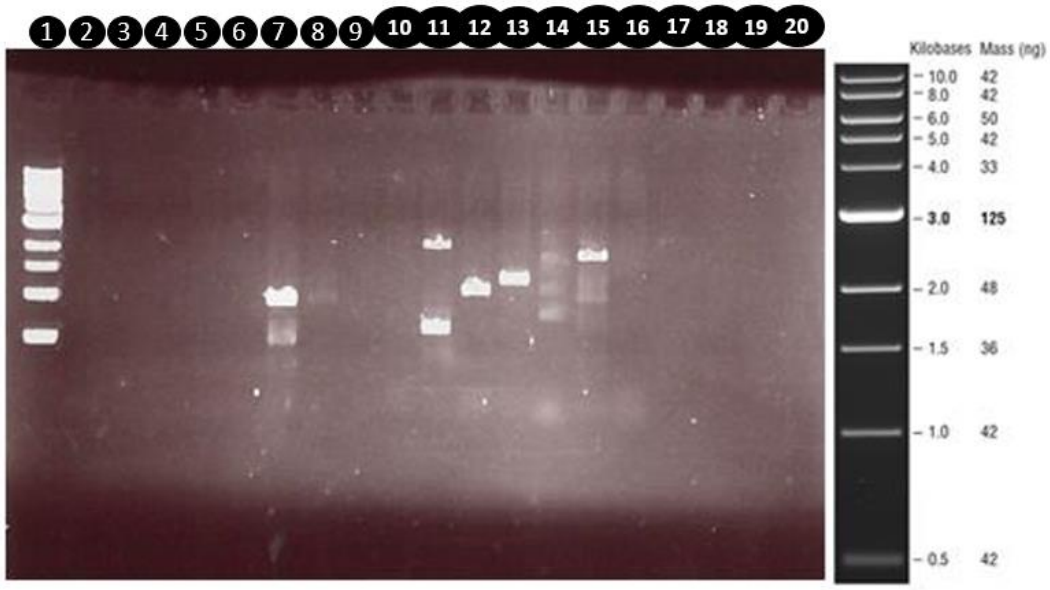


Figure 4.10. - Verification of successful chromosomal integration in ECIL02 (fusion between transposition elements). Genomic DNA was extracted from *E. coli* and amplification of the different genetic fusions was undertaken at an annealing temperature of 50°C.
Lane 1 - 1 KB NEB DNA ladder
Lanes 2 to 6 and 8 to 10 – Empty
Lane 7 – *pqsR* (~1-Kb)
Lane 11 – *luxC/*P_{pqsA} (~750-bp)
Lane 12 – *glmS/Tn7R* (~1.1-Kb)
Lane 13 – *phoS/Tn7L* (~1.2-Kb) *pqsR/Tn7L* (~1Kb)
Lane 14 – unrelated to this study
Lane 15 – $Tn7_1$*/Tn7R* (~714-bp)
Lane 16 – $Tn7_2$/Tn7L (~286-bp)

All controls applied revealed that the insertion of the engineered construct in the chromosome of the ECIL02 strain was successful as all elements were present and structurally complete. The next steps consisted in the assessment of the biosensor by means of bioluminescence assays.

4.2. Bioluminescence assays

Assessment of the newly constructed biosensor strain ECIL02 against C_7-PQS and C_9-PQS was carried out. The purpose of testing different compounds was to evaluate the bioreporting capacities of the single copy chromosomal version against a range of typical QS signalling molecules, e.g.,

C_7-PQS and C_9-PQS. By measuring luminescence during growth for up to 24 hours, measurements were taken every 30 minutes. However, strain ECIL02 did not produce any bioluminescence under the conditions used. This could be the result of: a) the concentration of alkyl quinolones used, i.e. for a single copy it could be that the PqsR produced and subsequently attaching to P_{pqsA} was of insufficient quantity, b) quality and strength of complex formed, c) faulty functional assembly of the composing parts or d) structural issues related to absence of a regulator. These hypotheses were therefore tested producing gateways to what the original problem could actually be:

a) **ECIL02 exposed to HHQ and C_7–HHQ–*N*–oxide proven incapable of biosensor activation** as both were unable to generate bioluminescence at a wide range of concentrations.

b) **Proofreading the functional elements of the biosensor**, offered an immediate idea on the reliability of the chromosomal insertion. A template of genomic DNA from ECIL02 comprising a region that included the inserted construct was sequenced. Genetic completeness of gene fusions and absence of SNPs discontinued the existence of any point mutations.

c) ***Pseudomonas aeruginosa* mutants pointed towards missing regulatory elements in our biosensor** (explored in the coming subsections) as being the probable origin of an inefficient light production, thus prompting an immediate assumption that *E. coli* as a recipient could be the defective part of our strategy.

The biosensor was assembled in a mini-Tn7 delivery vector containing single *attTn7* sites like PA (349). Different PA quorum sensing-related mutants were tried in order to recognise what missing or defective elements were responsible in the deficient reporter. The adequate functioning of the operational elements P_{pqsA} and *pqsR* was assessed with strain PAIL001 [PAO1-

N Δ*pqsA*, Δ*pqsR*, miniTn*7* (*lacI*^{Q}, P$_{tac}$-*pqsR*, P$_{pqsA}$-*luxCDABE*)], subsequently giving space to the scrutiny of the main regulatory QS candidates, *lasR* (mutant PAIL003) and *rhlR* (mutant PAIL004). Two other elements more directly related to the *pqsABCDE* operon and PQS productions were also examined; namely *pqsE* and *pqsH*. Table 4.1 summarises the reported activities of the biosensor in these strains:

Table 4.1. – Summary of luminescence scores generated by the different mutant strains carrying the PQS–based biosensor. All values were calculated based on area under curve produced by strains carrying the PQS–based biosensor growing under two different conditions: a) in the presence of 50 µM C_7–PQS and 1 mM IPTG and b) under the same conditions but with previous overnight growth exposure to 1 mM IPTG. Bold green and red values stand for the highest and lowest signal, respectively, in a specific exposure scenario.

Mutant strain	50 µM C_7-PQS plus 1 mM IPTG (RLU)*	Plain LB Control (RLU)*	50 µM C7-PQS plus 1 mM IPTG after overnight exposure to 1 mM IPTG (RLU)**	Plain LB Control after overnight exposure to 1 mM IPTG and Plain LB on the day (RLU)**
ECIL02 *E. coli ΔsdiA, ΔlacI, miniTn7* (*lacI*^{Q}, P$_{tac}$-*pqsR*, P$_{pqsA}$-*luxCDABE*)	**$4.8x10^2$**	**$3.6x10^2$**	**$1.3x10^4$**	**$5.8x10^3$**
PAIL001 [PAO1-N Δ*pqsA*, Δ*pqsR*, miniTn*7* (*lacI*^{Q}, P$_{tac}$-*pqsR*, P$_{pqsA}$-*luxCDABE*)	**$6.5x10^7$**	$2.6x10^7$	$5.5x10^7$	$4.1x10^7$
PAIL002 PAO1-N *ΔpqsA, ΔpqsH*, miniTn*7* (*lacI*^{Q}, P$_{tac}$-*pqsR*, P$_{pqsA}$-*luxCDABE*)	$5.1x10^7$	$2.6x10^7$	$4.6x10^7$	$2.7x10^7$
PAIL003 PAO1-N PASPD233 miniTn*7* (*lacI*^{Q}, P$_{tac}$-*pqsR*, P$_{pqsA}$-*luxCDABE*) [*lasR* mutant]	$2.5x10^7$	$2.3x10^7$	$5.9x10^7$	$3.6x10^7$
PAIL004 PAO1-N PACP10 *miniTn7* (*lacI*^{Q}, P$_{tac}$-*pqsR*, P$_{pqsA}$-*luxCDABE*) [*rhlR* mutant]	$6.9x10^4$	$2.7x10^4$	**$8.5x10^7$**	**$5.5x10^7$**
PAIL009 *PAO1 pqsEind*::miniTn*7* (*lacI*^{Q}, P$_{tac}$-*pqsR*, P$_{pqsA}$-*luxCDABE*)	$2.9x10^7$	**$3.4x10^7$**	$4.9x10^7$	$3.2x10^7$

* Corresponding to 48 cycles

* * Corresponding to 20 cycles

4.2.1. PAIL001 response to 50 µM C7-PQS and 1 mM IPTG (figure 4.11)

PAIL001 was constructed from a double Δ*pqsA/ΔpqsR* mutant; this strain uses the P_{pqsA} and the transcriptional regulator *pqsR* directly from the chromosomally inserted biosensor. The background signal is high, possibly due to leakage of the *lacI* repressor, but response to quinolone and inducer is nearly 3-fold stronger than the basal level (control constituted by plain LB). Overall, this experiment helped to clarify that the transcriptional regulator from the inserted biosensor as well as the *pqsA* promoter were not defective and therefore not the cause of the lack of activity in *E. coli*.

If no significant bioluminescence was ever produced, *pqsR* and/or P_{pqsA} were likely to be the faulty elements in the original integrated biosensor system. The bioluminescence assays conducted in the PAO1-N *ΔpqsA ΔpqsR* miniTn*7* (*lacI*^{Q}, P_{tac}-*pqsR*, P_{pqsA}-*luxCDABE*) strain PAIL001 clearly ruled it out. 50 µM C_7-PQS stimulus revealed a very good signal production, the induction curve being 3-fold that of the one produced in the control curve (Plain LB).

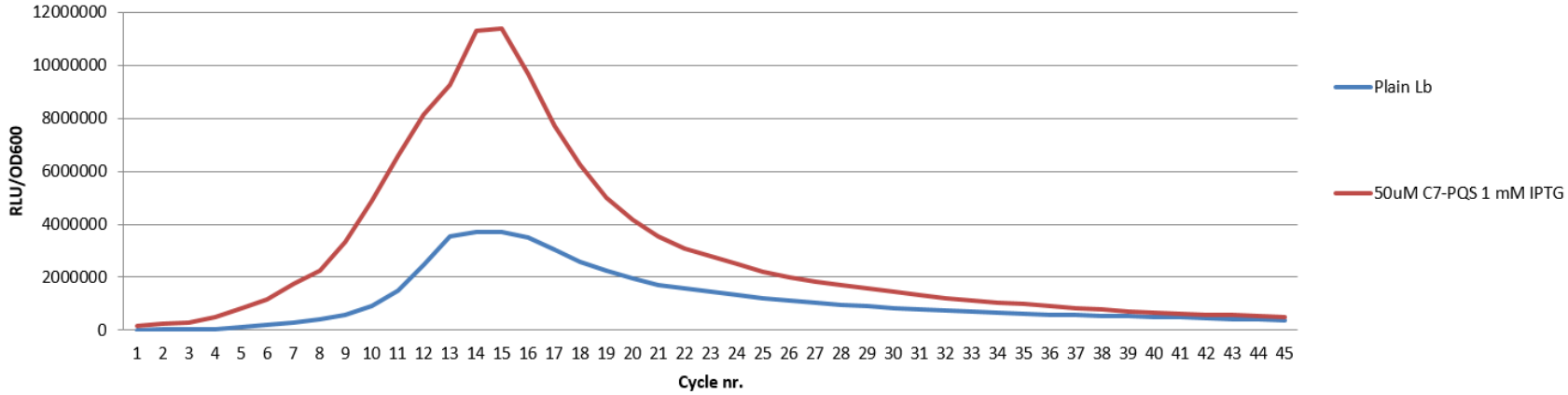


Figure 4.11. - Bioluminescence production in PAIL001 [PAO1-N *ΔpqsA ΔpqsR* miniTn*7, lacI*^{q}, P$_{tac}$-*pqsR*, P$_{pqsA}$-*luxCDABE*]. The test strain was presented to 50 µM C_7-PQS plus 1 mM IPTG and bioluminescence was read every 30 minutes (cycle) for a period of 24 hours. Initial OD_{600} of test strain was 0.5.

4.2.2. PAIL001 responsiveness after overnight exposure to 1 mM IPTG (figure 4.12)

To assess whether pre-induction of PqsR production was a requisite for a better response of the biosensor towards C_7-PQS, overnight cultures in preparation for the bioluminescence assays were grown in the presence of 1 mM IPTG. PAIL001 was grown as usual, except this time it was supplemented with 1 mM IPTG and repeated 1 mM IPTG addition before the luminescence testing took place. The results obtained helped distinguish between two ideas derived from previously presented data, 1) IPTG has a role in saturating the system and is not at all required for an adequate biosensor response, and 2) the presence of a strong background signal due to a possible leakage of the transcriptional repressor LacI associated to a very sensitive *luxCDABE* reporter operon. When comparing to data on figure 4.12 the biosensor system really gains from the overnight exposure to 1 mM IPTG because when tested against 50 µM C_7-PQS and 1 mM IPTG on the day, the curve generated with overnight exposure to IPTG produces a peak of slightly over $12x10^6$ relative light units (RLU), a much greater signal compared to $8x10^6$ RLU generated without overnight exposure to IPTG.

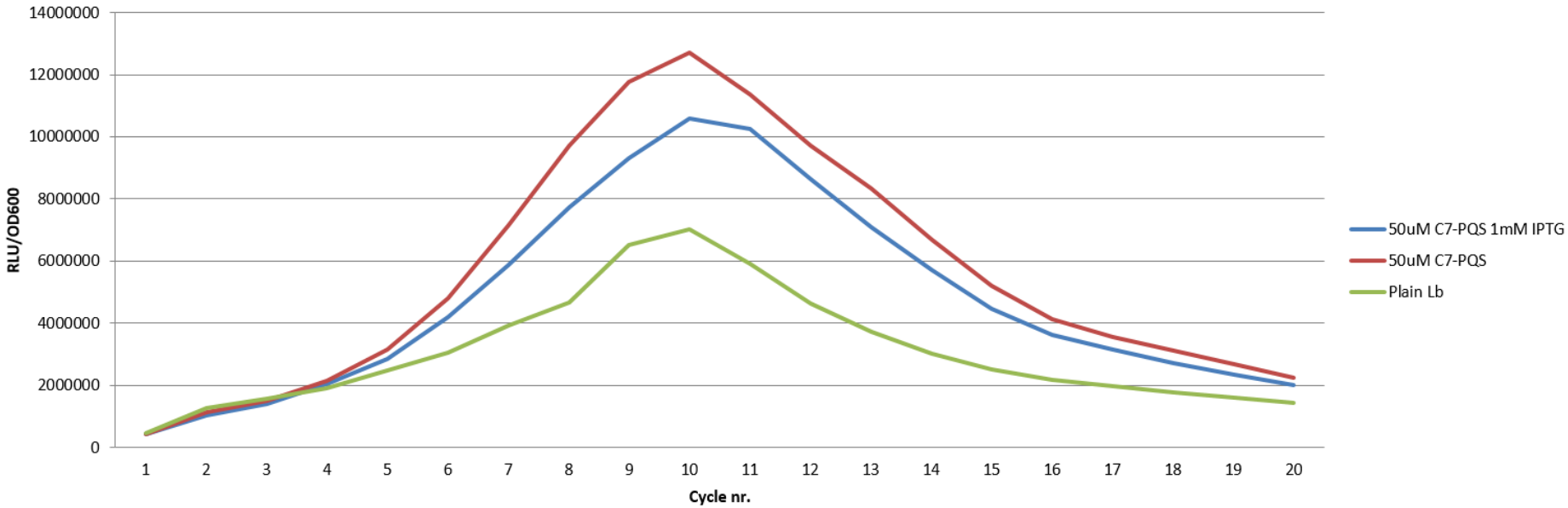


Figure 4.12. - Bioluminescence production in PAIL001 [PAO1-N *ΔpqsA ΔpqsR* miniTn*7, lacI*^{Q}, P$_{tac}$-*pqsR*, P$_{pqsA}$-*luxCDABE*]. The test strain was grown overnight in the presence of 1 mM IPTG. Subsequent 1 mM IPTG was added to the 50 µM C_7-PQS treatment prior to bioluminescence assay. Bioluminescence was read every 30 minutes (cycle) for a period of 10 hours (the time point where the response starts plateauing). Initial OD_{600} of test strain was 0.5.

Strain PAIL001 showed that the biosensor itself is not the cause of the lack of bioluminescence in *E. coli*. The P_{pqsA} and *pqsR* elements present in PAIL001 by means of the inducible biosensor indicate that these elements are functional, at least when supported by potential additional and still unknown factors, i.e., the regulatory genes that might exist in PA that are not present in *E. coli* and that contribute to an adequate functioning of the biosensor.

4.2.3. PAIL003 [*lasR* mutant]

Initial assays carried out with the *lasR* mutant strain PAIL003 [PAO1-N *ΔlasR*, $lacI^q$, P_{tac}-*pqsR*, P_{pqsA}-*luxCDABE*] obtained with exposure to 50 µM C_7-PQS and 1 mM IPTG, revealed an expected decrease in bioluminescence (figure 4.13). This is not surprising considering that the strain is devoid of its top hierarchical QS regulatory element that positively acts on its *pqsA* promoter. Some common traits are still present though, e.g., high background noise (baseline production of PqsR) reaching $6x10^6$ RLU, but at the same level of PAIL001 [PAO1-N Δ*pqsA*, Δ*pqsR*, miniTn*7* (*lacI*^{q}, P_{tac}-*pqsR*, P_{pqsA}-*luxCDABE*).

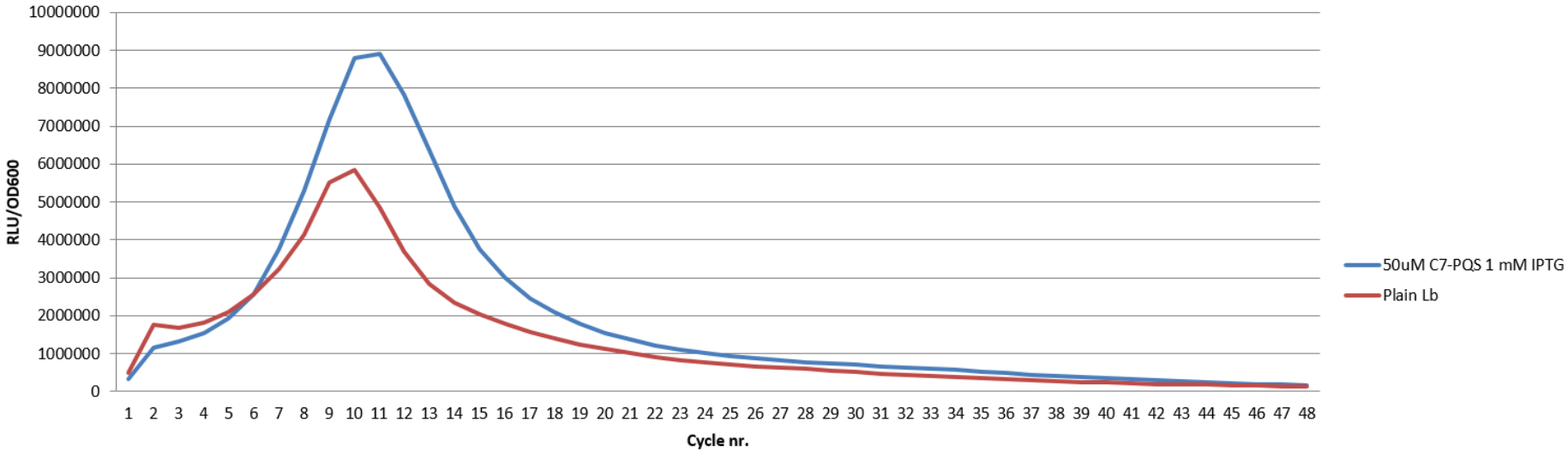


Figure 4.13 - Bioluminescence production in PAIL003 [PAO1-N *ΔlasR miniTn7, lacI*^{Q}, P$_{tac}$-*pqsR*, P$_{pqsA}$-*luxCDABE*]. The test strain was presented to 50 µM C$_7$-PQS plus 1 mM IPTG and bioluminescence was read every 30 minutes (cycle) for a period of 24 hours. Initial OD$_{600}$ of test strain was 0.5.

Inexistence of a *lasR* regulon was proved not to be the factor responsible for absence of light production in ECIL02, as shown with PAIL003. With the *lasR* regulatory role evaluated in terms of effects on the biosensor response spawned by the different stimulants the other major regulon hierarchically dependent on the first one, *rhlR*, was then assessed. The biosensor was chromosomally inserted in the PACP10 *ΔrhlR* resulting in PAIL004 [PAO1-N PACP10 miniTn*7* (*lacI*^{Q}, P_{tac}-*pqsR*, P_{pqsA}-*luxCDABE*)].

4.2.4. PAIL004 [*rhlR* mutant]

The *rhlR* mutant carrying a chromosomal integration of the biosensor system was created from the *ΔrhlR* mutant PACP10. This mutant strain tested against 50 µM C_7-PQS plus 1 mM IPTG revealed that there is basically no difference to its *lasR* counterpart mutant (figure 4.14).

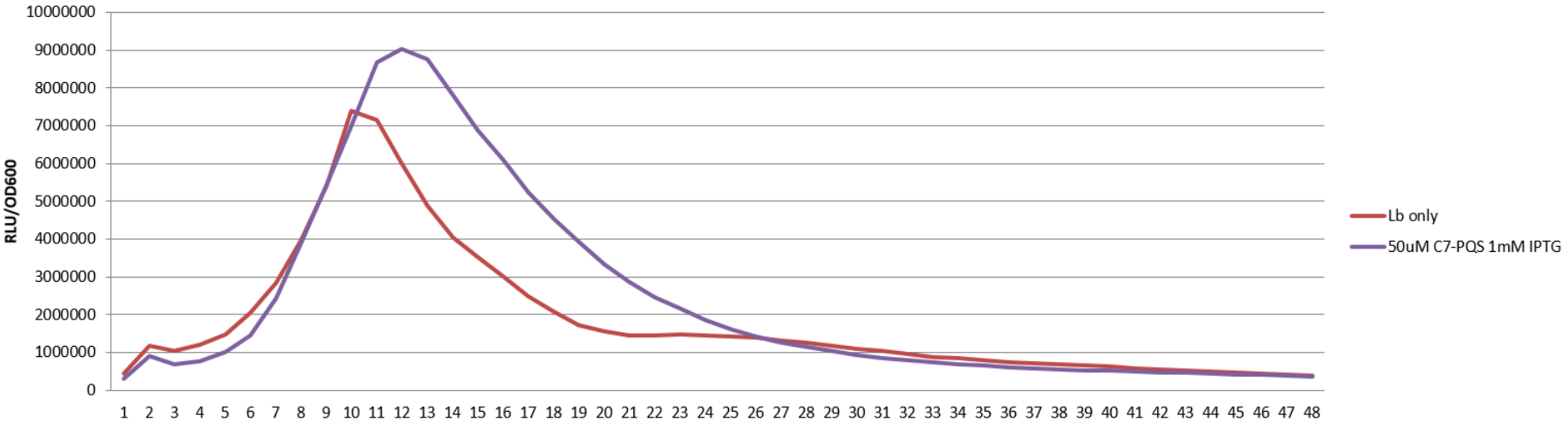


Figure 4.14 - Bioluminescence production in PAIL004 [PAO1-N *ΔrhlR miniTn7, lacI*^{Q}, P$_{tac}$-*pqsR*, P$_{pqsA}$-*luxCDABE*] under varying IPTG and C$_7$-PQS conditions. The test strain was presented to 50 µM C$_7$-PQS plus 1 mM IPTG and bioluminescence was read every 30 minutes (cycle) for a period of 24 hours. Initial OD$_{600}$ of test strain was 0.5.

4.2.5. Effect of overnight IPTG exposure in the reporter activity of PAIL004 (figure 4.15)

One of the most present effects observed in the biosensor system generated was the constant apparent leaking of LacI repression leading to constitutive PqsR production. The same pattern was seen with this *rhlR* mutant. The overnight exposure to 1 mM IPTG with subsequent fresh addition of the same concentration prior to testing confirmed the opposite behaviour in a strain devoid of the RhlR. Without the *rhlR* element there is space for more production of light to a record peak of ~$20x10^6$ RLU. The same strain was exposed overnight to 1 mM IPTG, but without subsequent addition of IPTG prior to the luminescence reading.

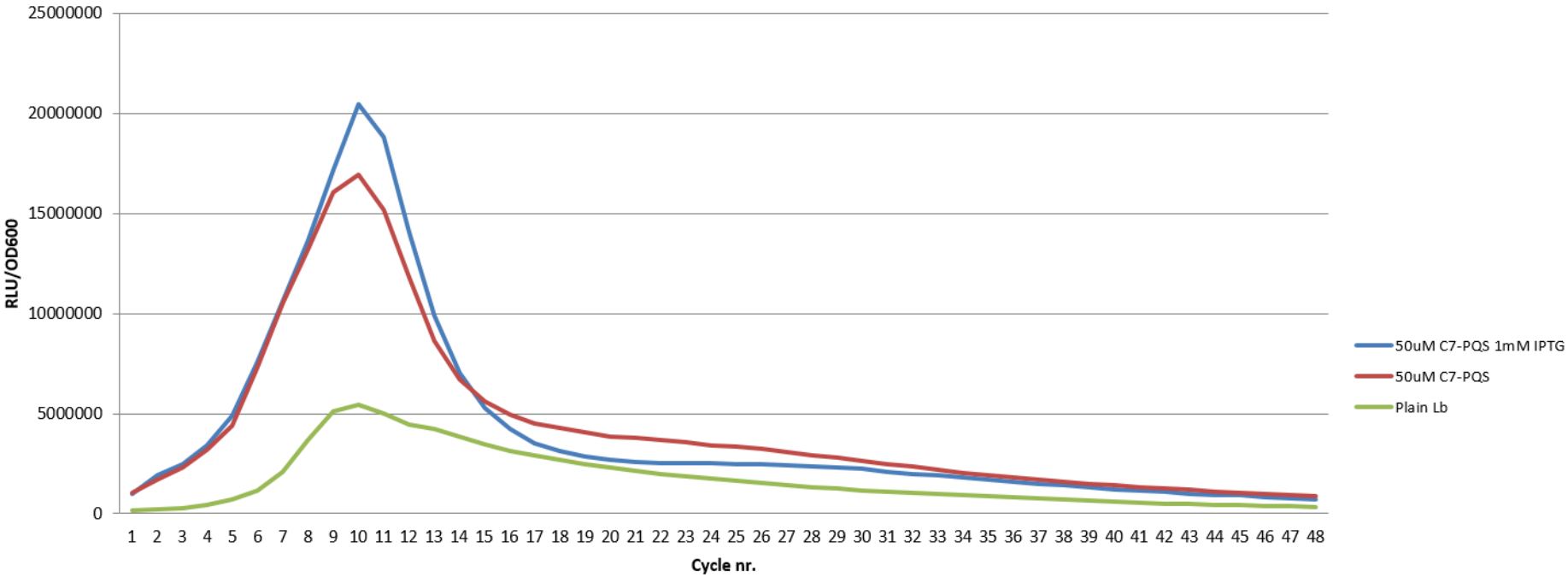


Figure 4.15. - Bioluminescence production in PAIL004 [PAO1-N *ΔrhlR miniTn7, lacI*^{Q}, P$_{tac}$-*pqsR*, P$_{pqsA}$-*luxCDABE*] after overnight exposure to 1 mM IPTG. The test strain was exposed overnight to 1 mM IPTG and presented to two different scenarios on the day of testing: 1) 50 µM C_7-PQS plus 1 mM IPTG and 2) 50 µM C_7-PQS and no IPTG. Bioluminescence was read every 30 minutes (cycle) for a period of 24 hours. Initial OD_{600} of test strain was 0.5.

In comparison to results obtained with strains PAIL001 and PAIL003 (figures 4.12 and 4.13) the strong negative feedback typical of *rhlR* does not appear to be in action anymore. In a way, the absence of *rhlR* reveals itself as causing twice as much reporter activity as with PAIL001. The result is a much increased quinolone-stimulated curve peak but approximately the same baseline production of light. Comparing results obtained with PAIL003 (*lasR* mutant) and PAIL004 (*rhlR* mutant), a negative feedback-loop regulation conducted by *rhlR* can be imagined, that would reduce the signal peak by a quinolone-induced mechanism. By inducing once again on the day with additional 1 mM IPTG, the luminescence peak rises from ~17x10^6 RLU to ~20x10^6 RLU.

4.3. Corrective measures towards a functional system in *E. coli*

Information obtained from further testing indicated that the QS systems *las* and *rhl*, as well as the analysed *pqsA* and *pqsR* genes, had no immediate accountability on the inactivity of the biosensor in *E. coli*. Cugini *et al* (2007) (191) reports briefly on the same type of heterologous *E. coli* system, in their case the *E. coli* pEAL08-2, containing a plasmid with the gene encoding PqsR, also induced by the *tac* promoter, and with the *pqsA* promoter driving *lacZ* expression rather than bioluminescence. This translational fusion accounts for the first three codons of P_{pqsA} and all the *lacZ* codons resulting naturally in production of more protein.

In another article by McGrath *et al* (2004) (168), the *pqsA* promoter is actually 99 bp shorter than the one used in this research project. These 99 bp were analysed and appear to contain the Shine-Dalgarno sequence with responsibilities in ribosomal binding and translating. A possibility would be to

reconstruct a *miniCTX-lux*-P_{pqsA} system including this additional region to compare.

The two problems initially thought to be directly associated to the lack of activity of the biosensor in the C_7/C_9-PQS tested chromosomal insertion in strain ECIL02 were related to: a) the fusion constituted by **P_{tac}-*pqsR*** being deficient, hence producing an insufficient quantity of PqsR that was consequently incapable of binding to the *pqsA* promoter fused to the *lux* operon in a way that generated light, or b) the set constituted by the P_{pqsA}-*lux* operon being deficient, therefore irrespective of PqsR being expressed, it was not adequately sensed by the established fusion *pqsA* promoter-*lux* cassette, regardless of binding to the P_{pqsA}.

Considering these possible problems, two underlying strategies were designed as corrective measures towards a functional system in *E. coli*: 1) Correcting a possibly defective P_{pqsA} by merging the *lacI*^{q}-P_{tac}-*pqsR* from pIL005 with the functional *luxCDABE*-P_{pqsA} obtained from a *miniCTX::*P_{pqsA}-*luxCDABE* plasmid containing the Shine-Dalgarno sequence; 2) Replacing the inducible P_{tac} promoter for a constitutive promoter, expected to enhance *PqsR* production in the *E. coli sdiA* mutant.

The possibly 'defective' P_{pqsA} could indicate low affinity to PqsR; therefore, strategy 1 intended to address this issue by replacing it with the P_{pqsA} element from a *miniCTX::*P_{pqsA}-*luxCDABE* template. In conjunction with a constitutive promoter it was thought to result in more PqsR being produced and higher rate of affinity in attaching to P*pqsA*. On the other side of the problem there is a fault thought to be related to a weak inductive P_{tac}-*pqsR* fusion, thus the solution was to replace these by a constitutive promoter, such as the *Em7* promoter.

Plasmid pIL007 [pUC18R6K mini Tn7T::pIL007 (*lacI*^{Q}, P_{tac}-*pqsR* from pIL005 and P_{pqsA}-*luxCDABE* from pminiCTX::*luxCDABE*-P_{pqsA}) is an improved

version of plasmid pIL005 (corresponding to an intermediate plasmid where the P_{pqsA} had been replaced). When integrated in the chromosome of ECIL01 [*E. coli ΔsdiA*, *ΔlacI, Km*^{S}] producing ECIL03 [*E. coli ΔsdiA*, *ΔlacI,* miniTn*7* (*lacI*^{Q}, P_{Em7}-*pqsR*, P_{pqsA}-*luxCDABE*)] still resulted in a silent system, disproving the hypothesis of an incomplete construct in pIL005. For that reason, a corrective approach was then designed for subsequent testing. In that sense, plasmid pIL008 [*E. coli S17-λ1pir* pUC18R6K miniTn7T::pIL005 (*lacI*^{Q}, *Em7, pqsR* from pIL005 and P_{pqsA}-*luxCDABE*) from pminiCTX:: P_{pqsA}-*luxCDABE*] resulted from a fusion of two functional regions of two different biosensors that when integrated in ECIL01 [*E. coli ΔsdiA*, *ΔlacI, Km*^{S}] produced ECIL04 [*E. coli ΔsdiA*, *ΔlacI,* miniTn*7* (*lacI*^{Q}, P_{Em7}-*pqsR*, P_{pqsA}-*luxCDABE*)].

On both plasmid versions of the new constructs pIL007 and pIL008, as well as in the resulting chromosomal integrations ECIL03/4, the phenotypical response in terms of light production was null. Both pIL007 (figure 4.16) and pIL008 (figure 4.17) showed just basal levels of light even with an *Em7* constitutive promoter offering a better initial pulse.

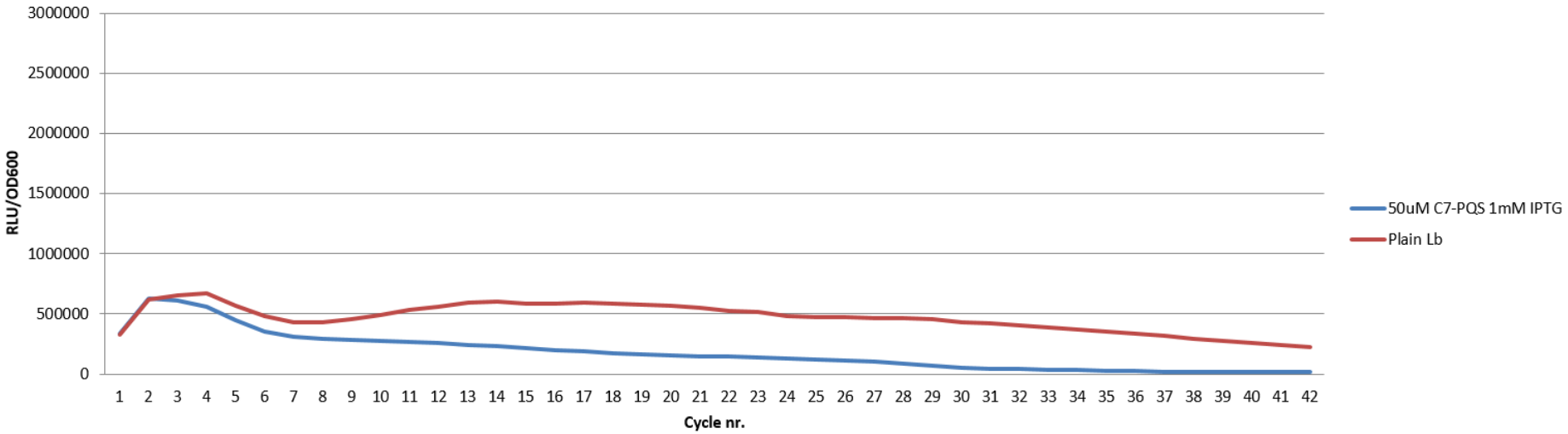


Figure 4.16. - Bioluminescence production in *E. coli S17-λ1pir* pUC18R6K miniTn7T::pIL007 (P_{pqsA}-*luxCDABE*, *lacI*^{Q}, P_{tac}-*pqsR*). The tested strain was stimulated with 50 µM C7-PQS and 1 mM IPTG added prior to the bioluminescence assay. Bioluminescence was read every 30 minutes (cycle) for a period of 24 hours. Initial OD_{600} of strain was 0.1.

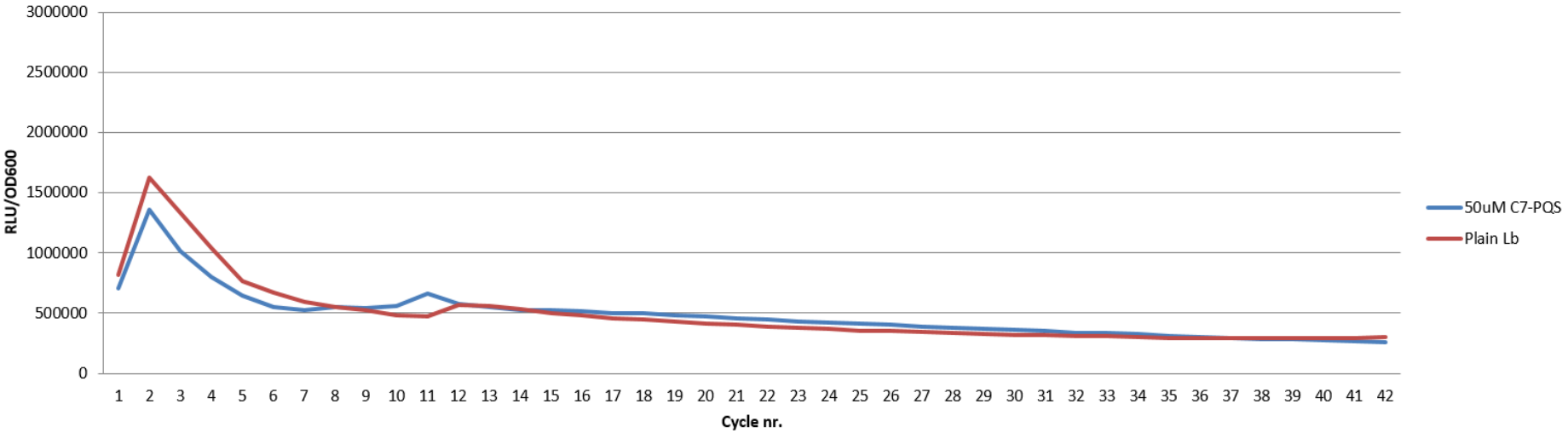


Figure 4.17. - Bioluminescence production in *E. coli S17-λ1pir* pUC18R6K miniTn7T::pIL008 (P_{pqsA}-*luxCDABE*, *lacI*^{Q}, *Em7-pqsR*). The tested strain was exposed to 50 µM C7-PQS. Bioluminescence was read every 30 minutes (cycle) for a period of 24 hours. Initial OD_{600} of strain was 0.1.

With the applied strategies unable to generate bioluminescence in alkyl quinolone-stimulated *E. coli* biosensors, the presumption that an important regulator being absent from the host system gains strength. The scrutiny to the different genetic elements of a PA functional biosensor indicates functioning of the P_{pqsA} and *PqsR* elements that become inactive in *E. coli*. Future work on this project points towards the screening of a PA genomic bank to identify any indispensable missing regulator(s) that switch(es) on the system in *E. coli*.

4.4. Discussion

In the context of semi-quantitative/qualitative sensing and reporting of QSSMs, biosensors have emerged as extremely versatile biological tools. These can be applied in assessing bacterial moieties for the presence of signalling molecules specific to either or both the AHL and the AQ systems in PA. They represent immediate advantages in contrast to the lengthy and expensive chromatographic procedures that are used in assaying bacterial culture supernatants. And considering that the AQ-associated QS system is still a fairly understudied target in the quest for AQ-based virulence attenuators, the sensing of its cognate molecules represent a primary point of focus for future nosocomial-preventive therapeutics.

Although AQ-sensing biosensors have already been constructed, these have been essentially based on PA (350) (310), (351), an organism that is not amenable to the development of biosensors to be used in clinical environments due to its potential pathogenicity. Consequently, *E. coli* was chosen for the development of a following generation of biosensors as it presented two basic yet crucial advantages: 1) non-interference with the system, and 2) no associated pathogenicity.

Overall, the AQ reporter system was designed to be specific, sensitive and robust. The bioluminescent reporter produced was based upon the system that is well proven in PA (310) (191) (145) (351) and its transplant into *E. coli* was not expected to present any major difficulties. However, despite all efforts, it unexpectedly resulted in silence in the heterologous host *E. coli* (Table 4.1, figures 4.16 and 4.17) while the same construct exhibited the expected behaviour when introduced into PA. Reasons for this discrepancy were extensively researched and possible explanations are explored below.

In general terms, the *E. coli* strain carrying the biosensor system integrated in the chromosome (strain ECIL02) can not be said to have responded specifically and in a direct relationship to the internal PQS levels when in *E. coli* (Table 4.1). Basic stimulatory elements, like for example an overinduction of the inducible promoter with an excess of IPTG (1 mM) and the replacing of the inducible promoter (*Ptac*) for a constitutive one (*Em7*), showed that the absence of light in the biosensor system was likely to derive from the absence of a regulatory effector other than PqsR, rather than a consequence of insensitivity. The testing of other AQs produced by PA (HHQ and C_7-HHQ-N-oxide) to which the reporter strain was exposed, were incapable of inducing the biosensor at wide ranges of concentrations (data not shown). Further sequence verification of the functional elements of the biosensor did not reveal any unexpected mutation in the chromosomally-inserted reporter. The part of ECIL02 chromosomal DNA comprising a region that included the inserted construct was amplified by PCR and sequenced, revealing genetic completeness (concerning fusions) and a total absence of SNPs. The fact that no point mutations were observed prompted the subsequent postulation of possible missing regulatory elements present in PA and absent in *E. coli*. The role of these elements, likely to be absent from the biosensor construct, but suspected to be an integral part of the regulatory pathways in virulence-associated phenotypes in PA, was evaluated by means of chromosomal integration of the biosensor in PA single and double mutants.

Introduction of the biosensor construct into a double PA *pqsA*/*pqsR* deletion mutant successfully resulted in light production when exposed to micromolar levels of exogenous PQS, confirming that no functional element embedded in the core construct could be deficient (figure 4.11). Additionally, strains singly devoid of the *lasR* and *rhlR* genes encoding AHL-related QS regulators reported strong light production when exposed to micromolar concentrations of exogenous PQS, in a way that aligns with the expected hierarchical dominance of *lasR* over *rhlR* and the *pqsA* promoter. Finally, *pqsH* and *pqsE* mutants carrying the biosensor were assessed and yet again resulted in strong bioluminescence activity to levels comparable to that of the parental strain PAO1 (Table 4.1).

The results obtained failed to explain the nature of this silent biosensor in *E. coli*, for all checked possibilities of a defective biosensor were discarded by the evidences collected. Nevertheless, Cugini *et al* (2007) (191) reported the development of a heterologous *E. coli* strain carrying the plasmid construct pEAL08-2, a similar type of AQ reporter construct but with two main differences: (a) the pEAL08-2 plasmid uses a metabolically inert reporter (*lacZ*) rather than a bioluminescence reporter (*luxCDABE*) that is heavy on metabolism, and (b) in this case the reporter construct is present in many copies on a plasmid in the cells as opposed to integrated in single copy in the chromosome. In plasmid pEAL08-2, *pqsR* expression is driven by the *tac* promoter as well, whereas the *pqsA* promoter is responsible for driving the β-galactosidase (*lacZ*) reporter gene expression (191). This reporter has been found by different authors as being fully functional in *E. coli* (308) (303) (351). Subsequent work carried out in our laboratory by Dr. Miguel Cocotl Yañez revealed that the *pqsA-lux* reporter constructed in this study exhibited bi-modal phenotypic activity when inserted into the chromosome of *E. coli* DH5α (Cocotl Yañez 2015, report). Although the reasons for obtaining different phenotypes from this same genetic construct are currently unknown and under investigation, this may explain its lack of responsiveness to AQs in *E. coli*.

Altogether, these findings initially lead to a number of hypotheses attempting to explain the deficient activity of the constructed reporter in *E. coli* compared to its successful functioning when in PA:

1) Missing regulatory elements, either occurring within the 500 bp region upstream to the *pqsA* promoter or part of the PA genome, but naturally absent from *E. coli*. The former is likely to potentiate promoter expression and the latter is likely to participate in the production of transcription factors whose absence leads to an impotent *pqsA* promoter.
2) Sick DH5α recipient (as in having accumulated structural alterations), since this lab strain is such a heavily modified organism that cannot be considered a wild-type *per se*, anymore.
3) An unpredicted *sdiA* binding effect as the element *sdiA* binds to *lux* boxes with definite PqsR binding consequences.

When comparing the PQS-based biosensor developed in this research project with a similar one developed by Cugini *et al* (2007) (191), two fundamental differences emerge: 1) the actual reporting approach and 2) the constituency of the 500 bp region upstream the *pqsA* promoter. In relation to the first fundamental difference and contrarily to the bioluminescence operon (*luxCDABE*) the authors made use of a non-metabolic, enzymatic reporter. However, this can be considered a mere option that on its own provides a different reporting method, therefore not offering a satisfactory explanation for an inactive construct. In regards to the second point, the authors placed in front of the reporter gene (*lacZ*) not only the 500 bp of the promoter fragment (500 bp upstream the ATG of the *pqsA* gene), but also the first 99 bp of the *pqsA* open reading frame itself. These additional 99 bp comprise part of the actual *pqsA* gene that is likely to enhance the strength of expression of the *pqsA* promoter. The missing fragment is believed to potentiate the expression of the gene promoter that will respond strongly to the binding of the PQS-PqsR complex. Consequently, it is supposed that this absence results in practically

basal levels of light production in the ECIL02 strain, whereas the levels accomplished by using the additional 99 bp of the *pqsA* gene in the *lacZ* reporter are much stronger (higher β-galactosidase expression).

In fact, Muller *et al* (2013) (351) successfully used this very same *lacZ* reporter construct in the sensing of HHQ and PQS, establishing it in *Pseudomonas putida* KT2440. The authors showed that the bioreporter responded to both quinolone molecules in the concentration range of 0.1 to 10 µM (HHQ) and 0.01 to 5 µM (PQS). Their engineering protocol used a smaller *pqsA* fragment of 440 bp (nucleotides -245 to +195 relative to the transcriptional start) amplified by PCR from genomic DNA of PAO1. The fragment was cloned into the promoter probe vector pPR9TT containing a 5'-truncated '*lacZ* gene. The '*lacZ* gene was fused to the *pqsA* promoter and the first codons of *pqsA* in the region corresponding to the transcription initiation site, and located 71 bp upstream to the *pqsA* start codon (168). This region is related to a LysR box that is placed at −45 bp and plays a central role in the transcriptional activation by PqsR and PQS (162) (Xiao et al. 2006b).

In conclusion and ideally, for obtaining a fully functional translational fusion in *E. coli*, the bioreporter developed may need to account for partial genomic locus of the *pqsA* gene, inserted upstream the promoter of the gene of interest, preferably at a site that does not disrupt protein function or topology. But even though the absence of the aforementioned 99 bp might function as a determinant that hypothetically results in a much weaker binding to the *pqsA* promoter, rendering it incapable of activating the expression of the reporter gene; yet another additional possibility shall not be discarded, i.e., that there is a protein in PA (either a transcription factor or a protein) inherently absent from *E. coli*. In that case, such *E. coli*-absent regulatory protein is naturally present in PA, hence whenever the bioreporter is integrated in elected PA mutants always resulted in a light productive reporting, and specifically and quantitatively responsive to the presence of AQs.

Even though intrinsic genomic differences may be responsible for the lacking of a crucial regulatory element, the successful expression of exogenous proteins in *E. coli* might not be immediately derived from genomic incapacity of the recipient strain. It could also be related to a recurrent problem in the expression of pseudomonad-derived genes that do not express properly in an *E. coli* background. This has been suggested by Allen (1989) (352) for there is evidence indicating that some Pseudomonas genes may possess different promoter sequences that are not recognised by *E. coli* RNA polymerase. In analysing the barrier to expression of Pseudomonas genes in *E. coli*, the author considers that even though a wide range of other underlying explanations can be stated, linked to differing transcriptional/translational machinery amid the two species, the most reliable piece of evidence relates to promoter signals in Pseudomonas. More specifically pinpointing the issue as deriving from different nucleotide sequences, mRNA start points, as well as the associated levels of mRNA production.

Some promoters in *E. coli* can actually display activity higher than the *E. coli* consensus (353) (354) (355), thus indicating that promoter recognition by RNA polymerase is likely to be just one of the overall determinants of promoter activity. *Pseudomonas* promoter sequences show that some of the species genes have *E. coli*-like or NIF-like promoters (356), whereas other genes have no homology whatsoever to these. PA genes with no homology to the *E. coli*-like promoters are usually weakly expressed in *E. coli* suggesting that there is a possibility that *Pseudomonas*-specific promoter sequences are apparently recognised by an alternative RNA polymerase holoenzyme (357) (358) (359). House-keeping genes are known to be expressed at significantly strong levels during the development of organisms, and the *Pseudomonas* "house-keeping" genes have a promoter specificity that is prepared for optimal expression in *Pseudomonas*, and not *E. coli*. Overall, what is here suggested as yet another possibility for a silent bioreporter, is the possible existence of a blockade to expression at the recognition level of *Pseudomonas* promoter signal in *E. coli*, something that might occur at least for some genes. This problem may not be

observed in *E. coli* if and when the promoter is in multiple copies on a plasmid, but may naturally appear when in single copy in the chromosome. Moreover, *E. coli* may naturally have different *pqsR* expression levels and/or quinolone uptaking rates, as well as and different efflux pumping mechanisms than Pseudomonads.

Additionally, Martinez-Antonio *et al* (2008) (360) conducted a structural analysis of the regulatory network of *E. coli* to find out that the mode of regulatory interaction between transcription factors (positive) is actually contrary to their autoregulation (negative). In addition, there are coherent and incoherent feedforward loops in this species like in any other living organisms. Thus, the presence of coexisting multiple bacterial phenotypes in *E. coli* is likely to be potentiated by long transcriptional cascades attached to regulatory shifts that happen differentially with the *pqsA* promoter and with respect to PA. The authors observed that in *E. coli* transcription factors that play a role in the end of transcriptional cascades are usually part of a two-component systems. Cell homeostasy is maintained through multiple regulatory cascades where transcription factors are usually self-repressed, but regulation within the network is maintained by sequential activation of both transcription factors and by multi-element circuits present at the core of the regulatory network. Downstream of the hierarchical network, two-component systems can memorise transient external signals through auto-activation loops, thus acting as molecular switches that allow the coexistence of alternative phenotypes, as observed by Cocotl Yañez in his report.

It is thus quite unlikely that the defect causing a silent reporter in *E. coli* is associated to a genetic problem of spontaneous mutations, or even due to the fact that the DH5α strain used for producing ECIL02 is actually a cloning strain, and not an expression host. In addition, it is important to take into account that the silent reporter in *E. coli* may be due to the fact that the fragment used for the *pqsA* promoter is unnecessarily extensive at the 3' end. Consequently, the additional part used might be producing post-transcriptional

artifacts with consequent destabilisation of the mRNA, leading to unsuccessful expression of the *luxCDABE* operon in *E. coli* (but not in PA). Destabilisation of the mRNA is indeed explored by Brouwer *et al* (2014) (169) as an important artifact based on findings showing that PqsR is not only regulated by the *las* and the *rhl* system, but also by the small RNA PhrS, an activator of the PqsR biosynthesis (177). Brouwer *et al* analysed His-tagged *pqsA*, studied the PqsA production *in vivo* and unravelled the presence of a secondary structure within the RhlR-induced long *pqsA* transcript that may control *pqsA* translation. The *pqsA* transcription was under the regulatory control of a *lac* promoter in a fashion dependent on the accessibility to the native SD sequence.

Similarly, Dötsch *et al* (2012) (172) have recently reported the presence of an alternative transcriptional start site (*pqsA* -339) located downstream of the RhlR-binding site, that points towards a posttranscriptional repression of PqsA by RhlR (at the RNA level between transcription and translation of the gene). The typical way posttranscriptional repression takes place in prokaryotes is through the binding of small regulatory RNAs aiming at mRNA molecules or even through the production of altered mRNA with secondary structures, and these play a pivotal role in the posttranscriptional regulation process in prokaryotes (174) (361). This conformational disguising of the translation initiation site of the *pqsABCDE* transcript, results in poorer PQS biosynthesis and delay association of the 30S ribosomal subunit with the mRNA, thus obstructing translation initiation. This alternative transcriptional start site (*pqsA* -339) of the *pqsABCDE* operon offers yet another regulatory point directly interfering with transcription of the PQS system.

Finally, with regards to the presence of bi-modal phenotypic activity, generated as the result of chromosomally integrating the bioreporter in *E. coli* DH5α, Martinez-Antonio *et al* (2008) (360) describes rather interesting findings. These concern transcriptional factors that induce alternative transcripts with strong effects on cell signaling-dependent phenotypes in *E. coli*. Once again the lack of approximately 99 bp upstream the *pqsA* promoter

might explain why gene expression did not respond to xenobiotic conditions tested when presenting ECIL02 to a range of AQs. As suggested by the authors, such response would be triggered either by the binding of transcription factors at specific points in the genome or by recognition of an appropriate effector protein. In some cases, the referred actions occur by means of two interacting proteins, as in the two-component systems of gram-negative bacteria, responding to external signals. What we also observed and has been extensively reported is that these can result in numerous phenotypes with wide metabolic and replicative heterogeneity (362) (363) (364), otherwise bacteria would not adapt to a panoply of different niches and condictions.

This interpreting of xenobiotic signals result in phenotypic alterations. These are linked to differing physiological capacities and may generate persister functionalities, e.g. more resistance to antimicrobial drugs. This is particularly true for biofilms and their associated multiple phenotypes for different Gram-negative bacteria (365) (366) (367) (368) (369).

It is also observed that usually those transcription factors that play an important role at the end of regulatory cascades in *E. coli* belong to two-component systems. This suggests that the equilibrium within the cellular moiety is kept by means of several regulatory cascades where transcription factors are usually autorepressed. But more importantly, such occurs whilst regulatory memory within the network is conserved by successive activations of these same transcription factors, and by a circuitry composed of multiple agents present at the centre of the network. Knowing that two-component systems are capable of recording temporary external signalling by means of autoactivation loops, these systems can behave as switches, i.e., chemical adjusters that act downstream the regulatory network will allow the coexistence of bi-modal phenotypes, as observed in this study. And has shown by Isalan *et al* (2008) (370) *E. coli* is versatile an organism to accommodate such interactions between upstream and downstream transcription factors and

effector proteins in the network hierarchy, without morphological disadvantages or compromising to their survival.

Chapter 5

5.1. Optimisation of liquid extraction surface analysis (LESA) as a new methodology for rapid screening of quorum sensing molecules in *ex vivo* PA bacterial extracts

5.1.1. Abstract

A new ambient mass spectrometry methodology was successfully developed and optimised allowing reliable screening of PA QS molecules at concentrations in the range of 15 nM to 10 µM in microliter sample volumes. The method is based on micro-liquid extractions from a solid surface with nano-electrospray mass spectrometry used for quantification of target molecules. Results obtained with analysis of bacterial overnight extracts suggest that adequate LESA-MS (liquid extraction surface analysis - mass spectrometry) extraction efficiency is attainable dependent on the organic:aqueous ratio of the extraction solvents, the physical/chemical identity of the sampling surface material, the nature of the sampling solution and the accessibility to molecular ionisation of the analytes.

Data obtained suggested the hydrophobic interactions established between substrate surface ultimately improve desorption and consequently ionisation rates of the analytes of interest. MS spectra produced have enhanced quality when the analytes of interest are ressuspended in less 'salty' media even if these are of a more complex composition, suggesting that protonation and sodiating interfere directly in the quality of the chromatograms. Considering additional pre-air space and a reading delay,

alongside reextracting from previously analysed sample spots, could help deliver improved spectra.

5.2. Introduction

5.2.1. Clinical and economic consequences of hospital-acquired PA infections

In terms of hospital acquired infections, PA is the most frequent Gram-negative pathogen associated with infections gained in healthcare premises all over the world. It is the number one causative agent of pneumonia in the United States where it is commonly implicated in detected nosocomial urinary tract and bloodstream infections (371) (372). In a 1995 point prevalence study (analysing a number of persons with disease in a time interval divided by number of persons in the population) conducted in Western European intensive care units (ICUs), PA was amongst the commonest organisms found and comprised almost a third (29%) of all Gram-negative isolates, being present in 17% of all positive cultures (12). More recently, PA has been included in the 'ESKAPE' (***E****nterococcus faecium*, ***S****taphylococcus aureus*, ***K****lebsiella pneumoniae*, ***A****cinetobacter*, ***P****seudomonas aeruginosa* and ***E****nterobacter*) list of pathogens posing the greatest public health threat by the Infectious Disease Society of America (373). Due to its increasing prevalence and low cell wall permeability intake, which together enhance its ability to acquire and express multiple resistance mechanisms (e.g., beta barrel protein deletion, overexpressing efflux pumps, etc.).

Despite data from the late 90s reporting a decline in β-lactam and aminoglycoside-resistant PA isolates in Europe, imipenem-resistant isolates in Canada and meropenem in Latin America (374), in the US the rates of multidrug resistance strains (resistant to over three of the following drugs: ceftazidime,

ciprofloxacin, tobramycin, and imipenem) did see a 10% increase from 1993 to 2002 (375). For instance, the latest numbers point towards a decrease in fluoroquinolone resistance in PA observed in countries of the European Economic Area (EEA) (376), whilst suggesting that carbapenem resistance in this same region is still a common feature. In fact, yearly in Europe around 400,000 patients with nosocomial infections are contaminated with an antimicrobial drug resistant strain and from these an estimated 25,000 patients die in consequence of that very same contagion (377). An immediate concern that arises from the very low number of treatment options in regards to the high prevalence of resistant strains is that inevitably a late diagnostic leads to inappropriate practical therapies (378), and this impacts economically as well as logistically on the national health services worldwide.

ICU-acquired infections are common and have been linked to resistant strains of microbiological isolates (379). Among the commonest pathogens found after ICU surveillance PA is the most predominant (12.4%), followed by *S. aureus* (12.3%), coagulase-negative *staphylococci* (10-2%), *Candida* spp. (10.1%), *Enterobacter* spp. and *enterococci* (with 8.6% each) (380). More recently, a 2012 study by Blackburn *et al* (2012) (381) on hospital-acquired bloodstream infections (HA-BSI), pointed towards high rates of multiple drug resistant PA (52%) in a paediatric setting.

Antimicrobial drug resistant agents and their growing prevalence is worrying, particularly PA resistant to broad spectra intravenous β-lactam antibiotics like Imipenem, a strong inhibitor of β-lactamases from Gram-negative bacteria resistant to most β-lactam antibiotics. Thus, a rapid detection of PA in the early stages of infection is the most desired preventive approach. An active cooperation merging the best knowledge of modern microbiological laboratory procedures alongside the most modern biochemical screening technologies represents an important synergy which could potentially improve the infection detection and control process.

Thus, the starting point for this method development optimisation was the need to tackle a time and specificity limitation associated to the traditional clinical/laboratory screening of putatively-infected samples. These time and handling limitations can only be overcome if a robust (rapid, accurate and specific) protocol, one that returns reproducible data, can be put in practice, thus avoiding the severe onset of an emerging infection even at its very initial detectable stages.

5.2.2. Traditional PA qualitative and quantitative detection methods

Traditionally, as recommended by the European Pharmacopoeia, the qualitative determination of the presence of PA in clinical samples is based on the microbiological examination of non-sterile products in selective broth media, homogenised and incubated at 35°C to 37°C for a time sufficient to revive the bacteria, but not enough to promote further development of the organisms (usually in between 2 to 5 hours), transfer to enriched media for incubation at 35°C to 37°C for 18h to 48h and subsequent culturing on plates of agar medium with incubation at 35°C to 37°C for 18h to 24h (382). The quantitative evaluation operates with inoculates in suitable quantities of enrichment broth in serial dilutions from 0.1 g to 0.001 g (or ml) of the product under examination, incubation at 35°C to 37°C for 24 to 48h, subculturing of the different cultures on plates of agar medium to obtain respective selective isolation, and consequently incubation at 35°C to 37°C for 18h to 24h (382). The growth of adequately established colonies of Gram-negative bacteria, generally of a reddish colour, constitutes a positive result.

This procedure comes with several limitations, namely the fact that sub-lethally injured organisms (relevant for the quality of the product) are not detected, and a fastidious handling protocol (from clinical sampling to final quantification) that involves a minimum of four days for analytical completion.

The classic bacterial biosensors mentioned in results chapters 4 are not at all prepared for simultaneous delivery of rapid detection and reliable quantification in a hospital setting. A limited number of techniques have been applied with varying rates of success, individually or as part of integrated protocols, in detecting the presence of QS-related molecules, for example thin layer chromatography (157), bacterial AHL biosensors (383), combined methodologies in high-throughput cell-based assays (384) and LC-MS/MS (liquid chromatography – mass spectrometry) methods (292, 385). But the increasing demand for simpler accessible tools with faster diagnostic output shapes the future of new methodologies to be developed in order to overcome these limitations.

Even with recent novel approaches, chromatographic procedures have been the main technique opted for when it comes to quantifying the different signalling molecules in PA QS, (386) (387). This is possibly due to the fact that high performance thin layer chromatography being more sensitive than biosensor-based methods. Even though chromatography-based techniques are the most applied in regards to molecular screening for detection and quantification of QS molecules, new screening methodologies, like liquid extraction surface analysis (LESA), are now emerging as future techniques with clear advantages, once optimised.

This chip-based electrospray technique has been recently explored in research broadly varying in target sample, for example, research involving drug distribution and metabolism analysis (388), analysis of food surfaces (389), surface analysis of lipids (390), analysis of proteins from biological substrates (391) and identification of skeletal muscle proteins (392).

5.2.3. LESA as a novel methodology for profiling PA QS-related molecules

LESA is the newest technological approach for the TriVersa NanoMate consisting of an automated chip-based nanoelectrospray infusion (nanoES) source for mass spectrometry, a new screening technique that combines micro-liquid extraction from a solid surface along with nano-electrospray mass spectrometry (388) (393) (394) (395). One of its many potential applications is the examination of the presence of target molecules, as well as their distribution, by means of analysing the surface of *ex-vivo* sample extracts without need for lengthy sampling preparation and time consuming analysis, an area where LC–MS/MS is traditionally employed.

The technique has been recently explored in a vast range of differing scientific approaches for generating successful molecular profiles. The nature of the approaches in which LESA has been applied show its versatile applicability in the direct analysis of chloroquine and metabolites from whole-body animal tissue (396), intact proteins from *E. coli* colonies (397), healthy and unhealthy human liver tissue (398), noncovalent protein complexes from dried substrates (399), intact proteins from biological substrates (391), just to name a few.

Immediate advantages presented by this technique are speed and simplicity, longer and more stable Electrospray ionisation mass-spectrometry (ESI), higher sensitivity with lower detection limits than other surface analysis techniques. With LESA (figure 5.1) it is possible to analyse directly from surfaces with extractable analytes, like for example, thin tissue sections, planar separation media (e.g., thin layer chromatography plates), dried blood spots on paper, Matrix Assisted Laser Desorption/Ionization (MALDI) plates for complementary information by ESI, and compatibility with the majority of mass spectrometers.

5.2.4. LESA-MS technology and equipment

Chip-based infusion The TriVersa NanoMate system uses the ESI Chip® (figure 5.2), a silicon-based integrated nanoelectrospray microchip device to where the extracted sample is sprayed for fragmentation after infusion.

LC/MS fraction collection/infusion – This is the component where the previously voltage-fragmented sample (effluent) will be collected for further analysis. The effluent is divided (split) post column where part is directed to a conventional LC/MS interface (with optional tandem MS) whereas the rest of the split effluent is collected at time segments into a multi-well plate.

LESA® - The liquid extraction surface analysis ultimately integrates the previously mentioned elements into a sequential analytical system. This starts with the samples being solvent-infused and collected from a variety of solid surfaces (figure 5.3) such as microtiter slides (figure 5.4), by means of desorption electrospray ionization (DESI). The infused samples are subsequently aimed at the automated chip-based nanoelectrospray (figure 5.2) for electrical fragmentation and finally analysed by means of mass spectrometry in conjunction with the TriVersa NanoMate system.

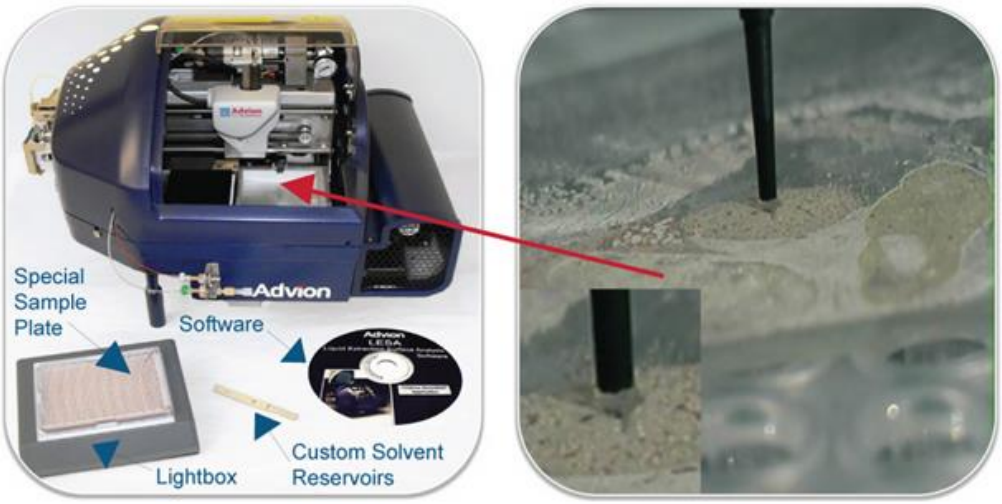


Figure 5.1. Composing parts of the Advion Mode 3 LESA® Triversa NanoMate bioanalyser. Left) LESA kit composed of software, solvent reservoirs, sample plate, lightbox and the complex TriVersa NanoMate. Right) An example of spot extracting in a tissue surface sampling.

Source: (400).

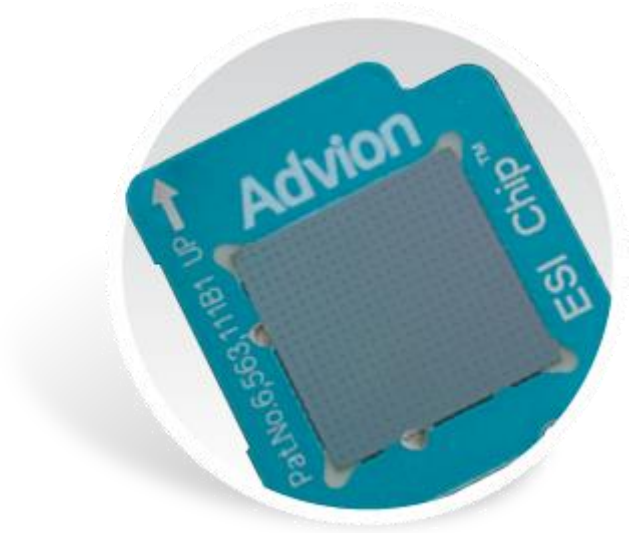


Figure 5.2. Advion Electrospray Injection Mode 1. ESI™ silicon-based integrated nanoelectrospray microchip device consisting of an array of 400 nanoelectrospray emitters with different inner diameters allowing for flow rates of 20 to 300 nL/min.
Source: (401).



Figure 5.3. Injection tips, sampling plate and culture slide. Advion Triversa Nanomate® mechanical sampling head with black tips for injection/infusion.
Source: (402)

5.2.5. Research objective

The lack of rapid screening methods for PA QS-related molecules obtained from clinical samples (sputum, plasma, urine, etc) has been thoroughly explored in the introduction of this thesis. A simple, cheap, straightforward and immediate methodology like the LESA-MS can potentially lead to improved analytical results of the aforementioned biological samples. In this scenario a novel methodology that is designed to offer a reliable detection as well as a rapid one, has in Liquid Extraction Surface Analysis Mass Spectrometry (LESA-MS) of bacterial extracts, a prolific opportunity to perfect the clinical response therapies in putatively infected patients.

Hence, the main objective of this research chapter was to adapt and optimise the LESA-MS methodology to the detecting and screening of five pre-defined PA QS-related molecules: *N*-butyryl-L-homoserine lactone (C_4-HSL), 2-heptyl-4-quinolone (C_7-HHQ), 4-hydroxy-2-heptylquinoline *N*-oxide (C_7-*N*-Oxide), C_7-PQS and *N*-(3-oxododecanoyl)-L-homoserine lactone. The analysis was performed on crude bacterial extracts obtained from two PA strains differing in virulence potential (PA14 and PAO1) and a few of their QS-related mutants.

5.3. Results and Discussion

The optimisation procedure developed in this research study covered three operational parts integrated in one system: (1) Chip-based infusion, (2) LESA-MS and (3) Accessories. After adequate optimisation of the referred parts, the system was used to scrutinise levels of QS molecules in PA mutants and wild-type strains listed in section 5.3.4. Results obtained with the LESA-MS bacterial scrutiny were then qualitatively compared with what is traditionally observed by LC-MS/MS and accepted in the specialised literature. An

approximation of the data acquired by means of an optimised LESA-MS methodology to the widely accepted LC-MS, reinforces the method reliability for validating its application in further researches.

It is important to mention that because LESA-MS analysis of bacterial smears has not been done before; there were no preparatory protocols available. However, guidance in regards to the different types of spray solvent and the correct settings for the mass spectrometer, as well as stage optimisation process and referred acquired results are described along the chapter. All calculations were performed in agreement to standard formulae established in Alankar (2011) (403).

5.3.1. Solvent and sampling mixture optimisation

To assess the different solvent mixtures prepared, calibration curves of standards were initially tested by means of infusion and later tried with LESA-MS. After a series of trials, the best calibration curve of standards obtained was the one using a solvent combination mixture of 75% methanol (with 0.1% formic acid) and 25% water, extracting from samples constituted by 80% LB and 20% methanol (figure 5.4). This new solvent composition allowed signal improvement for its associated replicates had more approximate values (Table 5.1), an effect strongly observed from 10 µM onward. The sample composition of 80:20 LB:Methanol (%:%) offered a much better performance in contrast to the previous results obtained with several other different sampling mixture compositions, especially the second best sampling solution entirely made of pure methanol (figure 5.5).

Table 5.1. Average MS response (NL counts) of QS molecules produced at two different solvent mixtures. Grey rows) Sample solvent composition comprised of 80% LB medium and 20% methanol. White rows) Sample solvent composition comprised of 100% methanol. Signal values were obtained by mass spec after collection of infusion samples from a 96-well plate. A range of seven concentrations was used for both scenarios differing only for the top concentration. Red bold values indicate the higher standard deviation in comparison. Values in brackets represent standard deviation values of six replicates.

[QS molecule] µM	C_4-HSL	HHQ	HQNO	C_7-PQS	3-OXO-C_{12}-HSL
Blank	**16 [5.7]**	40 [13.8]	24 [22.1]	**116 [36.8]**	**19 [6.2]**
Blank	3 [4.2	**57 [19.2]**	25 [22.1]	158 [33.4]	19 [5.7]
0.001	7.2 [3.5]	27 [12.7]	55 [28.6]	**80 [36.0]**	**80 [27.9]**
0.001	**3 [5.2]**	**53 [25.0]**	**51 [48.6]**	136 [20.9]	15 [3.1]
0.01	7 [2.7]	17 [13.1]	29 [18.3]	44 [27.5]	57 [33.6]
0.01	**4 [7.6]**	**1939 [2335.2]**	**5062 [6086.6]**	**2471 [4073.7]**	**167 [215.8]**
0.1	3 [4.1]	44 [36.5]	71 [58.6]	**61 [74.8]**	**27 [22.8]**
0.1	**4 [5.6]**	**205 [53.8]**	**404 [91.5]**	305 [54.8]	38 [9.3]
1	7 [3.1]	1285 [314.6]	2945 [814.3]	1820 [922.5]	108 [38.1]
1	**5 [5.9]**	**13729 [2053.5]**	**41799 [5225.2]**	**22614 [3720.2]**	**546 [59.8]**
10	10 [3.9]	12327 [1322.6]	30961 [7822]	21680 [4696.4]	232 [50.8]
10	**4 [4.9]**	**75644 [12509.7]**	**230435 [36648.5]**	**173661 [30251.0]**	**5125 [662.4]**
80	61 [43.9]	209315 [39222.4]	498610 [108987.7]	449111 [78854.1]	1552 [277.2]
100	**143 [216.7]**	**701045 [57252.5]**	**2257987 [154775.7]**	**1962403 [155770.6]**	**59462 [28369.9]**

The successful mixture composition allowed picking up a rather steady workable linear signal of the 3-oxo-C_{12}-HSL element down to a concentration of around 335.5 nM. Both C_4-HSL and 3-oxo-C_{12}-HSL were difficult to detect. Analytically speaking, the system sensitivity increases as expected at the higher concentrations and detection of both C_4-HSL and 3-oxo-C_{12}-HSL was observed from the 10 µM concentration thresholds. In addition, the differences registered by using a fully organic solvent or LB broth with 20% (V/V) of

methanol in it is nearly irrelevant for most, if not all, the compounds tested. The LOD and LOQ results obtained (Table 5.2) showed that a direct analysis of QS molecules present in overnight extracts can be very simply acquired just by adding methanol to the final test volume.

Table 5.2. Summary of standard mixture calibration curves and minimum limit of detection by means of LESA-MS. The curve was produced with a solvent effluent consisting on (A) Standard mixture calibration curve using a 100% methanol sample, (B) Standard mixture calibration curve using 80% LB plus 20% methanol sample. The solvent in the equipment was composed of 75% methanol + 25% water. The concentrations used were blank, 0.001 µM, 0.01 µM, 0.1 µM, 1 µM, 10 µM and 100 µM, but the maximum concentration tested on the bottom line was 80 µM rather than 100 µM. All values obtained from an average of six replicates.

	100% Methanol			80% LB 20% Methanol		
Compound	**Linear curve equation Y =**	**Linear curve R^2**	**LOD LOQ**	**Linear curve equation**	**Linear curve R^2**	**LOD LOQ**
C_4-HSL	Y = 1.405*X + 1.419	0.9907	11.1 µM 37 µM	Y = 0.6660*X + 7.217	0.9548	15.8 µM 52.6 µM
HHQ	Y = 6992*X + 2259	0.9999	10.7 nM 35.8 nM	Y = 2628*X - 2337	0.9957	14.8 nM 49.5 nM
HQNO	Y = 22537*X + 4530	0.9999	6.5 nM 21.7 nM	Y = 6259*X - 5368	0.9961	13.9 nM 46.3 nM
C_7-PQS	Y = 19633*X - 2812	0.9999	3.2 nM 10.7 nM	Y = 5643*X - 5887	0.9942	19.1 nM 63.8 nM
3-oxo-C_{12}-HSL	Y = 595.0*X - 104.9	0.9998	15.1 nM 50.4 nM	Y = 18.74*X + 52.57	0.9978	4.5 µM 14.9 µM

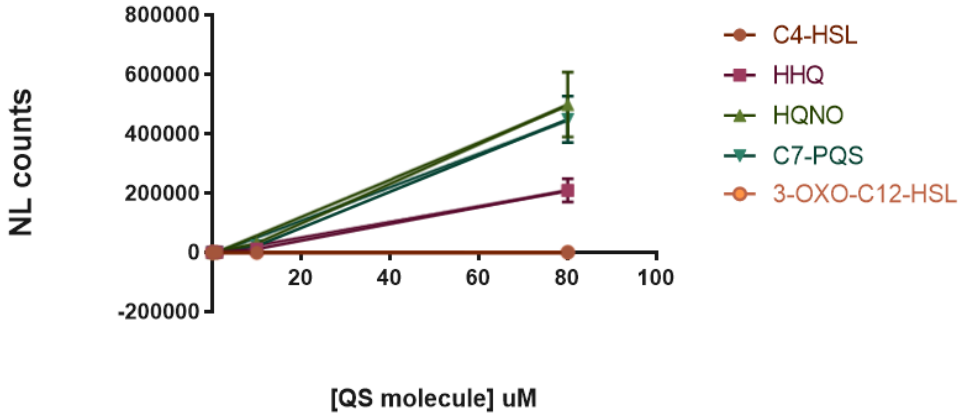


Figure 5.4. Standard mixture calibration curve using 80% LB plus 20% methanol sample. 1 µl of standards mixture (consisting of 80% LB medium and 20% methanol) was spotted onto each circular Prosolia cell slide spot. Results plotted correspond to an average of six replicates. The solvent in the equipment was composed of 75% methanol + 25% water. NL signal values were obtained by mass spec after collection of infusion samples from a 96-well plate. A range of seven concentrations (blank, 0.001 µM, 0.01 µM, 0.1 µM, 1 µM, 10 µM and 80 µM) was used for producing the calibration curve.

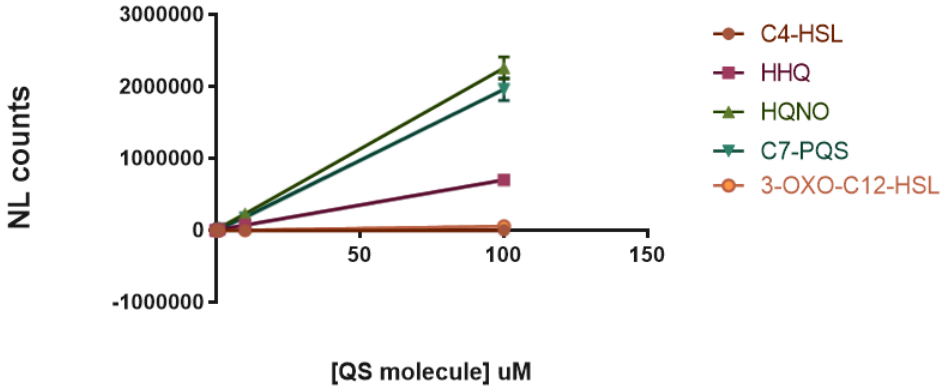


Figure 5.5. Standard mixture calibration curve using a 100% methanol sample. 1 µl of standards mixture (consisting of 100% methanol) was spotted onto each circular Prosolia cell slide spot. Results plotted correspond to an average of six replicates. The solvent in the equipment was composed of 75% methanol + 25% water. NL signal values were obtained by mass spec after collection of infusion samples from a 96-well plate. A range of seven concentrations (blank, 0.001 µM, 0.01 µM, 0.1 µM, 1 µM, 10 µM and 100 µM) was used for producing the calibration curve.

Regardless of improvements in the quality of signal output and approximation between replicates, it is clear from the results that the AHLs are

still molecules difficult to sense when using this methodology. But a clear conclusion from the improved effects suggested by the addition of methanol to the scrutinised samples also supports the idea that there is worth in working a balance between organic and aqueous phases in the samples. In addition, it is also necessary to assess how the organic:aqueous composition will impact on adherence to sampling slides differing in hydrophobic/hydrophilic properties.

5.3.2. Optimisation of aqueous and organic phases and substrate surface optimisation

Low aqueous-high organic (25%-75%) versus high aqueous-low organic (75%-25%) phases in the solvent mixture preparation were studied to improve extraction quality. Even though the high aqueous/low organic solvent mixture provides a slightly better detection of the chromatographic signal for most of the molecules studied (C_7-PQS, HHQ and HQNO), its counterpart, the low aqueous/high organic mixture improves on the signal picking up of the substances that throughout the study were the hardest to detect, i.e., C_4-HSL and 3-oxo-C_{12}-HSL (figure 5.6).

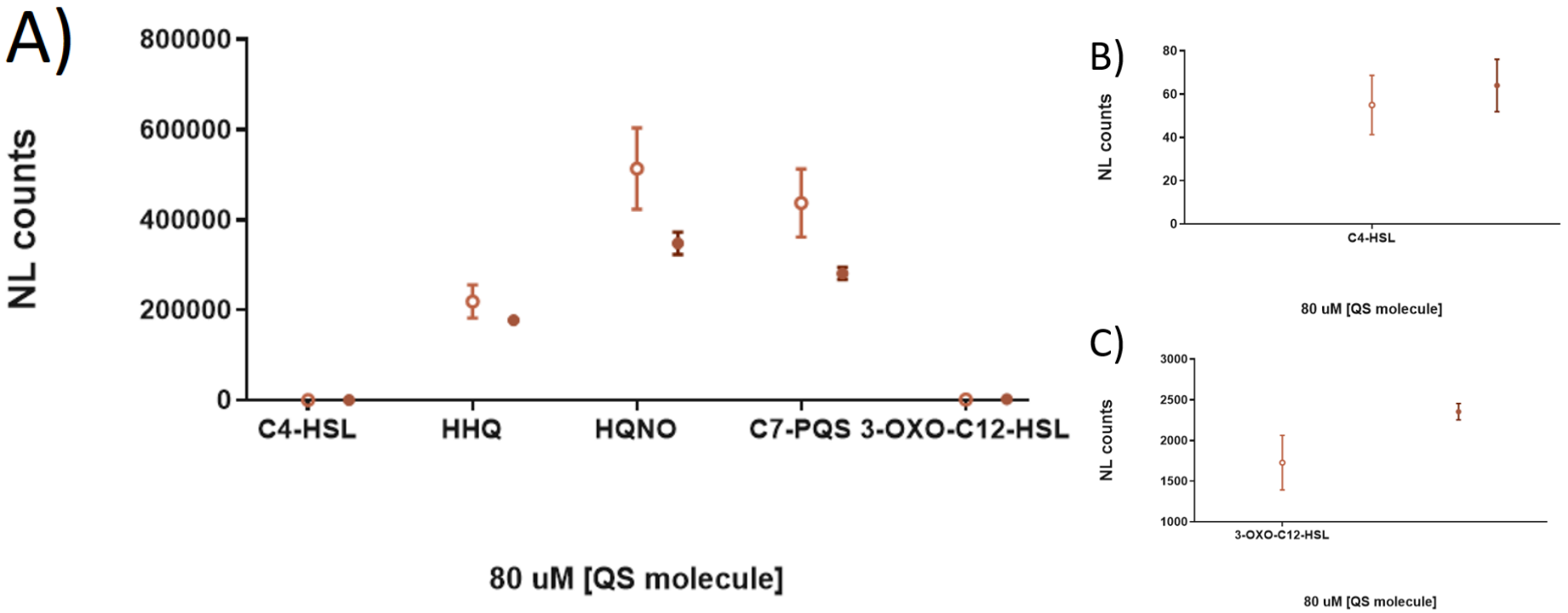


Figure 5.6. Effect of solvent composition in LESA extractions of a standard calibration mixture at a concentration of 80 µM. Open dots correspond to (75%-25%) high aqueous/low organic and closed dots correspond to (25%-75%) low aqueous/high organic phase. A) Overall results, B) Individualised C_4-HSL results, C) Individualised 3-oxo-C_{12}-HSL results. The extraction solvent in the equipment was composed of 75% methanol (0.1% formic acid) and 25% water. Extraction and analysis performed by LESA-MS from a PTFE substrate slide with an analysis time of 1 minute.

Based on the results obtained there isn't much difference in the outcome provided by the two analysed scenarios. Thus, opting for a 75/25 or a 25/75 aqueous:organic fraction is an option the analyst should take depending on the signal issues that concern AHLs C_4-HSL and 3-oxo-C_{12}-HSL. Nevertheless, improved extraction rates can be achieved by using solvent additives, such as substances that reduce surface tension of the liquids in which analytes are dissolved (404). Surfactants tend to be the best option as they help enhance the solubility of certain substrates by reducing the size of droplets and increasing their surface coverage. Other alternatives are at hand for improving detection of analytes by means of enhancing solubility in the initial droplet they are wrapped in, like for example, non-aqueous sprays. The advantages in using these sprays is that they reduce internal energy deposition, and if applied to ESI they are known to work much better in polar solvents (e.g., water, methanol, ethanol, formic acid, hydrogen fluoride, ammonia) rather than non-polar ones (benzene, toluene, hexane, pentane, octane, etc.).

In regards to the sampling surface material, two solid surfaces were available for sampling, Glass (hydrophilic) and PTFE (hydrophobic). The different adherence and extraction trials conducted allowed the understanding that ideally the hydrophobic surface of the Prosolia cell culture slide is the best option for sampling the overnight extract, due to forming a rigid droplet on the sampling surface. This is because the glass slide surface affects the quality of the extraction, registering peaks even in the absence of analytes in solution. Evidence is thus provided towards accepting that hydrophobic properties of the substrate matrix are relevant in the liquid film production. In fact, the importance of the solvent layer formation produced on the sampling surface has been observed in detail by Volny *et al* (2008) (405). The authors mention 'wettability' (also known as surface energy) as the crutial factor in the production of different surface tension values in a range of materials. The best surfaces for producing better behaved/controlled droplets are the super-hydrophobic materials where very high potentiate rigidity. Further than that, the electrical conductivity of the substrate itself is mentioned as playing an

important part in the process, mostly due to the fact that highly charged substrates will consequently produce secondary droplets with added electrical charges.

It is unequivocal that the layer of liquid produced on top of the sampling surface aids the extraction of the analyte. However, where one would very simply consider it as the only variable with strong implications in the removal of the substrate from the sampling surface, another very important factor is worth mentioning: playing with the organic/aqueous solvent ratio. This is considered by Green (2010) (406) as the most direct method for improving substrate solubility. The author suggests that it is commonly applied a solvent mixture ratio composed of 50−70% organic solvent (methanol or acetonitrile), and our best composition is just a little over the upper limit (75%). High organic solvent compositions directly affect the formation of small size, easier to collect and desolvate, less dispersive droplets. The opposite behaviour (e.g., more naturally spreadable droplets) is seen in those where the solvent is mainly aqueous. And finally considering other possible substrate sampling surfaces, Chipuk and Brodbelt (2008) (407) reported that for some solid surfaces of different electrostatic nature, such as paper, clothing fabrics, plastics and metallic surfaces, there is no significant loss of material when using desorption electrospray ionisation. Wiztorski *et al* (2016) (408) also showed that it is possible to generate a less dispersed droplet by reducing the amount of organic solvent used to extract the substrate, something that can be done by adding NH_4HCO_3, as suggested by the authors.

Like in any MS procedure, ion production can depend quite strongly on the molecular interactions (e.g., pyrolisis can have detrimental effects on heat-sensitive surfaces, etc.) and electrical charge-transfer established between samples and sampling surfaces. And even though the majority of the commonly used ambient ionisation methodologies that use solid surfaces are non-invasive, whenever droplets are used to dissolve the analytical matrix, typically some attrition/disarray is noticed. Hence, optimising the adherence of

sample matrix to the available substrate surface, for producing a stable analysable unspreaded droplet, is imperative. For example, acetonitrile, one of the default solvents in use in the system, is a polar aprotic solvent miscible with water but with slightly dispersive properties, hence causing unwanted smearing outwards of the sample on the hydrophilic slide side.

The basic principle of surface analysis states that any 'standard' sample, directly extracted from a sampling surface, has to produce quantifiable MS values, if in an aqueous solution that maintains rigidity on a hydrophobic surface. In conclusion, this section shows that LESA-MS extraction efficiency is to an extent dependent on the physical/chemical identity of the surface material. But surfaces can be altered to enhance droplet rigidity and better film consistency, nonetheless. For example, by producing a more hydrophobic structure that ultimately improves desorption, and consequently ionisation rates of the extracted analytes (409).

5.3.3. Growth media optimisation

Calibrants (Table 5.1) in LB and M9 growth media, from a mixture containing AQs and AHLs, were spotted onto the substrate surface and individually analysed using LESA-MS. The results obtained (figures 5.7 and 5.8) confirmed LB as the best of the two media after LESA-MS analysis due to the quality of the produced calibration curves (Table 5.3). All concentrations of QS molecules provided a good signal and the presence of the internal standards was detected for all molecules (in LB medium) but with poorer results for M9. For C_4-HSL and 3-oxo-C_{12}-HSL the LOD and LOQ levels responded differently when transiting from LB to M9, i.e., for C_4-HSL the levels increased approximately 27-fold in M9, but on the other hand for 3-oxo-C_{12}-HSL in M9 saw its value reduce approximately 5.7-fold. In addition, the best chromatograms produced were delivered by samples ressuspended in 80% LB medium with 20% methanol, indicating that the ionic complexity of the LB

medium was not the issue in producing a stable signal, as initially considered.

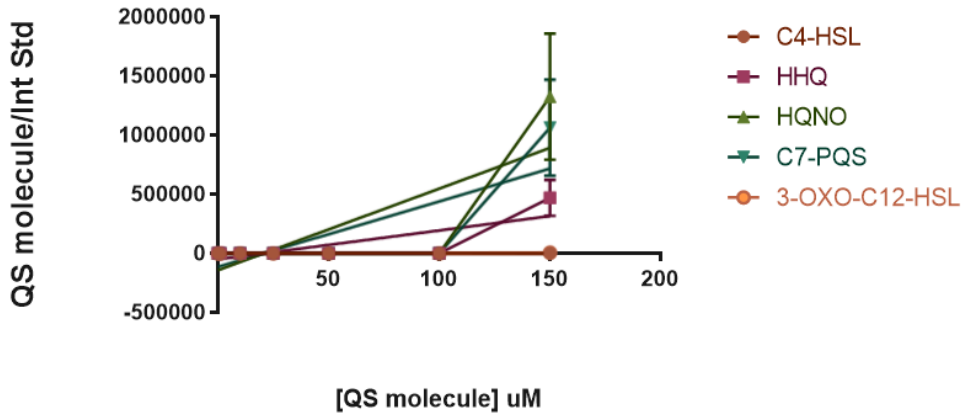


Figure 5.7. Standard mixture calibration curve in LB medium. 1 µl of standard mixture dissolved in LB medium was spotted onto each circular Prosolia cell slide spot. PQS-D_4 was used as internal standard. The extraction solvent in the equipment was composed of 75% methanol (0.1% formic acid) and 25% water. Results plotted correspond to an average of three replicates and an analysis time of 1 minute.

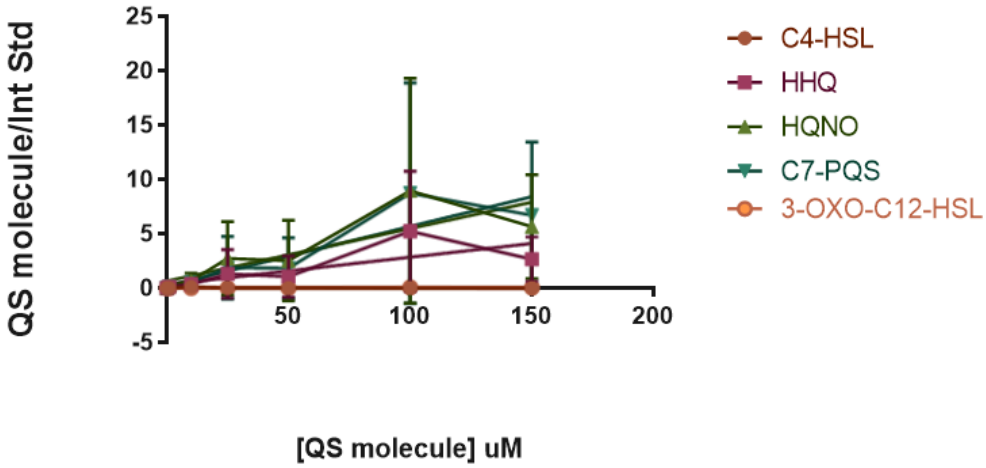


Figure 5.8. Standard mixture calibration curve in M9 medium. 1 µl of standard mixture dissolved in LB medium was spotted onto each circular Prosolia cell slide spot. PQS-D_4 was used as internal standard. The extraction solvent in the equipment was composed of 75% methanol (0.1% formic acid) and 25% water. Results plotted correspond to an average of three replicates and an analysis time of 1 minute.

Table 5.3. Summary of LOD and LOQ for standard mixture calibration solutions in LB and M9 media. The curve was produced with a spray solvent consisting on a standard mixture calibration curve using 100% LB or M9, respectively. The solvent in the equipment was composed of 75% methanol + 25% water. The concentrations used were blank, 0.001 µM, 0.01 µM, 0.1 µM, 1 µM, 10 µM, 100 µM and 150 µM of a mixture of standards. All values obtained with LESA-MS from an average of three replicates with an analysis time of 1 minute.

	LB			M9		
Compound	**Linear curve equation Y =**	**Linear curve R^2**	**LOD LOQ**	**Linear curve equation**	**Linear curve R^2**	**LOD LOQ**
C_4-HSL	Y = 1.298*X + 7.105	0.9887	13.9 nM 46.2 nM	Y = -55.06*X + 7102	0.07764	381.4 nM 1.273 µM
HHQ	Y = 3416*X - 3406	0.9580	693.8 nM 2.3 µM	Y = 8823*X - 4086	0.9801	504 nM 1.68 µM
HQNO	Y = 8335*X - 71407	0.9443	175.3 nM 584 nM	Y = 17883*X - 9818	0.9641	493.5 nM 1.645 µM
C_7-PQS	Y = 6988*X - 57472	0.9658	133.1 nM 443.6 nM	Y = 20919*X - 149722	0.9281	356.5 nM 1.188 µM
3-OXO-C_{12}-HSL	Y = 41.96*X + 50.78	0.9840	7.4 µM 24.7 µM	Y = 163.3*X - 30.77	0.9697	1.3 µM 4.4 µM

The presence of ions and other debris material in the growth medium can work as camouflage inhibiting capture of the ions of interest. In that sense, growth media with a high NaCl content can represent a problem because these salt ions will ultimately compete with the interesting ones. In this optimisation process it is believed that the high NaCl salt content present in the M9 medium indicates such interference. At the time of spotting M9 samples, the salts did not dissolve properly in the extraction solvents and ended up blocking the nozzle and damaging the first ESI-chip used. Nonetheless, another possibility for explaining the malfunction is that, instead, the droplet became sodiated (by the addition of sodium cations) or simply protonated (by the addition of protons).

Both ESI and nanospray ionisation are extremely sensitive analytical methods, and the presence of non-volatile ions reduces their sensitivity. Thus, the presence of debris or even salts is to be avoided whenever possible. Traces of formic acid are usually added to produce positive ionisation (protonation) and ammonia for negative ionisation (deprotonation); consequently, helping sample protonation. Either way the m/z scale needs calibrating; that is achieved by using a standard sample analogous to the sample of interest (the reason why calibrants are hereby ressuspended in LB medium prior to analysis), and then applying a mass correction. In addition, in positive ionisation mode, the one that directly relates to these results, the protonated ions become dominant over the remaining species in the moiety. However, there is a negative consequence to this interaction which is that the m/z value of the salt adducts, a trace of the bivalent-charged ion, sits approximately at half of the expected m/z value. This effect can mask the presence of our ions of interest by producing either or both adducts (single product of all added components) and/or dimers (joined oligomers), rather than dissociated molecules, as desired.

The high salt (Na^+ and Cl^- ions) content in M9 medium, in multiple molecular shapes, namely heptahydrate Na_2HPO_4, NaCl, NH_4Cl and $CaCl_2$, is clearly well above the salt content in LB broth (10 g of NaCl in 1 L of water). This resulted in LB samples producing better ionisation due to M9 samples possibly undergoing protonation/sodiating. LB broth samples ended up delivering better R square values and better LOD, LOQ, and furthermore it does allow a much improved overnight growth, so LB is the medium of choice in this sense.

Chang *et al* (2012) (410) observed that high salt adducts were only present in aqueous ESI solutions; supporting the hypothesis that their presence in high concentrations may be responsible for poor MS reliability. Precipitating these salts in organic ESI solutions is thus proposed by the authors as a procedure that is likely to improve MS measurements.

The calibration curves generated prompted the acceptance of LB medium as the choice vehicle for sampling the filtered bacterial extracts, prior to chromatography. In addition, LB medium also allows a faster overnight growth of the bacteria to a much higher OD_{600}. This is because the M9 medium and even the MMP medium also initially tested (data not shown) do not sufficiently support bacterial growth and their overnight cultures never reached an OD_{600} level higher than 0.5 (M9) and 0.05 (MMP) [PAO1-L grown for 30 hours at 37°C with 200 rpm shaking].

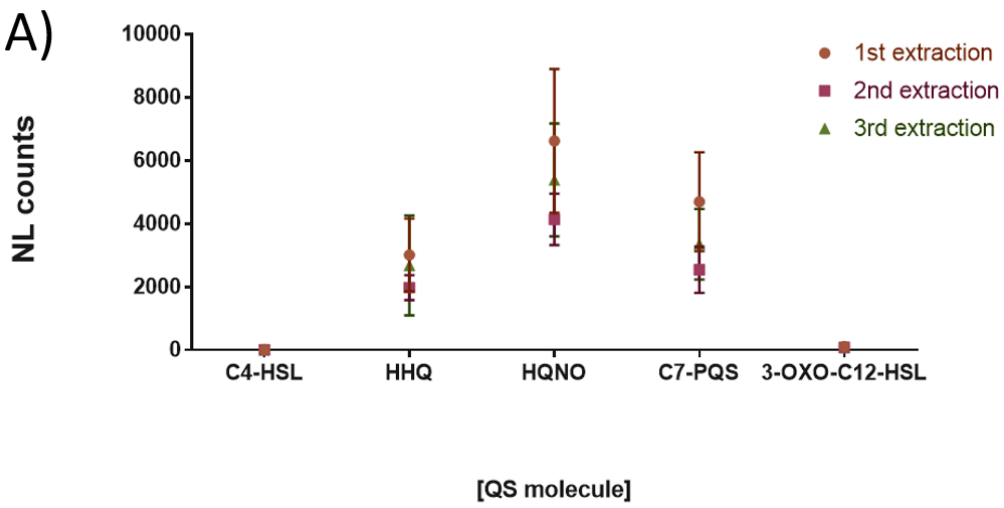
Moreover, the many results observed also showed that LB diluted samples cannot be spotted on their own on the Prosolia cell slide hydrophobic surface; it always requires at least 20% methanol (V/V) to improve sample preparation, but up to 50% (V/V) can be used. Nevertheless, this fact does not only relate to the solvent composition and its participation in the dispersion of the droplet; it is also directly affected by the composition of the growth medium itself as seen in the results obtained here.

Finally, another practical observation made possible by the optimisation results obtained with this study is that prolonged extraction times alongside slow extraction flow rates result in high signal intensities for the target analytes. Peak area increases with extraction time where 30 to 60 seconds represents the time range this study showed as delivering best results, as previously observed by Blatherwick *et al* (2011) (411). However, if the analyst is not willing to manipulate these variables, there is always a third option that can be explored, i.e., re-extracting from a previously analysed spot.

5.3.4. Advantage in re-extracting from previously analysed spots

Limited contact time established (some seconds) between the sampling solvent and the extraction substrate surface, alongside poor compound solubility, are two reasons our study revealed as limitating to the LESA-MS

outcome. In fact, the results obtained from several screenings indicated that a fair amount of analyte is left unused on the surface spot after the first and second extractions take place (Figure 5.9). Hence, there are immediate advantages in re-extracting from old spots; however, re-extracting does not improve the system's sensitivity to pick up certain molecules, what it does is improving the system's usage of available product. Incapacity to read the full presence of analyte is a major factor that supports the needs for subsequent same-spot extractions. But another factor that might help understand signal improvement with additional same-spot readings resides in the work of Bereman *et al* (2007) (412). The authors realised that the quality of the analysis is improved (higher signal-to-noise ratio) within the initial set of spectrums, and subsequent analysis deliver poorer results due to a possible washing and/or diluting of the remaining analytes.



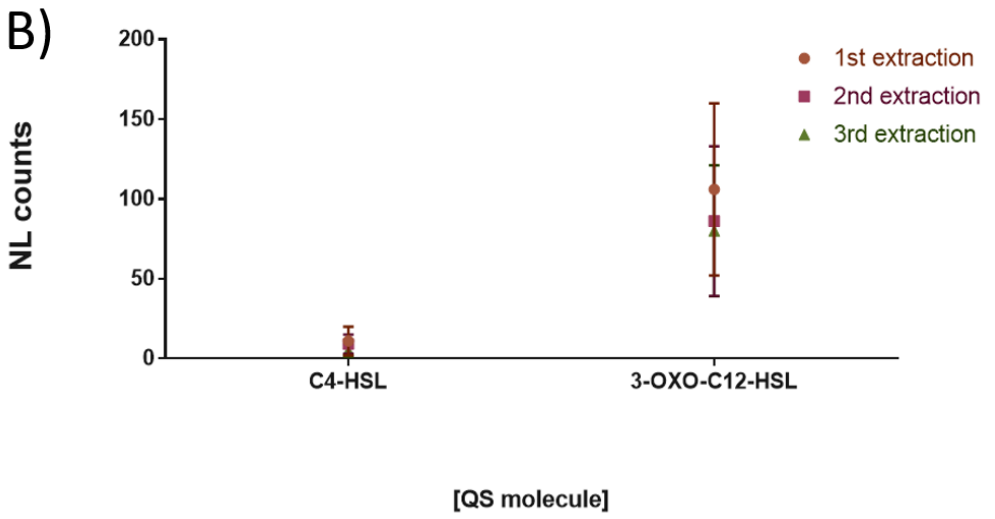


Figure 5.9. Re-extractions of a 10 µM standard calibration mixture in 100% methanol. Three consecutive extractions were performed in the same spot and analysed by means of LESA-MS. A) Overall results, B) Individualised C_4-HSL and 3-oxo-C_{12}-HSL results. The extraction solvent in the equipment was composed of 75% methanol (0.1% formic acid) and 25% water, and the sampling vehicle was made of 100% methanol. Results plotted correspond to an average of three replicates and an analysis time of 1 minute. Vertical bars correspond to standard deviation.

The observed results highlight the importance of reanalysing the same spot through a series of extractions**.** Actually, fast screening through the conventional acceptable minimum number of replicates jeopardises the integrity of the analytical process. For analytes below LOD in a given sample can still 'hide' a much higher concentration of analyte underneath the first screened layers. This effect has been reported before by García-Reyes *et al* (2009) (413) on their work with pesticide presence in fruit peel substrates.

Bereman and Muddiman (2007) (414) noticed a delay in generated ion current at the very beginning of an ESI experiment that the authors attributed to the length of time necessary to dissolve the compound of interest from its source surface into the liquid film. This effect has also been proved with an *in silico* model droplet as the most important of a series of possible interferences (size, speed, angular distribution) (415, 416). The authors defend that the putative momentum transfer proceedings taking place between the primary droplets and the liquid film determine the formation of droplets that do indeed

hold analyte. The effect is designated by the authors as due to the angle that reduced size droplets establish with the substrate.

In order to resolve the issue created by the need for serial extractions on the same spot, this study advises using a different gas pressure and different applied voltage in order to verify if the optimum spraying conditions, individually or together, impact on the readings. The recommended gas pressure and voltage to apply depend on the percentage and volume of organic solvent in the sample. Nevertheless, the most revealing strategy applied to correct the mentioned issue had to do with applying a pre-air space of 2 µl of air volume in the nozzle and a reading delay of a minimum of 10 seconds. Air space in the nozzle helped avoid leakage whenever the nozzle is engaging.

5.4. Application of an optimised protocol

5.4.1. Screening and detection in PAO1-L, PA14 and PAO1-L mutants using LESA-MS

In order to understand if the optimisation procedure delivered acceptably reliable results, different PA strains were compared to what would be theoretically expected. The comparison took into account that no LESA-MS reportings on the analysis of bacterial extracts have been made available previously.

PAO1-L and PA14 (wild-types), PAO1-L *ΔlasI*, PAO1-L *ΔrhlI*, PAO1-L *ΔpqsA*, PAO1-L *ΔpqsH* (figure 5.10) samples were obtained from overnight cultures grown in LB for 24 hours, at 37°C and 200 rpm shaking. The overnight cultures were reduced to a standard OD_{600} of 1.0, filter sterilised and aliquoted to vials containing 100 µl with 80% of this volume being LB medium and 20% methanol.

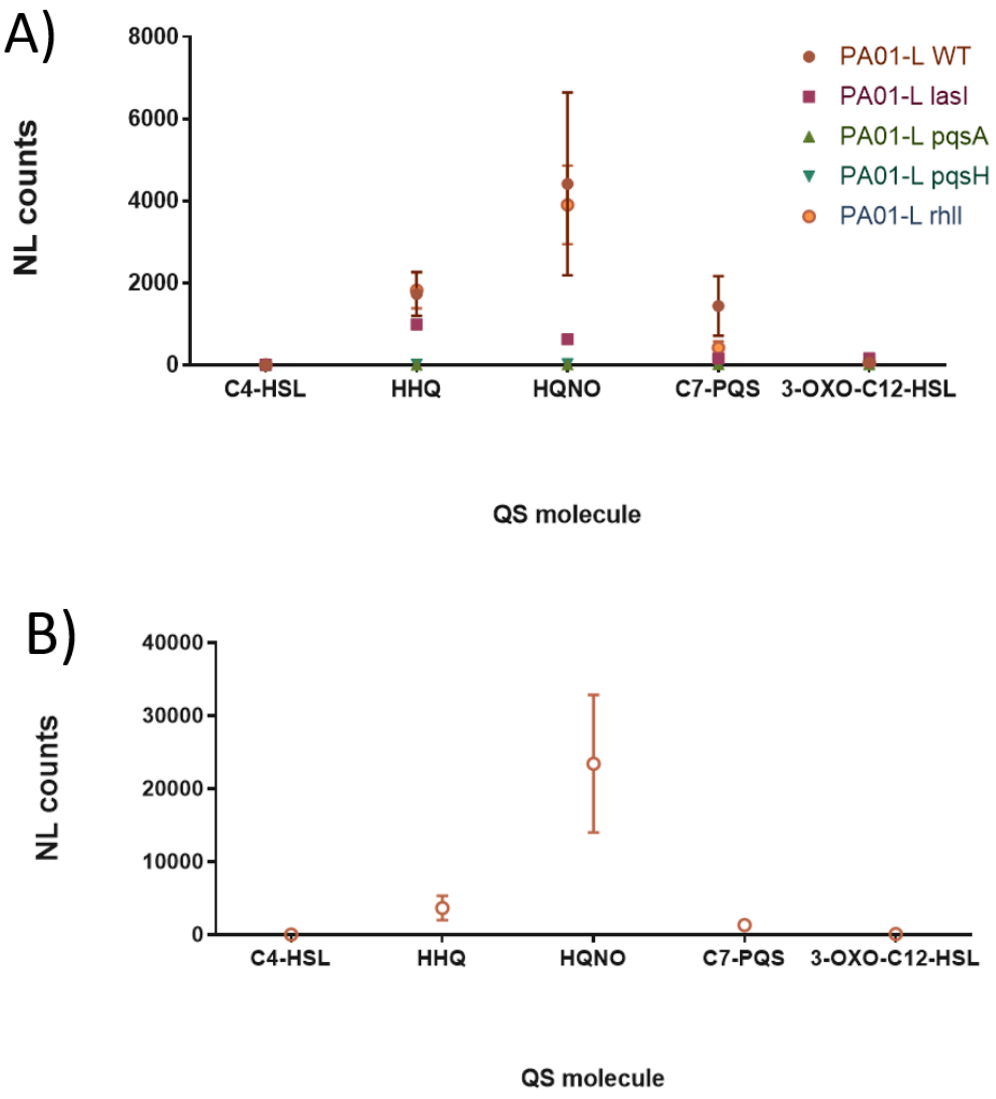


Figure 5.10. Liquid extraction surface analysis of (A)PAO1-L wild-type and mutant strains and (B) PA14 wild-type. 1 µl of a mixture composed by the original LB culture and methanol in an 80:20 proportion (%/%) was spotted onto each circular Prosolia cell slide spot. The extraction solvent in the equipment was composed of 75% methanol (0.1% formic acid) and 25% water. Retention time applied was of 1 minute. Results plotted correspond to a minimum of three to a maximum of six replicates. Plot of the bottom right end refers to analysis of a PA14 wild-type strain.

The results on the presence of QS molecules in PA bacterial extracts using an optimised LESA-MS protocol cannot be compared quantitatively, thus a purely qualitative comparison was made. The protocol optimised with this study is not yet capable of an absolute quantitation, but it is feasible to produce a reliable qualitative comparison based on the optimised LESA-MS protocol for

comparison of strains, detection of signalling molecules, and for mutant strains determining lower or higher levels expected in the wild-type counterparts.

It had been previously noticed that this methodology faced difficulties when attempting to sense AHLs, namely C_4-HSL and 3-oxo-C_{12}-HSL. And that was duly reported once again when analysing the bacterial extracts of virtually all studied wild-type and mutant strains. The focus was hence directed to the analysis of the remaining three molecules that have produced a visible and interpretable signal, i.e., the alkyl quinolone series of QS molecules HHQ, HQNO and C_7-PQS. The evidence that supports the potential of the optimised LESA-MS protocol is summarised below.

Evidence 1) in a *lasI* mutant (full purple square) the transcription of *pqsA* is compromised, showing reduced signals (168); but the *las* QS system is not at all pivotal in the bacterium for producing alkyl-quinolones. Some very low C_7-PQS sensing was reported. A *lasR* mutant is still capable of producing some PQS in the late stationary phase (157) (162). Nevertheless, when the *lasI* gene is present (as naturally is in a wild-type strain) these levels are taken back to their natural higher values.

Evidence 2) in a *lasR* mutant, the *lasI* element is dysfunctional or has its regulation turned off. Consequently, the *pqsH* expression is reduced (157) (162) but not entirely deleted. Thus, the sensing values of HHQ and C_7-PQS were reduced to very low levels in a *pqsH* mutant (downward green arrow).

Evidence 3) in a *rhlI* mutant (orange circle), transcription from the *pqsA* promoter is increased (168), and consequently so are the levels of PQS. The C_7-PQS values picked up by our methodology reported a much higher signal than what is produced by the *lasI* mutant, but obviously not to the normal levels typical of the wild-type. Once again our results are according to what was expected.

Evidence 4) a *pqsH* mutant is naturally lacking the 'equipment' for vesicle production that participates in converting HHQ into PQS (145). But *pqsH* is regulated by LasR; hence when *pqsH* is present (as in the wild-type) but *lasI* is absent, a difference is generated in terms of *pqsH*/*pqsR* regulation. This discrepancy ultimately affects the levels of HHQ that are overproduced in comparison to PQS (164). This effect is also noted in the PA *rhlI* mutant (orange circle) used in this study for the strain is devoid of the capacity to encode the monooxygenase used in the conversion reaction (417) (146).

Evidence 5) a *pqsA* mutant (upward green arrow) would not produce any significant HHQ, HQNO and especially C_7-PQS signal; and the results show exactly that. To be entirely sure that these results are not a technological analogy and derive directly from the absence of the *pqsA* gene, one has to compare this absence to what is seen in the wild-type (full orange circle). The wild-type strain suggests exactly that LESA-MS can indeed pick up strong signals for these three molecules, and the strength of the HQNO signal is actually quite visible.

Evidence 6) the *pqsA* and *pqsH* mutants are incapable of producing sensible levels of HHQ and PQS, whereas the wild-type strain is 'armed' with strong levels of both these quinolones (418). Both effects are easily observed in the image summarising the LESA-MS results.

Evidence 7) as in the LC-MS results reporting the presence of QS molecules in PA14 bacteria exposed to QS inhibitors (figure 3.14), the blank control only exposed to LB medium shows prominence in HQNO production. This is then followed by HHQ and C_7-PQS, respectively, just like in this section for PA14 and the PAO1 wild-type strains.

The collected evidence serves as enough proof that our optimised system is indeed functional and reliable for a qualitative evaluation. Nevertheless, the observed limitations of the system have to do mostly with

the sensing of the AHLs C_4-HSL and 3-oxo-C_{12}-HSL. And that is even the case for the highly pathogenic PA14 strain where the basal values for these two molecules are naturally higher than in PAO1.

An immediate suggestion to help amend the issues with the AHLs is to try and open the lactone cycle with 0.5 M ammonia overnight, followed by vaccum evaporation and resolubilisation in ethyl acetate. It is possible that this procedure will help sense the long AHL chain. For both these molecules we are very likely presented to a case of false negative reporting and not so much a situation where these molecules are at concentrations below the LESA-MS detection level. In addition, AHLs are very sensitive compounds that can face degradation quite rapidly (419), thus its sensing might be compromised by having undergone a differentiated ionisation. In *Pseudomonas putida*, AHLs see their concentration reduced to near zero 36 hours post early logarithmic phase.

In this optimisation study, we demonstrate that LESA combined with high-resolution mass spectrometry is a promising ambient extraction tool to analyse virtually unprepared bacterial extracts. The extraction performed directly from a surface where dried bacterial extracts have been spotted shows a fast and simple technique to screen and qualitatively detect QS compounds. This methodology represents an initial step towards a rapid and reliable screening process, not only for the ever demanding clinical enviroment, but also in regards to highthroughput extractions or screens.

Chapter 6
General conclusions and future directions

To successfully challenge a growing menace with serious health and financial implications, the origin of its alarming emergence has got to be understood and targetted. In the rise of hyper-resistant/-mutable nosocomial pathogens with an 'appetite' for immunosuppressed subjects, like PA is in respect to cystic fibrosis patients, the problem resides in poor global investment and even poorer generalised malpractice.

Antibiotics being used as growth factors for intensive meat production, overprescription by clinicians and misusage of antibiotic drugs by both medical staff and patients, only add up to the problem. Moreover, the upsurgence of hyper-resistant and hyper-mutable strains demands that more last resort antimicrobials (e.g., Carbapenems, Imipenem) are applied regardless of their associated nephrotoxicity and hepatotoxicity. The problem gains ever more relevance when analysing the numbers of new antibiotics recently developed worldwide, in decreasing numbers over the years. Compared to researching other pharmaceuticals, like bronchiolitis medication that exageratedly overflood the market, investing on antibiotic research still represents a very low financial gain due to weak return on investment (205). With such an immense problem, that converges financial, scientific and pharmaceutical limitations, the development of approaches that take into account time and investment restrictions are the most desirable ones.

In silico engineering of antimicrobials is likely to be the best response to the challenges posed, for it combines a preliminary screening based on virtual docking strategies which facilitate an immediate adaptive redesign in response

to undesirable docking scores. It is true that the designing of novel synthetic PA QS antagonists has long been directed to activity on AHLs, with the AQs regulatory pathways usually being overlooked. Besides AHL and 4-AQ systems, little progress has been accomplished towards delivering new antimicrobial drugs that target QS systems. The basic reasons for it is that the identity and profile of many of these QS signals remain unknown, and insufficient focus has been granted to these pathways. The targeting of AQs only recently became an option because of development of synthetic small molecules intended to limit PA pathogeneicity. The molecules chemically engineered for the control of regulatory proteins depend to a certain extent, on their chemical structure and composition, the effects they exert on the biological systems, their pharmacokinetics and thermodynamic profiles. A slight difference in particular residues is capable of huge effect, eventually culminating in shifts that turn antagonists onto potent agonists, and vice-versa. Building on the protein-ligand interaction dynamics, whilst gaining knowledge of the topology of their active binding pockets, constitutes a promising yet essential strategy in the design of antimicrobial drugs. In this aspect, it is important to exploit key regulatory functions that are determined by the activity of proteins and also substantially supported by information provided by mutants.

In Chapter 3 an immediate future approach points towards understanding the mode of action (competitive/non-competitive) of the GP QSIs. One possible experiment would be to add increasing levels of agonist molecule (PQS) and antagonist molecule (individual GP QSIs) together in a liquid culture. Subsequently, inhibition of *pqsA* expression would be measured by means of a P_{pqsA}-*luxCDABE* bioluminescent reporter in a dual scenario, i.e., (1) with a normal parental strain carrying the reporter, and (2) with a *pqsA* mutant (hence impaired in regards to AQs synthesis). When levels of PQS and antagonist are individually increased the resulting dose-response curve produces a vertical shift for PqsR and *pqs* inhibition (toward inhibition of *pqsA* expression). A non-competitive mode of action by the antagonist would be disclosed. It is possible however that the GP QSIs involve, in fact, an allosteric

interaction with the PqsR protein; or even that a horizontal shift of the tested dose-response curve occurs, thus suggesting that the compounds are competitive for PqsR. Another possible experiment would be to measure their specific kinetics, supported by qPCR assays to determine a real-time rate of *pqsA* expression when a known concentration of PQS (to form a complex with PqsR) is challenged at a range of concentrations of GP QSIs. In a case where inhibition can be overcome when adding growing concentrations of substrate.

Besides the mode of action of the PqsR antagonists, the optimisation of their ulterior structure has been determined as a crucial factor in the synthesis of potent agonists. Divergent synthesis producing parental compounds and their derivatives/analogs with proven antagonistic activity can offer insights into their binding modes. But the level of knowledge acquired gains ever more depth when the protein structure is also challenged in a way that promotes not only competitiveness, but above all synergy. Thus, in the context of virulence, epistatic interactions are important relations to scrutinise for their nature is also commonly synergistic, additive or even antagonistic (420). Therefore, they demand a strategic approach that makes use of highthroughput screening adapted to large-scale systems for uncovering underlying antimicrobial drug interactions (421). Accepting that a combination delivers synergistic effects will depend entirely on observing whether a combined effect is greater than, equal to or less than predicted taking individual effects as the basis for comparison, as it is proposed by Klein *et al* (2012) (304). The resulting drug engineering strategy accounts for an intramolecular design based on fragment optimisation, using PqsR antagonistic scaffolds with reported success against the virulence pathway regulated by PqsR.

Amidst many other suggestions already debated in the respective discussion sections, the presence of halogenated elements has been thoroughly reported as successful in the production of PqsR antagonists. Special attention must be addressed to the use of fluoride atoms that successfuly constitute, for example, the fluoroquinolone compounds with

reported strong specific antimicrobial effects. In that sense, engineering derivatives based on the scaffold of these GP QSIs would offer an intriguing perspective on optimisation towards 'killing' of the *pqsA* expression by full repression of the PqsR protein. Moreover, the testing of small variants where localised fluoride atoms are swapped by other also successful elements in the antagonistic composition, like sulphur, chloride and amino groups (that enhance ligand-receptor affinity when in aqueous moieties), would also have the potential to produce interesting derivatives with putative antagonistic behaviour. Finally, selecting an appropriate scaffold is especially challenging when considering the paradoxical nature of the intervening agents, i.e., the hydrophobic character of HHQ and PQS, and the mainly lipophilic nature of the ligand binding domain in the PqsR protein.

In terms of arrest of biofilm formation and disruption of the matrix integrity, there is a definite need for testing the GP QSIs under two scenarios: 1) Including a *pqsA* mutant that was not considered in the initial testings made, and 2) testing the PqsR antagonists alongside sub-inhibitory concentrations of more traditional antibiotic drugs, like Tobramycin, Gentamycin, Carbenicillin, Ciprofloxacin, etc. The first point is based on the fact that AQ-dependent QS contributes to biofilm maturation and even though the impact of the PqsR antagonists produced convincing reductions in biofilm thickness, some of the tested compounds do not seem to inhibit completely AQ synthesis (see section 3.4). But recent antimicrobials that have not been widely used in the clinical setting, thus not so prone to finding resistant PA haplotypes, should also be evaluated in combination with these PqsR antagonists. Hence, there is a definite need to also consider drugs with reported success in treating chronic PA infections, like Ticarcillin and Piperacillin. In fact, serious PA infections have been recently approached with a combinatory therapeutics of Ceftolozane, Ticarcillin, Piperacillin or Imipenem associated or not to an aminoglycoside, and results against hospital outbreaks isolates have been fairly positive (422) (423) (424). The authors refer a principle behind the major benefits presented by combinatory antimicrobial therapy, i.e., that its success emerges from the very

simple probability that one of the parts will be an effective agent. However, there is more to this simplistic prerogative for in an optimum scenario it could also result in additive or synergistic effects. And even if a bactericidal strategy making use of last resort antibiotics (e.g., Imipenem) is not advised, a successful synergistic partnership between these and novel synthetic PqsR antagonists can represent a fruitful alternative approach, especially when considering that these nosocomial strains often act as persisters.

An imperative future consideration is the testing of these GP QSIs in a number of bioreporting QS-related PA mutants, mainly because the type of screening used reports action by the loss of *pqsA* stimulation. This potentiates an immediate problem for influences other than those from the GP QSIs can also generate a reduction in *pqsA* expression. In that sense, whenever the bacteria are challenged with sub-inhibitory concentrations of a toxic compound, growth will be impaired. When this study focused on remaining *pqsA* activity, it was also accepting that such resulted from a reduction in PqsR made available for binding to the *pqsA* promoter, but it could also be the case that the effects are not only directly exerted on the PqsR protein, but for example epistatic influences with pleiotropic consequences impacting on protein synthesis occur. To avoid a misleading 'false positive', growth was also constantly monitored and the strains responded naturally. Finally, with regards to chapter 3, it is also important to recognise whether the GP QSIs are able to rescue the survival of macrophages or virulence-infected mice (affected by attenuated PqsR mutant cells). This would help confirm if the GP QSIs directly target PqsR and that its anti-virulence efficacy is not an off-target effect.

In chapter 4, a PQS-based luminescent bioreporter based on the binding of PqsR to a *lux*-fused *pqsA* promoter was chromosomally inserted in an *E. coli* recipient, resulting was silence. Differences in genetic backgrounds of *E. coli* and PA were debated (see section 4.4) as playing a probable part in this deficiency and for that matter should be addressed with the building of, for instance, a genomic bank. Partial digestions producing fragments of 2 to 3 Kb

would then be screened for corrected activity (seeking for the missing regulatory protein) in the bioreporter-bearing *E. coli* (ECIL02). In addition, the strategy of applying part of the *pqsA* fragment upstream the gene promoter is thought to validate higher PqsR-PQS binding, and therefore luminescence. Also the multiphenotypical issue generated with the chromosomal insertion of the bioreporter in *E. coli* needs addressing, possibly through isolation of phenotypes of interest.

Another important aspect in need of clarification has to do with ECIL02 expression of *pqsA* when exposed to a range of concentrations of C_7-PQS, mostly because PqsA production via RhlR might be postrancriptional (169). A real-time assessment by qPCR of the different phenotypes generated in ECIL02 could then clarify a supposed fluctuating/differing transcription rate in these 'variants'.

And finally, chapter 5 brought an optimised LESA approach for the rapid and simplified screening of bacterial extracts intended for use in the testing of clinical samples. Future work shall also look further into using *in vivo* analysis, especially those obtained from clinical settings. LESA-MS ambient ionisation *in vivo* analysis is something that has been thoroughly used with for example with plants, flowers, human fluids and tissue sections, food proteins, etc., but not so well characterised in microbiological samples. Another issue that needs solving has to do with the presence of organic solvents in the electrospray solution mixture. Methanol, for example, delivers good performance, but the balancing with the aqueous phase cannot be left aside for methanol is not *in vivo*-friendly. And because even after optimisation the system revealed difficulties in picking up C_4-HSL and 3-oxo-C_{12}-HSL, improvements to the protocol should address more sensitivity to AHLs, but in regards to AQs the system has been finely tuned and has responded well. The other important aspects to cover in future endeavours concerns the variability inherent to the chemical composition of samples, as these can naturally differ quite strongly from one another, but variability is also added by the vechicles in which

analytes are sampled. Finally, any future refining must cover the enhancing of the quantitative determination in this methodology, as presently the optimised technique is rather qualitative.

Bibliography

1. Defez C, Fabbro-Peray P, Bouziges N, Gouby A, Mahamat A, Daurès JP, et al. (2004). "Risk factors for multidrug-resistant *Pseudomonas aeruginosa* nosocomial infection". *Journal of Hospital Infection*; **57**(3):209-216.

2. Bodey GP, Bolivar R, Fainstein V, Jadeja L (1983). "Infections Caused by *Pseudomonas aeruginosa*". *Review of Infectious Diseases*; **5**(2):279-313.

3. Koch C, Høiby N (1993). "Pathogenesis of cystic fibrosis". *The Lancet*; **341**(8852):1065-1069.

4. Hirsch EB, Tam VH (2010). "Impact of multidrug-resistant *Pseudomonas aeruginosa* infection on patient outcomes". *Expert review of pharmacoeconomics & outcomes research*; **10**(4):441-451.

5. Bonten M, Bergmans D, Speijer H, Stobberingh E (1999). "Characteristics of polyclonal endemicity of *Pseudomonas aeruginosa* colonization in Intensive Care Units". *American Journal of Respiratory and Critical Care Medicine*; **160**:1212 - 1219.

6. Palmer KL, Mashburn LM, Singh PK, Whiteley M (2005). "Cystic Fibrosis Sputum Supports Growth and Cues Key Aspects of *Pseudomonas aeruginosa* Physiology". *Journal of Bacteriology*; **187**(15):5267-5277.

7. Smith RS, Iglewski BH (2003). "*P. aeruginosa* quorum-sensing systems and virulence". *Current Opinion in Microbiology*; **6**(1):56-60.

8. Latifi A, Winson MK, Foglino M, Bycroft BW, Stewart GSAB, Lazdunski A, et al. (1995). "Multiple homologues of LuxR and LuxI control expression of virulence determinants and secondary metabolites through quorum sensing in *Pseudomonas aeruginosa* PAO1". *Molecular Microbiology*; **17**(2):333-343.

9. Driscoll JA, Brody SL, Kollef MH (2012). "The Epidemiology, Pathogenesis and Treatment of *Pseudomonas aeruginosa* Infections". *Drugs*; **67**(3):351-368.

10. Høiby N, Bjarnsholt T, Givskov M, Molin S, Ciofu O (2010). "Antibiotic resistance of bacterial biofilms". *International Journal of Antimicrobial Agents*; **35**(4):322-332.

11. Neuhauser MM, Weinstein RA, Rydman R, Danziger LH, Karam G, Quinn JP (2003). "Antibiotic resistance among gram-negative bacilli in us intensive care units: Implications for fluoroquinolone use". *JAMA*; **289**(7):885-888.

12. Vincent J, Bihari DJ, Suter PM, et al. (1995). "The prevalence of nosocomial infection in intensive care units in europe: Results of the european prevalence of infection in intensive care (epic) study". *JAMA*; **274**(8):639-644.

13. Jones RN, Kirby JT, Beach ML, Biedenbach DJ, Pfaller MA (2002). "Geographic variations in activity of broad-spectrum β-lactams against *Pseudomonas aeruginosa*: summary of the worldwide SENTRY Antimicrobial Surveillance Program (1997–2000)". *Diagnostic Microbiology and Infectious Disease*; **43**(3):239-243.

14. Mayor S (2000). "Hospital acquired infections kill 5000 patients a year in England". *BMJ : British Medical Journal*; **321**(7273):1370-1370.

15. Hidron AI, Edwards JR, Patel J, Horan TC, Sievert DM, Pollock DA, et al. (2008). "Antimicrobial-Resistant Pathogens Associated With Healthcare-Associated Infections: Annual Summary of Data Reported to the National Healthcare Safety Network at the Centers for Disease Control and Prevention, 2006–2007". *Infection Control & Hospital Epidemiology*; **29**(11):996-1011.

16. Osmon S, Ward S, Fraser VJ, Kollef MH (2004). "Hospital Mortality for Patients With Bacteremia Due to *Staphylococcus aureus* or *Pseudomonas aeruginosa*". *Chest*; **125**(2):607-616.

17. Ibrahim EH, Sherman G, Ward S, Fraser VJ, Kollef MH (2000). "The influence of inadequate antimicrobial treatment of bloodstream infections on patient outcomes in the icu setting*". *Chest*; **118**(1):146-155.

18. Kollef MH (2000). "Inadequate Antimicrobial Treatment: An Important Determinant of Outcome for Hospitalized Patients". *Clinical Infectious Diseases*; **31**(Supplement 4):S131-S138.

19. Kollef MH, Sherman G, Ward S, Fraser VJ (1999). "Inadequate antimicrobial treatment of infections: A risk factor for hospital mortality among critically ill patients". *Chest*; **115**(2):462-474.

20. Micek ST, Lloyd AE, Ritchie DJ, Reichley RM, Fraser VJ, Kollef MH (2005). "*Pseudomonas aeruginosa* Bloodstream Infection: Importance of Appropriate Initial Antimicrobial Treatment". *Antimicrobial Agents and Chemotherapy*; **49**(4):1306-1311.

21. Hogardt M, Heesemann J. Microevolution of *Pseudomonas aeruginosa* to a Chronic Pathogen of the Cystic Fibrosis Lung. In: Dobrindt U, Hacker HJ, Svanborg C, editors. Between Pathogenicity and Commensalism. Berlin, Heidelberg: Springer Berlin Heidelberg; 2013. p. 91-118.

22. Pedersen SS, Høiby N, Espersen F, Koch C (1992). "Role of alginate in infection with mucoid *Pseudomonas aeruginosa* in cystic fibrosis". *Thorax*; **47**(1):6-13.

23. Boyd A, Chakrabarty AM (1994). "Role of alginate lyase in cell detachment of *Pseudomonas aeruginosa*". *Applied and Environmental Microbiology*; **60**(7):2355-2359.

24. Laarman AJ, Bardoel BW, Ruyken M, Fernie J, Milder FJ, van Strijp JAG, et al. (2012). "*Pseudomonas aeruginosa* Alkaline Protease Blocks Complement Activation via the Classical and Lectin Pathways". *The Journal of Immunology*; **188**(1):386-393.

25. Hobden JA (2002). "*Pseudomonas aeruginosa* Proteases and Corneal Virulence". *DNA and Cell Biology*; **21**(5-6):391-396.

26. Peters JE, Park SJ, Darzins A, Freck LC, Saulnier JM, Wallach JM, et al. (1992). "Further studies on *Pseudomonas aeruginosa* LasA: analysis of specificity". *Molecular Microbiology*; **6**(9):1155-1162.

27. Muhlebach MS, Noah TL (2002). "Endotoxin Activity and Inflammatory Markers in the Airways of Young Patients with Cystic Fibrosis". *American Journal of Respiratory and Critical Care Medicine*; **165**(7):911-915.

28. Weinrauch Y, Zychlinsky A (1999). "The Induction of Apoptosis by Bacterial Pathogens". *Annual Review of Microbiology*; **53**(1):155-187.

29. Frithz-Lindsten E, Du Y, Rosqvist R, Forsberg Å (1997). "Intracellular targeting of exoenzyme S of *Pseudomonas aeruginosa* via type III-dependent translocation induces phagocytosis resistance, cytotoxicity and disruption of actin microfilaments". *Molecular Microbiology*; **25**(6):1125-1139.

30. Khalifa ABH, Moissenet D, Thien HV, Kheder M (2011). "Virulence factors in *Pseudomonas aeruginosa*: mechanisms and modes of regulation". *Annales de Biologie Clinique*; **69**(4):393-403.

31. Sokol PA, Iglewski BH, Hager TA, Sadoff JC, Cross AS, McManus A, et al. (1981). "Production of exoenzyme S by clinical isolates of *Pseudomonas aeruginosa*". *Infection and Immunity*; **34**(1):147-153.

32. El-Solh AA, Hattemer A, Hauser AR, Alhajhusain A, Vora H (2012). "Clinical Outcomes of Type III *Pseudomonas aeruginosa* Bacteremia". *Critical Care Medicine*; **40**(4):1157-1163.

33. Doyle TB, Hawkins AC, McCarter LL (2004). "The Complex Flagellar Torque Generator of *Pseudomonas aeruginosa*". *Journal of Bacteriology*; **186**(19):6341-6350.

34. Mahenthiralingam E, Speert DP (1995). "Nonopsonic phagocytosis of *Pseudomonas aeruginosa* by macrophages and polymorphonuclear leukocytes requires the presence of the bacterial flagellum". *Infection and Immunity*; **63**(11):4519-4523.

35. Bajolet-Laudinat O, Girod-de Bentzmann S, Tournier JM, Madoulet C, Plotkowski MC, Chippaux C, et al. (1994). "Cytotoxicity of *Pseudomonas aeruginosa* internal lectin PA-I to respiratory epithelial cells in primary culture". *Infection and Immunity*; **62**(10):4481-4487.

36. Chemani C, Imberty A, de Bentzmann S, Pierre M, Wimmerová M, Guery BP, et al. (2009). "Role of LecA and LecB Lectins in *Pseudomonas aeruginosa*-Induced Lung Injury and Effect of Carbohydrate Ligands". *Infection and Immunity*; **77**(5):2065-2075.

37. Tielker D, Hacker S, Loris R, Strathmann M, Wingender J, Wilhelm S, et al. (2005). "*Pseudomonas aeruginosa* lectin LecB is located in the outer membrane and is involved in biofilm formation". *Microbiology*; **151**(5):1313-1323.

38. Zaidi TS, Fleiszig SM, Preston MJ, Goldberg JB, Pier GB (1996). "Lipopolysaccharide outer core is a ligand for corneal cell binding and ingestion of *Pseudomonas aeruginosa*". *Investigative Ophthalmology & Visual Science*; **37**(6):976-986.

39. Cho J-S, Kang J-H, Um J-Y, Han I-H, Park I-H, Lee H-M (2014). "Lipopolysaccharide Induces Pro-Inflammatory Cytokines and MMP Production via TLR4 in Nasal Polyp-Derived Fibroblast and Organ Culture". *PLoS One*; **9**(11):e90683.

40. Bryant CE, Spring DR, Gangloff M, Gay NJ (2010). "The molecular basis of the host response to lipopolysaccharide". *Nat Rev Micro*; **8**(1):8-14.

41. Doig P, Todd T, Sastry PA, Lee KK, Hodges RS, Paranchych W, et al. (1988). "Role of pili in adhesion of *Pseudomonas aeruginosa* to human respiratory epithelial cells". *Infection and Immunity*; **56**(6):1641-1646.

42. Persat A, Inclan YF, Engel JN, Stone HA, Gitai Z (2015). "Type IV pili mechanochemically regulate virulence factors in *Pseudomonas aeruginosa*". *Proceedings of the National Academy of Sciences*; **112**(24):7563-7568.

43. Titball RW (1993). "Bacterial phospholipases C". *Microbiological Reviews*; **57**(2):347-366.

44. Liu PV. *Pseudomonas aeruginosa*. Clinical manifestations of infection and current therapy. Doggett RG, editor: New York: Academic Press; 1979.

45. Wieland CW, Siegmund B, Senaldi G, Vasil ML, Dinarello CA, Fantuzzi G (2002). "Pulmonary Inflammation Induced by *Pseudomonas aeruginosa* Lipopolysaccharide, Phospholipase C, and Exotoxin A: Role of Interferon Regulatory Factor 1". *Infection and Immunity*; **70**(3):1352-1358.

46. Terada LS, Johansen KA, Nowbar S, Vasil AI, Vasil ML (1999). "*Pseudomonas aeruginosa* Hemolytic Phospholipase C Suppresses Neutrophil Respiratory Burst Activity". *Infection and Immunity*; **67**(5):2371-2376.

47. Lau GW, Hassett DJ, Ran H, Kong F (2004). "The role of pyocyanin in *Pseudomonas aeruginosa* infection". *Trends in Molecular Medicine*; **10**(12):599-606.

48. Ulmer AJ, Pryjma J, Tarnok Z, Ernst M, Flad HD (1990). "Inhibitory and stimulatory effects of *Pseudomonas aeruginosa* pyocyanine on human T and B lymphocytes and human monocytes". *Infection and Immunity*; **58**(3):808-815.

49. Britigan BE, Railsback MA, Cox CD (1999). "The *Pseudomonas aeruginosa* Secretory Product Pyocyanin Inactivates α1 Protease Inhibitor: Implications for the Pathogenesis of Cystic Fibrosis Lung Disease". *Infection and Immunity*; **67**(3):1207-1212.

50. Lamont IL, Beare PA, Ochsner U, Vasil AI, Vasil ML (2002). "Siderophore-mediated signaling regulates virulence factor production in *Pseudomonas aeruginosa*". *Proceedings of the National Academy of Sciences of the United States of America*; **99**(10):7072-7077.

51. Cox CD (1982). "Effect of pyochelin on the virulence of *Pseudomonas aeruginosa*". *Infection and Immunity*; **36**(1):17-23.

52. Milena GR, Gordana GC, Miroslav MV, Ivanka K (2012). "Production and characterization of rhamnolipids from *Pseudomonas aeruginosa* san-ai". *Journal of the Serbian Chemical Society*; **77**(1):27-42.

53. Zulianello L, Canard C, Köhler T, Caille D, Lacroix J-S, Meda P (2006). "Rhamnolipids Are Virulence Factors That Promote Early Infiltration of Primary Human Airway Epithelia by *Pseudomonas aeruginosa*". *Infection and Immunity*; **74**(6):3134-3147.

54. O'Malley YQ, Abdalla MY, McCormick ML, Reszka KJ, Denning GM, Britigan BE (2003). "Subcellular localization of Pseudomonas pyocyanin cytotoxicity in human lung epithelial cells". *American Journal of Physiology - Lung Cellular and Molecular Physiology*; **284**(2):L420-L430.

55. Nutman J CP, Dearborn DG, Berger M, Sorensen RU (1988). "Suppression of lymphocyte proliferation by *Pseudomonas aeruginosa* phenazine pigments". *Israel Journal of Medical Sciences*; **24**(4-5):228-232.

56. Wilson R, Sykes DA, Watson D, Rutman A, Taylor GW, Cole PJ (1988). "Measurement of *Pseudomonas aeruginosa* phenazine pigments in sputum and assessment of their contribution to sputum sol toxicity for respiratory epithelium". *Infection and Immunity*; **56**(9):2515-2517.

57. Britigan BE, Roeder TL, Rasmussen GT, Shasby DM, McCormick ML, Cox CD (1992). "Interaction of the *Pseudomonas aeruginosa* secretory products pyocyanin and pyochelin generates hydroxyl radical and causes synergistic damage to endothelial cells. Implications for Pseudomonas-associated tissue injury". *The Journal of Clinical Investigation*; **90**(6):2187-2196.

58. Hao Y, Kuang Z, Xu Y, Walling BE, Lau GW (2013). "Pyocyanin-induced mucin production is associated with redox modification of FOXA2". *Respiratory Research*; **14**(1):1-14.

59. Chai W, Zhang J, Duan Y, Pan D, Liu W, Li Y, et al. (2014). "Pseudomonas pyocyanin stimulates IL-8 expression through MAPK and NF-κB pathways in differentiated U937 cells". *BioMed Central Microbiology*; **14**(1):1-12.

60. Ran H, Hassett DJ, Lau GW (2003). "Human targets of *Pseudomonas aeruginosa* pyocyanin". *Proceedings of the National Academy of Sciences of the United States of America*; **100**(24):14315-14320.

61. Mavrodi DV, Bonsall RF, Delaney SM, Soule MJ, Phillips G, Thomashow LS (2001). "Functional Analysis of Genes for Biosynthesis of Pyocyanin and Phenazine-1-Carboxamide from *Pseudomonas aeruginosa* PAO1". *Journal of Bacteriology*; **183**(21):6454-6465.

62. Dietrich LEP, Price-Whelan A, Petersen A, Whiteley M, Newman DK (2006). "The phenazine pyocyanin is a terminal signalling factor in the quorum

sensing network of *Pseudomonas aeruginosa*". *Molecular Microbiology*; **61**(5):1308-1321.

63. Nadal Jimenez P, Koch G, Thompson JA, Xavier KB, Cool RH, Quax WJ (2012). "The Multiple Signaling Systems Regulating Virulence in *Pseudomonas aeruginosa*". *Microbiology and Molecular Biology Reviews*; **76**(1):46-65.

64. Twining SS, Kirschner SE, Mahnke LA, Frank DW (1993). "Effect of *Pseudomonas aeruginosa* elastase, alkaline protease, and exotoxin A on corneal proteinases and proteins". *Investigative Ophthalmology & Visual Science*; **34**(9):2699-2712.

65. Tang HB, DiMango E, Bryan R, Gambello M, Iglewski BH, Goldberg JB, et al. (1996). "Contribution of specific *Pseudomonas aeruginosa* virulence factors to pathogenesis of pneumonia in a neonatal mouse model of infection". *Infection and Immunity*; **64**(1):37-43.

66. Kessler E, Safrin M, Abrams WR, Rosenbloom J, Ohman DE (1997). "Inhibitors and Specificity of *Pseudomonas aeruginosa* LasA". *Journal of Biological Chemistry*; **272**(15):9884-9889.

67. Braun P, de Groot A, Bitter W, Tommassen J (1998). "Secretion of Elastinolytic Enzymes and Their Propeptides by *Pseudomonas aeruginosa*". *Journal of Bacteriology*; **180**(13):3467-3469.

68. Kessler E, Safrin M, Gustin JK, Ohman DE (1998). "Elastase and the LasA Protease of *Pseudomonas aeruginosa* Are Secreted with Their Propeptides". *Journal of Biological Chemistry*; **273**(46):30225-30231.

69. Peters JE, Galloway DR (1990). "Purification and characterization of an active fragment of the LasA protein from *Pseudomonas aeruginosa*: enhancement of elastase activity". *Journal of Bacteriology*; **172**(5):2236-2240.

70. Wolz C, Hellstern E, Haug M, Galloway DR, Vasil ML, Döring G (1991). "*Pseudomonas aeruginosa* LasB mutant constructed by insertional mutagenesis reveais elastolytic activity due to alkaline proteinase and the LasA fragment". *Molecular Microbiology*; **5**(9):2125-2131.

71. Cowell BA, Twining SS, Hobden JA, Kwong MSF, Fleiszig SMJ (2003). "Mutation of lasA and lasB reduces *Pseudomonas aeruginosa* invasion of epithelial cells". *Microbiology*; **149**(8):2291-2299.

72. Gustin JK, Kessler E, Ohman DE (1996). "A substitution at His-120 in the LasA protease of *Pseudomonas aeruginosa* blocks enzymatic activity without

affecting propeptide processing or extracellular secretion". *Journal of Bacteriology*; **178**(22):6608-6617.

73. Engel LS, Hill JM, Caballero AR, Green LC, O'Callaghan RJ (1998). "Protease IV, a Unique Extracellular Protease and Virulence Factor from *Pseudomonas aeruginosa*". *Journal of Biological Chemistry*; **273**(27):16792-16797.

74. Wilderman PJ, Vasil AI, Johnson Z, Wilson MJ, Cunliffe HE, Lamont IL, et al. (2001). "Characterization of an Endoprotease (PrpL) Encoded by a PvdS-Regulated Gene in *Pseudomonas aeruginosa*". *Infection and Immunity*; **69**(9):5385-5394.

75. Fleiszig SM, Evans DJ, Do N, Vallas V, Shin S, Mostov KE (1997). "Epithelial cell polarity affects susceptibility to *Pseudomonas aeruginosa* invasion and cytotoxicity". *Infection and Immunity*; **65**(7):2861-2867.

76. Elliott BW, Cohen C (1986). "Isolation and characterization of a lysine-specific protease from *Pseudomonas aeruginosa*". *Journal of Biological Chemistry*; **261**(24):11259-11265.

77. Traidej M, Caballero AR, Marquart ME, Thibodeaux BA, O'Callaghan RJ (2003). "Molecular Analysis of *Pseudomonas aeruginosa* Protease IV Expressed in *Pseudomonas putida*". *Investigative Ophthalmology & Visual Science*; **44**(1):190-196.

78. Walsh PN, Ahmad SS (2002). "Proteases in blood clotting". *Essays In Biochemistry*; **38**:95-111.

79. Malloy JL, Veldhuizen RAW, Thibodeaux BA, O'Callaghan RJ, Wright JR (2005). "*Pseudomonas aeruginosa* protease IV degrades surfactant proteins and inhibits surfactant host defense and biophysical functions". *American Journal of Physiology - Lung Cellular and Molecular Physiology*; **288**(2):L409-L418.

80. McCormick CC, Hobden JA, Balzli CL, Reed JM, Caballero AR, Denard BS, et al. (2007). "Surfactant Protein D in *Pseudomonas aeruginosa* Keratitis". *Ocular Immunology and Inflammation*; **15**(5):371-379.

81. Horvat RT, Parmely MJ (1988). "*Pseudomonas aeruginosa* alkaline protease degrades human gamma interferon and inhibits its bioactivity". *Infection and Immunity*; **56**(11):2925-2932.

82. Parmely M, Gale A, Clabaugh M, Horvat R, Zhou WW (1990). "Proteolytic inactivation of cytokines by *Pseudomonas aeruginosa*". *Infection and Immunity*; **58**(9):3009-3014.

83. Kharazmi A, Høiby N, Döring G, Valerius NH (1984). "*Pseudomonas aeruginosa* exoproteases inhibit human neutrophil chemiluminescence". *Infection and Immunity*; **44**(3):587-591.

84. Kharazmi A, Eriksen HO, DÖRing G, Goldstein W, HØIby N (1986). "Effect of *Pseudomonas aeruginosa* Proteases on Human Leukocyte Phagocytosis and Bactericidal Activity". *Acta Pathologica Microbiologica Scandinavica Series C: Immunology*; **94C**(1-6):175-179.

85. Pedersen BK, Kharazmi A (1987). "Inhibition of human natural killer cell activity by *Pseudomonas aeruginosa* alkaline protease and elastase". *Infection and Immunity*; **55**(4):986-989.

86. Maier MR, Soberón-Chávez G (2000). "*Pseudomonas aeruginosa* rhamnolipids: biosynthesis and potential applications". *Applied Microbiology and Biotechnology*; **54**(5):625-633.

87. Syldatk C, Lang S, Matulovic U, Wagner F (1985). "Production of four interfacial active rhamnolipids from n-alkanes or glycerol by resting cells of Pseudomonas species DSM 2874". *Z Naturforsch*; **40**(1-2):61-67.

88. Rendell NB, Taylor GW, Somerville M, Todd H, Wilson R, Cole PJ (1990). "Characterisation of Pseudomonas rhamnolipids". *Biochimica et Biophysica Acta (BBA) - Lipids and Lipid Metabolism*; **1045**(2):189-193.

89. Kownatzki R, Tümmler B, Döring G (1987). "Rhamnolipid of *Pseudomonas aeruginosa* in sputum of cystic fibrosis patients". *The Lancet*; **329**(8540):1026-1027.

90. Abalos A, Pinazo A, Infante MR, Casals M, García F, Manresa A (2001). "Physicochemical and Antimicrobial Properties of New Rhamnolipids Produced by *Pseudomonas aeruginosa* AT10 from Soybean Oil Refinery Wastes". *Langmuir*; **17**(5):1367-1371.

91. Davey ME, Caiazza NC, O'Toole GA (2003). "Rhamnolipid Surfactant Production Affects Biofilm Architecture in *Pseudomonas aeruginosa* PAO1". *Journal of Bacteriology*; **185**(3):1027-1036.

92. Köhler T, Curty LK, Barja F, van Delden C, Pechère J-C (2000). "Swarming of *Pseudomonas aeruginosa* Is Dependent on Cell-to-Cell Signaling and Requires Flagella and Pili". *Journal of Bacteriology*; **182**(21):5990-5996.

93. Déziel E, Lépine F, Milot S, Villemur R (2003). "rhlA is required for the production of a novel biosurfactant promoting swarming motility in *Pseudomonas aeruginosa*: 3-(3-hydroxyalkanoyloxy)alkanoic acids (HAAs), the precursors of rhamnolipids". *Microbiology*; **149**(8):2005-2013.

94. Pelicic V (2008). "Type IV pili: *et pluribus unum*?". *Molecular Microbiology*; **68**(4):827-837.

95. O'Toole GA, Kolter R (1998). "Flagellar and twitching motility are necessary for *Pseudomonas aeruginosa* biofilm development". *Molecular Microbiology*; **30**(2):295-304.

96. Wolfgang MC, Lee VT, Gilmore ME, Lory S (2003). "Coordinate Regulation of Bacterial Virulence Genes by a Novel Adenylate Cyclase-Dependent Signaling Pathway". *Developmental Cell*; **4**(2):253-263.

97. Borlee BR, Goldman AD, Murakami K, Samudrala R, Wozniak DJ, Parsek MR (2010). "*Pseudomonas aeruginosa* uses a cyclic-di-GMP-regulated adhesin to reinforce the biofilm extracellular matrix". *Molecular Microbiology*; **75**(4):827-842.

98. Mahenthiralingam E, Campbell ME, Speert DP (1994). "Nonmotility and phagocytic resistance of *Pseudomonas aeruginosa* isolates from chronically colonized patients with cystic fibrosis". *Infection and Immunity*; **62**(2):596-605.

99. Klausen M, Aaes-Jørgensen A, Molin S, Tolker-Nielsen T (2003). "Involvement of bacterial migration in the development of complex multicellular structures in *Pseudomonas aeruginosa* biofilms". *Molecular Microbiology*; **50**(1):61-68.

100. Barken KB, Pamp SJ, Yang L, Gjermansen M, Bertrand JJ, Klausen M, et al. (2008). "Roles of type IV pili, flagellum-mediated motility and extracellular DNA in the formation of mature multicellular structures in *Pseudomonas aeruginosa* biofilms". *Environmental Microbiology*; **10**(9):2331-2343.

101. Sauer K, Camper AK, Ehrlich GD, Costerton JW, Davies DG (2002). "*Pseudomonas aeruginosa* Displays Multiple Phenotypes during Development as a Biofilm". *Journal of Bacteriology*; **184**(4):1140-1154.

102. Drake D, Montie TC (1987). "Protection against *Pseudomonas aeruginosa* infection by passive transfer of anti-flagellar serum". *Canadian Journal of Microbiology*; **33**(9):755-763.

103. Laughlin RS, Musch MW, Hollbrook CJ, Rocha FM, Chang EB, Alverdy JC (2000). "The Key Role of *Pseudomonas aeruginosa* PA-I Lectin on Experimental Gut-Derived Sepsis". *Annals of Surgery*; **232**(1):133-142.

104. Wu L, Estrada O, Zaborina O, Bains M, Shen L, Kohler JE, et al. (2005). "Recognition of Host Immune Activation by *Pseudomonas aeruginosa*". *Science*; **309**(5735):774-777.

105. Mitchell E, Houles C, Sudakevitz D, Wimmerova M, Gautier C, Perez S, et al. (2002). "Structural basis for oligosaccharide-mediated adhesion of *Pseudomonas aeruginosa* in the lungs of cystic fibrosis patients". *Nat Struct Mol Biol*; **9**(12):918-921.

106. Adam EC, Mitchell BS, Schumacher DU, Grant G, Schumacher U (1997). "*Pseudomonas aeruginosa* II lectin stops human ciliary beating: therapeutic implications of fucose". *American Journal of Respiratory and Critical Care Medicine*; **155**(6):2102-2104.

107. Adam EC, Schumacher DU, Schumacher U (1997). "Cilia from a cystic fibrosis patient react to the ciliotoxic *Pseudomonas aeruginosa* II lectin in a similar manner to normal control cilia – a case report". *The Journal of Laryngology & Otology*; **111**(08):760-762.

108. Sonawane A, Jyot J, Ramphal R (2006). "*Pseudomonas aeruginosa* LecB Is Involved in Pilus Biogenesis and Protease IV Activity but Not in Adhesion to Respiratory Mucins". *Infection and Immunity*; **74**(12):7035-7039.

109. Diggle SP, Stacey RE, Dodd C, Cámara M, Williams P, Winzer K (2006). "The galactophilic lectin, LecA, contributes to biofilm development in *Pseudomonas aeruginosa*". *Environmental Microbiology*; **8**(6):1095-1104.

110. Johansson EMV, Crusz SA, Kolomiets E, Buts L, Kadam RU, Cacciarini M, et al. (2008). "Inhibition and Dispersion of *Pseudomonas aeruginosa* Biofilms by Glycopeptide Dendrimers Targeting the Fucose-Specific Lectin LecB". *Chemistry & Biology*; **15**(12):1249-1257.

111. Kadam RU, Bergmann M, Hurley M, Garg D, Cacciarini M, Swiderska MA, et al. (2011). "A Glycopeptide Dendrimer Inhibitor of the Galactose-Specific Lectin LecA and of *Pseudomonas aeruginosa* Biofilms". *Angewandte Chemie International Edition*; **50**(45):10631-10635.

112. Ryder C, Byrd M, Wozniak DJ (2007). "Role of polysaccharides in *Pseudomonas aeruginosa* biofilm development". *Current Opinion in Microbiology*; **10**(6):644-648.

113. Lee VT, Matewish JM, Kessler JL, Hyodo M, Hayakawa Y, Lory S (2007). "A cyclic-di-GMP receptor required for bacterial exopolysaccharide production". *Molecular Microbiology*; **65**(6):1474-1484.

114. Ma L, Conover M, Lu H, Parsek MR, Bayles K, Wozniak DJ (2009). "Assembly and Development of the *Pseudomonas aeruginosa* Biofilm Matrix". *PLoS Pathogens*; **5**(3):e1000354.

115. Ghafoor A, Hay ID, Rehm BHA (2011). "Role of Exopolysaccharides in *Pseudomonas aeruginosa* Biofilm Formation and Architecture". *Applied and Environmental Microbiology*; **77**(15):5238-5246.

116. Colvin KM, Gordon VD, Murakami K, Borlee BR, Wozniak DJ, Wong GCL, et al. (2011). "The Pel Polysaccharide Can Serve a Structural and Protective Role in the Biofilm Matrix of *Pseudomonas aeruginosa*". *PLoS Pathogens*; **7**(1):e1001264.

117. Yang L, Hu Y, Liu Y, Zhang J, Ulstrup J, Molin S (2011). "Distinct roles of extracellular polymeric substances in *Pseudomonas aeruginosa* biofilm development". *Environmental Microbiology*; **13**(7):1705-1717.

118. Vasseur P, Vallet-Gely I, Soscia C, Genin S, Filloux A (2005). "The pel genes of the *Pseudomonas aeruginosa* PAK strain are involved at early and late stages of biofilm formation". *Microbiology*; **151**(3):985-997.

119. Friedman L, Kolter R (2004). "Two Genetic Loci Produce Distinct Carbohydrate-Rich Structural Components of the *Pseudomonas aeruginosa* Biofilm Matrix". *Journal of Bacteriology*; **186**(14):4457-4465.

120. P. Stoodley, K. Sauer, D. G. Davies, Costerton JW (2002). "Biofilms as Complex Differentiated Communities". *Annual Review of Microbiology*; **56**(1):187-209.

121. Byrd MS, Sadovskaya I, Vinogradov E, Lu H, Sprinkle AB, Richardson SH, et al. (2009). "Genetic and biochemical analyses of the *Pseudomonas aeruginosa* Psl exopolysaccharide reveal overlapping roles for polysaccharide synthesis enzymes in Psl and LPS production". *Molecular Microbiology*; **73**(4):622-638.

122. Winsor GL, Lam DKW, Fleming L, Lo R, Whiteside MD, Yu NY, et al. (2011). "Pseudomonas Genome Database: improved comparative analysis and population genomics capability for Pseudomonas genomes". *Nucleic Acids Research*; **39**(suppl 1):D596-D600.

123. Ma L, Jackson KD, Landry RM, Parsek MR, Wozniak DJ (2006). "Analysis of *Pseudomonas aeruginosa* Conditional Psl Variants Reveals Roles for the Psl Polysaccharide in Adhesion and Maintaining Biofilm Structure Postattachment". *Journal of Bacteriology*; **188**(23):8213-8221.

124. Matsukawa M, Greenberg EP (2004). "Putative Exopolysaccharide Synthesis Genes Influence *Pseudomonas aeruginosa* Biofilm Development". *Journal of Bacteriology*; **186**(14):4449-4456.

125. Allesen-Holm M, Barken KB, Yang L, Klausen M, Webb JS, Kjelleberg S, et al. (2006). "A characterization of DNA release in *Pseudomonas aeruginosa* cultures and biofilms". *Molecular Microbiology*; **59**(4):1114-1128.

126. Whitchurch CB, Tolker-Nielsen T, Ragas PC, Mattick JS (2002). "Extracellular DNA Required for Bacterial Biofilm Formation". *Science*; **295**(5559):1487-1487.

127. Smith RS, Kelly R, Iglewski BH, Phipps RP (2002). "The Pseudomonas Autoinducer N-(3-Oxododecanoyl) Homoserine Lactone Induces Cyclooxygenase-2 and Prostaglandin E2 Production in Human Lung Fibroblasts: Implications for Inflammation". *The Journal of Immunology*; **169**(5):2636-2642.

128. Wu H, Song Z, Givskov M, Doring G, Worlitzsch D, Mathee K, et al. (2001). "*Pseudomonas aeruginosa* mutations in lasI and rhlI quorum sensing systems result in milder chronic lung infection". *Microbiology*; **147**(5):1105-1113.

129. Zhu H, Bandara R, Conibear TCR, Thuruthyil SJ, Rice SA, Kjelleberg S, et al. (2004). "*Pseudomonas aeruginosa* with LasI Quorum-Sensing Deficiency during Corneal Infection". *Investigative Ophthalmology & Visual Science*; **45**(6):1897-1903.

130. Wu H, Song Z, Hentzer M, Andersen JB, Heydorn A, Mathee K, et al. (2000). "Detection of N-acylhomoserine lactones in lung tissues of mice infected with *Pseudomonas aeruginosa*". *Microbiology*; **146**(10):2481-2493.

131. Senturk S, Ulusoy S, Bosgelmez-Tinaz G, Yagci A. Quorum sensing and virulence of *Pseudomonas aeruginosa* during urinary tract infections2012.

132. Blier A-S, Veron W, Bazire A, Gerault E, Taupin L, Vieillard J, et al. (2011). "C-type natriuretic peptide modulates quorum sensing molecule and toxin production in *Pseudomonas aeruginosa*". *Microbiology*; **157**(Pt 7):1929-1944.

133. Palliyil S, Downham C, Broadbent I, Charlton K, Porter AJ (2013). "High sensitivity monoclonal antibodies specific for homoserine lactones protect

mice from lethal *Pseudomonas aeruginosa* infections". *Applied and Environmental Microbiology*.

134. Dekimpe V, Déziel E (2009). "Revisiting the quorum-sensing hierarchy in *Pseudomonas aeruginosa*: the transcriptional regulator RhlR regulates LasR-specific factors". *Microbiology*; **155**(3):712-723.

135. Croda-García G, Grosso-Becerra V, Gonzalez-Valdez A, Servín-González L, Soberón-Chávez G (2011). "Transcriptional regulation of *Pseudomonas aeruginosa* rhlR: role of the CRP orthologue Vfr (virulence factor regulator) and quorum-sensing regulators LasR and RhlR". *Microbiology*; **157**(9):2545-2555.

136. Branny P, Pearson JP, Pesci EC, Köhler T, Iglewski BH, Van Delden C (2001). "Inhibition of Quorum Sensing by a *Pseudomonas aeruginosa* dksA Homologue". *Journal of Bacteriology*; **183**(5):1531-1539.

137. Subramoni S, Venturi V (2009). "LuxR-family 'solos': bachelor sensors/regulators of signalling molecules". *Microbiology*; **155**(5):1377-1385.

138. Patankar AV, González JE (2009). "Orphan LuxR regulators of quorum sensing". *FEMS Microbiology Reviews*; **33**(4):739-756.

139. Lequette Y, Lee J-H, Ledgham F, Lazdunski A, Greenberg EP (2006). "A Distinct QscR Regulon in the *Pseudomonas aeruginosa* Quorum-Sensing Circuit". *Journal of Bacteriology*; **188**(9):3365-3370.

140. Chugani SA, Whiteley M, Lee KM, D'Argenio D, Manoil C, Greenberg EP (2001). "QscR, a modulator of quorum-sensing signal synthesis and virulence in *Pseudomonas aeruginosa*". *Proceedings of the National Academy of Sciences*; **98**(5):2752-2757.

141. Fuqua C (2006). "The QscR Quorum-Sensing Regulon of *Pseudomonas aeruginosa*: an Orphan Claims Its Identity". *Journal of Bacteriology*; **188**(9):3169-3171.

142. Pearson JP, Pesci EC, Iglewski BH (1997). "Roles of *Pseudomonas aeruginosa* las and rhl quorum-sensing systems in control of elastase and rhamnolipid biosynthesis genes". *Journal of Bacteriology*; **179**(18):5756-5767.

143. Pesci EC, Milbank JBJ, Pearson JP, McKnight S, Kende AS, Greenberg EP, et al. (1999). "Quinolone signaling in the cell-to-cell communication system of *Pseudomonas aeruginosa*". *Proceedings of the National Academy of Sciences of the United States of America*; **96**(20):11229-11234.

144. Lépine F, Milot S, Déziel E, He J, Rahme LG (2004). "Electrospray/mass spectrometric identification and analysis of 4-hydroxy-2-alkylquinolines (HAQs) produced by *Pseudomonas aeruginosa*". *Journal of The American Society for Mass Spectrometry*; **15**(6):862-869.

145. Heeb S, Fletcher MP, Chhabra SR, Diggle SP, Williams P, Cámara M (2011). "Quinolones: from antibiotics to autoinducers". *FEMS Microbiology Reviews*; **35**(2):247-274.

146. Gallagher LA, McKnight SL, Kuznetsova MS, Pesci EC, Manoil C (2002). "Functions Required for Extracellular Quinolone Signaling by *Pseudomonas aeruginosa*". *Journal of Bacteriology*; **184**(23):6472-6480.

147. Coleman JP, Hudson LL, McKnight SL, Farrow JM, Calfee MW, Lindsey CA, et al. (2008). "*Pseudomonas aeruginosa* PqsA Is an Anthranilate-Coenzyme A Ligase". *Journal of Bacteriology*; **190**(4):1247-1255.

148. Farrow JM, Pesci EC (2007). "Two Distinct Pathways Supply Anthranilate as a Precursor of the Pseudomonas Quinolone Signal". *Journal of Bacteriology*; **189**(9):3425-3433.

149. Knoten CA, Wells G, Coleman JP, Pesci EC (2014). "A Conserved Suppressor Mutation in a Tryptophan Auxotroph Results in Dysregulation of Pseudomonas Quinolone Signal Synthesis". *Journal of Bacteriology*; **196**(13):2413-2422.

150. Zhang Y-M, Frank MW, Zhu K, Mayasundari A, Rock CO (2008). "PqsD Is Responsible for the Synthesis of 2,4-Dihydroxyquinoline, an Extracellular Metabolite Produced by *Pseudomonas aeruginosa*". *Journal of Biological Chemistry*; **283**(43):28788-28794.

151. Dulcey Carlos E, Dekimpe V, Fauvelle D-A, Milot S, Groleau M-C, Doucet N, et al. (2013). "The End of an Old Hypothesis: The Pseudomonas Signaling Molecules 4-Hydroxy-2-Alkylquinolines Derive from Fatty Acids, Not 3-Ketofatty Acids". *Chemistry & Biology*; **20**(12):1481-1491.

152. Drees Steffen L, Fetzner S (2015). "PqsE of Pseudomonas aeruginosa Acts as Pathway-Specific Thioesterase in the Biosynthesis of Alkylquinolone Signaling Molecules". *Chemistry & Biology*; **22**(5):611-618.

153. Diggle SP, Matthijs S, Wright VJ, Fletcher MP, Chhabra SR, Lamont IL, et al. (2007). "The *Pseudomonas aeruginosa* 4-quinolone signal molecules HHQ and PQS play multifunctional roles in quorum sensing and iron entrapment". *Chemistry & Biology*; **14**(1):87-96.

154. Pain A, Cooney JJ (1998). "Characterization of Organotin-Resistant Bacteria from Boston Harbor Sediments". *Archives of Environmental Contamination and Toxicology*; **35**:412-416.

155. Ramos JL, Filloux A. Pseudomonas Springer Netherlands; 2010. 287 p.

156. McKnight SL, Iglewski BH, Pesci EC (2000). "The Pseudomonas Quinolone Signal Regulates rhl Quorum Sensing in *Pseudomonas aeruginosa*". *Journal of Bacteriology*; **182**(10):2702-2708.

157. Diggle SP, Winzer K, Chhabra SR, Worrall KE, Cámara M, Williams P (2003). "The *Pseudomonas aeruginosa* quinolone signal molecule overcomes the cell density-dependency of the quorum sensing hierarchy, regulates rhl-dependent genes at the onset of stationary phase and can be produced in the absence of LasR". *Molecular Microbiology*; **50**(1):29-43.

158. Déziel E, Lépine F, Milot S, He J, Mindrinos MN, Tompkins RG, et al. (2004). "Analysis of *Pseudomonas aeruginosa* 4-hydroxy-2-alkylquinolines (HAQs) reveals a role for 4-hydroxy-2-heptylquinoline in cell-to-cell communication". *Proceedings of the National Academy of Sciences of the United States of America*; **101**(5):1339-1344.

159. Bredenbruch F, Geffers R, Nimtz M, Buer J, Häussler S (2006). "The *Pseudomonas aeruginosa* quinolone signal (PQS) has an iron-chelating activity". *Environmental Microbiology*; **8**(8):1318-1329.

160. Rampioni G, Pustelny C, Fletcher MP, Wright VJ, Bruce M, Rumbaugh KP, et al. (2010). "Transcriptomic analysis reveals a global alkyl-quinolone-independent regulatory role for PqsE in facilitating the environmental adaptation of *Pseudomonas aeruginosa* to plant and animal hosts". *Environmental Microbiology*; **12**(6):1659-1673.

161. Wade DS, Calfee MW, Rocha ER, Ling EA, Engstrom E, Coleman JP, et al. (2005). "Regulation of Pseudomonas Quinolone Signal Synthesis in *Pseudomonas aeruginosa*". *Journal of Bacteriology*; **187**(13):4372-4380.

162. Xiao G, Déziel E, He J, Lépine F, Lesic B, Castonguay M-H, et al. (2006). "MvfR, a key *Pseudomonas aeruginosa* pathogenicity LTTR-class regulatory protein, has dual ligands". *Molecular Microbiology*; **62**(6):1689-1699.

163. Farrow JM, Sund ZM, Ellison ML, Wade DS, Coleman JP, Pesci EC (2008). "PqsE Functions Independently of PqsR-Pseudomonas Quinolone Signal and Enhances the rhl Quorum-Sensing System". *Journal of Bacteriology*; **190**(21):7043-7051.

164. Déziel E, Gopalan S, Tampakaki AP, Lépine F, Padfield KE, Saucier M, et al. (2005). "The contribution of MvfR to *Pseudomonas aeruginosa* pathogenesis and quorum sensing circuitry regulation: multiple quorum sensing-regulated genes are modulated without affecting lasRI, rhlRI or the production of N-acyl-l-homoserine lactones". *Molecular Microbiology*; **55**(4):998-1014.

165. Rahme L, Stevens E, Wolfort S, Shao J, Tompkins R, Ausubel F (1995). "Common virulence factors for bacterial pathogenicity in plants and animals". *Science*; **268**(5219):1899-1902.

166. Mahajan-Miklos S, Tan M-W, Rahme LG, Ausubel FM (1999). "Molecular Mechanisms of Bacterial Virulence Elucidated Using a *Pseudomonas aeruginosa*– Caenorhabditis elegans Pathogenesis Model". *Cell*; **96**(1):47-56.

167. Jander G, Rahme LG, Ausubel FM (2000). "Positive Correlation between Virulence of *Pseudomonas aeruginosa* Mutants in Mice and Insects". *Journal of Bacteriology*; **182**(13):3843-3845.

168. McGrath S, Wade DS, Pesci EC (2004). "Dueling quorum sensing systems in *Pseudomonas aeruginosa* control the production of the Pseudomonas quinolone signal (PQS)". *FEMS Microbiology Letters*; **230**(1):27-34.

169. Brouwer S, Pustelny C, Ritter C, Klinkert B, Narberhaus F, Häussler S (2014). "The PqsR and RhlR Transcriptional Regulators Determine the Level of Pseudomonas Quinolone Signal Synthesis in *Pseudomonas aeruginosa* by Producing Two Different pqsABCDE mRNA Isoforms". *Journal of Bacteriology*; **196**(23):4163-4171.

170. Schell MA (1993). "Molecular Biology of the LysR Family of Transcriptional Regulators". *Annual Review of Microbiology*; **47**(1):597-626.

171. Cao H, Krishnan G, Goumnerov B, Tsongalis J, Tompkins R, Rahme LG (2001). "A quorum sensing-associated virulence gene of *Pseudomonas aeruginosa* encodes a LysR-like transcription regulator with a unique self-regulatory mechanism". *Proceedings of the National Academy of Sciences*; **98**(25):14613-14618.

172. Dötsch A, Eckweiler D, Schniederjans M, Zimmermann A, Jensen V, Scharfe M, et al. (2012). "The *Pseudomonas aeruginosa* Transcriptome in Planktonic Cultures and Static Biofilms Using RNA Sequencing". *PLoS One*; **7**(2):e31092.

173. Fletcher M, Heeb S, Chhabra S, Diggle S, Williams P, Cámara M. 2-Alkyl-4(1H)-Quinolone Signalling in *Pseudomonas aeruginosa*. In: Ramos JL, Filloux A, editors. Pseudomonas: Springer Netherlands; 2010. p. 29-57.

174. Kozak M (2005). "Regulation of translation via mRNA structure in prokaryotes and eukaryotes". *Gene*; **361**:13-37.

175. de Smit MH, van Duin J (1990). "Secondary structure of the ribosome binding site determines translational efficiency: a quantitative analysis". *Proceedings of the National Academy of Sciences*; **87**(19):7668-7672.

176. Krajewski SS, Nagel M, Narberhaus F (2013). "Short ROSE-Like RNA Thermometers Control IbpA Synthesis in Pseudomonas Species". *PLoS One*; **8**(5):e65168.

177. Sonnleitner E, Gonzalez N, Sorger-Domenigg T, Heeb S, Richter AS, Backofen R, et al. (2011). "The small RNA PhrS stimulates synthesis of the *Pseudomonas aeruginosa* quinolone signal". *Molecular Microbiology*; **80**(4):868-885.

178. Toyofuku M, Nomura N, Kuno E, Tashiro Y, Nakajima T, Uchiyama H (2008). "Influence of the Pseudomonas Quinolone Signal on Denitrification in *Pseudomonas aeruginosa*". *Journal of Bacteriology*; **190**(24):7947-7956.

179. Cai Z, Liu Y, Chen Y, Yam JKH, Chew SC, Chua SL, et al. (2015). "RpoN Regulates Virulence Factors of *Pseudomonas aeruginosa* via Modulating the PqsR Quorum Sensing Regulator". *International Journal of Molecular Sciences*; **16**(12):28311-28319.

180. Heurlier K, Dénervaud V, Pessi G, Reimmann C, Haas D (2003). "Negative Control of Quorum Sensing by RpoN (σ54) in *Pseudomonas aeruginosa* PAO1". *Journal of Bacteriology*; **185**(7):2227-2235.

181. Farrow JM, Hudson LL, Wells G, Coleman JP, Pesci EC (2015). "CysB Negatively Affects the Transcription of pqsR and Pseudomonas Quinolone Signal Production in *Pseudomonas aeruginosa*". *Journal of Bacteriology*.

182. Medina G, Juárez K, Díaz R, Soberón-Chávez G (2003). "Transcriptional regulation of *Pseudomonas aeruginosa* rhlR, encoding a quorum-sensing regulatory protein". *Microbiology*; **149**(11):3073-3081.

183. Middleton B, Rodgers HC, Cámara M, Knox AJ, Williams P, Hardman A (2002). "Direct detection of N-acylhomoserine lactones in cystic fibrosis sputum". *FEMS Microbiology Letters*; **207**(1):1-7.

184. Barr HL, Halliday N, Cámara M, Barrett DA, Williams P, Forrester DL, et al. (2015). "*Pseudomonas aeruginosa* quorum sensing molecules correlate with clinical status in cystic fibrosis". *The European Respiratory Journal*; **46**(4):1046-1054.

185. Qazi S, Middleton B, Muharram SH, Cockayne A, Hill P, O'Shea P, et al. (2006). "N-Acylhomoserine Lactones Antagonize Virulence Gene Expression and Quorum Sensing in *Staphylococcus aureus*". *Infection and Immunity*; **74**(2):910-919.

186. Machan ZA, Taylor GW, Pitt TL, Cole PJ, Wilson R (1992). "2-Heptyl-4-hydroxyquinoline N-oxide, an antistaphylococcal agent produced by *Pseudomonas aeruginosa*". *Journal of Antimicrobial Chemotherapy*; **30**(5):615-623.

187. Hoffman LR, Déziel E, D'Argenio DA, Lépine F, Emerson J, McNamara S, et al. (2006). "Selection for *Staphylococcus aureus* small-colony variants due to growth in the presence of *Pseudomonas aeruginosa*". *Proceedings of the National Academy of Sciences*; **103**(52):19890-19895.

188. Goerke C, Wolz C (2010). "Adaptation of *Staphylococcus aureus* to the cystic fibrosis lung". *International Journal of Medical Microbiology*; **300**(8):520-525.

189. Fugère A, Lalonde Séguin D, Mitchell G, Déziel E, Dekimpe V, Cantin AM, et al. (2014). "Interspecific Small Molecule Interactions between Clinical Isolates of *Pseudomonas aeruginosa* and *Staphylococcus aureus* from Adult Cystic Fibrosis Patients". *PLoS One*; **9**(1):e86705.

190. Hornby JM, Jensen EC, Lisec AD, Tasto JJ, Jahnke B, Shoemaker R, et al. (2001). "Quorum Sensing in the Dimorphic Fungus *Candida albicans* Is Mediated by Farnesol". *Applied and Environmental Microbiology*; **67**(7):2982-2992.

191. Cugini C, Calfee MW, Farrow JM, Morales DK, Pesci EC, Hogan DA (2007). "Farnesol, a common sesquiterpene, inhibits PQS production in *Pseudomonas aeruginosa*". *Molecular Microbiology*; **65**(4):896-906.

192. Cugini C, Morales DK, Hogan DA (2010). "Candida albicans-produced farnesol stimulates Pseudomonas quinolone signal production in LasR-defective *Pseudomonas aeruginosa* strains". *Microbiology*; **156**(10):3096-3107.

193. Chen H, Fujita M, Feng Q, Clardy J, Fink GR (2004). "Tyrosol is a quorum-sensing molecule in *Candida albicans*". *Proceedings of the National Academy of Sciences of the United States of America*; **101**(14):5048-5052.

194. Alem MAS, Oteef MDY, Flowers TH, Douglas LJ (2006). "Production of Tyrosol by *Candida albicans* Biofilms and Its Role in Quorum Sensing and Biofilm Development". *Eukaryotic Cell*; **5**(10):1770-1779.

195. Hassan Abdel-Rhman S, Mostafa El-Mahdy A, El-Mowafy M (2015). "Effect of Tyrosol and Farnesol on Virulence and Antibiotic Resistance of Clinical Isolates of *Pseudomonas aeruginosa*". *BioMed Research International*; **2015**:7.

196. Ichikawa JK, Norris A, Bangera MG, Geiss GK, van 't Wout AB, Bumgarner RE, et al. (2000). "Interaction of *Pseudomonas aeruginosa* with epithelial cells: Identification of differentially regulated genes by expression microarray analysis of human cDNAs". *Proceedings of the National Academy of Sciences*; **97**(17):9659-9664.

197. Heeckeren A, Walenga R, Konstan MW, Bonfield T, Davis PB, Ferkol T (1997). "Excessive inflammatory response of cystic fibrosis mice to bronchopulmonary infection with *Pseudomonas aeruginosa*". *Journal of Clinical Investigation*; **100**(11):2810-2815.

198. Muhlebach MS, Stewart PW, Leigh MW, Noah TL (1999). "Quantitation of Inflammatory Responses to Bacteria in Young Cystic Fibrosis and Control Patients". *American Journal of Respiratory and Critical Care Medicine*; **160**(1):186-191.

199. Meyer JM, Neely A, Stintzi A, Georges C, Holder IA (1996). "Pyoverdin is essential for virulence of *Pseudomonas aeruginosa*". *Infection and Immunity*; **64**(2):518-523.

200. Takase H, Nitanai H, Hoshino K, Otani T (2000). "Impact of Siderophore Production on *Pseudomonas aeruginosa* Infections in Immunosuppressed Mice". *Infection and Immunity*; **68**(4):1834-1839.

201. Xiao R, Kisaalita WS (1997). "Iron acquisition from transferrin and lactoferrin by *Pseudomonas aeruginosa* pyoverdin". *Microbiology*; **143**(7):2509-2515.

202. Telford G, Wheeler D, Williams P, Tomkins PT, Appleby P, Sewell H, et al. (1998). "The *Pseudomonas aeruginosa* Quorum-Sensing Signal MoleculeN-(3-Oxododecanoyl)-l-Homoserine Lactone Has Immunomodulatory Activity". *Infection and Immunity*; **66**(1):36-42.

203. Smith RS, Fedyk ER, Springer TA, Mukaida N, Iglewski BH, Phipps RP (2001). "IL-8 Production in Human Lung Fibroblasts and Epithelial Cells Activated by the Pseudomonas Autoinducer N-3-Oxododecanoyl Homoserine Lactone Is Transcriptionally Regulated by NF-κB and Activator Protein-2". *The Journal of Immunology*; **167**(1):366-374.

204. Sabuda DM, Laupland K, Pitout J, Dalton B, Rabin H, Louie T, et al. (2008). "Utilization of colistin for treatment of multidrug-resistant

Pseudomonas aeruginosa". *The Canadian Journal of Infectious Diseases & Medical Microbiology*; **19**(6):413-418.

205. Norrby SR, Nord CE, Finch R (2005). "Lack of development of new antimicrobial drugs: a potential serious threat to public health". *The Lancet Infectious Diseases*; **5**(2):115-119.

206. Smeianov V, Scott K, Reid G (2000). "Activity of cecropin P1 and FA-LL-37 against urogenital microflora". *Microbes and Infection*; **2**(7):773-777.

207. Albrecht MT, Wang W, Shamova O, Lehrer RI, Schiller NL (2002). "Binding of protegrin-1 to *Pseudomonas aeruginosa* and *Burkholderia cepacia*". *Respiratory Research*; **3**(1):18-18.

208. Overhage J, Campisano A, Bains M, Torfs ECW, Rehm BHA, Hancock REW (2008). "Human Host Defense Peptide LL-37 Prevents Bacterial Biofilm Formation". *Infection and Immunity*; **76**(9):4176-4182.

209. Giacometti A, Cirioni O, Barchiesi F, Fortuna M, Scalise G (1999). "In-vitro activity of cationic peptides alone and in combination with clinically used antimicrobial agents against *Pseudomonas aeruginosa*". *Journal of Antimicrobial Chemotherapy*; **44**(5):641-645.

210. Bucki R, Pastore JJ, Randhawa P, Vegners R, Weiner DJ, Janmey PA (2004). "Antibacterial Activities of Rhodamine B-Conjugated Gelsolin-Derived Peptides Compared to Those of the Antimicrobial Peptides Cathelicidin LL37, Magainin II, and Melittin". *Antimicrobial Agents and Chemotherapy*; **48**(5):1526-1533.

211. Bellemare A, Vernoux N, Morin S, Gagné SM, Bourbonnais Y (2010). "Structural and antimicrobial properties of human pre-elafin/trappin-2 and derived peptides against *Pseudomonas aeruginosa*". *BMC Microbiology*; **10**(1):1-13.

212. Kaneko Y, Thoendel M, Olakanmi O, Britigan BE, Singh PK (2007). "The transition metal gallium disrupts *Pseudomonas aeruginosa* iron metabolism and has antimicrobial and antibiofilm activity". *The Journal of Clinical Investigation*; **117**(4):877-888.

213. Rangel-Vega A, Bernstein LR, Mandujano Tinoco E-A, García-Contreras S-J, García-Contreras R (2015). "Drug repurposing as an alternative for the treatment of recalcitrant bacterial infections". *Frontiers in Microbiology*; **6**.

214. Banin E, Lozinski A, Brady KM, Berenshtein E, Butterfield PW, Moshe M, et al. (2008). "The potential of desferrioxamine-gallium as an anti-

Pseudomonas therapeutic agent". *Proceedings of the National Academy of Sciences*; **105**(43):16761-16766.

215. Moreau-Marquis S, O'Toole GA, Stanton BA (2009). "Tobramycin and FDA-Approved Iron Chelators Eliminate *Pseudomonas aeruginosa* Biofilms on Cystic Fibrosis Cells". *American Journal of Respiratory Cell and Molecular Biology*; **41**(3):305-313.

216. Moreau-Marquis S, Coutermarsh B, Stanton BA (2015). "Combination of hypothiocyanite and lactoferrin (ALX-109) enhances the ability of tobramycin and aztreonam to eliminate *Pseudomonas aeruginosa* biofilms growing on cystic fibrosis airway epithelial cells". *Journal of Antimicrobial Chemotherapy*; **70**(1):160-166.

217. Hauber H-P, Schulz M, Pforte A, Mack D, Zabel P, Schumacher U (2008). "Inhalation with Fucose and Galactose for Treatment of *Pseudomonas aeruginosa* in Cystic Fibrosis Patients". *International Journal of Medical Sciences*; **5**(6):371-376.

218. Kolomiets E, Swiderska MA, Kadam RU, Johansson EMV, Jaeger K-E, Darbre T, et al. (2009). "Glycopeptide Dendrimers with High Affinity for the Fucose-Binding Lectin LecB from *Pseudomonas aeruginosa*". *ChemMedChem*; **4**(4):562-569.

219. Lee J-H, Kim Y-G, Cho MH, Lee J (2014). "ZnO nanoparticles inhibit *Pseudomonas aeruginosa* biofilm formation and virulence factor production". *Microbiological Research*; **169**(12):888-896.

220. Tsuang Y-H, Sun J-S, Huang Y-C, Lu C-H, Chang WH-S, Wang C-C (2008). "Studies of Photokilling of Bacteria Using Titanium Dioxide Nanoparticles". *Artificial Organs*; **32**(2):167-174.

221. Salehi AH, Montazer M, Toliyat T, Mahmoudi-Rad M (2015). "A new route for synthesis of silver:gold alloy nanoparticles loaded within phosphatidylcholine liposome structure as an effective antibacterial agent against *Pseudomonas aeruginosa*". *Journal of Liposome Research*; **25**(1):38-45.

222. Debarbieux L, Leduc D, Maura D, Morello E, Criscuolo A, Grossi O, et al. (2010). "Bacteriophages Can Treat and Prevent *Pseudomonas aeruginosa* Lung Infections". *Journal of Infectious Diseases*; **201**(7):1096-1104.

223. Garbe J, Wesche A, Bunk B, Kazmierczak M, Selezska K, Rohde C, et al. (2010). "Characterization of JG024, a *Pseudomonas aeruginosa* PB1-like broad host range phage under simulated infection conditions". *BMC Microbiology*; **10**(1):1-10.

224. Torres-Barceló C, Arias-Sánchez FI, Vasse M, Ramsayer J, Kaltz O, Hochberg ME (2014). "A Window of Opportunity to Control the Bacterial Pathogen *Pseudomonas aeruginosa* Combining Antibiotics and Phages". *PLoS One*; **9**(9):e106628.

225. Valdéz JC, Peral MC, Rachid M, Santana M, Perdigón G (2005). "Interference of Lactobacillus plantarum with *Pseudomonas aeruginosa* in vitro and in infected burns: the potential use of probiotics in wound treatment". *Clinical Microbiology and Infection*; **11**(6):472-479.

226. Alexandre Y, Le Berre R, Barbier G, Le Blay G (2014). "Screening of *Lactobacillus spp.* for the prevention of *Pseudomonas aeruginosa* pulmonary infections". *BMC Microbiology*; **14**(1):1-10.

227. Varma P, Nisha N, Dinesh KR, Kumar AV, Biswas R (2011). "Anti-Infective Properties of *Lactobacillus fermentum* against *Staphylococcus aureus* and *Pseudomonas aeruginosa*". *Journal of Molecular Microbiology and Biotechnology*; **20**(3):137-143.

228. Lamers RP, Cavallari JF, Burrows LL (2013). "The Efflux Inhibitor Phenylalanine-Arginine Beta-Naphthylamide (PA?N) Permeabilizes the Outer Membrane of Gram-Negative Bacteria". *PLoS One*; **8**(3):e60666.

229. Gill EE, Franco OL, Hancock REW (2015). "Antibiotic Adjuvants: Diverse Strategies for Controlling Drug-Resistant Pathogens". *Chemical Biology & Drug Design*; **85**(1):56-78.

230. Liu Y, Yang L, Molin S (2010). "Synergistic Activities of an Efflux Pump Inhibitor and Iron Chelators against *Pseudomonas aeruginosa* Growth and Biofilm Formation". *Antimicrobial Agents and Chemotherapy*; **54**(9):3960-3963.

231. Tambekar DH, Dahikar SB (2011). "Antibacterial activity of some Indian Ayurvedic preparations against enteric bacterial pathogens". *Journal of Advanced Pharmaceutical Technology & Research*; **2**(1):24-29.

232. Jayaraman P, Sakharkar MK, Lim CS, Tang TH, Sakharkar KR (2010). "Activity and interactions of antibiotic and phytochemical combinations against *Pseudomonas aeruginosa* in vitro.". *Int J Biol Sci*; **6**(6):556-568.

233. Hertle R, Mrsny R, Fitzgerald DJ (2001). "Dual-Function Vaccine for *Pseudomonas aeruginosa*: Characterization of Chimeric Exotoxin A-Pilin Protein". *Infection and Immunity*; **69**(11):6962-6969.

234. Miyairi S, Tateda K, Fuse ET, Ueda C, Saito H, Takabatake T, et al. (2006). "Immunization with 3-oxododecanoyl-l-homoserine lactone–protein conjugate

protects mice from lethal *Pseudomonas aeruginosa* lung infection". *Journal of Medical Microbiology*; **55**(10):1381-1387.

235. Jiang M, Yao J, Feng G (2014). "Protective Effect of DNA Vaccine Encoding Pseudomonas Exotoxin A and PcrV against Acute Pulmonary *Pseudomonas aeruginosa* Infection". *PLoS One*; **9**(5):e96609.

236. Adonizio A, Kong K-F, Mathee K (2008). "Inhibition of Quorum Sensing-Controlled Virulence Factor Production in *Pseudomonas aeruginosa* by South Florida Plant Extracts". *Antimicrobial Agents and Chemotherapy*; **52**(1):198-203.

237. Hurley MN, Cámara M, Smyth AR (2012). "Novel approaches to the treatment of *Pseudomonas aeruginosa* infections in cystic fibrosis". *The European Respiratory Journal*; **40**(4):1014-1023.

238. Tang K, Zhang X-H (2014). "Quorum Quenching Agents: Resources for Antivirulence Therapy". *Marine Drugs*; **12**(6):3245-3282.

239. Hentzer M, Givskov M (2003). "Pharmacological inhibition of quorum sensing for the treatment of chronic bacterial infections". *Journal of Clinical Investigation*; **112**(9):1300-1307.

240. Clatworthy AE, Pierson E, Hung DT (2007). "Targeting virulence: a new paradigm for antimicrobial therapy". *Nat Chem Biol*; **3**(9):541-548.

241. Roy V, Fernandes R, Tsao C-Y, Bentley WE (2010). "Cross Species Quorum Quenching Using a Native AI-2 Processing Enzyme". *ACS Chemical Biology*; **5**(2):223-232.

242. Yang L, Liu Y, Sternberg C, Molin S (2010). "Evaluation of Enoyl-Acyl Carrier Protein Reductase Inhibitors as *Pseudomonas aeruginosa* Quorum-Quenching Reagents". *Molecules*; **15**(2):780.

243. Ramos J-L. Pseudomonas. Media SSB, editor2004. 740 p.

244. Storz MP, Maurer CK, Zimmer C, Wagner N, Brengel C, de Jong JC, et al. (2012). "Validation of PqsD as an Anti-biofilm Target in *Pseudomonas aeruginosa* by Development of Small-Molecule Inhibitors". *Journal of the American Chemical Society*; **134**(39):16143-16146.

245. Pistorius D, Ullrich A, Lucas S, Hartmann RW, Kazmaier U, Müller R (2011). "Biosynthesis of 2-Alkyl-4(1H)-Quinolones in *Pseudomonas aeruginosa*: Potential for Therapeutic Interference with Pathogenicity". *ChemBioChem*; **12**(6):850-853.

246. Weidel E, de Jong JC, Brengel C, Storz MP, Braunshausen A, Negri M, et al. (2013). "Structure Optimization of 2-Benzamidobenzoic Acids as PqsD Inhibitors for *Pseudomonas aeruginosa* Infections and Elucidation of Binding Mode by SPR, STD NMR, and Molecular Docking". *Journal of Medicinal Chemistry*; **56**(15):6146-6155.

247. Sahner JH, Brengel C, Storz MP, Groh M, Plaza A, Müller R, et al. (2013). "Combining in Silico and Biophysical Methods for the Development of *Pseudomonas aeruginosa* Quorum Sensing Inhibitors: An Alternative Approach for Structure-Based Drug Design". *Journal of Medicinal Chemistry*; **56**(21):8656-8664.

248. Storz MP, Brengel C, Weidel E, Hoffmann M, Hollemeyer K, Steinbach A, et al. (2013). "Biochemical and Biophysical Analysis of a Chiral PqsD Inhibitor Revealing Tight-binding Behavior and Enantiomers with Contrary Thermodynamic Signatures". *ACS Chemical Biology*; **8**(12):2794-2801.

249. Migiyama Y, Kaneko Y, Yanagihara K, Morohoshi T, Morinaga Y, Nakamura S, et al. (2013). "Efficacy of AiiM, an N-Acylhomoserine Lactonase, against *Pseudomonas aeruginosa* in a Mouse Model of Acute Pneumonia". *Antimicrobial Agents and Chemotherapy*; **57**(8):3653-3658.

250. Wang Y, Dai Y, Zhang Y, Hu Y, Yang B, Chen S (2007). "Effects of quorum sensing autoinducer degradation gene on virulence and biofilm formation of *Pseudomonas aeruginosa*". *Science in China Series C: Life Sciences*; **50**(3):385-391.

251. Rajesh PS, Ravishankar Rai V (2014). "Quorum quenching activity in cell-free lysate of endophytic bacteria isolated from Pterocarpus santalinus Linn., and its effect on quorum sensing regulated biofilm in *Pseudomonas aeruginosa* PAO1". *Microbiological Research*; **169**(7–8):561-569.

252. Hraiech S, Hiblot J, Lafleur J, Lepidi H, Papazian L, Rolain J-M, et al. (2014). "Inhaled Lactonase Reduces *Pseudomonas aeruginosa* Quorum Sensing and Mortality in Rat Pneumonia". *PLoS One*; **9**(10):e107125.

253. Aybey A, Demirkan E (2016). "Inhibition of quorum sensing-controlled virulence factors in *Pseudomonas aeruginosa* by human serum paraoxonase". *Journal of Medical Microbiology*; **65**(2):105-113.

254. Theriault JR, Wurst J, Jewett I, Verplank L, Perez JR, Gulick AM, et al. Identification of a small molecule inhibitor of *Pseudomonas aeruginosa* PvdQ acylase, an enzyme involved in siderophore pyoverdine synthesis. Information NCfB, editor2013.

255. Wurst JM, Drake EJ, Theriault JR, Jewett IT, VerPlank L, Perez JR, et al. (2014). "Identification of Inhibitors of PvdQ, an Enzyme Involved in the Synthesis of the Siderophore Pyoverdine". *ACS Chemical Biology*; **9**(7):1536-1544.

256. Pustelny C, Albers A, Büldt-Karentzopoulos K, Parschat K, Chhabra SR, Cámara M, et al. (2009). "Dioxygenase-Mediated Quenching of Quinolone-Dependent Quorum Sensing in *Pseudomonas aeruginosa*". *Chemistry & Biology*; **16**(12):1259-1267.

257. Müller C, Birmes FS, Rückert C, Kalinowski J, Fetzner S (2015). "*Rhodococcus erythropolis* BG43 Genes Mediating *Pseudomonas aeruginosa* Quinolone Signal Degradation and Virulence Factor Attenuation". *Applied and Environmental Microbiology*; **81**(22):7720-7729.

258. Hauser AR, Mecsas J, Moir DT (2016). "Beyond Antibiotics: New Therapeutic Approaches for Bacterial Infections". *Clinical Infectious Diseases*.

259. Kaufmann GF, Sartorio R, Lee S-H, Mee JM, Altobell LJ, Kujawa DP, et al. (2006). "Antibody Interference with N-Acyl Homoserine Lactone-Mediated Bacterial Quorum Sensing". *Journal of the American Chemical Society*; **128**(9):2802-2803.

260. Golpasha ID, Mousavi SF, Owlia P, Siadat SD, Irani S (2015). "Immunization with 3-oxododecanoyl-L-homoserine lactone-r-PcrV conjugate enhances survival of mice against lethal burn infections caused by *Pseudomonas aeruginosa*". *Bosnian Journal of Basic Medical Sciences*; **15**(2):15-24.

261. Goure J, Pastor A, Faudry E, Chabert J, Dessen A, Attree I (2004). "The V Antigen of *Pseudomonas aeruginosa* Is Required for Assembly of the Functional PopB/PopD Translocation Pore in Host Cell Membranes". *Infection and Immunity*; **72**(8):4741-4750.

262. Piletska EV, Stavroulakis G, Larcombe LD, Whitcombe MJ, Sharma A, Primrose S, et al. (2011). "Passive Control of Quorum Sensing: Prevention of *Pseudomonas aeruginosa* Biofilm Formation by Imprinted Polymers". *Biomacromolecules*; **12**(4):1067-1071.

263. Maddocks SE, Oyston PCF (2008). "Structure and function of the LysR-type transcriptional regulator (LTTR) family proteins". *Microbiology*; **154**(12):3609-3623.

264. Reen FJ, Barret M, Fargier E, O'Muinneacháin M, O'Gara F (2013). "Molecular evolution of LysR-type transcriptional regulation in *Pseudomonas aeruginosa*". *Molecular Phylogenetics and Evolution*; **66**(3):1041-1049.

265. Muraoka S, Okumura R, Ogawa N, Nonaka T, Miyashita K, Senda T (2003). "Crystal Structure of a Full-length LysR-type Transcriptional Regulator, CbnR: Unusual Combination of Two Subunit Forms and Molecular Bases for Causing and Changing DNA Bend". *Journal of Molecular Biology*; **328**(3):555-566.

266. Zhou X, Lou Z, Fu S, Yang A, Shen H, Li Z, et al. (2010). "Crystal Structure of ArgP from *Mycobacterium tuberculosis* Confirms Two Distinct Conformations of Full-length LysR Transcriptional Regulators and Reveals Its Function in DNA Binding and Transcriptional Regulation". *Journal of Molecular Biology*; **396**(4):1012-1024.

267. Xu N, Yu S, Moniot S, Weyand M, Blankenfeldt W (2012). "Crystallization and preliminary crystal structure analysis of the ligand-binding domain of PqsR (MvfR), the Pseudomonas quinolone signal (PQS) responsive quorum-sensing transcription factor of *Pseudomonas aeruginosa*". *Acta Crystallographica Section F: Structural Biology and Crystallization Communications*; **68**(Pt 9):1034-1039.

268. Ilangovan A, Fletcher M, Rampioni G, Pustelny C, Rumbaugh K, Heeb S, et al. (2013). "Structural Basis for Native Agonist and Synthetic Inhibitor Recognition by the *Pseudomonas aeruginosa* Quorum Sensing Regulator PqsR (MvfR)". *PLoS Pathogens*; **9**(7):e1003508.

269. Hentzer M, Riedel K, Rasmussen TB, Heydorn A, Andersen JB, Parsek MR, et al. (2002). "Inhibition of quorum sensing in *Pseudomonas aeruginosa* biofilm bacteria by a halogenated furanone compound". *Microbiology*; **148**(1):87-102.

270. Wu H, Song Z, Hentzer M, Andersen JB, Molin S, Givskov M, et al. (2004). "Synthetic furanones inhibit quorum-sensing and enhance bacterial clearance in *Pseudomonas aeruginosa* lung infection in mice". *Journal of Antimicrobial Chemotherapy*; **53**(6):1054-1061.

271. Smith KM, Bu Y, Suga H (2003). "Induction and Inhibition of *Pseudomonas aeruginosa* Quorum Sensing by Synthetic Autoinducer Analogs". *Chemistry & Biology*; **10**(1):81-89.

272. Ishida T, Ikeda T, Takiguchi N, Kuroda A, Ohtake H, Kato J (2007). "Inhibition of Quorum Sensing in *Pseudomonas aeruginosa* by N-Acyl

Cyclopentylamides". *Applied and Environmental Microbiology*; **73**(10):3183-3188.

273. Annapoorani A, Umamageswaran V, Parameswari R, Pandian SK, Ravi AV (2012). "Computational discovery of putative quorum sensing inhibitors against LasR and RhlR receptor proteins of *Pseudomonas aeruginosa*". *Journal of Computer-Aided Molecular Design*; **26**(9):1067-1077.

274. Ahumedo M, Drosos JC, Vivas-Reyes R (2014). "Application of molecular docking and ONIOM methods for the description of interactions between anti-quorum sensing active (AHL) analogues and the *Pseudomonas aeruginosa* LasR binding site". *Molecular BioSystems*; **10**(5):1162-1171.

275. Goh W-K, Gardner CR, Chandra Sekhar KVG, Biswas NN, Nizalapur S, Rice SA, et al. (2015). "Synthesis, quorum sensing inhibition and docking studies of 1,5-dihydropyrrol-2-ones". *Bioorganic & Medicinal Chemistry*; **23**(23):7366-7377.

276. O'Loughlin CT, Miller LC, Siryaporn A, Drescher K, Semmelhack MF, Bassler BL (2013). "A quorum-sensing inhibitor blocks *Pseudomonas aeruginosa* virulence and biofilm formation". *Proceedings of the National Academy of Sciences*; **110**(44):17981-17986.

277. Simon R, Priefer U, Puhler A (1983). "A Broad Host Range Mobilization System for In Vivo Genetic Engineering: Transposon Mutagenesis in Gram Negative Bacteria". *Nature Biotechnology*; **1**(9):784-791.

278. Ilangovan A, Fletcher M, Rampioni G, Pustelny C, Rumbaugh K, Heeb S, et al. (2013). "Structural Basis for Native Agonist and Synthetic Inhibitor Recognition by the *Pseudomonas aeruginosa* Quorum Sensing Regulator PqsR (MvfR)". *PLoS Pathog*; **9**(7):e1003508.

279. Winzer K, Falconer C, Garber NC, Diggle SP, Camara M, Williams P (2000). "The *Pseudomonas aeruginosa* Lectins PA-IL and PA-IIL Are Controlled by Quorum Sensing and by RpoS". *Journal of Bacteriology*; **182**(22):6401-6411.

280. Darch SE, McNally A, Harrison F, Corander J, Barr HL, Paszkiewicz K, et al. (2015). "Recombination is a key driver of genomic and phenotypic diversity in a *Pseudomonas aeruginosa* population during cystic fibrosis infection". *Scientific Reports*; **5**:7649.

281. Hoang TT, Karkhoff-Schweizer RR, Kutchma AJ, Schweizer HP (1998). "A broad-host-range Flp-FRT recombination system for site-specific excision of chromosomally-located DNA sequences: application for isolation of unmarked *Pseudomonas aeruginosa* mutants". *Gene*; **212**(1):77-86.

282. Atkinson S, Chang C-Y, Patrick HL, Buckley CMF, Wang Y, Sockett RE, et al. (2008). "Functional interplay between the *Yersinia pseudotuberculosis* YpsRI and YtbRI quorum sensing systems modulates swimming motility by controlling expression of flhDC and fliA". *Molecular Microbiology*; **69**(1):137-151.

283. Choi K-HaS, H. P (2005). "An improved method for rapid generation of unmarked

Pseudomonas aeruginosa deletion mutants". *BMC Microbiology*; **5**(30):11.

284. Prentki P, Krisch HM (1984). "In vitro insertional mutagenesis with a selectable DNA fragment". *Gene*; **29**(3):303-313.

285. Choi K-H, Gaynor JB, White KG, Lopez C, Bosio CM, Karkhoff-Schweizer RR, et al. (2005). "A Tn7-based broad-range bacterial cloning and expression system". *Nat Meth*; **2**(6):443-448.

286. Becher A, Schweizer HP (2000). "Integration-proficient *Pseudomonas aeruginosa* vectors for isolation of single-copy chromosomal lacZ and lux gene fusions". *BioTechniques*; **29**(5):948-950, 952.

287. Schweizer HP (1991). "Escherichia-Pseudomonas shuttle vectors derived from pUC18/19". *Gene*; **97**(1):109-112.

288. Heeb S, Blumer C, Haas D (2002). "Regulatory RNA as Mediator in GacA/RsmA-Dependent Global Control of Exoproduct Formation in Pseudomonas fluorescens CHA0". *Journal of Bacteriology*; **184**(4):1046-1056.

289. Sambrook J. FEF, Maniatis T. Molecular cloning: a laboratory manual. Cold Spring Harbor Laboratory Press NY, editor1989.

290. Chhabra SR, Harty C, Hooi DSW, Daykin M, Williams P, Telford G, et al. (2003). "Synthetic Analogues of the Bacterial Signal (Quorum Sensing) Molecule N-(3-Oxododecanoyl)-l-homoserine Lactone as Immune Modulators". *Journal of Medicinal Chemistry*; **46**(1):97-104.

291. Saiki R, Gelfand D, Stoffel S, Scharf S, Higuchi R, Horn G, et al. (1988). "Primer-directed enzymatic amplification of DNA with a thermostable DNA polymerase". *Science*; **239**(4839):487-491.

292. Ortori CA, Halliday N, Cámara M, Williams P, Barrett DA. LC-MS/MS Quantitative Analysis of Quorum Sensing Signal Molecules. In: Filloux A, Ramos J-L, editors. Pseudomonas Methods and Protocols. New York, NY: Springer New York; 2014. p. 255-270.

293. Chang PC, Blackwood AC (1969). "Simultaneous production of three phenazine pigments by *Pseudomonas aeruginosa* Mac 436". *Canadian Journal of Microbiology*; **15**(5):439-444.

294. Ingledew WM, Campbell JJR (1969). "A new resuspension medium for pyocyanin production". *Canadian Journal of Microbiology*; **15**(6):595-598.

295. Essar DW, Eberly L, Hadero A, Crawford IP (1990). "Identification and characterization of genes for a second anthranilate synthase in *Pseudomonas aeruginosa*: interchangeability of the two anthranilate synthases and evolutionary implications". *Journal of Bacteriology*; **172**(2):884-900.

296. Kittler J, Illingworth J (1985). "On threshold selection using clustering criteria". *Systems, Man and Cybernetics, IEEE Transactions on*; **SMC-15**(5):652-655.

297. Prosolia. Prosolia 2012 DESI Product Brochure 2012 [Available from: http://www.prosolia.com/sites/default/files/Prosolia_2012_DESI_Product_Brochure.pdf.

298. Lesic B, Lépine F, Déziel E, Zhang J, Zhang Q, Padfield K, et al. (2007). "Inhibitors of Pathogen Intercellular Signals as Selective Anti-Infective Compounds". *PLoS Pathog*; **3**(9):e126.

299. Messmer EM (2007). "Osmoprotection as a new therapeutic principle". *Der Ophthalmologe*; **104**(11):987-990.

300. Kesarwani M, Hazan R, He J, Que Y, Apidianakis Y, Lesic B, et al. (2011). "A Quorum Sensing Regulated Small Volatile Molecule Reduces Acute Virulence and Promotes Chronic Infection Phenotypes". *PLoS Pathog*; **7**(8):e1002192.

301. Lu C, Maurer CK, Kirsch B, Steinbach A, Hartmann RW (2014). "Overcoming the Unexpected Functional Inversion of a PqsR Antagonist in *Pseudomonas aeruginosa*: An In Vivo Potent Antivirulence Agent Targeting pqs Quorum Sensing". *Angewandte Chemie International Edition*; **53**(4):1109-1112.

302. Lu C, Kirsch B, Maurer CK, de Jong JC, Braunshausen A, Steinbach A, et al. (2014). "Optimization of anti-virulence PqsR antagonists regarding aqueous solubility and biological properties resulting in new insights in structure–activity relationships". *European Journal of Medicinal Chemistry*; **79**:173-183.

303. Lu C, Kirsch B, Zimmer C, de Jong Johannes C, Henn C, Maurer Christine K, et al. (2012). "Discovery of Antagonists of PqsR, a Key Player in 2-Alkyl-4-quinolone-Dependent Quorum Sensing in *Pseudomonas aeruginosa*". *Chemistry & Biology*; **19**(3):381-390.

304. Klein T, Henn C, de Jong JC, Zimmer C, Kirsch B, Maurer CK, et al. (2012). "Identification of Small-Molecule Antagonists of the *Pseudomonas aeruginosa* Transcriptional Regulator PqsR: Biophysically Guided Hit Discovery and Optimization". *ACS Chemical Biology*; **7**(9):1496-1501.

305. Hartmann RW, Kranzfelder G, Von Angerer E, Schoenenberger H (1980). "Antiestrogens. Synthesis and evaluation of mammary tumor inhibiting activity of 1,1,2,2-tetraalkyl-1,2-diphenylethanes". *Journal of Medicinal Chemistry*; **23**(8):841-848.

306. Cheng A, Merz KM (2003). "Prediction of Aqueous Solubility of a Diverse Set of Compounds Using Quantitative Structure−Property Relationships". *Journal of Medicinal Chemistry*; **46**(17):3572-3580.

307. Veber DF, Johnson SR, Cheng H-Y, Smith BR, Ward KW, Kopple KD (2002). "Molecular Properties That Influence the Oral Bioavailability of Drug Candidates". *Journal of Medicinal Chemistry*; **45**(12):2615-2623.

308. Hodgkinson J, Bowden SD, Galloway WRJD, Spring DR, Welch M (2010). "Structure-Activity Analysis of the Pseudomonas Quinolone Signal Molecule". *Journal of Bacteriology*; **192**(14):3833-3837.

309. Brandl M, Weiss MS, Jabs A, Sühnel J, Hilgenfeld R (2001). "C-h···π-interactions in proteins". *Journal of Molecular Biology*; **307**(1):357-377.

310. Fletcher MP, Diggle SP, Camara M, Williams P (2007). "Biosensor-based assays for PQS, HHQ and related 2-alkyl-4-quinolone quorum sensing signal molecules". *Nature Protocols*; **2**(5):1254-1262.

311. Frei R, Breitbach AS, Blackwell HE (2012). "2-Aminobenzimidazole Derivatives Strongly Inhibit and Disperse *Pseudomonas aeruginosa* Biofilms". *Angewandte Chemie International Edition*; **51**(21):5226-5229.

312. Zender M, Klein T, Henn C, Kirsch B, Maurer CK, Kail D, et al. (2013). "Discovery and Biophysical Characterization of 2-Amino-oxadiazoles as Novel Antagonists of PqsR, an Important Regulator of *Pseudomonas aeruginosa* Virulence". *Journal of Medicinal Chemistry*; **56**(17):6761-6774.

313. Starkey M, Lepine F, Maura D, Bandyopadhaya A, Lesic B, He J, et al. (2014). "Identification of Anti-virulence Compounds That Disrupt Quorum-Sensing Regulated Acute and Persistent Pathogenicity". *PLoS Pathog*; **10**(8):e1004321.

314. Abraham RT, Weiss A (2004). "Jurkat T cells and development of the T-cell receptor signalling paradigm". *Nature Reviews Immunology*; **4**(4):301-308.

315. Waldrop GL (2009). "Smaller Is Better for Antibiotic Discovery". *ACS Chemical Biology*; **4**(6):397-399.

316. Persson T, Hansen TH, Rasmussen TB, Skinderso ME, Givskov M, Nielsen J (2005). "Rational design and synthesis of new quorum-sensing inhibitors derived from acylated homoserine lactones and natural products from garlic". *Organic & Biomolecular Chemistry*; **3**(2):253-262.

317. Schaefer AL, Hanzelka BL, Eberhard A, Greenberg EP (1996). "Quorum sensing in Vibrio fischeri: probing autoinducer-LuxR interactions with autoinducer analogs". *Journal of Bacteriology*; **178**(10):2897-2901.

318. Jakobsen TH, Bragason SK, Phipps RK, Christensen LD, van Gennip M, Alhede M, et al. (2012). "Food as a source for QS inhibitors: Iberin from Horseradish Revealed as a Quorum Sensing Inhibitor of *Pseudomonas aeruginosa*". *Applied and Environmental Microbiology*.

319. Li M, Ni N, Chou H-T, Lu C-D, Tai PC, Wang B (2008). "Structure-Based Discovery and Experimental Verification of Novel AI-2 Quorum Sensing Inhibitors against *Vibrio harveyi*". *ChemMedChem*; **3**(8):1242-1249.

320. Peng H, Cheng Y, Ni N, Li M, Choudhary G, Chou HT, et al. (2009). "Synthesis and Evaluation of New Antagonists of Bacterial Quorum Sensing in *Vibrio harveyi*". *ChemMedChem*; **4**(9):1457-1468.

321. Koch B, Liljefors T, Persson T, Nielsen J, Kjelleberg S, Givskov M (2005). "The LuxR receptor: the sites of interaction with quorum-sensing signals and inhibitors". *Microbiology*; **151**(11):3589-3602.

322. Kahnert A, Vermeij P, Wietek C, James P, Leisinger T, Kertesz MA (2000). "The ssu Locus Plays a Key Role in Organosulfur Metabolism in *Pseudomonas putida* S-313". *Journal of Bacteriology*; **182**(10):2869-2878.

323. Kobayashi K, Tagawa S (2004). "Activation of SoxR-Dependent Transcription in *Pseudomonas aeruginosa*". *Journal of Biochemistry*; **136**(5):607-615.

324. Lee J-H, Kim Y-G, Cho MH, Kim J-A, Lee J (2012). "7-fluoroindole as an antivirulence compound against *Pseudomonas aeruginosa*". *FEMS Microbiology Letters*; **329**(1):36-44.

325. Borchardt SA, Allain EJ, Michels JJ, Stearns GW, Kelly RF, McCoy WF (2001). "Reaction of Acylated Homoserine Lactone Bacterial Signaling Molecules with Oxidized Halogen Antimicrobials". *Applied and Environmental Microbiology*; **67**(7):3174-3179.

326. Bomberger JM, MacEachran DP, Coutermarsh BA, Ye S, O'Toole GA, Stanton BA (2009). "Long-Distance Delivery of Bacterial Virulence Factors by *Pseudomonas aeruginosa* Outer Membrane Vesicles". *PLoS Pathog*; **5**(4):e1000382.

327. Blanke SR (2006). "Portals and Pathways: Principles of Bacterial Toxin Entry into Host Cells". *Microbes and Infection*; **1**(1):26-32.

328. Rasmussen TB, Bjarnsholt T, Skindersoe ME, Hentzer M, Kristoffersen P, Köte M, et al. (2005). "Screening for Quorum-Sensing Inhibitors (QSI) by Use of a Novel Genetic System, the QSI Selector". *Journal of Bacteriology*; **187**(5):1799-1814.

329. Cady NC, McKean KA, Behnke J, Kubec R, Mosier AP, Kasper SH, et al. (2012). "Inhibition of Biofilm Formation, Quorum Sensing and Infection in *Pseudomonas aeruginosa* by Natural Products-Inspired Organosulfur Compounds". *PLoS One*; **7**(6):e38492.

330. Swem LR, Swem DL, O'Loughlin CT, Gatmaitan R, Zhao B, Ulrich SM, et al. (2009). "A Quorum-Sensing Antagonist Targets Both Membrane-Bound and Cytoplasmic Receptors and Controls Bacterial Pathogenicity". *Molecular Cell*; **35**(2):143-153.

331. Mattmann ME, Geske GD, Worzalla GA, Chandler JR, Sappington KJ, Greenberg EP, et al. (2008). "Synthetic ligands that activate and inhibit a quorum-sensing regulator in *Pseudomonas aeruginosa*". *Bioorganic & Medicinal Chemistry Letters*; **18**(10):3072-3075.

332. Storz MP, Allegretta G, Kirsch B, Empting M, Hartmann RW (2014). "From in vitro to in cellulo: structure-activity relationship of (2-nitrophenyl)methanol derivatives as inhibitors of PqsD in *Pseudomonas aeruginosa*". *Organic & Biomolecular Chemistry*; **12**(32):6094-6104.

333. Kiessling LL, Gestwicki JE, Strong LE (2006). "Synthetic Multivalent Ligands as Probes of Signal Transduction". *Angewandte Chemie International Edition*; **45**(15):2348-2368.

334. Mammen M, Choi S-K, Whitesides GM (1998). "Polyvalent Interactions in Biological Systems: Implications for Design and Use of Multivalent Ligands and Inhibitors". *Angew Chem Int Ed*; **37**:2754-2794.

335. Newkome GR, Moorefield CN, Vögtle F. Dendritic Molecules: Concepts, Syntheses, Perspectives. mbH VV, editor1996.

336. Lee CC, MacKay JA, Frechet JMJ, Szoka FC (2005). "Designing dendrimers for biological applications". *Nature Biotechnology*; **23**(12):1517-1526.

337. Deguise I, Lagnoux D, Roy R (2007). "Synthesis of glycodendrimers containing both fucoside and galactoside residues and their binding properties to Pa-IL and PA-IIL lectins from *Pseudomonas aeruginosa*". *New Journal of Chemistry*; **31**(7):1321-1331.

338. Galloway WRJD, Hodgkinson JT, Bowden SD, Welch M, Spring DR (2011). "Quorum Sensing in Gram-Negative Bacteria: Small-Molecule Modulation of AHL and AI-2 Quorum Sensing Pathways". *Chemical Reviews*; **111**(1):28-67.

339. Miller LC, O'Loughlin CT, Zhang Z, Siryaporn A, Silpe JE, Bassler BL, et al. (2015). "Development of Potent Inhibitors of Pyocyanin Production in *Pseudomonas aeruginosa*". *Journal of Medicinal Chemistry*; **58**(3):1298-1306.

340. Giamarellou H (1986). "Aminoglycosides plus beta-lactams against gram-negative organisms. Evaluation of in vitro synergy and chemical interactions". *The American Journal of Medicine*; **80**(6B):126-137.

341. Forrest GN, Tamura K (2010). "Rifampin Combination Therapy for Nonmycobacterial Infections". *Clinical Microbiology Reviews*; **23**(1):14-34.

342. Tamma PD, Cosgrove SE, Maragakis LL (2012). "Combination Therapy for Treatment of Infections with Gram-Negative Bacteria". *Clinical Microbiology Reviews*; **25**(3):450-470.

343. Kanj SS, Kanafani ZA (2011). "Current Concepts in Antimicrobial Therapy Against Resistant Gram-Negative Organisms: Extended-Spectrum β-Lactamase–Producing Enterobacteriaceae, Carbapenem-Resistant Enterobacteriaceae, and Multidrug-Resistant *Pseudomonas aeruginosa*". *Mayo Clinic Proceedings*; **86**(3):250-259.

344. Choi H, Lee DG (2012). "Synergistic effect of antimicrobial peptide arenicin-1 in combination with antibiotics against pathogenic bacteria". *Research in Microbiology*; **163**(6–7):479-486.

345. Schneider EK, Azad MAK, Han M-L, Zhou Q, Wang J, Huang JX, et al. (2016). "An "Unlikely" Pair: The Antimicrobial Synergy of Polymyxin B in Combination with the Cystic Fibrosis Transmembrane Conductance Regulator Drugs KALYDECO and ORKAMBI". *ACS Infectious Diseases*; **2**(7):478-488.

346. Nissen KB, Haugaard-Kedström LM, Wilbek TS, Nielsen LS, Åberg E, Kristensen AS, et al. (2015). "Targeting Protein-Protein Interactions with Trimeric Ligands: High Affinity Inhibitors of the MAGUK Protein Family". *PLoS One*; **10**(2):e0117668.

347. Qin Y, Luo Z-Q, Smyth AJ, Gao P, Beck von Bodman S, Farrand SK (2000). "Quorum-sensing signal binding results in dimerization of TraR and its release from membranes into the cytoplasm". *The EMBO Journal*; **19**(19):5212-5221.

348. Luo Z-Q, Farrand SK (1999). "Signal-dependent DNA binding and functional domains of the quorum-sensing activator TraR as identified by repressor activity". *Proceedings of the National Academy of Sciences*; **96**(16):9009-9014.

349. Choi K-H, Schweizer HP (2006). "mini-Tn7 insertion in bacteria with single attTn7 sites: example *Pseudomonas aeruginosa*". *Nat Protocols*; **1**(1):153-161.

350. Diggle SP, Fletcher MP, Cámara M, Williams P. Detection of 2-Alkyl-4-Quinolones Using Biosensors. In: Rumbaugh PK, editor. Quorum Sensing: Methods and Protocols. Totowa, NJ: Humana Press; 2011. p. 21-30.

351. Müller C, Fetzner S (2013). "A Pseudomonas putida bioreporter for the detection of enzymes active on 2-alkyl-4(1H)-quinolone signalling molecules". *Applied Microbiology and Biotechnology*; **97**(2):751-760.

352. Allen RL. A study of gene expression in Pseudomonas: University of Leicester; 1989 14/04/1989. 156 p.

353. Estrem ST, Gaal T, Ross W, Gourse RL (1998). "Identification of an UP element consensus sequence for bacterial promoters". *Proceedings of the National Academy of Sciences of the United States of America*; **95**(17):9761-9766.

354. Mitchell JE, Zheng D, Busby SJW, Minchin SD (2003). "Identification and analysis of 'extended –10' promoters in *Escherichia coli*". *Nucleic Acids Research*; **31**(16):4689-4695.

355. Haugen SP, Ross W, Gourse RL (2008). "Advances in bacterial promoter recognition and its control by factors that do not bind DNA". *Nat Rev Micro*; **6**(7):507-519.

356. Frantz B, Chakrabarty AM. CHAPTER 9 - Degradative Plasmids in Pseudomonas A2 - Sokatch, J.R. The Biology of Pseudomonas: Academic Press; 1986. p. 295-323.

357. Varshney U, Hutcheon T, van de Sande JH (1988). "Sequence analysis, expression, and conservation of *Escherichia coli* uracil DNA glycosylase and its gene (ung)". *Journal of Biological Chemistry*; **263**(16):7776-7784.

358. Canosa I, Yuste L, Rojo F (1999). "Role of the Alternative Sigma Factor ς(S) in Expression of the AlkS Regulator of the Pseudomonas oleovorans Alkane Degradation Pathway". *Journal of Bacteriology*; **181**(6):1748-1754.

359. Warren RL, Freeman JD, Levesque RC, Smailus DE, Flibotte S, Holt RA (2008). "Transcription of foreign DNA in *Escherichia coli*". *Genome Research*; **18**(11):1798-1805.

360. Martínez-Antonio A, Janga SC, Thieffry D (2008). "Functional organisation of *Escherichia coli* transcriptional regulatory network". *Journal of Molecular Biology*; **381**(1):238-247.

361. Geissmann T., Marzi S., Romby P. (2009). "The role of mRNA structure in translational control in bacteria". *RNA Biology*; **6**(2):153-160.

362. Balaban NQ, Merrin J, Chait R, Kowalik L, Leibler S (2004). "Bacterial Persistence as a Phenotypic Switch". *Science*; **305**(5690):1622-1625.

363. Keren I, Shah D, Spoering A, Kaldalu N, Lewis K (2004). "Specialized Persister Cells and the Mechanism of Multidrug Tolerance in *Escherichia coli*". *Journal of Bacteriology*; **186**(24):8172-8180.

364. Ehrlich GD, Hu FZ, Shen K, Stoodley P, Post JC (2005). "Bacterial Plurality as a General Mechanism Driving Persistence in Chronic Infections". *Clinical orthopaedics and related research*; (437):20-24.

365. Kamoun S, Kado CI (1990). "Phenotypic Switching Affecting Chemotaxis, Xanthan Production, and Virulence in *Xanthomonas campestris*". *Applied and Environmental Microbiology*; **56**(12):3855-3860.

366. Massey RC, Buckling A, Peacock SJ (2001). "Phenotypic switching of antibiotic resistance circumvents permanent costs in *Staphylococcus aureus*". *Current Biology*; **11**(22):1810-1814.

367. Handke LD, Conlon KM, Slater SR, Elbaruni S, Fitzpatrick F, Humphreys H, et al. (2004). "Genetic and phenotypic analysis of biofilm phenotypic variation in multiple *Staphylococcus epidermidis* isolates". *Journal of Medical Microbiology*; **53**(5):367-374.

368. Guerrero A, Jain N, Goldman DL, Fries BC (2006). "Phenotypic switching in *Cryptococcus neoformans*". *Microbiology (Reading, England)*; **152**(Pt 1):3-9.

369. Chantratita N, Wuthiekanun V, Boonbumrung K, Tiyawisutsri R, Vesaratchavest M, Limmathurotsakul D, et al. (2007). "Biological Relevance of Colony Morphology and Phenotypic Switching by B*urkholderia pseudomallei*". *Journal of Bacteriology*; **189**(3):807-817.

370. Isalan M, Lemerle C, Michalodimitrakis K, Horn C, Beltrao P, Raineri E, et al. (2008). "Evolvability and hierarchy in rewired bacterial gene networks". *Nature*; **452**(7189):840-845.

371. Emori TG, Gaynes RP (1993). "An overview of nosocomial infections, including the role of the microbiology laboratory". *Clinical Microbiology Reviews*; **6**(4):428-442.

372. Streit JM, Jones RN, Sader HS, Fritsche TR (2004). "Assessment of pathogen occurrences and resistance profiles among infected patients in the intensive care unit: report from the SENTRY Antimicrobial Surveillance Program (North America, 2001)". *International Journal of Antimicrobial Agents*; **24**(2):111-118.

373. Boucher HW, Talbot GH, Bradley JS, Edwards JE, Gilbert D, Rice LB, et al. (2009). "Bad Bugs, No Drugs: No ESKAPE! An Update from the Infectious Diseases Society of America". *Clinical Infectious Diseases*; **48**(1):1-12.

374. Gales AC, Jones RN, Turnidge J, Rennie R, Ramphal R (2001). "Characterization of *Pseudomonas aeruginosa* Isolates: Occurrence Rates, Antimicrobial Susceptibility Patterns, and Molecular Typing in the Global SENTRY Antimicrobial Surveillance Program, 1997–1999". *Clinical Infectious Diseases*; **32**(Supplement 2):S146-S155.

375. Obritsch MD, Fish DN, MacLaren R, Jung R (2004). "National Surveillance of Antimicrobial Resistance in *Pseudomonas aeruginosa* Isolates Obtained from Intensive Care Unit Patients from 1993 to 2002". *Antimicrobial Agents and Chemotherapy*; **48**(12):4606-4610.

376. (ECDPC) ECfDPaC. Antimicrobial resistance surveillance in Europe 2012 2013 [Available from: http://ecdc.europa.eu/en/publications/_layouts/forms/Publication_DispForm.aspx?List=4f55ad51-4aed-4d32-b960-af70113dbb90&ID=963.

377. (WHO) RofE-WHO. Antimicrobial Resistance: World Health organisation; 2016 [Available from: http://www.euro.who.int/en/health-topics/disease-prevention/antimicrobial-resistance/antimicrobial-resistance.

378. Nathwani D, Raman G, Sulham K, Gavaghan M, Menon V (2014). "Clinical and economic consequences of hospital-acquired resistant and

multidrug-resistant *Pseudomonas aeruginosa* infections: a systematic review and meta-analysis". *Antimicrobial Resistance and Infection Control*; **3**(1):1-16.

379. Vincent J, Rello J, Marshall J, et al. (2009). "International study of the prevalence and outcomes of infection in intensive care units". *JAMA*; **302**(21):2323-2329.

380. Jarvis WR, Martone WJ (1992). "Predominant pathogens in hospital infections". *Journal of Antimicrobial Chemotherapy*; **29**(suppl A):19-24.

381. Blackburn RM, Henderson KL, Minaji M, Muller-Pebody B, Johnson AP, Sharland M (2012). "Exploring the Epidemiology of Hospital-Acquired Bloodstream Infections in Children in England (January 2009–March 2010) by Linkage of National Hospital Admissions and Microbiological Databases". *Journal of the Pediatric Infectious Diseases Society*.

382. Pharmacopoeia E. Methods of analysis - abstracts. 22002. p. 24-139.

383. Steindler L, Venturi V (2007). "Detection of quorum-sensing N-acyl homoserine lactone signal molecules by bacterial biosensors". *FEMS Microbiology Letters*; **266**(1):1-9.

384. Müh U, Schuster M, Heim R, Singh A, Olson ER, Greenberg EP (2006). "Novel *Pseudomonas aeruginosa* Quorum-Sensing Inhibitors Identified in an Ultra-High-Throughput Screen". *Antimicrobial Agents and Chemotherapy*; **50**(11):3674-3679.

385. Ortori CA, Dubern J-F, Chhabra SR, Cámara M, Hardie K, Williams P, et al. (2010). "Simultaneous quantitative profiling of N-acyl-l-homoserine lactone and 2-alkyl-4(1H)-quinolone families of quorum-sensing signaling molecules using LC-MS/MS". *Analytical and Bioanalytical Chemistry*; **399**(2):839-850.

386. Bala A, Gupta RK, Chhibber S, Harjai K (2013). "Detection and quantification of quinolone signalling molecule: A third quorum sensing molecule of *Pseudomonas aeruginosa* by high performance-thin layer chromatography". *Journal of Chromatography B*; **930**:30-35.

387. Maurer CK, Steinbach A, Hartmann RW (2013). "Development and validation of a UHPLC–MS/MS procedure for quantification of the Pseudomonas Quinolone Signal in bacterial culture after acetylation for characterization of new quorum sensing inhibitors". *Journal of Pharmaceutical and Biomedical Analysis*; **86**:127-134.

388. Eikel D, Vavrek M, Smith S, Bason C, Yeh S, Korfmacher WA, et al. (2011). "Liquid extraction surface analysis mass spectrometry (LESA-MS) as a novel

profiling tool for drug distribution and metabolism analysis: the terfenadine example". *Rapid Communications in Mass Spectrometry*; **25**(23):3587-3596.

389. Eikel D, Henion J (2011). "Liquid extraction surface analysis (LESA) of food surfaces employing chip-based nano-electrospray mass spectrometry". *Rapid Communications in Mass Spectrometry*; **25**(16):2345-2354.

390. Ellis SR, Brown SH, in het Panhuis M, Blanksby SJ, Mitchell TW (2013). "Surface analysis of lipids by mass spectrometry: More than just imaging". *Progress in Lipid Research*; **52**(4):329-353.

391. Sarsby J, Griffiths RL, Race AM, Bunch J, Randall EC, Creese AJ, et al. (2015). "Liquid Extraction Surface Analysis Mass Spectrometry Coupled with Field Asymmetric Waveform Ion Mobility Spectrometry for Analysis of Intact Proteins from Biological Substrates". *Analytical Chemistry*; **87**(13):6794-6800.

392. Montowska M, Rao W, Alexander MR, Tucker GA, Barrett DA (2014). "Tryptic Digestion Coupled with Ambient Desorption Electrospray Ionization and Liquid Extraction Surface Analysis Mass Spectrometry Enabling Identification of Skeletal Muscle Proteins in Mixtures and Distinguishing between Beef, Pork, Horse, Chicken, and Turkey Meat". *Analytical Chemistry*; **86**(9):4479-4487.

393. Himmelsbach M, Varesio E, Hopfgartner G (2014). "Liquid Extraction Surface Analysis (LESA) of Hydrophobic TLC Plates Coupled to Chip-Based Nanoelectrospray High-resolution Mass Spectrometry". *CHIMIA International Journal for Chemistry*; **68**(3):150-154.

394. Lorenz M, Ovchinnikova OS, Van Berkel GJ (2014). "Fully automated laser ablation liquid capture surface analysis using nanoelectrospray ionization mass spectrometry". *Rapid Communications in Mass Spectrometry*; **28**(11):1312-1320.

395. Walworth MJ, ElNaggar MS, Stankovich JJ, Witkowski C, Norris JL, Van Berkel GJ (2011). "Direct sampling and analysis from solid-phase extraction cards using an automated liquid extraction surface analysis nanoelectrospray mass spectrometry system". *Rapid Communications in Mass Spectrometry*; **25**(17):2389-2396.

396. Parson WB, Koeniger SL, Johnson RW, Erickson J, Tian Y, Stedman C, et al. (2012). "Analysis of chloroquine and metabolites directly from whole-body animal tissue sections by liquid extraction surface analysis (LESA) and tandem mass spectrometry". *Journal of Mass Spectrometry*; **47**(11):1420-1428.

397. Randall EC, Bunch J, Cooper HJ (2014). "Direct Analysis of Intact Proteins from *Escherichia coli* Colonies by Liquid Extraction Surface Analysis Mass Spectrometry". *Analytical Chemistry*; **86**(21):10504-10510.

398. Sarsby J, Martin NJ, Lalor PF, Bunch J, Cooper HJ (2014). "Top-Down and Bottom-Up Identification of Proteins by Liquid Extraction Surface Analysis Mass Spectrometry of Healthy and Diseased Human Liver Tissue". *Journal of The American Society for Mass Spectrometry*; **25**(11):1953-1961.

399. Martin NJ, Griffiths RL, Edwards RL, Cooper HJ (2015). "Native Liquid Extraction Surface Analysis Mass Spectrometry: Analysis of Noncovalent Protein Complexes Directly from Dried Substrates". *Journal of The American Society for Mass Spectrometry*; **26**(8):1320-1327.

400. laboratory ORN. AB SCIEX Partners with Advion BioSystems to Commercialize ORNL Sampling System 2010 [Available from: http://web.ornl.gov/adm/partnerships/success_stories/ab_sciex_partners.shtml.

401. Advion. Mode 1: Chip-Based Infusion. 2016.

402. Biomec. TriVersa NanoMate® 2015 [Available from: http://www.biomec.co.kr/purification.

403. Alankar SV, G. (2011). "Methods for the determination of limit of detection and limit of quantitation of the analytical methods". *Chronicles of Young Scientists*; **2**(1):21-25

404. Badu-Tawiah A, Cooks RG (2010). "Enhanced ion signals in desorption electrospray ionization using surfactant spray solutions". *Journal of The American Society for Mass Spectrometry*; **21**(8):1423-1431.

405. Volny M, Venter A, Smith SA, Pazzi M, Cooks RG (2008). "Surface effects and electrochemical cell capacitance in desorption electrospray ionization". *Analyst*; **133**(4):525-531.

406. Green FMS, T. L.; Gilmore, I. S.; Stokes, P.; O'Connor, G. (2010). "The effect of electrospray solvent composition on desorption electrospray ionisation (DESI) efficiency and spatial resolution". *Analyst*; **135**:731-737.

407. Chipuk JE, Brodbelt JS (2008). "Transmission Mode Desorption Electrospray Ionization". *Journal of The American Society for Mass Spectrometry*; **19**(11):1612-1620.

408. Wisztorski M, Desmons A, Quanico J, Fatou B, Gimeno J-P, Franck J, et al. (2016). "Spatially-resolved protein surface microsampling from tissue sections using liquid extraction surface analysis". *PROTEOMICS*:n/a-n/a.

409. Penna A, Elviri L, Careri M, Mangia A, Predieri G (2011). "Investigation of novel sol–gel hydrophobic surfaces for desorption electrospray ionization-mass spectrometry analysis". *Analytical and Bioanalytical Chemistry*; **400**(5):1515-1523.

410. Chang D-Y, Lee C-C, Shiea J (2002). "Detecting Large Biomolecules from High-Salt Solutions by Fused-Droplet Electrospray Ionization Mass Spectrometry". *Analytical Chemistry*; **74**(11):2465-2469.

411. Blatherwick EQ, Van Berkel GJ, Pickup K, Johansson MK, Beaudoin M-E, Cole RO, et al. (2011). "Utility of spatially-resolved atmospheric pressure surface sampling and ionization techniques as alternatives to mass spectrometric imaging (MSI) in drug metabolism". *Xenobiotica*; **41**(8):720-734.

412. Bereman MS, Williams TI, Muddiman DC (2007). "Carbohydrate Analysis by Desorption Electrospray Ionization Fourier Transform Ion Cyclotron Resonance Mass Spectrometry". *Analytical Chemistry*; **79**(22):8812-8815.

413. García-Reyes JF, Jackson AU, Molina-Díaz A, Cooks RG (2009). "Desorption Electrospray Ionization Mass Spectrometry for Trace Analysis of Agrochemicals in Food". *Analytical Chemistry*; **81**(2):820-829.

414. Bereman MS, Muddiman DC (2007). "Detection of Attomole Amounts of Analyte by Desorption Electrospray Ionization Mass Spectrometry (DESI-MS) Determined Using Fluorescence Spectroscopy". *Journal of The American Society for Mass Spectrometry*; **18**(6):1093-1096.

415. Costa AB, Cooks RG (2007). "Simulation of atmospheric transport and droplet-thin film collisions in desorption electrospray ionization". *Chemical Communications*; (38):3915-3917.

416. Costa AB, Graham Cooks R (2008). "Simulated splashes: Elucidating the mechanism of desorption electrospray ionization mass spectrometry". *Chemical Physics Letters*; **464**(1–3):1-8.

417. Whiteley M, Parsek MR, Greenberg EP (2000). "Regulation of Quorum Sensing by RpoS in *Pseudomonas aeruginosa*". *Journal of Bacteriology*; **182**(15):4356-4360.

418. Kim K, Kim YU, Koh BH, Hwang SS, Kim S-H, Lépine F, et al. (2010). "HHQ and PQS, two *Pseudomonas aeruginosa* quorum-sensing molecules, down-

regulate the innate immune responses through the nuclear factor-κB pathway". *Immunology*; **129**(4):578-588.

419. Fekete A, Kuttler C, Rothballer M, Hense BA, Fischer D, Buddrus-Schiemann K, et al. (2010). "Dynamic regulation of N-acyl-homoserine lactone production and degradation in *Pseudomonas putida* IsoF". *FEMS Microbiology Ecology*; **72**(1):22-34.

420. Mani R, St.Onge RP, Hartman JL, Giaever G, Roth FP (2008). "Defining genetic interaction". *Proceedings of the National Academy of Sciences*; **105**(9):3461-3466.

421. Yeh PJ, Hegreness MJ, Aiden AP, Kishony R (2009). "Drug interactions and the evolution of antibiotic resistance". *Nature reviews Microbiology*; **7**(6):460-466.

422. Roussel-Delvallez M, Wallet F, Delpierre F, Courcol RJ (1996). "In Vitro Bactericidal Effect of a β-lactam + Aminoglycoside Combination Against Multiresistant *Pseudomonas aeruginosa* and *Acinetobacter baumannii*". *Journal of Chemotherapy*; **8**(5):365-368.

423. Lodise TP, Lomaestro B, Drusano GL (2007). "Piperacillin-Tazobactam for *Pseudomonas aeruginosa* Infection: Clinical Implications of an Extended-Infusion Dosing Strategy". *Clinical Infectious Diseases*; **44**(3):357-363.

424. Farrell DJ, Flamm RK, Sader HS, Jones RN (2013). "Antimicrobial activity of ceftolozane/tazobactam tested against Enterobacteriaceae and *Pseudomonas aeruginosa* with various resistance patterns isolated in U.S. hospitals (2011-2012)". *Antimicrobial Agents and Chemotherapy*.

Annexes

A1.1. Synergistic effects of GP QS-inhibiting compounds in PAO1-L CTX::P_{Km}-*luxCDABE* after double exposure (Table A1.1)

Most of the tested double combinations produce additional work in the Kanamycin reporter generating upregulation that results in remaining activity over the 100% threshold. Having in mind that these double combinations use only a fourth of the standard concentration to what they are compared to, any metabolical rate delivering results below such level needs to be considered a very acceptable synergistic starting point. In that sense, only three compounds (GPZ824390, GPZ002966 and GPZ273902) maintain at points the bacterial metabolical rate when combined with other compounds. However, in most of the double combinations involving GPZ273902 the bacterial metabolical rate is kept within what can be called a normal range, i.e., not exerting a metabolical effort to percentages higher than the worst of the involved compounds. The outstanding combination emerging from the pool of tested ones is definitely GPZ824390 with GPZ273902; an association that produced a lower metabolical rate than the best of its counterparts. This represents a good indication towards a combinatory group that is already known to reduce *pqsA* expression also to levels below the ones produced by its counterparts.

Table A1.1. Summary of synergistic effects in PAO1-L CTX::P$_{Km}$-*luxCDABE* after combinatory exposure (vertical columns combined with horizontal column). Green stands for percentage of remaining activity lower than the better of the two individual compounds combined, and red for percentage of remaining activity above the worst of the two individual compounds combined. Black stands for inert combinations. The last vertical and horizontal lines present the values corresponding to the exposure of the PAO1-L CTX::P$_{Km}$-*luxCDABE* to the compound individually. Percentages were obtained by comparing the AUC of the different double ombinations to the 1% DMSO control (DMSO percentage in the 100 µM exposure). Initial OD_{600} equals to 0.05. Values in brackets correspond to standard deviation.

PAO1-L CTX::P$_{Km}$-*luxCDABE* VS. 25µM each	GPZ406918	GPZ244801	GPZ738715	GPZ850128	GPZ349236	GPZ961685	GPZ683975	GPZ555169	GPZ535307	GPZ687738	GPZ870387	GPZ775924	GPZ481832	GPZ824390	GPZ002966	GPZ004927	GPZ273902	Individual variation (% of remaining activity @ 100 µM)
GPZ406918	X	1720809 (73%) [143301]	1984509 (84%) [134898]	2055415 (87%) [138479]	2106096 (89%) [143784]	2029484 (86%) [141722]	2094633 (89%) [145691]	2116356 (90%) [147305]	2123905 (90%) [151738]	2089871 (89%) [152203]	2113975 (90%) [161330]	2101305 (89%) [151635]	2209762 (94%) [154955]	3105848 (132%) [165106]	3144046 (133%) [220386]	1911321 (81%) [151162]	1718322 (73%) [144181]	1624517 (69%) [62345]
GPZ244801	X	X	1785690 (76%) [128054]	1723292 (73%) [123059]	1828641 (78%) [132530	1969822 (84%) [142181	3239580 (137%) [153213]	1907014 (81%) [138267]	1955356 (83%) [90810]	1880346 (80%) [143150]	1864515 (79%) [101961]	1810533 (77%) [102163]	2048265 (87%) [144118]	1829275 (78%) [137735]	4235562 (180%) [261112]	1931778 (82%) [151580]	1962456 (83%) [255453]	949967 (40%) [51752]
GPZ738715	X	X	X	3620010 (154%) [204055]	3768988 (160%) [214022]	2634392 (112%) [187412]	3999307 (170%) [219446]	3999169 (170%) [227730]	4074673 (173%) [203692]	3802678 (161%) [197170]	2561174 (109%) [82737]	4205799 (178%) [94079]	5718513 (243%) [145717]	5739227 (243%) [129894]	1014339 (43%) [34564]	1746928 (74%) [137090]	1711394 (73%) [147024]	1062865 (45%) [50297]
GPZ850128	X	X	X	X	3841231 (163%) [121627]	4493023 (191%) [158754]	3956866 (168%) [131282]	4039761 (171%) [144458]	4075327 (173%) [148908]	3444498 (146%) [109403]	2912439 (124%) [137726]	3719730 (158%) [141552]	4720733 (200%) [131166]	4934811 (209%) [123563]	3253149 (138%) [232700]	1649496 (70%) [121893]	1690475 (72%) [135026]	1199529 (51%) [50774]
GPZ349236	X	X	X	X	X	4122620 (175%) [117233]	3742727 (159%) [109030]	3830468 (162%) [123474]	3263022 (138%) [57016]	3389528 (144%) [64145]	3323758 (141%) [57460]	3378346 (143%) [59773]	2281887 (97%) [52505]	3316719 (141%) [163898]	3102818 (132%) [226453]	3167239 (134%) [197630]	1748130 (74%) [145835]	1280692 (54%) [56865]
GPZ961685	X	X	X	X	X	X	3020691 (128%) [128759]	3882002 (165%) [211270]	5378560 (228%) [256611]	3644501 (155%) [66915]	3616118 (153%) [69033]	3392063 (144%) [69446]	2605939 (111%) [65745]	3635279 (154%) [159073]	2950863 (125%) [233312]	3304171 (140%) [299779]	1748008 (74%) [152050]	1340317 (57%) [39354]
GPZ683975	X	X	X	X	X	X	X	4452401 (189%) [145961]	4671806 (198%) [142430]	5230055 (222%) [154676]	4018797 (170%) [78474]	4008085 (170%) [184740]	4083843 (173%) [198579]	4223385 (179%) [196094]	3168370 (134%) [217719]	3025139 (128%) [195562]	1719235 (73%) [146717]	1292732 (55%) [38321]
GPZ555169	X	X	X	X	X	X	X	X	4067975 (173%) [178917]	4291966 (182%) [199186]	3857018 (164%) [209674]	4281824 (182%) [193423]	4237928 (180%) [200338]	3471226 (147%) [161482]	3150256 (134%) [230958]	3150256 (134%) [230958]	1747406 (74%) [147124]	1279873 (54%) [53420]
GPZ535307	X	X	X	X	X	X	X	X	X	2177391 (92%) [118829]	2119418 (90%) [125055]	4191073 (178%) [102163]	4141218 (176%) [203952]	3744753 (159%) [158724]	1532771 (65%) [233312]	2908677 (123%) [204998]	1729777 (73%) [146119]	1240534 (53%) [51621]
GPZ687738	X	X	X	X	X	X	X	X	X	X	2404928 (102%) [148315]	2780875 (118%) [142316]	2281216 (97%) [115753]	4241496 (180%) [206254]	3272402 (139%) [231513]	3136287 (133%) [94891]	1851241 (79%) [153592]	1244147 (53%) [48172]
GPZ870387	X	X	X	X	X	X	X	X	X	X	X	2376146 (101%) [84812]	1526894 (65%) [94891]	3551535 (151%) [149086]	3336893 (142%) [252783]	2887388 (122%) [210677]	1530529 (65%) [131556]	1001238 (42%) [35434]
GPZ775924	X	X	X	X	X	X	X	X	X	X	X	X	3359634 (143%) [111479]	3627471 (154%) [173781]	3457988 (147%) [242569]	3044691 (129%) [200334]	3143954 (133%) [111479]	1331702 (56%) [48571]
GPZ481832	X	X	X	X	X	X	X	X	X	X	X	X	X	3453341 (146%) [134384]	3489993 (148%) [141069]	3484143 (148%) [145856]	3110022 (132%) [122241]	1078950 (46%) [34431]
GPZ824390	X	X	X	X	X	X	X	X	X	X	X	X	X	X	5488351 (233%) [310174]	2274548 (96%) [180925]	1389745 (59%) [178015]	2014396 (85%) [88479]
GPZ002966	X	X	X	X	X	X	X	X	X	X	X	X	X	X	X	3180334 (135%) [214312]	1934794 (82%) [250942]	1000420 (42%) [53665]

GPZ004927	**X**	**X**	**X**	**X**	**X**	**X**	**X**	**X**	**X**	**X**	**X**	**X**	**X**	**X**	**X**	**X**	**1898738 (81%) [243994]**	**1272663 (54%) [41885]**
GPZ273902	**X**	**X**	**X**	**X**	**X**	**X**	**X**	**X**	**X**	**X**	**X**	**X**	**X**	**X**	**X**	**X**	**X**	**1995172 (85%) 168808]**
Average 0% DMSO	**X**	**X**	**X**	**X**	**X**	**X**	**X**	**X**	**X**	**X**	**X**	**X**	**X**	**X**	**X**	**X**	**X**	**X**
Average 0.5% DMSO	**X**	**X**	**X**	**X**	**X**	**X**	**X**	**X**	**X**	**X**	**X**	**X**	**X**	**X**	**X**	**X**	**X**	**X**
Individual variation (% of remaining activity @ 100 µM)	1624517 (69%)	949967 (40%)	1062865 (45%)	1199529 (51%)	1280692 (54%)	1340317 (57%)	1292732 (55%)	1279873 (54%)	1240534 (53%)	1244147 (53%)	1001238 (42%)	1331702 (56%)	1078950 (46%)	2014396 (85%)	1000420 (42%)	1272663 (54%)	**1995172 (85%)**	**X**

A1.2. Synergistic effects of GP QS-inhibiting compounds in PAO1-L after triple exposure

An imposing idea emerges from exposing *pqsA-luxCDABE* to double combinations of GP QS-inhibiting compounds, using smaller concentrations of product that result in improved inhibition, i.e., the idea that it might be possible to use fewer and fewer amounts of GP QS-inhibiting compounds by working the different ligation cores of the *PqsR* molecular structure. In that sense, the *pqsA* remaining activity was once again read only this time against triple (Tables A1.2 and A1.3) and quadruple combinations (Table A1.4). Triple combinations used 16.5 μM of each of the participating compounds whereas quadruple combinations used 6.25 μM of each the involved agents. Both *pqsA* and *PKm* biosensors were tested for triple combinations, with only *pqsA*-luxCDABE tested for quadruple combinations, in order to associate successful *pqsA*-inhibiting results with maintenance of metabolical exertion in the bacteria.

Table A1.2. Inhibitory effects of triple synergistic combinations in PAO1-L CTX::P_{pqsA}-*luxCDABE*. Strain was grown overnight at 37°C in LB medium and exposed to a triple combination of GP QS-inhibiting compounds at an individual concentration of 16.5 µM. Luminescence was read every 30 minutes for a period of 24 hours. Green stands for percentage of remaining activity lower than the better of the two individual compounds combined, and red for percentage of remaining activity above the worst of the two individual compounds combined. Black stands for inert combinations. Percentages were obtained by comparing the AUC of the different triple combinations to the 1% DMSO control (DMSO percentage in the 100 µM exposure). Legend: (A) GPZ824390 (B) GPZ002966 (C) GPZ004927 (D) GPZ244801 (E) GPZ687738 (F) GPZ870387 (G) GPZ481832 (H) GPZ273902. Initial OD_{600} was of 0.05.

Triple Combination of top 7 inhibitors (16.5µM each)	Percentage of remaining activity with compound 1 at 100µM	Percentage of remaining activity with compound 2 at 100µM	Percentage of remaining activity with compound 3 at 100µM	Percentage of remaining activity with triple combination	Δ of remaining activity to best inhibitory compound
ABC	15%	11%	22%	38%	>27%
ABD	15%	11%	43%	43%	>32%
ABE	15%	11%	42%	29%	>18%
ABF	15%	11%	27%	42%	>31%
ABG	15%	11%	33%	33%	>21%
ACD	15%	22%	43%	16%	>1%
ACE	15%	22%	42%	21%	>6%
ACF	15%	22%	27%	52%	>37%
ACG	15%	22%	33%	14%	**<1%**
ADE	15%	43%	42%	14%	**<1%**
ADF	15%	43%	27%	14%	**<1%**
ADG	15%	43%	33%	14%	**<1%**
AEG	15%	42%	33%	16%	>1%
AEF	15%	42%	27%	14%	**<1%**
AFG	15%	27%	33%	16%	>1%
BCD	11%	22%	43%	42%	>31%
BCE	11%	22%	42%	37%	>26%
BCF	11%	22%	27%	31%	>20%
BCG	11%	22%	33%	66%	>55%
BDE	11%	43%	42%	**9%**	**<2%**
BDF	11%	43%	27%	14%	**>3%**
BDG	11%	43%	33%	14%	**>3%**
CDE	22%	43%	42%	19%	**<3%**
CDF	22%	43%	27%	18%	**<4%**
CDG	22%	43%	33%	20%	**<2%**

DEF	43%	42%	27%	81%	>54%
DFG	43%	27%	33%	104%	>77%
DEG	42%	42%	33%	55%	>22%
EFG	42%	27%	33%	69%	>42%
EFG	42%	27%	33%	53%	>26%

An important fact to retain immediately is that 1/6 of the standard individual concentration is being applied in measuring the effects of triple combination on inhibiting *pqsA* expression. Hence, any produced effect that indicates maintenance of a *pqsA*-inhibiting pattern is to be considered successful for less quantity of compound is being used. Results obtained show that apart from the DFG association comprised by GPZ244801, GPZ687738 and GPZ481832 (maintains an inaltered *pqsA* remaining activity at 104%) all other triple combinations reduce the remaining activity overall. However, only a few reduce it to a level of activity lower than the better of the involved compounds at an initial concentration of 100 µM. Thus, by combining at an individual concentration of 16.5 µM three GP QS-inhibiting compounds interacting 'simultaneously' with the PqsR tetradimeric strucuture, the *pqsA* expression rate is actually reduced to lower levels. Analysing the involved elements in the pool of successful triple combinations, one can stress the frequent surgence of GPZ824390 and GPZ244801.

Looking at the effects produced by exposing PAO1-N CTX::P_{Km}-*luxCDABE* to triple combinations of GP QS-inhibiting compounds (Table R2.6) it is possible to highlight three groups that reduce the reporter activity, namely BDE (GPZ002966/GPZ244801/GPZ687738), BDF (GPZ002966/ GPZ244801/GPZ870387) and ADF (GPZ824390/GPZ244801/GPZ870387). From these three groups two combinations (ADF and BDE) have previously been mentioned as *pqsA*-inhibiting triple combinations (Table A1.3).

Table A1.3. Inhibitory effects of triple synergistic combinations in PAO1-L CTX::P_{Km}-*luxCDABE*. Strain was grown overnight at 37°C in Lb medium and exposed to a triple combination of GP QS-inhibiting compounds at an individual concentration of 16.5 µM. Luminescence was read every 30 minutes for a period of 24 hours. Green stands for percentage of remaining activity lower than the better of the two individual compounds combined, and red for percentage of remaining activity above the worst of the two individual compounds combined. Black stands for inert combinations. Percentages were obtained by comparing the AUC of the different triple combinations to the 1% DMSO control (DMSO percentage in the 100 µM exposure). Legend: (A) GPZ824390 (B) GPZ002966 (C) GPZ004927 (D) GPZ244801 (E) GPZ687738 (F) GPZ870387 (G) GPZ481832 (H) GPZ273902. Initial OD_{600} was of 0.05.

Triple Combination of top 7 inhibitors (16.5µM each)	Percentage of remaining activity with compound 1 @ 100µM	Percentage of remaining activity with compound 2 @ 100µM	Percentage of remaining activity with compound 3 @ 100µM	Percentage of remaining activity with triple combination	Δ of remaining activity to best inhibitory compound
ABC	73%	73%	80%	135%	>62%
ABD	73%	73%	106%	112%	>39%
ABE	73%	73%	74%	108%	>35%
ABF	73%	73%	74%	115%	>42%
ABH	73%	73%	67%	101%	>34%
ACD	73%	80%	106%	96%	>23%
ADE	73%	106%	74%	80%	>7%
ADF	73%	74%	74%	**55%**	**<18%**
ADG	73%	74%	100%	114%	>41%
ADH	73%	74%	67%	106%	>39%
AEF	73%	106%	74%	116%	>43%
AEG	73%	106%	100%	97%	>24%
AEH	73%	106%	67%	100%	>33%
AFH	73%	74%	67%	108%	>41%
AGH	73%	100%	67%	110%	>43%
BCD	73%	80%	74%	88%	>15%

BCE	73%	80%	106%	88%	>15%
BCF	73%	80%	74%	95%	>22%
BCG	73%	80%	100%	116%	>43%
BCH	73%	80%	67%	102%	>29%
BDE	73%	74%	106%	**16%**	**<57%**
BDF	73%	74%	74%	**42%**	**<31%**
BDG	73%	74%	100%	30%	<43%
CDE	80%	74%	106%	108%	>28%
CDF	80%	74%	74%	105%	>31%
CDG	80%	74%	100%	106%	>32%
CDH	80%	74%	67%	89%	>22%
DEF	106%	106%	74%	98%	>24%
DEG	106%	74%	100%	68%	<14%
DEH	106%	74%	67%	99%	>25%
EFG	106%	74%	74%	77%	>3%
Average 0% DMSO	2244259	-	-	-	-
Average 0.5% DMSO	2385559	-	-	-	-

A1.3. Synergistic effects of GP QS-inhibiting compounds in PAO1-L after quadruple exposure

Making full use of the tetrameric structure of PqsR set the premise for trialing *pqsA* response to quadruple combinatory exposures (Table A1.4). As in previous experiments where combinatory sets were prepared in smaller concentrations than the preceeding exposures, the quadruple exposure accounted for individual concentrations of 6.25 µM of the participating GP QS-inhibiting compounds. Overall, a full use of the tetrameric structure of the PqsR molecule resulted in very strong *pqsA*-inhibiting rates to approximately an average of 20 to 33% in all prepared combinations. The sets composed by:

ABCD (GPZ824390/GPZ002966/GPZ004927/GPZ244801),

ABCE (GPZ824390/GPZ002966/GPZ004927/GPZ687738),

CDEF (GPZ004927/GPZ244801/GPZ687738/GPZ870387),

CDEG (GPZ004927/GPZ244801/GPZ687738/GPZ481832),

had noticeable variations of remaining percentage of activity to best inhibition compound of over 50%, whilst showing remaining *pqsA* percentage of activity sitting in between 21 and 24%.

No inert interactions were generated with exposing to quadruple combinations possibly indicating an overbearing effect on the PqsR protein structure.

Table A1.4. Inhibitory effects of quadruple synergistic combinations in PAO1-L CTX::P_{pqsA}-*lux*. Strain was grown overnight at 37°C in LB medium and exposed to quadruple combinations of GP QS-inhibiting compounds at an individual concentration of 6.25 µM. Luminescence was read every 30 minutes for a period of 24 hours. Green stands for percentage of remaining activity lower than the better of the four individual compounds combined, and red for percentage of remaining activity above the worst of the four individual compounds combined. Black stands for inert combinations. Percentages were obtained by comparing the AUC of the different triple combinations to the 1% DMSO control (DMSO percentage in the 100 µM exposure). Legend: (A) GPZ824390 (B) GPZ002966 (C) GPZ004927 (D) GPZ244801 (E) GPZ687738 (F) GPZ870387 (G) GPZ481832 (H) GPZ273902. Initial OD_{600} was of 0.05.

Quadruple combination of top 7 inhibitors at an individual concentration of 6.25µM	Percentage of remaining activity with compound 1 @ 100µM	Percentage of remaining activity with compound 2 @ 100µM	Percentage of remaining activity with compound 3 @ 100µM	Percentage of remaining activity with compound 4 @ 100µM	Percentage of remaining activity with quadruple combination	Δ of remaining activity to best inhibitory compound
ABCD	73%	73%	80%	106%	**23%**	**<50%**
ABCE	73%	73%	80%	106%	**21%**	**<52%**
ABCF	73%	73%	80%	74%	**25%**	<48%
ABCG	73%	73%	80%	77%	**25%**	<48%
BCDE	73%	80%	106%	106%	**24%**	<49%
BCDF	73%	80%	106%	74%	**24%**	<49%
BCDG	73%	80%	106%	77%	**24%**	<49%
CDEF	80%	106%	106%	74%	**24%**	**<50%**
CDEG	80%	106%	106%	77%	**25%**	**<52%**
DEFG	106%	106%	74%	77%	**33%**	<41%
ADEF	73%	106%	106%	74%	**25%**	<48%
ADEH	73%	106%	106%	67%	**23%**	<44%
ADFH	73%	106%	74%	67%	**22%**	<45%
ADGH	73%	106%	77%	67%	**24%**	<43%
AEFG	73%	106%	74%	77%	**26%**	<47%
BDEF	73%	106%	106%	74%	**30%**	<43%
BDEG	73%	106%	106%	77%	**32%**	<41%
EFGH	106%	74%	77%	67%	**23%**	<44%

In order to verify that when all ligation cores in the PqsR protein structure are occupied no further added compounds generate a *pqsA*-inhibiting effect, a quintuple combination of ABCDE using individual compound concentrations of 6.25 µM was presented to PAO1-N CTX::P_{pqsA}-*luxCDABE*. The aforementioned association composed of five of the best compounds did not result in better than 22% remaining activity, i.e., the very same repression region individually produced by the quadruple associations ABCD (23%) and ABCE (21%).

A1.4. Synergistic effects of GP QS-inhibiting compounds in PA14

The last analysis to the strength of the synergistic effects produced on the P_{pqsA}-*luxCDABE* reporter were conducted on PA14, known to be a more pathogenic PA strain (Table A1.5), and therefore expectedly more resistant to the candidate molecules under scrutiny. However, the extent PA14 would show an increased resistance to combinatory groups comprised by the most successful *pqsA*-inhibiting molecules needed to be assessed. Even though the number of combinations is very small to adequately represent significant statistics, the overall results reinforce the idea that a more pathogenic strain is still very sensitive to the inhibiting power of the double combination of GP QS-inhibiting compounds, but GPZ004927 is more effective in this more pathogenic strain. This indicates a possible molecular participation of an agent related to the pathogenic islands present in this strain that is affected by GPZ004927 and reduces its defensive capabilities. Nonetheless, this was merely an observation to open space for future interactions rather than an indepth assessment of these synergistic effects on more pathogenic strains.

Table A1.5. Summary of synergistic effects in PA14 CTX*::*P_{pqsA}-*luxCDABE* after combinatory exposure (vertical columns combined with horizontal column). Strain was grown overnight at 37°C in LB medium and exposed to double combinations of GP QS-inhibiting compounds at an individual concentration of 25 µM. Luminescence was read every 30 minutes for a period of 24 hours. Percentages were obtained by comparing the AUC of the different triple combinations to the 1% DMSO control (DMSO percentage in the 100 µM exposure).

PA14 CTX::P_{pqsA}-*luxCDABE* exposed to 25µM of each compound	GPZ824390	GPZ002966	GPZ273902
GPZ824390	*	24% (15% in PAO1-L)	23% (9% in PAO1-L)
GPZ002966	*	*	23% (9% in PAO1-L)
GPZ004927	13% (17% in PAO1-L)	16% (12% in PAO1-L)	12% (10% in PAO1-L)

A1.5. Synergistic effects in PAO1-N *lecA/lecB* after triple exposure

Triple combination exposures with individual concentrations of 16.5 µM were presented to PAO1-N *lecA* only (Table A1.6). Overall, the double combinations produced repression of the *lecA* activity with only one exception DEF (GPZ244801/GPZ687738/GPZ870387). The most effective triple combination was ABD (GPZ824390/GPZ002966/GPZ244801) reducing percentage of remaining activity of *lecA* to mere 24% corresponding to a decrease of 24% in relation to the best of the compounds used when at a concentration of 100 µM. CDF (GPZ004927/GPZ244801/GPZ870387) and CDG (GPZ004927/GPZ244801/GPZ481832) were capable of reducing the percentage of remaining activity to 34% and 37%, respectively. Both CDF and CDG had variations of remaining activity to best inhibitory compound of over 38%.

Table A1.6. Summary of synergistic effects over *lecA* activity after triple combinatory exposure to selected GreenPharma inhibitors. PAO1-N CTX::P$_{lecA}$-*luxCDABE* was grown overnight at 37°C and exposed to individual concentrations of 16.5 µM of each of the intervening compounds. Green stands for improved reduction in comparison to best individual compound and red stands for enhanced activity in comparison to worst individual compound when at a concentration of 100 µM. Legend: (A) GPZ824390 (B) GPZ002966 (C) GPZ004927 (D) GPZ244801 (E) GPZ687738 (F) GPZ870387 (G) GPZ481832 (H) GPZ273902. Initial OD_{600} was of 0.05.

QS-inhibitor at an individual concentration of 16.5 µM	Percentage of remaining activity with compound 1 at 100µM	Percentage of remaining activity with compound 2 at 100µM	Percentage of remaining activity with compound 3 at 100µM	Percentage of remaining activity with individual exposure at 100 µM	Δ of remaining activity to best inhibitory compound
ABC	48%	56%	83%	**36%**	<12%
ABD	48%	56%	87%	**24%**	**<24%**
ABE	48%	56%	46%	55%	>9%
ABF	48%	56%	76%	**37%**	<11%
ABG	48%	56%	106%	**39%**	<9%
BCD	56%	83%	87%	**36%**	<20%
BCE	56%	83%	46%	**31%**	<15%
BCF	56%	83%	76%	**41%**	<15%
BCG	56%	83%	106%	**44%**	<12%
CDE	83%	87%	46%	**27%**	<19%
CDF	83%	87%	76%	**37%**	**<39%**
CDG	83%	87%	106%	**34%**	**<49%**
DEF	87%	46%	76%	**121%**	>75%
DEG	87%	46%	106%	**54%**	>8%
EFG	46%	76%	106%	**58%**	>12%

A1.6. Effect of mixtures of GP QSIs on pyocyanin production

Table A1.7. Effect of GP QS-inhibiting compounds on pyocyanin production. Strains were grown overnight at 37°C and then standardised to an OD_{600} of 1.0 to be exposed to the GP QS-inhibiting compounds whilst reincubating at 37°C and 200 rpm for 18 hours. Exposures were performed to individual concentrations of 10 µM, 100 µM and IC_{50} values. Whenever possible the samples were exposed to IC_{10} and IC_{90} values and mixtures for an understanding of the synergistic effects. Three replicates of each treatment were analysed. Green and red bold values stand for percentage of remaining activity at least 20% below and above control, respectively.

PAO1-N	Mean [Pyocyanin] µg/ml	Remaining Pyocyanin Production %	Standard deviation ± 95% confidence (µg/ml)
Mixture of GPZ870387, GPZ535307 and GPZ481832 (@ 16.5 µM each)	3.67	**59.2%**	5.00 ±0.25
PA14	**Mean [Pyocyanin] µg/ml**	**Remaining Pyocyanin Production %**	**Standard deviation ± 95% confidence (µg/ml)**
Mixture of GPZ002966 and GPZ824390 (@ 5 µM each)	2.851	**13%**	1.60 ±0.08
Mixture of GPZ002966 andGPZ481832 (@ 5 µM each)	6.376	**56%**	1.60 ±0.08
Mixture of GPZ824390 and GPZ244801 (@ 5 µM each)	1.152	**10%**	0.60 ±0.03
PA SED2-LES	**Mean [Pyocyanin] µg/ml**	**Remaining Pyocyanin Production %**	**Standard deviation ± 95% confidence (µg/ml)**
Mixture of GPZ244801 and GPZ824390 (@ 5 µM each)	7.307	**24%**	1.00 ±0.05
Mixture of GPZ870387 and GPZ244801 (@ 12.5 µM each)	16.82	**59%**	N/A

A1.7. Ligand receptor binding and docking affinity of the GP QSIs to the PqsR protein (Figures A1.1 to A1.8)

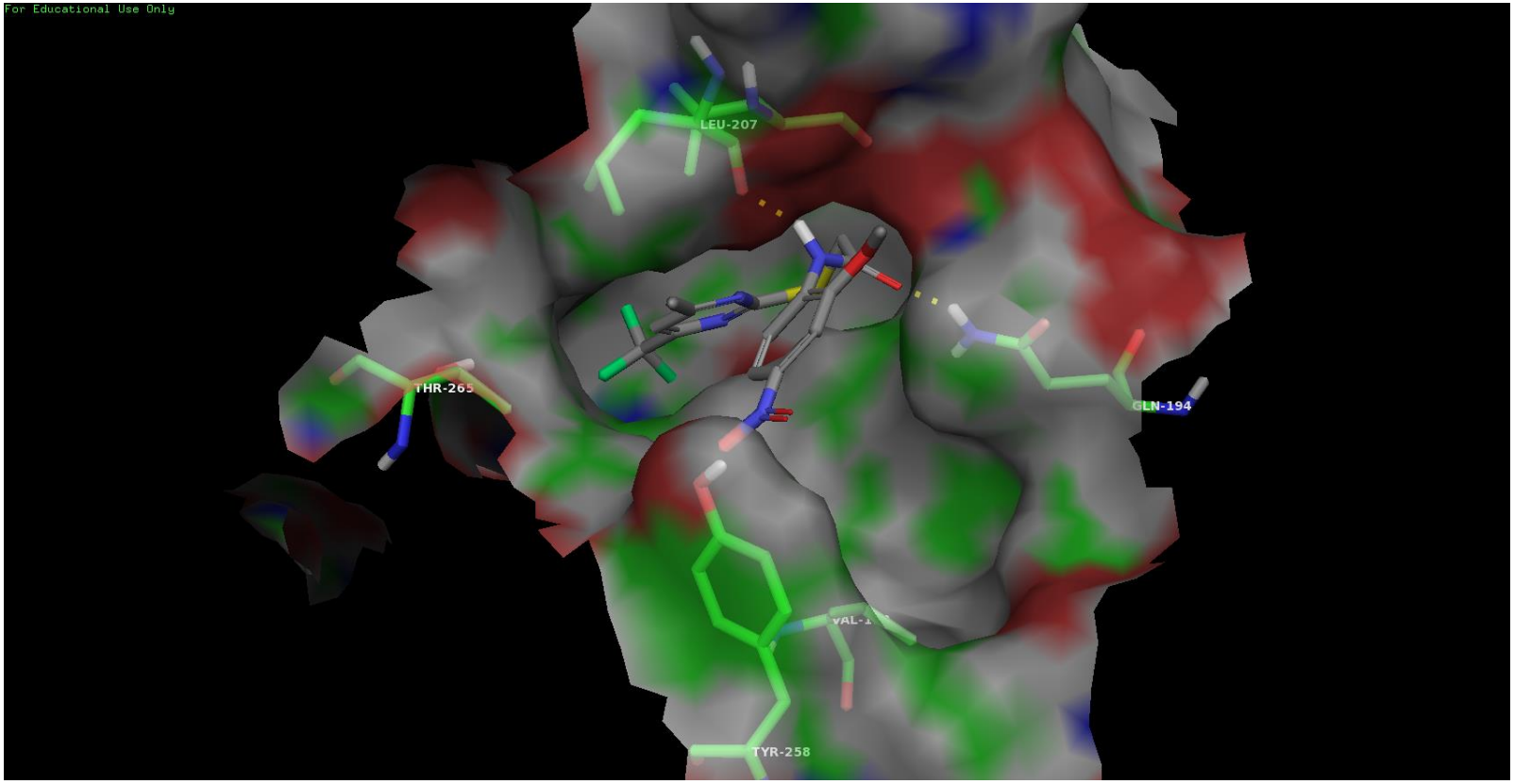


Figure A1.1. GPZ002966 (side view).

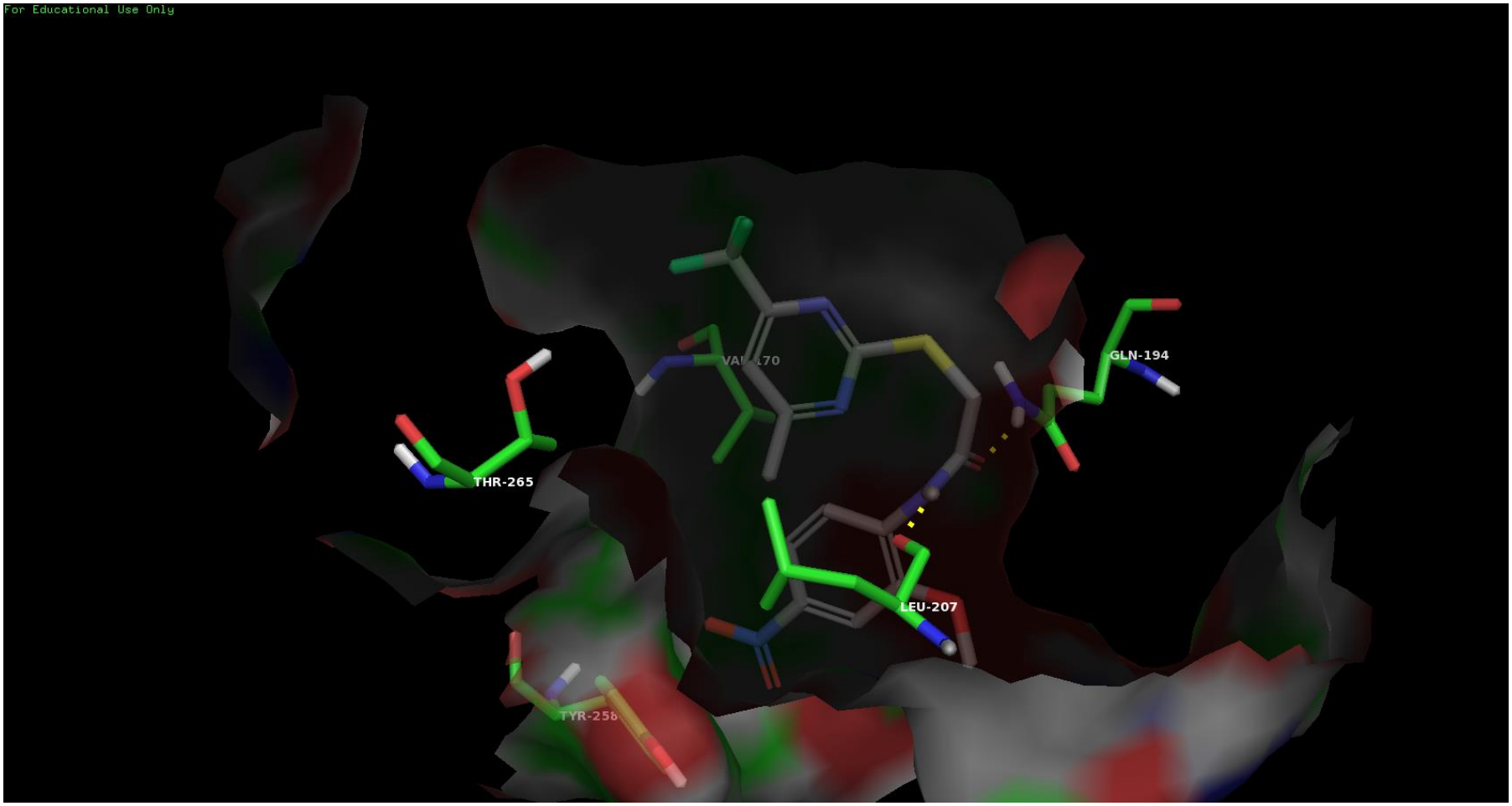


Figure A1.2. GPZ002966 (top view)

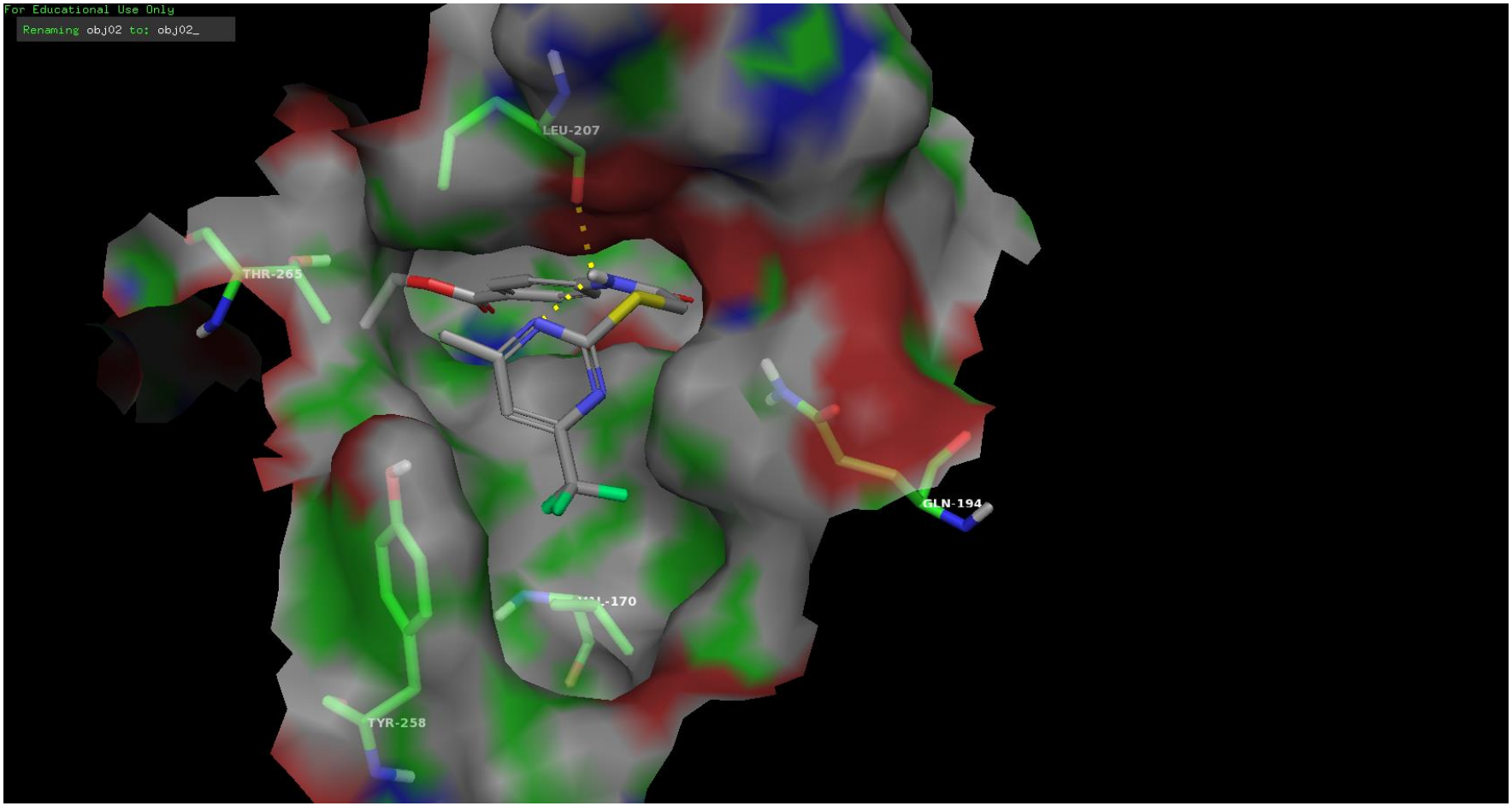


Figure A1.3. GPZ004927 (side view)

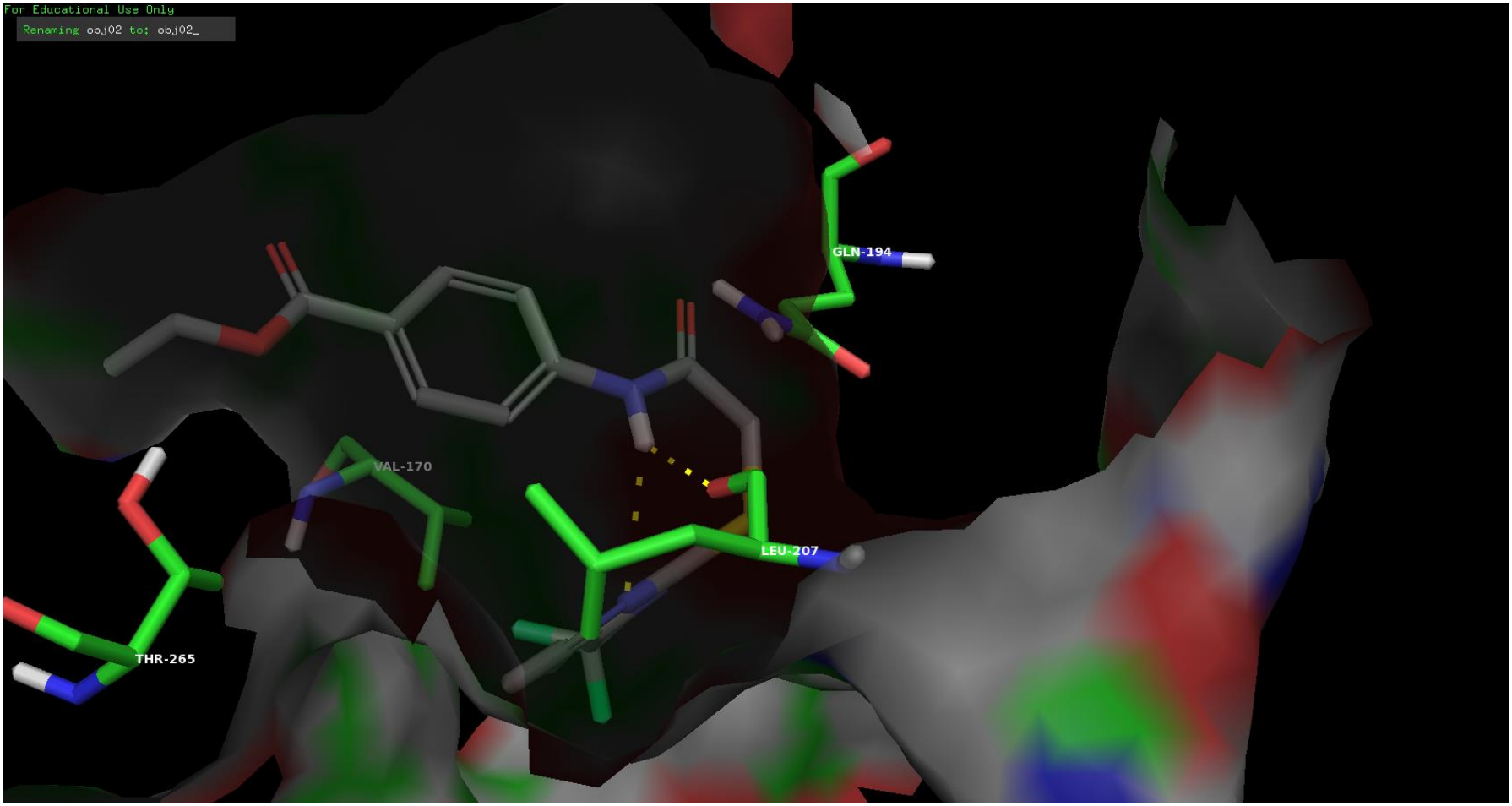


Figure A1.4. GPZ004927 (top view)

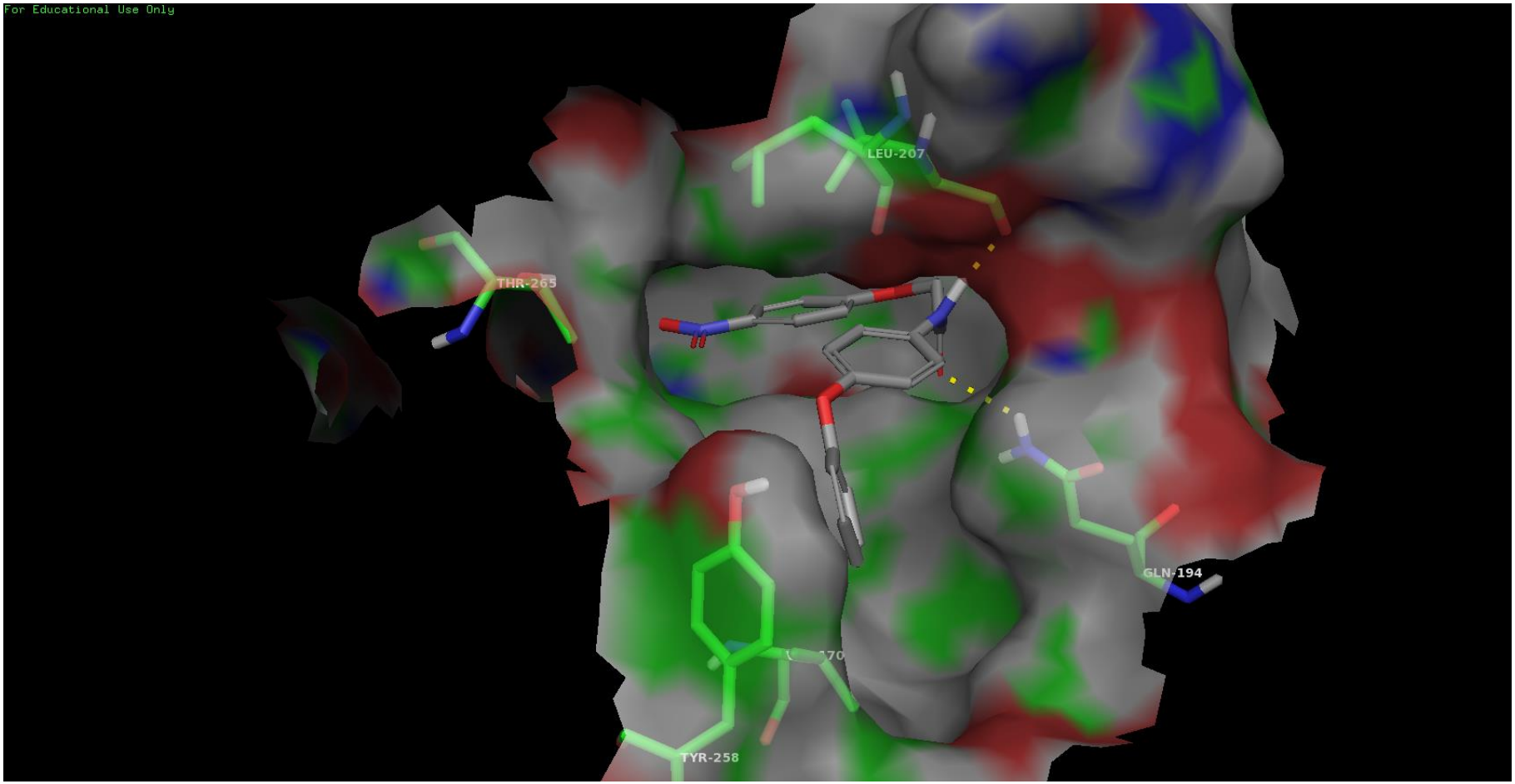


Figure A1.5. GPZ273902 (side view)

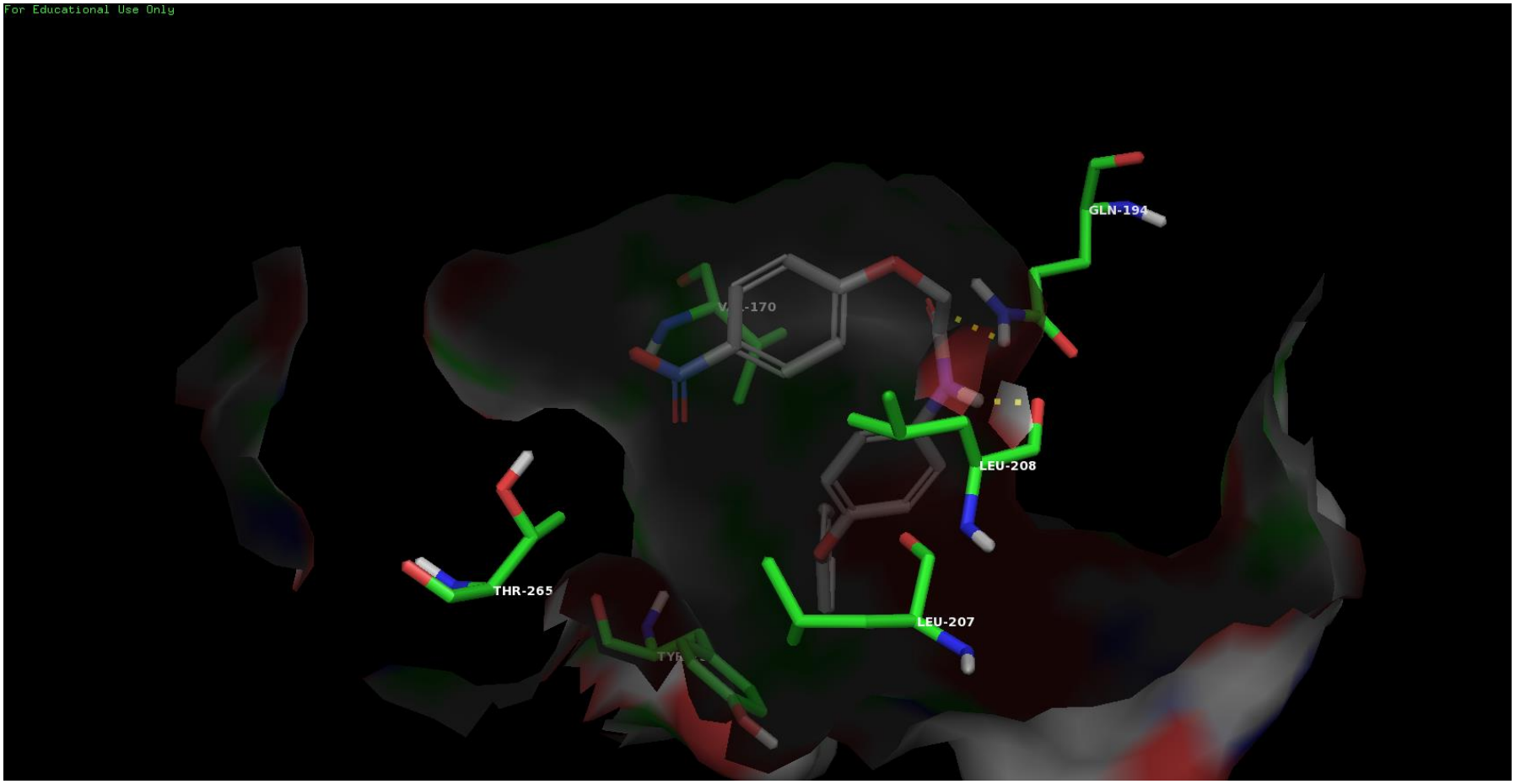


Figure A1.6. GPZ273902 (top view)

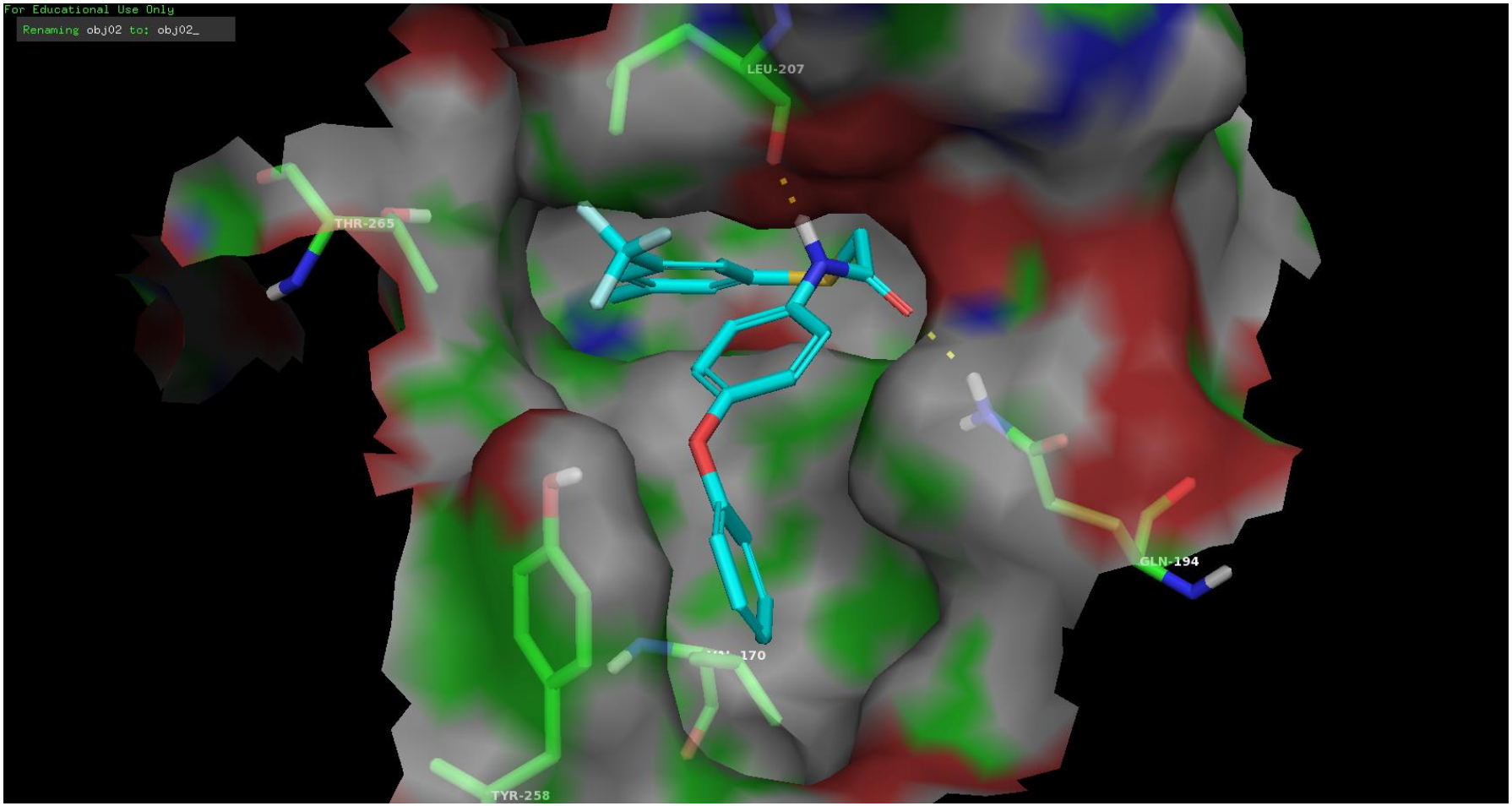


Figure A1.7. GPZ824390 (side view)

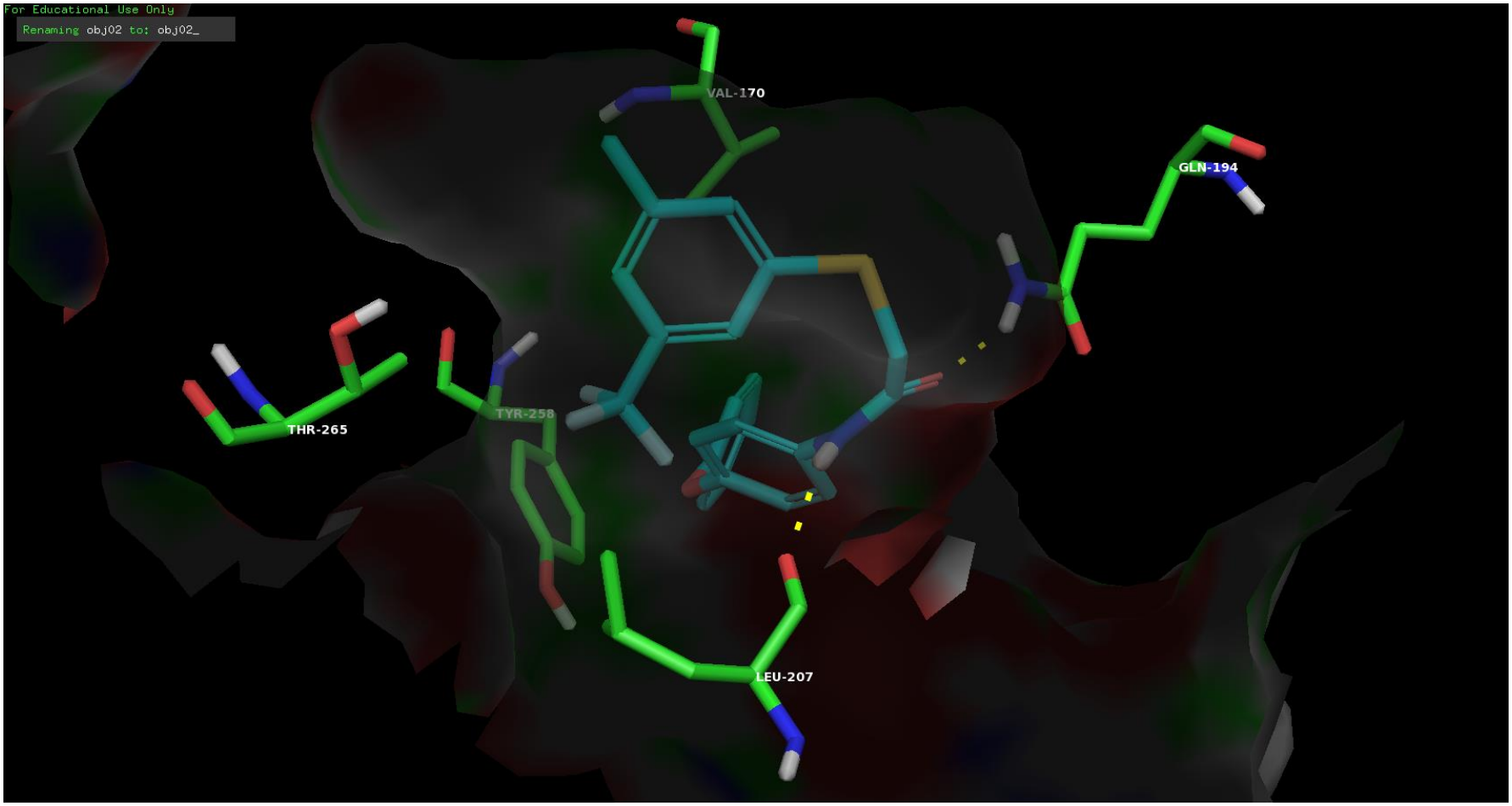


Figure A1.8. GPZ824390 (top view)